

**Relationship between altered myoepithelial  
phenotype and the inflammatory cell infiltrate  
in progression of DCIS**

**Thesis submitted for the degree of Doctor of Philosophy at the  
University of London**

**Khairiya O Ahmed**

**MBBS, MSC**

**2014**

**Centre for Tumour Biology Institute of Cancer  
Barts and the London Queen Mary school of Medicine and Dentistry  
John Van Science Centre, Charterhouse Square, London EC1M 6BQ**

## Abstract

Changes in the microenvironment have been implicated in the transition of pre-invasive ductal carcinoma in-situ (DCIS) to invasive breast cancer. Normal myoepithelial cells have a tumour suppressor phenotype but they are altered in DCIS and ultimately lost with transition to invasive cancer. A consistent change in DCIS is up-regulation of the integrin  $\alpha\beta6$  in myoepithelial cells. Preliminary observations identified a correlation between myoepithelial  $\alpha\beta6$  and an increased peri-ductal inflammatory infiltrate.

The hypothesis of this study is that the altered myoepithelial phenotype influences the peri-ductal inflammatory environment, which in turn mediates a pro-apoptotic effect on myoepithelial cells contributing to their loss.

To investigate this, the inflammatory infiltrate was characterised in a series of DCIS tissue in relation to  $\alpha\beta6$  status. This demonstrated significantly higher levels of CD4<sup>+</sup>ve and FOXP3<sup>+</sup>ve T cells around  $\alpha\beta6$ <sup>+</sup>ve DCIS ducts compared to  $\alpha\beta6$ <sup>-</sup>ve ducts ( $P < 0.01$ ), suggesting an increase in Treg cells. In-vivo, Matrigel plugs containing injected into the flanks of female C57/Blk6 normal mice generated influx of higher levels of CD4<sup>+</sup>ve cells ( $p = 0.005$ ) and FOXP3<sup>+</sup> T cells ( $p = 0.007$ ) in the presence of  $\alpha\beta6$ <sup>+</sup>ve myoepithelial cells compared to  $\alpha\beta6$ <sup>-</sup>ve cells, supporting the findings in human tissue samples.

Since Treg cells produce TRAIL that can induce apoptosis, we investigated the influence of  $\alpha\beta6$  on myoepithelial cells on the levels of TRAIL in T cells and the hypothesis that  $\alpha\beta6$ -positive myoepithelial cells may be more susceptible to TRAIL-induced apoptosis, leading to loss of the myoepithelial barrier. Firstly, levels of TRAIL in Jurkat and primary T cell populations co-cultured with  $\beta4$

or  $\beta 6$  myoepithelial cells were measured. This demonstrated a higher level of TRAIL in primary T cells co-cultured  $\beta 6$  myoepithelial cells compared to those co-cultured with  $\beta 4$  myoepithelial cells.  $\beta 6^{+ve}$  and  $\beta 6^{-ve}$  myoepithelial cells were exposed to TRAIL, and this demonstrated that TRAIL enhanced apoptosis, measured by cleaved PARP, in  $\beta 6^{+ve}$  cells. Furthermore, these cells showed loss of the anti-apoptotic protein Galectin-7, and knockdown of Galectin-7 in normal  $\beta 6^{-ve}$  myoepithelial cells rendered them more susceptible to TRAIL-induced apoptosis. In DCIS tissues, an inverse relationship between  $\alpha\beta 6$  and Galectin-7 in myoepithelial cells was demonstrated, and Cytokine Array analysis showed that  $\alpha\beta 6^{+ve}$  myoepithelial cells express higher levels of IL-16, which has a role in Treg cell recruitment.

Taken together these results suggest that expression of  $\alpha\beta 6$  by myoepithelial cells in DCIS generates a tumour-promoter peri-ductal inflammatory infiltrate through altered cytokine release, is associated with reduced galectin-7 expression and enhances myoepithelial cell apoptosis in response to TRAIL. This provides a potential mechanism by which myoepithelial cells may be lost during evolution of DCIS and so contribute to progression to invasive disease.

## **Declaration of work**

I hereby certify that this material, which I submit for assessment on the programme of study leading to the award of PhD is entirely my own work and has not been taken from the work of others save and to the extent that such work has been cited and acknowledged within the text of my work.

Signed: Dr. Khairiya Ahmed



## Acknowledgment

I would like to thank my supervisor, Prof. Louise J Jones for her ongoing guidance, encouragement and great support. I am grateful to her for giving me the honour to be one of her students.

Many thanks to my second supervisor, Dr. John Marshall for helping me when I needed him. Special thanks Dr. Michael Allen, Dr. Jenny Gomm and Dr. George Elia for teaching me and helping me through various lab techniques. I would also like to thank all my colleagues in breast group for making my life enjoyable during the course of my research.

I am grateful to Alahdy University, Iben sina teaching hospital and Libyan goverement for providing the scholarship.

I am glad to have a chance to thank people who had a positive impact in my life. My family for their support, love, care and prayers throughout my life.

# Table of Contents

---

Abstract .....	i-ii
Declaration of work.....	iii
Acknowledgment.....	iv
Table of Contents .....	v-xii
List of figures .....	xiii-xv
List of Tables.....	xvi
Abbreviations .....	xvii-xxii
Chapter 1: Introduction .....	1
1.1 The Breast .....	2
1.2 Cancer.....	3
1.3 Breast cancer .....	4
1.3.1 History of breast cancer.....	6
1.3.2 Geographic variation .....	9
1.3.3 Risk factors.....	9
1.3.4 Age .....	9
1.3.5 Reproductive history .....	10
1.3.6 Age of menarche.....	11
1.3.7 Age at menopause.....	11
1.3.8 Hormones .....	11
I. Endogenous.....	11
II. Exogenous.....	12
1.3.9 Breast density .....	12
1.3.10 Family history.....	13
1.3.11 Physical activity.....	14
1.3.12 Alcohol consumption.....	14
1.4 Ductal carcinoma in situ (DCIS) .....	15
1.5 Classification of DCIS.....	16
1.6 Progression of DCIS to invasive cancer.....	18
1.7 DCIS microenvironment .....	19
1.8 Myoepithelial cells .....	20
1.8.1 Markers of myoepithelial cells .....	20
1.8.2 Function of myoepithelial cells in normal breast .....	22
1.8.3 Role of myoepithelial cells in breast cancer.....	23
1.9 Immune system.....	27
1.10 Overview of immune cell function in cancer .....	28

1.11 Inflammation and cancer: progression versus elimination .....	29
1.11.1 Anti-tumour response of immune cells .....	29
1.11.2 Pro-tumour response of immune cells .....	29
1.12 The role of the immune system in breast cancer .....	30
1.13 T lymphocytes .....	32
1.13.1 CD69 T cells.....	33
1.13.1.1 The role of CD69 T cells in malignancy .....	33
1.13.1.2 Role of CD69+ cells in breast cancer .....	34
1.13.2 CD4 T cells.....	34
1.13.2.1 Role of CD4 T cells in immunity .....	35
1.13.2.2 Role of CD4 T cells in cancer .....	35
1.13.2.3 Role of CD4 T cells in breast cancer .....	36
1.13.3 FOXP3+ cells .....	37
1.13.3.1 Role of FOXP3 T cells in cancer.....	37
1.13.3.2 Role of FOXP3+ cells in breast cancer .....	38
1.13.4 CD8 T cells.....	39
1.13.4.1 Role of CD8 T cells in cancer .....	39
1.13.4.2 Role of CD8 T cells in breast cancer .....	40
1.13.5 CD45RO+ cells .....	40
1.13.5.1 Role of CD45RO+ cells in cancer .....	41
1.13.5.2 Role of CD45RO+ cells in breast cancer.....	42
1.14 Macrophages .....	42
1.14.1 Macrophages in cancer .....	43
1.14.2 Macrophages in breast cancer.....	44
1.14.3 CD68+ macrophages .....	44
1.14.3.1 CD68 + macrophages in cancer.....	44
1.14.3.2 CD68+ macrophages in breast cancer .....	45
1.14.4 CD74+ cells.....	46
1.14.4.1 CD74+ cells in cancer .....	46
1.14.4.2 CD74+ cells in breast cancer .....	47
1.14.5 Macrophage inhibitory factor (MIF) .....	47
1.14.5.1 Role of MIF in cancer.....	47
1.14.6 Arginase-positive macrophages.....	48
1.15 Apoptosis (programmed cell death) .....	49
1.16 Mechanism of apoptosis .....	51
I. Extrinsic pathway.....	51
II. Intrinsic pathway.....	51
1.17 Markers of apoptosis .....	54

I. Cleavage of Poly (ADP-ribose) polymerase (PARP) .....	54
II. Cleavage of $\beta$ – actin.....	54
1.18 Role of apoptosis in breast cancer .....	56
1.19 TRAIL (APO-2L).....	56
1.20 Galectin-7 expression in tissue.....	57
1.21 Hypothesis .....	59
Chapter 2: Materials & Methods .....	61
2.1 Clinical materials.....	62
2.1.1 Tissue samples.....	62
2.1.1.1 UK tissue samples .....	62
2.1.1.2 Netherland tissue samples .....	63
2.1.2 Tissue block selection.....	64
2.2 Origin of primary cells and cell lines .....	64
2.2.1 Primary cells.....	65
2.1.3.1 Breast myoepithelial cells.....	65
2.1.3.2 Primary T lymphocytes .....	67
2.3 Matrigel plug assays .....	67
2.4 Immunohistochemistry .....	69
2.4.1 Slide preparation.....	69
2.4.2 Haematoxylin and eosin staining.....	69
2.4.3 Immunohistochemistry technique.....	69
2.4.4 Slide preparation for staining .....	70
2.4.5 Antigen retrieval.....	70
2.4.6 Blocking .....	71
2.4.7 Primary antibody .....	71
2.4.8 Secondary antibody .....	73
2.4.9 Avidin biotin complex (ABC) .....	73
2.4.10 Detection.....	73
2.4.11 Dehydration .....	74
2.5 Scoring of Immunohistochemistry .....	74
2.5.1 Scoring of $\alpha\beta$ 6 IHC staining.....	74
2.5.2 Relationship between $\alpha\beta$ 6 and galectin-7 expression.....	74
2.5.3 Scoring of inflammatory cell infiltrate in DCIS .....	75
2.5.3.1 Photography.....	75
2.5.3.2 Process Image program .....	77
2.5.4 Scoring of inflammatory cell infiltrate in Matrigel plugs.....	78
2.5.4.1 Photography.....	78

2.5.4.2 Aperio Imagescope software .....	78
2.5.4.3 Quantitation of the inflammatory cell infiltrate in Matrigel plugs containing myoepithelial cells .....	78
2.6 Measuring of DCIS duct size .....	81
2.7 Statistical analysis .....	83
2.8 Cell culture .....	83
2.8.1 Myoepithelial cell line culture .....	83
2.8.2 Maintenance of myoepithelial cell line .....	84
2.8.3 Primary myoepithelial cell culture .....	84
2.8.4 Jurkat cell line culture .....	84
2.8.5 Primary T cell culture .....	85
2.8.6 Counting of cells.....	85
2.8.7 Cryopreservation of cells.....	85
2.8.8 Generation of condition medium.....	86
2.8.9 Magnetic activated cell sorting.....	86
2.8.10 Co-culture of myoepithelial cells with T cells.....	87
2.9 Cell treatment .....	89
2.10 Western blotting .....	89
2.10.1 Preparation of whole cell lysates .....	89
2.10.2 Estimation of protein concentration .....	90
2.10.3 Immunoblotting .....	90
2.10.4 Antibody detection .....	91
2.10.5 Blotting for $\beta$ -actin/HSC70 .....	92
2.11 siRNA Transfection.....	93
2.12 Detection of apoptosis .....	93
2.13 RNA extraction.....	93
2.14 Quantitation of RNA .....	94
2.15 Complementary DNA (cDNA) synthesis .....	94
2.16 Polymerase chain reaction (PCR).....	95
2.17 qPCR .....	97
2.17.1 Relative expression level.....	97
2.18 Proteome Profiler .....	98
2.19 Flow cytometry.....	99
Chapter 3: Inflammatory cell infiltrate in DCIS.....	102
3.1 Introduction .....	103
3.1.1 Role of Inflammatory cells in cancer .....	103
3.2 Rationale for investigation .....	105

3.3 Selection of inflammatory cell markers.....	106
3.4 Methods and Materials .....	107
3.4.1 Immunohistochemistry .....	107
3.4.2 Scoring of $\alpha\beta6$ IHC staining .....	107
3.4.3 Scoring of inflammatory cell infiltrate in DCIS .....	107
3.4.5 Scoring of inflammatory cell infiltrate in Matrigel plugs.....	108
3.5 Results .....	109
3.5.1 Selection of DCIS cases .....	109
3.5.2 Inflammatory cell infiltrate in DCIS in relation to altered myoepithelial cell phenotype.....	110
3.5.2.1 CD69+ve cells in DCIS in relation to $\alpha\beta6$ expression .....	110
3.5.2.2 CD4+ve cells in DCIS microenvironment.....	113
3.5.2.4 CD8 cytotoxic T cell density in DCIS cases .....	119
3.5.2.5 DCIS-associated CD45RO+ve cells.....	122
3.5.2.6 MHC-II+ve cells in DCIS .....	125
3.5.2.7 CD74+ve cell infiltrate in DCIS microenvironment .....	128
3.5.2.8 CD68+ve cells in DCIS cases.....	131
3.5.2.9 Arginase-1+ve cells in DCIS microenvironment .....	134
3.5.3 Inflammatory cell profile in relation to $\alpha\beta6$ status .....	137
3.5.4 Analysis of the inflammatory cell infiltrate in relation to myoepithelial $\alpha\beta6$ status <i>in-vivo</i> .....	139
3.5.4.1 Quantitation of CD4+ve T cells in Matrigel plug assays .....	139
3.5.4.2 Density of FOXP3+ve cell in Matrigel plugs .....	142
3.5.4.3 Density of CD8+ve T cells in Matrigel plugs.....	145
3.5.4.4 Quantitation of CD74+ve cells in Matrigel plugs .....	148
3.5.4.5 Distribution of Arginase-1+ve cells in Matrigel plugs assays.....	151
3.6 Discussion .....	154
3.7 Conclusion.....	158
Chapter 4: Role of T cells in progression of DCIS.....	159
4.1 Introduction .....	160
4.2 Hypothesis .....	162
4.3 Methods and Materials .....	163
4.3.1 Measuring TRAIL levels in T cells .....	163
4.3.2 Measuring TRAIL receptors in myoepithelial cells .....	163
4.3.3 Analysing the susceptibility of myoepithelial cell lines to apoptosis.....	163
4.3.4 Detection of apoptosis in DCIS-associated myoepithelial cells by immunohistochemistry.....	164
4.4 Results .....	165

4.4.1 Impact of myoepithelial cells on T-cell derived TRAIL .....	165
4.4.2 Expression of TRAIL receptors DR4 & DR5 in myoepithelial cell populations.....	167
4.4.3 Detection of apoptosis in TRAIL-treated myoepithelial cell lines .....	169
4.4.4 Detection of cleaved caspase-3 as a marker of apoptosis in DCIS.....	175
4.5 Discussion .....	177
4.6 Conclusion.....	181
Chapter 5: Galectin-7 in relation to $\alpha\beta 6$ .....	182
5.1 Introduction .....	183
5.1.1 Galectin-7 expression in myoepithelial cells.....	183
5.2 Hypothesis .....	183
5.2.1 Aims of this chapter.....	184
5.3 Methods and Materials .....	184
5.3.1 Investigation of galectin-7 and $\alpha\beta 6$ expression in DCIS.....	184
5.3.2 Analysis of the relationship between galectin-7 and $\alpha\beta 6$ in DCIS.....	184
5.3.4 Measurement of galectin-7 in myoepithelial cells.....	185
5.3.5 Knockdown of galectin-7 in primary myoepithelial cells and $\beta 4$ myoepithelial cell line.....	185
5.3.6 Measuring duct size .....	185
5.4 Results .....	186
5.4.1 Expression of galectin-7 in control tissues .....	186
5.4.2 Galectin-7 expression in DCIS cases and its correlation with $\alpha\beta 6$ .....	188
5.4.3 Galectin- 7 expression in myoepithelial breast cell lines .....	192
5.4.4 Impact of galectin-7 knockdown on $\alpha\beta 6$ expression.....	194
5.4.5 Relationship between Galectin-7 expression and apoptotic response .....	196
5.4.6 Relationship between galectin-7 and $\alpha\beta 6$ expression and DCIS duct size	202
5.4.7 Relationship between galectin-7 and $\alpha\beta 6$ expression and clinical outcome .....	206
5.5 Discussion .....	209
5.6 Conclusion.....	212
Chapter 6: Myoepithelial- T cell interaction .....	213
6.1 Introduction .....	214
6.1.1 Cytokines expressed in normal breast and breast cancer.....	214
6.2 Hypothesis .....	215
6.3 Methods and Materials .....	216
6.3.1 Co-culture of myoepithelial cells with T cells.....	216
6.3.2 Measurement of CD4 and CD8 in T cells co-cultured with myoepithelial cells.....	216

6.3.3 Investigation of cytokine levels in myoepithelial cells .....	216
6.4 Results .....	217
6.4.2 Analysis of CD3 expression in primary T cell .....	218
6.4.3 Analysis of CD4 expression in primary T cells and Jurkat T cells .....	219
6.4.4 Analysis of CD8 expression in primary T cells and Jurkat T cells .....	221
6.4.5 Effect of myoepithelial cells on expression of CD4 in primary T cells .....	223
6.4.6 Effect of myoepithelial cells on expression of CD4 in Jurkat T cells .....	227
6.4.7 Impact of myoepithelial cells on expression of CD8 in primary T cells ....	231
6.4.8 Impact of myoepithelial cells on expression of CD8 in Jurkat T cells .....	235
6.4.9 Cytokine profile of myoepithelial cells .....	239
6.4.10 Cytokines released by myoepithelial cells.....	241
6.4.11 Influence of T cells on myoepithelial cytokine expression .....	243
6.5 Discussion .....	245
6.6 Conclusion.....	247
7.1 Overview of the study aims .....	249
7.2 $\alpha\beta 6$ positive DCIS-associated myoepithelial cells and the inflammatory cell infiltrate.....	250
7.3 Role of T cells in progression of DCIS .....	251
7.4 Increased expression of TRAIL.....	251
7.5 Effect of TRAIL on DCIS-associated myoepithelial cells .....	252
7.6 Clinical relevance of myoepithelial cell apoptosis .....	255
7.7 Down-regulation of galectin-7 in myoepithelial cells and its relationship to $\alpha\beta 6$ .....	255
7.8 Clinical impact of galectin-7 expression in DCIS-associated myoepithelial cells .....	257
7.9 Putative mechanisms to explain the impact of $\alpha\beta 6$ on inflammatory cell phenotype .....	258
7.9.1 Effect of $\alpha\beta 6$ on phenotype of T cells .....	258
7.9.2 Altered cytokine expression by myoepithelial cells .....	259
7.10 Strengths and Weaknesses of the Study .....	260
Chapter 8 Summary and Conclusion .....	262
8.1 Influence of DCIS-associated myoepithelial cell phenotype on inflammatory cell infiltrate .....	263
8.2 Impact of up-regulation of $\beta 6$ on DCIS-associated myoepithelial cells on T cell TRAIL levels.....	264
8.3 Role of T cells in progression of DCIS .....	264
8.4 Altered myoepithelial cell phenotype during DCIS .....	265
Chapter 9 Futures directions 9.0 Future directions.....	266
9.0 Future directions.....	267



References .....	269
Appendices .....	309
Appendix 1 .....	310
1.1 Mycoplasma PCR.....	310
1.4 Stacking gel .....	312
1.5 SDS-PAGE: Running buffer .....	313
1.6 SDS- PAGE: Transfer buffer.....	313
Appendix 2 .....	315
Source of reagents .....	315
Appendix3 .....	319
Presentations.....	319

## List of figures

---

Figure 1.1 Normal Breast Histology H&E Stain .....	3
Figure 1. 2 The cancer hallmarks.....	4
Figure 1.3 Column VIII of The Edwin Smith Surgical Papyrus, a copy of the first document believed to describe cancer of the breast.....	8
Figure 1.4 Progression of DCIS to invasive breast cancer.....	16
Figure 1.5 Schematic diagram of microenvironmental alterations during breast cancer progression.....	20
Figure 1.6 Myoepithelial cells in normal and DCIS ducts. ....	27
Figure 1.7 Key morphological changes exhibited in apoptosis and necrosis .....	50
Figure 1.8 The extrinsic and intrinsic apoptosis pathways .....	53
Figure 2.1 Scheme depicting preparation and purification of breast cell types.....	66
Figure 2.2 Scheme depicting investigation of the interaction between myoepithelial cells and the inflammatory infiltrate <i>in vivo</i> . ....	68
Figure 2.3 NDP Image software .....	76
Figure 2.4 Process Image Software.....	77
Figure 2.5 Imagescope software .....	80
Figure 2.6 Measuring DCIS duct size.....	82
Figure 2.7 Co-culture of myoepithelial cells with Jurkat or Primary T cells.....	88
Figure 3.1 Representative images of DCIS with myoepithelial cells homogenously negative (A) or positive (B) for $\alpha\beta6$ integrin.....	109
Figure 3.2 Representative images of CD69 staining in DCIS cases .....	111
Figure 3.3 CD69+ve cells in DCIS in relation to myoepithelial $\alpha\beta6$ status.....	112
Figure 3.4 Representative images of CD4 staining in DCIS cases .....	114
Figure 3.5 Quantification of CD4+ve cells around DCIS ducts in relation to $\alpha\beta6$ expression .....	115
Figure 3.6 Representative images of FOXP3+ve cells in DCIS cases.....	117
Figure 3.7 FOXP3+ve cell density in DCIS microenvironment in relation to $\alpha\beta6$ expression .....	118
Figure 3.8 Representative IHC images of CD8+ve cells in DCIS .....	120
Figure 3.9 CD8+ve cell density in DCIS in relation to $\alpha\beta6$ expression.....	121
Figure 3.10 Representative IHC images of CD45RO in DCIS.....	123
Figure 3.11 CD45RO+ve cell density in DCIS microenvironment in relation to $\alpha\beta6$ status .....	124
Figure 3.12 Representative images of MHCII+ve cells in DCIS microenvironment in relation to $\alpha\beta6$ status.....	126
Figure 3.13 MHC-II+ve cell in DCIS microenvironment in relation to $\alpha\beta6$ status .	127
Figure 3.14 Representative images of CD74+ve cell in DCIS cases.....	129
Figure 3.15 CD74+ve cell infiltration in DCIS microenvironment in relation to $\alpha\beta6$ expression .....	130
Figure 3.16 Representative images of CD68+ve cells in DCIS stroma in relation to $\alpha\beta6$ status .....	132

Figure 3.17 CD68+ve cells in DCIS microenvironment in relation to $\alpha\beta6$ expression .....	133
Figure 3.18 Representative images of arginase-1+ve cells in DCIS stroma in relation to $\alpha\beta6$ status .....	135
Figure 3.19 Arginase-1+ve cells in DCIS microenvironment in relation to $\alpha\beta6$ expression .....	136
Figure 3.20 Percentage of inflammatory cell populations in the peri-ductal microenvironment of DCIS in relation to $\alpha\beta6$ status .....	138
Figure 3.21 Representative images of CD4+ve cells in Matrigel plugs..... خطأ! الإشارة المرجعية غير معرفة.	
Figure 3.22 CD4+ve cells in Matrigel plugs containing myoepithelial cells.....	141
Figure 3.23 Representative images of FOXP3+ve cells in Matrigel plugs.....	143
Figure 3.24 Distribution of FOXP3+ve cells in Matrigel plugs containing myoepithelial cells .....	144
Figure 3.25 Representative images of CD8+ve cells in Matrigel plugs.....	146
Figure 3.26 Distribution of CD8+ve cells in Matrigel plugs .....	147
Figure 3.27 Representative images of CD74+ve cells in Matrigel plugs assays .....	149
Figure 3.28 Density of CD74+ve cell in Matrigel plugs.....	150
Figure 3.29 Representative images of arginase-1+ve cells in matrigel plugs.....	152
Figure 3.30 Density of arginase+ve cell in Matrigel plugs.....	153
Figure 4.1 Measurement of TRAIL levels in Jurkat T cells and primary T cells co-cultured with $\beta4$ or $\beta6$ myoepithelial cells for 48 hrs	166
Figure 4.2 RNA expression of DR4 in myoepithelial cells .....	168
Figure 4.3 RNA expression of DR5 in myoepithelial cells .....	168
Figure 4.4 A: Detection of apoptosis by cleaved PARP in $\beta4$ and $\beta6$ myoepithelial cells exposed to TRAIL .....	170
Figure 4.4 B: Detection of apoptosis by cleaved PARP in $\beta4$ and $\beta6$ myoepithelial cells exposed to TRAIL.....	171
Figure 4.5 A: Induction of morphological changes in $\beta4$ and $\beta6$ myoepithelial cell lines on exposure to etoposide chemotherapy.....	172
Figure 4.5 B: Induction of morphological changes in $\beta4$ and $\beta6$ myoepithelial cell lines on exposure to etoposide chemotherapy.....	173
Figure 4.5 C Induction of morphological changes in $\beta6$ myoepithelial cell lines on exposure to etoposide chemotherapy. ....	174
Figure 4.6 Representative example of caspase-3 immunohistochemistry staining in $\alpha\beta6$ +ve DCIS case with high peri-ductal infiltration of Treg cells.....	176
Figure 5.1 Galectin-7 expression in normal mammary gland and skin tissue.....	187
Figure 5.2 Immunohistochemical staining of DCIS for Galectin 7 and $\alpha\beta6$ .....	189
Figure 5.3 Immunohistochemical staining of DCIS for Galectin 7 and $\alpha\beta6$ .....	190
Figure 5.4 Analysis of galectin-7 and $\alpha\beta6$ expression in DCIS cases .....	191
Figure 5.5 Analysis of Galectin-7 in myoepithelial cell lines.....	193
Figure 5.6 Knockdown of galectin-7 in primary myoepithelial cells .....	194
Figure 5.7 Knockdown of galectin-7 in primary myoepithelial cells at extended time-points.....	195
Figure 5.8 Analysis of $\beta6$ expression following knockdown of galectin-7 in primary myoepithelial cells .....	195
Figure 5.9 Knockdown of galectin-7 in $\beta4$ cells for 24hrs .....	198
Figure 5.10 Knockdown of galectin-7 in $\beta4$ cells for 48hrs .....	198
Figure 5.11 Knockdown of galectin-7 in $\beta4$ myoepithelial cells at 24 hrs .....	199

Figure 5. 12 Knockdown of galectin-7 in  $\beta$ 4 myoepithelial cells at 48 hrs ..... 199

Figure 5. 13 Detection of apoptosis by cleaved PARP in $\beta$ 4 cells exposed to TRAIL following knockdown of galectin-7 .....	200
Figure 5. 14 Induction of morphological changes in $\beta$ 4 cells treated with G7 siRNA (A) or control siRNA (B) on exposure to etoposide .....	201
Figure 5. 15 Measurement of the area of ducts in DCIS cases where the ducts are positive or negative for galectin-7 .....	203
Figure 5. 16 Measurement of area of ducts in DCIS cases where the ducts are positive or negative for $\alpha\beta$ 6 .....	204
Figure 5. 17 Measurement of size of ducts in DCIS cases where the ducts are positive or negative for both galectin-7 and $\alpha\beta$ 6 or positive for one and negative for the other .....	205
Figure 6.1 Expression of CD3 in Jurkat T cells.....	217
Figure 6.2 Representative dot plot of CD3 expression in primary T cells.....	218
Figure 6.3 Expression of CD4 in the primary T cells .....	219
Figure 6.4 Representative dot plot of CD4 expression in Jurkat T cells.....	220
Figure 6.5 Expression of CD8 in primary T cells .....	221
Figure 6.6 Expression of CD8 in Jurkat T cells .....	222
Figure 6.7 Representative dot plots of CD4 expression in primary T cells co-cultured with $\beta$ 4 or $\beta$ 6 myoepithelial cells for 24hrs .....	224
Figure 6.8 Expression of CD4 in primary T cells co-cultured with $\beta$ 4 or $\beta$ 6 cells for 48 hrs.....	225
Figure 6.9 Expression of CD4 in primary T cells co-cultured with $\beta$ 4 or $\beta$ 6 cells for 72 hrs.....	226
Figure 6.10 Representative dot plots of CD4 expression in Jurkat T cells co-cultured with $\beta$ 4 or $\beta$ 6 myoepithelial cells for 24hrs .....	228
Figure 6.11 Expression of CD4 in Jurkat T cells co-cultured with $\beta$ 4 or $\beta$ 6 myoepithelial cells for 48 hrs.....	229
Figure 6.12 Expression of CD4 in Jurkat T cells co-cultured with $\beta$ 4 or $\beta$ 6 myoepithelial cells for 72 hrs.....	230
Figure 6.13 Representative dot plots for expression of CD8 in primary T cells co-cultured with $\beta$ 4 or $\beta$ 6 myoepithelial cells for 24 hrs .....	232
Figure 6.14 Representative dot plots for expression of CD8 in primary T cells co-cultured with $\beta$ 4 or $\beta$ 6 myoepithelial cells for 48 hrs .....	233
Figure 6.15 Representative dot plots for expression of CD8 in primary T cells co-cultured with $\beta$ 4 or $\beta$ 6 myoepithelial cells for 48 hrs .....	234
Figure 6.16 Expression of CD8 in Jurkat T cells co-cultured with $\beta$ 4 or $\beta$ 6 myoepithelial cells for 24 hrs.....	236
Figure 6.17 Expression of CD8 in Jurkat T cells co-cultured with $\beta$ 4 or $\beta$ 6 myoepithelial cells for 48 hrs.....	237
Figure 6.18 Representative dot plots of expression of CD8 in Jurkat T cells co-cultured with $\beta$ 4 or $\beta$ 6 myoepithelial cells for 72 hrs .....	238
Figure 6.19 Cytokines expressed in $\beta$ 4 and $\beta$ 6 myoepithelial cells .....	240
Figure 6.20 Cytokine profile released by $\beta$ 4 and $\beta$ 6 myoepithelial cells.....	242
Figure 6.21 Influence of Jurkat T cells on cytokines expressed on myoepithelial cells.....	242

## List of Tables

---

Table 1.1 Distribution of histological types of breast disease .	6
Table.1. 2 Estimated risk of developing breast cancer by age	10
Table 1.3 High penetrance mutations predisposing to the development of breast cancer	13
Table 1.4 Low penetrance SNPs predisposing to the development of breast cancer...	14
Table 1.5 Phenotypic traits of normal human breast myoepithelial cells	21
Table 2.1 Details of patient demographics and pathology	62
Table 2.2 Details of patient demographics and pathology	63
Table 2. 3 Source and Characteristics of cells used in <i>in vitro</i> experiments.....	65
Table 2.4 Details of Antibodies for mouse tissue: working dilutions and antigen retrieval technique.....	73
Table.2.5 Details of Antibodies for human tissue: working dilutions and antigen retrieval techniques	72
Table 2.6 Details of antibodies used in Western blot.....	92
Table 2.7 Recipe for the PCR mixture	95
Table 2.8 cDNA amplification programme	96
Table 2.9 Primary antibodies used for Flow cytometry	99
Table 5.1: Summary of case numbers with interpretable staining and other continuous attributes.....	206
Table 5.2 : Categorical pathological data relating to core biopsies with interpretable staining.....	207
Table 5.3 Relationship between $\alpha\beta6$ and ER	208

## Abbreviations

<b>A</b>	<b>Details</b>
AIF	Apoptosis inducing factor
AP	Alkaline phosphatase
AP-1	Activator protein-1
Apaf-1	Apoptosis activating factor-1
APC	Antigen presenting cell
$\alpha$ SMA	$\alpha$ Smooth muscle actin
<b>B</b>	
Bcl	B cell lymphoma
BM	Basement Membrane
BSA	Bovine serum albumin
<b>C</b>	
cDNA	Complementary DNA
COX2	Cyclooxygenase 2
CK	Cytokeratin
CRD	Carbohydrate recognition domain
CTLA4	Cytotoxic T lymphocyte antigen
CXCL	Chemokines (C-X-C motif) ligand

<b>D</b>	
DAB	3,3-diaminobenzidine tetrahydrochloride
DCIS	Ductal carcinoma in situ
DCs	Dendritic cells
DISC	death-inducing signalling complex
DMSO	Dimethylsulphoxide
<b>E</b>	
ECL	Enhanced chemiluminescence
ECM	Extracellular matrix
EDTA	Ethylenediamine tetraacetic acid
EGF	Epidermal growth factor
EGFR	Epidermal Growth Factor Receptor
EMT	Epithelial mesenchymal transition
EPIC	European Prospective Investigation of Cancer
ER	Estrogen Receptor
<b>F</b>	
FADD	Fas associated death domain
FCS	Foetal calf serum
FGF	Fibroblast growth factor
FITC	Fluorescein isothiocyanate
FOXP3	Forkhead box P3
FS	Forward scatter



<b>G</b>	
GAPDH	Glyceraldehyde3-phosphate dehydrogenase
G-CSF	Granulocyte colony stimulating factor
GM-CSF	Granulocyte-macrophage colony stimulating factor
<b>H</b>	
HC	Hydrocortisone
H&E	Haematoxylin and Eosin
Her2	Human Epidermal Growth Factor Receptor 2
HGF	Hepatocyte growth factor
HIF1 $\alpha$	Hypoxic inducible factor 1 $\alpha$
HRP	Horseradish peroxidase
HRT	Hormone Replacement Therapy
<b>I</b>	
IDC	Infiltrating Ductal carcinoma
IFN $\gamma$	Interferon gamma
IHC	Immunohistochemistry
IGF	Insulin-like growth factor
Ig	Immunoglobulin
iNOS	inducible nitric oxide synthesis
ILC	Invasive lobular carcinoma
IL	Interleukin
IL-1 ra	Interleukin-1 receptor antagonist

<b>K</b>	
Kda	Kilo dalton
<b>L</b>	
LAP-1	Latency-associated peptide-1
<b>M</b>	
MC	Medullary carcinoma
ME	Myoepithelial cells
MEGM	Mammary epithelial growth medium
MIF	Macrophage migration inhibitory factor
MHC II	Major histocompatibility complex class II
MMPs	Matrix metalloproteinase
mRNA	Messenger RNA
Myos	Myoepithelial cells

<b>N</b>	
NBF	Neutral buffered formalin
NF-Kb	Nuclear factor Kappa B
NFW	Nuclease free water
NK	Natural killer cells
NRS	Normal Rabbit serum
<b>O</b>	
OMM	Outer mitochondrial membrane
<b>P</b>	
PARP	Poly ADP-ribose polymerase
PBS	Phosphate buffered saline
PCR	Polymerase chain reaction
PE	Phycoerythrin
PFA	Paraformaldehyde
PI	Propidium iodide
PR	Progesterone Receptor
<b>Q</b>	
QMUL	Queen Mary University of London

<b>R</b>	
RANTES	Regulated upon Activation, Normal T-cell Expressed, and Secreted
RNA	Ribonucleic acid
rpm	Revolutions per minute
<b>S</b>	
SAGE	Serial analysis of gene expression
SDS	Sodium dodecyl sulfate polyacrylamide gel electrophoresis
STAT3	Signal transducer and activation of transcription 3
siRNA	Small interfering RNA
SS	Side scatter
<b>T</b>	
TAMs	Tumour associated macrophages
TBS	Tris buffered saline
TCR	T cell receptor
TDLU	Terminal duct lobular unit
TGF $\beta$	Transforming growth factor beta
Th	T helper cells
TNF $\alpha$	Tumour necrosis factor alpha
TRAIL	Tumour necrosis factor-related apoptosis-induced ligand
Treg	T regulatory cells
<b>U</b>	
<b>V</b>	
<b>W</b>	
<b>X</b>	
<b>Y</b>	
<b>Z</b>	

# **Chapter 1: Introduction**

# Introduction

---

## 1.1 The Breast

In simple terms the breast is a modified sweat gland, comprised of a lobular cluster of bilayered glands, known as acini, which have the potential to express milk, draining into bilayered ducts, distributed within a fibro-adipose stroma. The ducts branch repeatedly and ultimately give rise to the terminal ductal lobular units (TDLU) (Bissell, Radisky et al. 2002). Six to ten major ductal systems originate at the nipple. These ductal systems form independent but overlapping breast lobes, the size of which is variable. The terminal duct branches into a grapelike cluster of small acini to form a lobule. Each ductal system typically occupies over a quarter of the breast, and the systems extensively overlap each other.

In cross section, mammary ducts and lobules have a similar structure, with a lining of a single layer of epithelial cells, surrounded by a low, flattened discontinuous layer of contractile cells containing myofilaments (myoepithelial cells), which are separated from stroma by the basement membrane (Figure 1.1) (Ross 2006). In the larger ducts the luminal cells are columnar whereas in the smaller ducts the luminal cells are cuboidal. The luminal cells produce milk and myoepithelial cells assist in milk ejection during lactation (Ross 2006). The lobules are separated by moderately dense collagenous interlobular stroma, whilst the intralobular stroma surrounding the ducts within each lobule is less collagenous and more vascular. The amount of glandular tissue is controlled by progesterone and oestrogen secretion during

the menstrual cycle (Ferguson and Anderson 1981), pregnancy, lactation (Salazar, Tobon et al. 1975) and menopause (Huseby 1954).

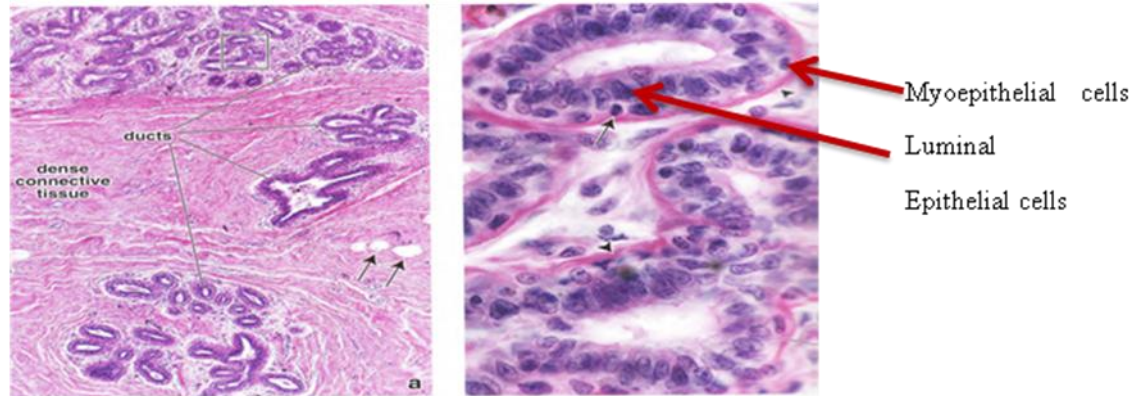


**Figure 1.1 Normal Breast Histology H&E Stain (Ross 2006)**

## 1.2 Cancer

Cancer is a disease in which a group of cells show uncontrolled growth, invasion of surrounding tissue and sometimes spread to other organs in the body, primarily through lymphatics or the blood stream. The hallmarks of cancer were described many years ago by Hanahan and his colleagues and they characterised cancer development by six features (Figure 1.2) (Hanahan and Weinberg 2000) . These processes are apoptosis evasion, self-sufficiency in growth signals, insensitivity to antigrowth signals, sustained angiogenesis, tissue invasion and metastasis, and limitless replicative potential. Several years later, other hallmarks have been added to describe the cancer cell state including DNA damage, oxidative stress, proteotoxic stress, mitotic stress, metabolic stress and immune surveillance evasion (Hanahan and Weinberg 2000). Recently, in 2010, instability of genes was presented by Negrini and his

colleagues as a further major factor involved in tumorigenesis (Negrini, Gorgoulis et al. 2010).

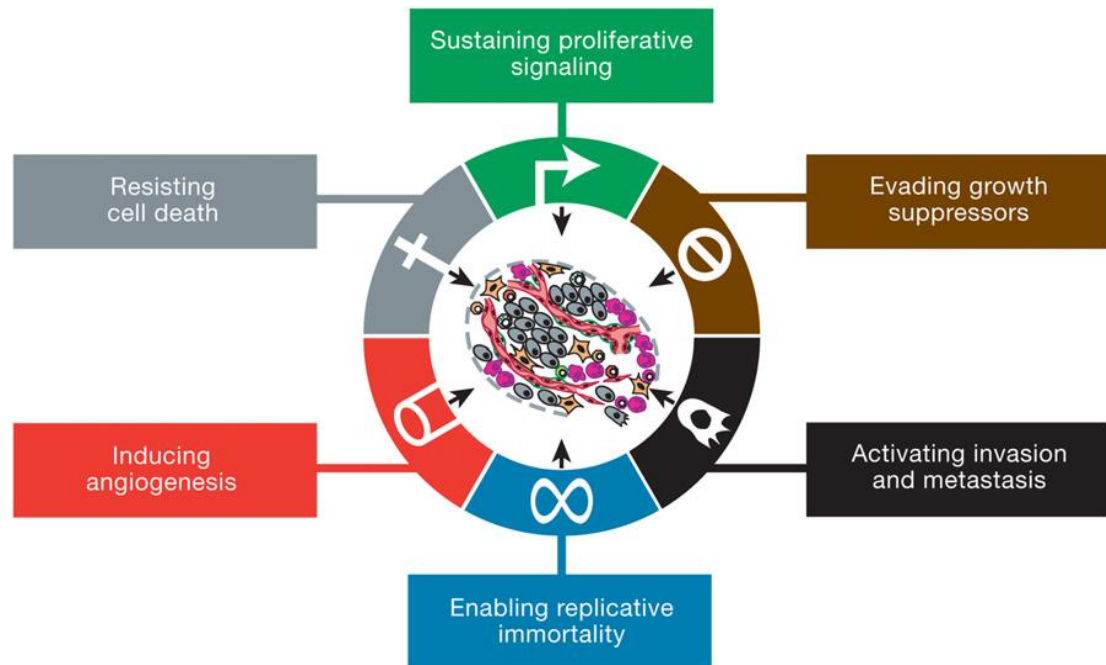


**Figure 1. 2 The cancer hallmarks**

The hallmarks that are involved in development of cancer (Hanahan and Weinberg 2000).

### 1.3Breast cancer

Breast cancer is the most frequent malignancy among women in Western countries and its incidence is still increasing. A number of factors are thought to contribute to this increase. Mammographic screening temporarily increased frequency by discovering incident, as well as prevalent cases. Higher exposure to risk factors for breast cancer, such as low and late parity, alcohol intake and use of hormonal replacement therapy could also contribute towards this increased incidence (MacMahon 2006). Depending on histological features, breast cancer can be classified into many subtypes. The first sub-classification is into pre-invasive versus invasive disease. Pre- invasive disease refers to a



neoplastic population that remains within the ductal-lobular framework and does not penetrate the surrounding stroma. This will be discussed in more detail below. Invasive disease is where the neoplastic population penetrates the basement membrane surrounding the ducts and lobules. Infiltrating ductal carcinoma (IDC) is the most common invasive breast cancer subtype, accounting for 70-80% of cases in most series (Kumar 2005). Infiltrating lobular carcinoma (ILC) is the second most common subtype accounting for ~10% of cases, with the so-called “special types” making up the remaining 10% of cases (Table 1.1). The importance of the morphological classification is that it impacts on patient prognosis, with IDC having poorest prognosis and the special types having a much better prognosis (Kumar 2005). More recently there has been an emerging molecular classification of breast cancer. This was first established by the report from Perou and his group (Perou, Sorlie et al. 2000), which used gene expression arrays to define an intrinsic molecular subtype classification of breast cancer. This identified four major classes, later expanded to six subtypes, shown to have a significant impact on prognosis. Most recently, this complexity has been further increased, with the description of 10 “integrated subtypes” of breast cancer with differing clinical behaviour emphasising the enormous heterogeneity of the disease (Curtis, Shah et al. 2012).

**Table 1.1 Distribution of histological types of breast disease (Kumar 2005).**

Total cancers	%
<b>In situ carcinomas</b>	15-30
Ductal carcinomas in situ	80
Lobular carcinomas in situ	20
<b>Invasive carcinomas</b>	70-85
Infiltrating ductal carcinoma	79
Infiltrating Lobular carcinomas	10
Tubular/cribriform carcinomas	6
Mucinous (colloid)	2
Medullary carcinomas	2
Papillary carcinomas	1
Metaplastic carcinomas	<1

### 1.3.1 History of breast cancer

The story of breast cancer is illustrated in the acts and artefacts of the human fight against illness. It is an epic tale that describes the concepts of disease from the work of evil spirits to the results of specific physical factors, and the healing arts from mysticism to modern science tools. The first reference to breast cancer was possibly written by Imhotep, the physician –architect in Egypt in the 30<sup>th</sup> century and is included in The Edwin Smith Surgical Papyrus as an incomplete and fragmented copy of the original document (figure 1.3) (Breasted JH 1930). This text provides the earliest references to suturing of wounds and cauterization with fire drills. Moreover, it includes the diagnosis and treatment of eight cases of breast cancer. Between 460-375 BC, Hippocrates describes some cases of breast cancer in detail. One of these cases was a woman who had breast carcinoma associated with bloody nipple discharge. He noted that when the discharge stopped the patient died so he concluded that there was a beneficial effect of the bloody discharge. Also he

linked menstrual cessation with breast cancer and sought to restore the menstrual cycle in young sufferers. His description of the course of advancing breast cancer sounds true today (De Moulin 1983). The invention of the microscope led to significant progress in breast histopathology. Johannes Muller (1801-1859) is the first one who reported that cancers are composed of living cells. Also, he noted the similarity of cells of primary breast cancer and its metastasis to the ribs, and that cancer cells had lost the characteristics of the normal cells. William S. Halsted, Professor of Surgery at Johns Hopkins Hospital in Baltimore (1852-1922), performed an operation which later became known as the radical mastectomy to treat breast cancer (Banks 1882). As the nineteenth century came to a close, the mastectomy seemed better than no treatment (Donegan 2002). Modified radical mastectomy was applied in the late 1940s (Patey and Dyson 1948). Moreover, in the 1970s, a more limited surgical option came into use, focusing on removal of the tumor and a small amount of surrounding tissue known as lumpectomy. In 1985, the lumpectomy combined with radiation therapy became the accepted surgical approach (Cotlar, Dubose et al. 2003). Landmark advances in the diagnostic fields include the use of ultrasound started in the late 1970's to aid differentiation between solid lesions and fluid-filled cysts. More recently, Magnetic Resonance Imaging (MRI) was optimized and annual MRI is now recommended by the American Cancer Society for women at high risk for breast cancer, but it is an expensive procedure and only available in larger cities (Saslow, Boetes et al. 2007). In addition, in 1895, discovery of X-ray led to mammography and formed the basis of radiotherapy for breast cancer. Radiotherapy was applied by Herman Goeth in Hamburg and Emile Herman

Grubbe in Chicago to treat cancer (De Moulin 1983). Endocrine surgery was replaced by hormonal treatment by Henry Starling in 1905, then by pharmacological methods of decreasing oestrogen secretion or its effects. Discovery of the oestrogen receptor (ER) in breast cancers by Elwood Jensen in Chicago in 1967 was another landmark in hormone therapy, differentiating the patients who could respond to this treatment from those could not (Jensen . 1967). However, as medicine and science reach the third millennium, breast cancer remains a daunting problem, but it is becoming more clearly defined than ever before as the tools of the modern science are used to gain better understanding of the disease.

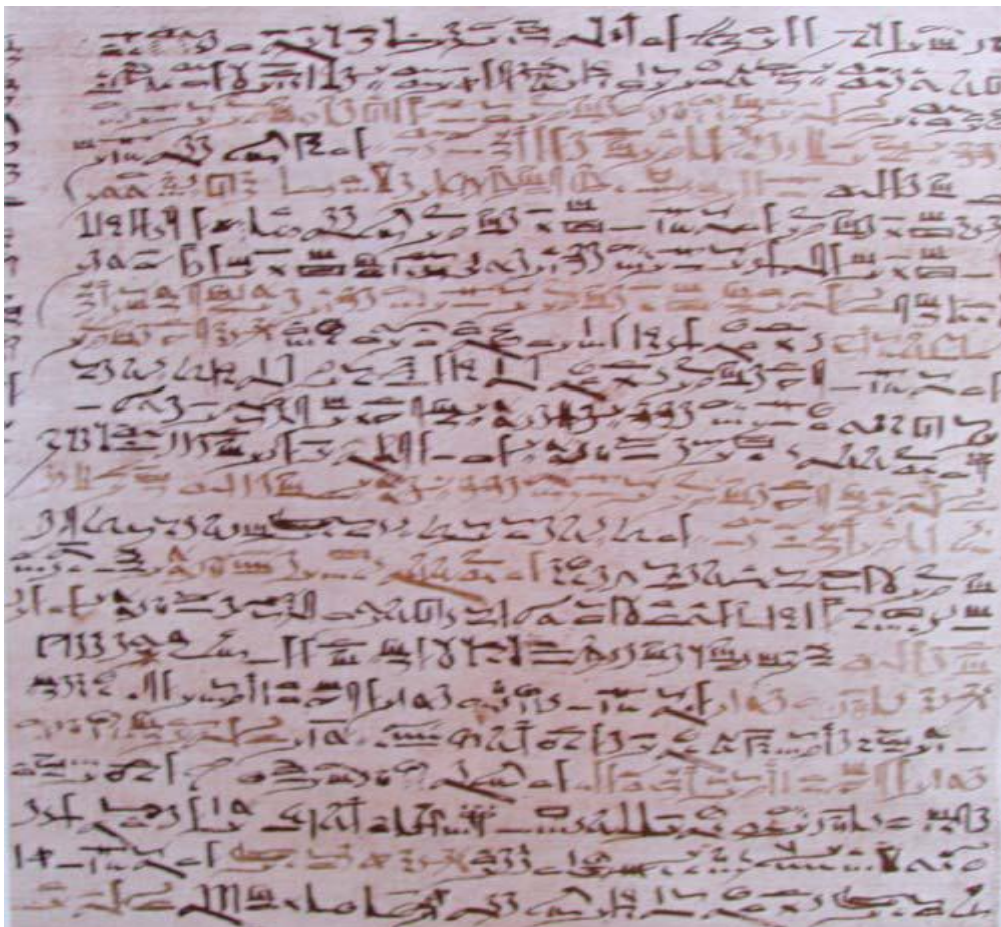


**Figure 1.3** Column VIII of The Edwin Smith Surgical Papyrus, a copy of the first document believed to describe cancer of the breast, circa 3000 BC. (Breasted, 1930).

### **1.3.2 Geographic variation**

Worldwide, every year more than a million people are diagnosed with breast cancer which accounts for 23% of all new cases of cancer in women and 10% of all new cases of cancers overall (Ferlay, Parkin et al. 2010). The incidence varies considerably worldwide with the highest rate in North America. Conversely, Africa and Asia show the lowest rates of breast cancer (Ferlay, Parkin et al. 2010). Around 332,670 of new cases of breast cancer occur each year in Europe and 182,460 in the USA (Ferlay, Parkin et al. 2010). The risk of breast cancer increases in women who migrate from low to high risk countries suggesting a strong role for environmental or lifestyle factors (Ziegler, Hoover et al. 1993, Deapen, Liu et al. 2002).

### **1.3.3 Risk factors**

There are many factors that influence the risk of breast cancer such as age, hormones, alcohol, obesity, physical activity and reproductive history.

### **1.3.4 Age**

Age is the strongest risk factor for breast cancer development in which the risk is increased with advancing age (Table 1.2). This estimate is based on data for 2008 in the UK (Sasieni, Shelton et al. 2011).

Table.1. 2 Estimated risk of developing breast cancer by age (Sasieni, Shelton et al. 2011)

Estimated risk at birth up to and including:	UK (2008)
Age 29	1 in 2,000
Age 39	1 in 215
Age 49	1 in 50
Age 59	1 in 22
Age 69	1 in 13
Lifetime risk	1 in 8

### 1.3.5 Reproductive history

The rise in breast cancer in developed countries is partly explained by the fact that women in these countries have, on average, fewer children and limit the period of lactation. A study suggested that breast cancer can be reduced by more than half from 6.3% to 2.7% by increasing duration of breast feeding from 8 months to 24 months for each child (Collaborative Group on Hormonal Factors in Breast 2002).

A meta-analysis study showed that the risk of breast cancer is 4% lower for every 12 months of breastfeeding (Collaborative Group on Hormonal Factors in Breast 2002). An estimated 3% of female breast cancers in the UK are linked to women breastfeeding each of their children for fewer than 6 months (Parkin 2011). Among BRCA1 mutation carriers, meta-analysis study showed that breast cancer risk may be lower in those breastfeeding for at least 12-24 months. This study also demonstrated that the risk of breast cancer in BRCA2 mutation carriers is not associated with breastfeeding (Pan, He et al. 2014).

### **1.3.6 Age of menarche**

The risk of breast cancer has consistently been associated with younger age at menarche. Estimates show the risk is decreased by 22% per five years delay in menarche (Garcia-Closas, Brinton et al. 2006).

### **1.3.7 Age at menopause**

Early menopause reduces the risk of breast cancer. Pre-menopausal women have a higher risk of breast cancer than women who have undergone menopause at the same age and with the same childbearing pattern. Risk rises by 3% for each year older at menopause (natural or induced by surgery) (Collaborative Group on Hormonal Factors in Breast 2012).

### **1.3.8 Hormones**

#### **I. Endogenous**

The risk of breast cancer increases with higher level of endogenous hormones. Many studies have demonstrated that post-menopausal women with the highest levels of oestrogen and testosterone have 2-3 times the risk of women with the lowest levels (Key, Appleby et al. 2002). However, the relation between hormones levels and pre-menopausal breast cancer risk is less defined (Kaaks, Berrino et al. 2005, Eliassen, Missmer et al. 2006). Also higher levels of prolactin hormone are associated with an increased risk, especially for oestrogen-receptor-positive tumours (Tworoger, Eliassen et al. 2007). Furthermore, higher levels of insulin have been connected to elevated risk of breast cancer in postmenopausal women not taking hormone replacement therapy (Gunter, Hoover et al. 2009). This link between breast cancer and

insulin level might clarify the 20% raised risk of breast cancer in diabetic women (Larsson, Mantzoros et al. 2007). Moreover, insulin-like growth factor 1 level shows a positive correlation with breast cancer risk (Key, Appleby et al. 2010).

## **II. Exogenous**

### **a) Oral contraceptives**

Use of the oral contraceptive is associated with an increased risk of breast cancer (Rosenberg, Boggs et al. 2010).

### **b) Hormone Replacement Therapy (HRT)**

There is a 66% increased risk of breast cancer in women currently taking HRT compared to non users. This elevated risk is seen with use of oestrogen-progesterone therapy rather than oestrogen only. In 2003, a study demonstrated that 20,000 extra breast cancer cases had arisen in women aged 50-64 years in the UK over the previous decade due to use of HRT and three-quarters of these cases were as a result of oestrogen-progesterone HRT use (Beral 2003).

## **1.3.9 Breast density**

Breast density is considered a strong and independent risk factor for breast cancer (Oza and Boyd 1993, Tamimi, Byrne et al. 2007). Normal breast is composed of fat, connective tissue and epithelial tissue. Low breast density is formed of a high proportion of fatty tissue. The risk of breast cancer is five times higher in women with >75% dense breast tissue compared to women with <10% dense tissue (McCormack and dos Santos Silva 2006). There are many factors that influence breast density such as menopausal status, weight



and number of children but the most important factor is inheritance (Boyd, Dite et al. 2002) .

### 1.3.10 Family history

The risk of breast cancer is doubled in women with one affected first-degree relative (mother or sister) compared to a women with no family history of the disease (Pharoah, Day et al. 1997). The risk also is higher if the relative is diagnosed under the age of 50 years. Mutations in the breast cancer susceptibility genes BRCA1 and BRAC2 account for the majority of families that have four or more affected members and about 2% of all breast cancers (Peto 2001). Women carrying these mutations have a 45-65% chance of developing the disease by the age of 70 (Antoniou, Pharoah et al. 2003). A number of other high prevalence susceptibility genes have been described, (Table 1.3) and altogether account for ~ 20-25% of breast cancers. More recently, a series of low prevalence SNP's conferring low-level risk for breast cancer also have been described (Table 1.4) (Mavaddat, Antoniou et al. 2010).

**Table 1.3 High penetrance mutations predisposing to the development of breast cancer (Mavaddat, Antoniou et al. 2010)**

LOCUS	GENE	SYNDROME	RR
17q21	BRCA1	BRCA1	5-45
13q12.3	BRCA2	BRCA2	9-21
17p13.1	TP53	Li-Fraumeni	2-10
10q23.3	PTEN	Cowden	2-10
19p13.3	STK11	Peutz-Jegher	2-10
16q22.1	CDH1		2-10

**Table 1.4 Low penetrance SNPs predisposing to the development of breast cancer (Mavaddat, Antoniou et al. 2010)**

LOCUS	GENE	VARIANT	RR
10q26	FGFR2	rs2981582	1.26
16q12	TOX3	rs3803662	1.20
5q11	MAP3K1	rs889312	1.13
8q24	FAM84B/c-MYC	rs13281615	1.08
11p15	LSP1	rs3817198	1.07
3p24	NEK10/SLC4A7	rs4973768	1.11
17q23.2	COX11	rs6504950	0.95
10p14	CASP8	rs1045485	0.88
2q35	TNP1/IGFBP5/2/TNS1	rs13387042	1.12
1p11.2	NOTCH2/FCGR1B	rs11249433	1.14
14q24.1	RAD51L1	rs999737	0.84
5p12	MRPS30/FGFR10	rs10941679	1.19
6q25	ESR1	rs2046210	1.29

### 1.3.11 Physical activity

Studies conclude that there is 15- 20% risk reduction among women with the highest category of physical activity (Monninkhof, Elias et al. 2007). The link is clearer for post-menopausal women. The influence of physical activity on breast cancer risk might be explained by how it affects hormone levels. A recent European Prospective Investigation of Cancer (EPIC) research study illustrated lower levels of oestrogen and testosterone in post-menopausal women with high levels of physical activity (Chan, Dowsett et al. 2007).

### 1.3.12 Alcohol consumption

A significant association between alcohol consumption and breast cancer has been shown by epidemiological studies (Baan, Straif et al. 2007). Analyses included 58 515 women with invasive breast cancer and 95 067 controls from 53 studies. These studies showed that daily consumption of about 50 g of

alcohol is associated with a relative risk of about 1.5 compared with that in non-drinkers (Hamajima, Hirose et al. 2002). The relationship between alcohol consumption and breast cancer was studied in 1.905 invasive breast cancer cases in related to different subtypes of breast cancer. This demonstrated that the risk increased steadily with increasing amount of alcohol consumption for ER+ and PR+ cancers but not for ER- and PR- cancer (Falk, Maas et al. 2014).

## **1.4 Ductal carcinoma in situ (DCIS)**

Ductal carcinoma in situ (DCIS) is the earliest clinical diagnosis of breast cancer and is usually detected through mammographic screening that identifies areas of calcification in the breast. This type of breast cancer is considered to be a pre-invasive neoplastic proliferation of cells within the ductal-lobular structures of the breast that does not penetrate the myoepithelial- basement membrane interface (figure 1.4). In the symptomatic setting, it accounts for 3-5% of cancers, but in the screening setting it accounts for up to 30% of cases (Ernster, Barclay et al. 2000).

According to epidemiological, histopathological and genetic studies, there is evidence that supports the concept that DCIS represents the precursor of invasive carcinoma in the majority of cases (Bombonati and Sgroi 2011). This model of progression of breast cancer has been refined, with columnar cell lesions and atypical ductal hyperplasia now being recognised as precursor lesions of low grade of DCIS (Schnitt 2003).

Because the aim of screening is to detect cancer as early as possible and treat so as to prevent life-threatening disease, it could be argued that DCIS represents the ideal stage to target to prevent invasive breast cancer. However,

the behaviour of DCIS is not clearly understood because opportunities to study its natural history are limited (Sanders, Schuyler et al. 2005), and it has been suggested that only 50% of cases will progress to invasive disease during the lifetime of a woman, though currently it is not possible to distinguish between those that will progress and those that will not (Collins, Tamimi et al. 2005).

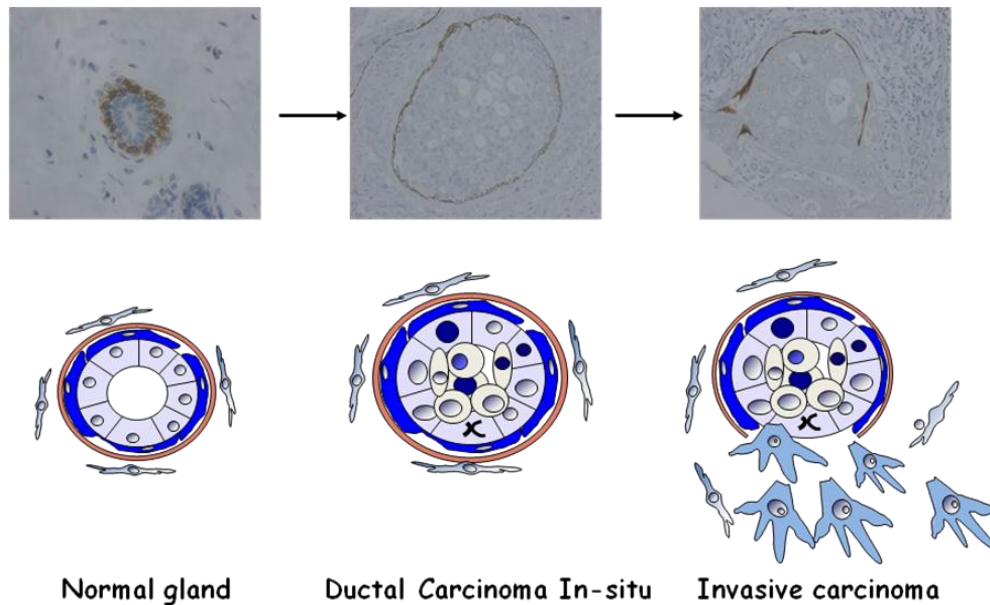


Figure 1.4 Progression of DCIS to invasive breast cancer (Allen, Thomas et al. 2014)

## 1.5 Classification of DCIS

DCIS is a heterogeneous disease that shows a variation in its clinical manifestation, morphology and biological behaviour. Many histological classification systems have been developed based on growth pattern, nuclear morphology and presence or absence of necrosis, in different combinations (van Dongen, Holland et al. 1992). In the UK, the National Coordinating Group for Breast Screening Pathology has proposed a classification system based on an assessment of nuclear pleomorphism and on the frequency of mitoses within the luminal cells. This classification defines low, intermediate

and high grade DCIS. Low grade DCIS is composed of small regular cells, usually with cribriform or micropapillary architecture and infrequent mitosis while high grade is composed of large, pleomorphic cells associated with frequent mitosis, also often showing a solid architecture with necrosis. The intermediate grade lesions present manifestations between low and high grade DCIS (Badve, A'Hern et al. 1998). Several studies have used biomarkers to identify different molecular subtypes of breast cancer (Perou, Sorlie et al. 2000, Curtis, Shah et al. 2012). Whilst mainly applied to invasive breast cancer, similar subtypes can be identified in DCIS, further supporting the heterogeneous nature of this disease (Tamimi, Baer et al. 2008, Clark, Warwick et al. 2011). Based on expression of oestrogen receptor (ER), progesterone receptor (PR), human epidermal growth factor receptor 2 (Her2) and cytokeratins, DCIS can be classified as: Luminal A (ER+/PR+/HER-), Luminal B (ER+/ PR+or-/HER2+), HER2 (ER-/PR-/HER2+), Triple Negative (ER-/PR-/HER2-) and basal (ER-/PR-/HER2-/CK5/6 and or CK14 and or EGFR-) so reflecting the major molecular subtypes of breast cancer (Clarke, Brunner et al. 1989, Livasy, Perou et al. 2007, Tamimi, Baer et al. 2008). There are some significant differences in the proportion of DCIS subtypes compared to invasive breast cancer (Clarke, Brunner et al. 1989), for example, according to some studies the basal-like phenotype is seen more frequently in invasive cancer than DCIS (Clarke, Brunner et al. 1989). Furthermore, HER-2 positive invasive breast cancer is less frequently identified than HER2 positive DCIS (Tamimi, Baer et al. 2008). The explanation for these differences is unclear but there is a proposal that either expression of HER2 is switched off during invasion or that HER2 positive DCIS cases frequently do not transform to

invasive cancer (Reis-Filho and Lakhani 2003). In current clinical practice, the molecular subtype classification is not applied to DCIS. In current clinical practice, treatment of DCIS is surgical with no routine adjuvant medical therapy. Indeed, most NHS units do not assess hormone receptor and Her2 receptor status in DCIS outside clinical trials. Whether this is best practice remains uncertain. Chemopreventive trials such as international Breast Cancer Intervention Study IBIS-I, in which patients diagnosed with DCIS were randomized to 5yrs adjuvant tamoxifen or no tamoxifen indicates that tamoxifen does reduce the incidence of recurrent invasive and non-invasive (ie DCIS) breast cancer, so it could be argued that knowing the subtype of DCIS could influence treatment, however, this does not yet appear to have become accepted clinical practice (Sestak, Kealy et al. 2012). Whether trials such as LORIS, which aims to randomize patients with non-high grade DCIS to surgery or surveillance, will open the way to medical treatment of DCIS, dependent on the subtype characteristics, remains to be seen.

## **1.6 Progression of DCIS to invasive cancer**

There are few opportunities to observe the natural history of DCIS but those limited studies that report on long-term follow up of DCIS provide an interesting insight (Sanders, Schuyler et al. 2005). There are two different models that have been described to explain the transition of DCIS to invasive carcinomas. The first model suggests that the progression of DCIS to invasive breast cancer (IBC) is a multistep process in which tumour progression follows a linear pattern - known as the theory of linear progression (Bodian, Perzin et al. 1993, Dupont, Parl et al. 1993, Lakhani, Chaggar et al. 1999). In this model it is suggested that low-grade DCIS progresses to high-grade DCIS and then to

invasive breast carcinoma (Bodian, Perzin et al. 1993, Dupont, Parl et al. 1993, Lakhani, Chaggar et al. 1999). The second model, known as the theory of parallel disease, suggests that low grade-DCIS tends to develop into low-grade invasive breast cancer. This theory implies commitment of a subtype of DCIS to a specific subtype of invasive breast cancer. The second model is supported by chromosomal-alteration studies along with data that shows that during the progression of DCIS to invasive disease, the grade of DCIS corresponds to the grade of the subsequent invasive breast cancer (Stratton, Collins et al. 1995, O'Connell, Pekkel et al. 1998, Hwang, DeVries et al. 2004, Irvine and Fentiman 2007). Clearly, the idea that both theories are mutually exclusive may represent an oversimplification (Wiechmann and Kuerer 2008). Several studies have compared gene expression and genetic profile between DCIS and its invasive counterpart (Krop, Sgroi et al. 2001, Ma, Salunga et al. 2003, Porter, Lahti-Domenici et al. 2003, Chin, de Solorzano et al. 2004). In general, these studies have failed to show consistent changes between in-situ and invasive disease and suggest that all the genetic changes associated with invasive breast cancer are already present at the DCIS stage. This has focussed attention on potential changes in the microenvironment that may contribute to development of invasive disease.

## **1.7 DCIS microenvironment**

The role of the microenvironment in invasive breast cancer has received much attention but there has been less focus on what role the microenvironment might play in DCIS. The DCIS microenvironment is complex, with contributions from myoepithelial cells, as well as stromal fibroblasts, blood vessels and the immune cells (Figure 1.5) (Polyak and Kalluri 2010).

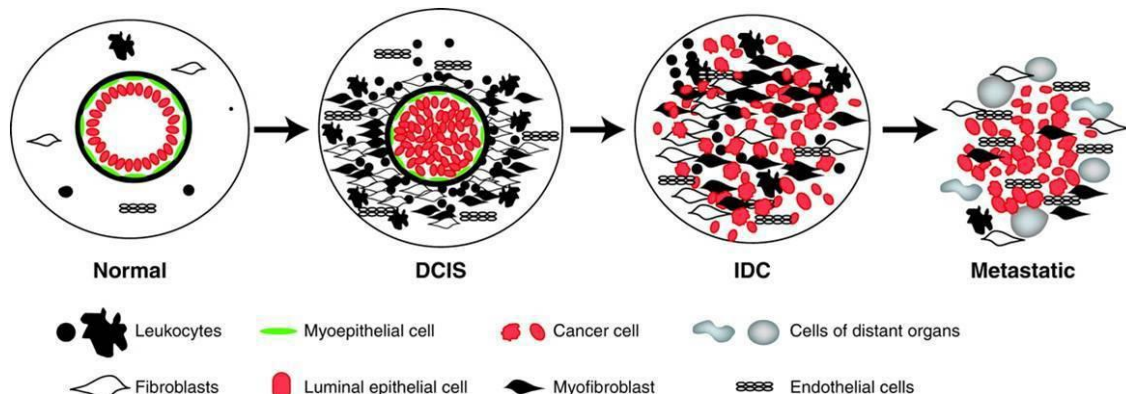


**Figure 1.5 Schematic diagram of microenvironmental alterations during breast cancer progression (Polyak and Kalluri 2010)**

Normal breast ducts are composed of the basement membrane (BM) and an inner layer of luminal epithelial cells in contact with an outer layer of myoepithelial cells. Cells composing the stroma include various leukocytes, fibroblasts, myofibroblasts, and endothelial cells. In DCIS, the myoepithelial cells are epigenetically and phenotypically altered. The number of stromal fibroblasts, myofibroblasts, lymphocytes, and endothelial cells increases as tumour progresses, although the degree of this is tumour subtype-specific.

## 1.8 Myoepithelial cells

In the normal breast the myoepithelial cells provide the major interface with basement membrane (BM). They attach to the basement membrane via hemidesmosomes and to the adjacent luminal epithelial and myoepithelial cells by desmosomes (Glukhova, Koteliansky et al. 1995). The myoepithelial cells are spindle-shaped cells oriented parallel to the long axis of mammary ducts as a continuous layer (Adriance, Inman et al. 2005).

### 1.8.1 Markers of myoepithelial cells

The presence of myoepithelial cells is frequently used as a marker of benign disease in the breast and as such there are continued efforts to identify specific markers that differentiate between luminal epithelial cells and myoepithelial cells in the normal resting human breast using different techniques (Table 1.5). Microarray studies have indicated that 42 genes can distinguish luminal and myoepithelial cells in the breast tissue (Jones, Mackay et al. 2004).



**Table 1.5** Examples of genes expressed by normal myoepithelial cells contributing to their tumour-suppressor phenotype.

Myoepithelial markers	References
CK5	(Nagle, Bocker et al. 1986)
Galectin-7	(Jones, Mackay et al. 2004)
CK14	(Dairkee, Blayney et al. 1985)
CK17	(Guelstein, Tchypysheva et al. 1988)
BG3C8	(Ronnov-Jessen, Van Deurs et al. 1992)
Vimentin	(Mork, van Deurs et al. 1990)
GFA	(Moll 1993)
$\alpha$ -Smooth muscle actin	(Gordon, Mulligan et al. 2003)
Smooth muscle-MHC	(Lazard, Sastre et al. 1993)
Calponin	(Lazard, Sastre et al. 1993)
CALLA	(Gusterson, Monaghan et al. 1986)
Thy-1	(Gudjonsson, Ronnov-Jessen et al. 2002)
P-cadherin	(Rasbridge, Gillett et al. 1993)
$\alpha$ 1 integrin	(Lazard, Sastre et al. 1993)
$\alpha$ 6 integrin	(Natali, Nicotra et al. 1992)
$\beta$ 4 integrin	(Koukoulis, Howeedy et al. 1993)
Connexin-43	(Wilgenbus, Kirkpatrick et al. 1992)
bFGF	(Gomm, Smith et al. 1991)
Laminin	(Rudland, Hughes et al. 1989)
Maspin	(Zou, Anisowicz et al. 1994)
Methallothionein	(Schmid, Ellis et al. 1993)
Calcium binding protein A2 (S100A2) SPARC	(Jones, Mackay et al. 2004)

## 1.8.2 Function of myoepithelial cells in normal breast

During development, myoepithelial cells act to induce luminal cell polarity (Runswick, O'Hare et al. 2001, Gudjonsson, Ronnov-Jessen et al. 2002), and to regulate ductal morphogenesis (Niranjan, Buluwela et al. 1995); here, connection to the BM and the desmosomal interactions with epithelial cells facilitate paracrine regulatory functions.

During lactation, myoepithelial cells contract in response to oxytocin and push milk to the ducts (Hamperl 1970), and gap junctions and cadherin-based interactions connecting myoepithelial cells function to coordinate the ejection of milk smoothly (Monaghan, Clarke et al. 1996). In addition, myoepithelial cells play a key role in synthesis of BM components such as collagen IV, laminin-1, laminin-5 and fibronectin that regulate ductal growth (Warburton, Mitchell et al. 1982). They further facilitate the remodeling of BM through the production of matrix metalloproteinases (MMPs), including MMP2 and MMP3 (Dickson and Warburton 1992).

Normal myoepithelial cells have been shown to exhibit a tumour suppressor action. For example, they express many ECM structural proteins, proteinase inhibitors and angiogenic inhibitors (Sternlicht, Safarians et al. 1996, Barsky 2003). Myoepithelial cell also express a number of type II tumour suppressor genes such as CK5, maspin,  $\alpha 6$  integrin and  $\alpha$  smooth muscle actin ( $\alpha$  SMA) (Sager 1997, Bissell and Radisky 2001). The first functional assays were carried out by Barsky and co-workers and demonstrated that myoepithelial cells exhibit many anti-tumourigenic properties, such as the ability to inhibit tumour cell invasion and angiogenesis (Sternlicht, Safarians et al. 1996,

Nguyen, Lee et al. 2000). Further studies using myoepithelial cell lines derived from canine tumours revealed that myoepithelial conditioned media inhibited the growth of breast cancer cells (Shao, Nguyen et al. 1998).

### **1.8.3 Role of myoepithelial cells in breast cancer**

In general, it is believed that myoepithelial cells rarely become malignant (Lakhani and O'Hare 2001). Luminal and myoepithelial cells are different in their capacity for DNA repair, and this contributes to the lower rate of transformation in myoepithelial cells (Angele, Jones et al. 2004). Moreover, when myoepithelial cells do undergo transformation, they usually form benign or low-grade neoplasms. They express many ECM structural proteins, proteinase inhibitors and angiogenic inhibitors, which may explain in part why these lesions are generally not invasive (Sternlicht, Safarians et al. 1996, Barsky 2003). However, there is growing evidence that myoepithelial cells change in DCIS.

Despite the fact that the myoepithelial layer remains largely intact in DCIS, the cells appear to differ from normal myoepithelial cells in gene expression (figure 1.6). Polyak and her team used SAGE (serial analysis of gene expression) to identify differences between normal myoepithelial cells and DCIS myoepithelial cells. They found that DCIS-associated myoepithelial cells exhibited the greatest change in gene expression of all cells in DCIS, including up-regulation of certain chemokines such as CXCL14 (Allinen, Beroukhim et al. 2004). This suggests that although myoepithelial cells are present, they may no longer send the correct signals to epithelial cells. One study found that myoepithelial cells derived from breast carcinoma express no or low level of laminin-1, and that these purified myoepithelial cells were

unable to polarize epithelial cells in three-dimensional collagen assays. This suggests that cancer associated myoepithelial cells may fail to transmit the necessary signals to produce proper epithelial cell polarity due to their inability to induce laminin-1 (Gudjonsson, Ronnov-Jessen et al. 2002).

A study carried out by Man et al (2007) aimed to identify the steps involved in development from normal breast through hyperplasia, in-situ disease to invasive cancer; they suggest that breast cancer invasion is triggered by a multi-step process of events targeting the microenvironment. They proposed that internal or external injuries such as trauma, inflammation or exposure to some chemicals result in disruption of the myoepithelial cell layer with subsequent infiltration of inflammatory cells. These inflammatory cells lead to further degeneration of the myoepithelial cells and basement membrane resulting in a gap that allows direct contact between the tumour cells and stromal cells. This gap in the myoepithelial cell layer is proposed to lead to a localized loss of tumour suppressors and paracrine inhibitory function, a local increase in oxygen level, nutrients and growth factors, and a focal increase of inflammatory cell infiltration, resulting in substantial changes in the micro-environment that ultimately facilitate cell proliferation.

Furthermore, direct contact between the luminal cell clusters and stromal cells stimulates the production of tenascin and other invasion-associated molecules that lead to tissue remodelling, angiogenesis and epithelial mesenchymal transition (EMT), offering a favourable micro-environment for invasion and proliferation (Man 2007). Work in our lab has shown that one of the most consistent changes in myoepithelial cells in DCIS is up-regulation of the integrin  $\alpha\beta 6$ . Normal myoepithelial cells do not express this integrin, but it is

induced in ~60% of DCIS cases with no evidence of invasion, and in >90% of cases of DCIS which is associated with established invasion. 69% of high grade DCIS cases were positive for  $\alpha\beta6$  expression, while 52% of non-high grade DCIS showed positivity for  $\alpha\beta6$  expression (Allen, Thomas et al. 2014).  $\alpha\beta6$  integrin is an epithelial-specific integrin and is a receptor for the extracellular matrix (ECM) proteins fibronectin (Weinacker, Chen et al. 1994), vitronectin (Huang, Wu et al. 1998), and tenascin (Yokosaki, Monis et al. 1996). It also binds to latency-associated peptide 1 (LAP-1), a protein which maintains TGF $\beta$  in its inactive form. On binding to  $\alpha\beta6$ , latent TGF $\beta$  becomes activated (Munger, Huang et al. 1999).  $\alpha\beta6$  integrin expression levels are low in normal healthy epithelia but are up-regulated in association with wound healing and inflammation. Suppression of the  $\beta6$  integrin in mice has demonstrated its role in down-regulation of inflammation in skin and the respiratory tract (Huang, Wu et al. 1996).

In addition,  $\alpha\beta6$  plays a significant role in the migration of keratinocytes (Huang, Wu et al. 1996). Moreover, it has been reported that  $\alpha\beta6$  is up regulated in several invasive cancers such as oral squamous cell carcinoma and colonic cancer (Bates, Bellovin et al. 2005, Thomas, Nystrom et al. 2006). Many studies have indicated that  $\alpha\beta6$  integrin may promote cancer progression by regulating expression of matrix metalloproteinases (MMPs) and activation of TGF- $\beta$ 1 (Agrez, Chen et al. 1994, Dixit, Chen et al. 1996, Li, Yang et al. 2003, Janes and Watt 2004, Morgan, Thomas et al. 2004, Thomas, Nystrom et al. 2006). It also is suggested to play a role in inducing tumour tolerance as a recent study has shown that there is a positive correlation between the number of Treg cells and the levels of  $\alpha\beta6$  in colorectal cancer

(Yang, Du et al. 2012) . In addition,  $\alpha\beta6$  integrin converts the precursor TGF $\beta$  to active TGF- $\beta$  in dendritic cells (DCs), which converts immature DCs to tolerogenic DCs (Chen, Yao et al. 2011). Tolerogenic DCs generates Treg cells (Li, Guo et al. 2008). Loss of  $\alpha\beta6$  leads to inflammation by impairing the immune-suppressive activity of Treg cells (Munger, Huang et al. 1999). Thus, there is a body of evidence linking expression of  $\alpha\beta6$  to a shift in the inflammatory microenvironment towards a more pro-tumourigenic phenotype.

The role of the myoepithelial cell in the process of tumour progression and invasion is still incompletely understood, but there is emerging evidence, as cited above, to indicate that their phenotype becomes altered in DCIS, and this may lead to acquisition of a pro-invasive phenotype. When invasive carcinoma is established there are few myoepithelial cells detectable, a characteristic that is sometimes used in clinical practice to confirm invasive phenotype. What happens to the myoepithelial population is unknown: it is possible the population is simply overgrown by the expanding tumour population, however, it may be that loss of the myoepithelial population is achieved through other mechanisms such as apoptosis, and factors leading to myoepithelial cell apoptosis may be contributory to the transition on in-situ to invasive disease.

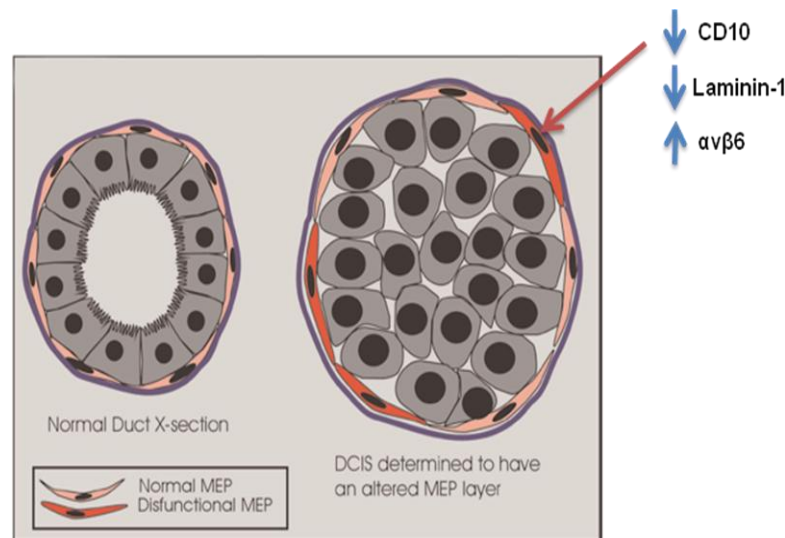


**Figure 1.6 Myoepithelial cells in normal and DCIS ducts (Adriance, Inman et al. 2005) .**

In DCIS, the myoepithelial cell layer remains intact, however, they exhibit an altered phenotype, including down-regulation of CD10 and laminin-1, and up-regulation of  $\alpha v \beta 6$  integrin.

## 1.9 Immune system

Structurally, the immune system is a collection of tissue, organs, circulatory cells and molecules (Charles 2001). Immune cells are produced and mature in primary lymphoid organs such as the bone marrow and thymus. They are transported via lymphatic and blood vessels to peripheral tissues or secondary lymphoid organs such as the lymph nodes or spleen. Functionally, the immune system is responsible for the location and removal of pathogens from the body. This system is divided into two categories; the innate system and adaptive system.

The innate immune system functions as a host defence in the early stages through nonspecific recognition of pathogens, induction of adaptive immune responses and determination of the type of adaptive response (Janeway 1998). The main function of adaptive system is specific recognition of pathogen resulting in induction of pathogen- specific long-term memory (Charles 2001).

The adaptive system includes two types of cells: T cells and B cells. The innate system includes macrophages, natural killer cells (NK) and dendritic cells (DCs).

## **1.10 Overview of immune cell function in cancer**

In general, the relationship between cancer and inflammation can be classified into two categories: an intrinsic pathway and an extrinsic pathway. The intrinsic pathway is mediated by genetic events that induce inflammation and neoplasia (Mantovani, Allavena et al. 2008). These events include the activation of different types of oncogenes by mutation, rearrangement or amplification of genes and inactivation of tumour-suppressor genes. Cells that are altered in this manner induce inflammatory mediators resulting in generation of an inflammatory microenvironment in tumours without an underlying inflammatory condition, such as in breast cancer (Mantovani, Allavena et al. 2008). In contrast, in the extrinsic pathway, inflammatory or infectious conditions enhance the risk of cancer development. Both pathways lead to activation of transcription factors, mainly Nuclear Factor Kappa B (NF- $\kappa$ B), signal transducer and activation of transcription 3 (STAT3) and hypoxia-inducible factor 1  $\alpha$  (HIF-1 $\alpha$ ), in tumour cells. These transcription factors coordinate the production of inflammatory mediators including cytokines, chemokines and cyclooxygenase 2 (COX2). Moreover, these factors are responsible for the recruitment and activation of various leukocyte populations (Mantovani, Allavena et al. 2008). The cytokines activate transcription factors in inflammatory cells, stromal cells and tumour cells leading to more inflammatory mediators being induced and the cancer-inflammatory microenvironment is generated (Mantovani, Allavena et al. 2008).



## **1.11 Inflammation and cancer: progression versus elimination**

The immune system has a dual role in cancer. It has the ability to inhibit tumour growth by killing cancer cells, for example, through the cytotoxic effect of CD8 T cells (Nosho, Baba et al. 2010). It also can promote tumour growth via proliferation of T regulatory cells (Treg) in the cancer microenvironment that can suppress the cytotoxic activity of CD8 T cells (Wang and Wang 2007).

### **1.11.1 Anti-tumour response of immune cells**

In colorectal cancer, tumour-infiltrating CD8 T cells are thought to have an important role in the elimination of cancer cells, and CD8 T cells are associated with good prognosis for colorectal cancer patients (Nosho, Baba et al. 2010). Activated CD4 T helper cells are classified into Th1 or Th2. Th1 cells secrete  $\text{IFN}\gamma$ ,  $\text{TGF}\beta$ ,  $\text{TNF}\alpha$  and IL-2. These cytokines collaborate with CD8 cytotoxic functions (Romagnani 1997). Moreover, Th1 CD4 cells can enhance the antitumor immune response via secretion of  $\text{IFN}\gamma$ , which in turn induces cytotoxic activity of macrophages (Stout and Bottomly 1989).

### **1.11.2 Pro-tumour response of immune cells**

Th2 CD4 T cells and T regulatory cells function together to repress CD8 cytotoxicity and to induce pro-tumoural polarization of innate immune responses such as polarization of tumour associated macrophages (TAMS) through secretion of cytokine such as IL-4, IL-3, IL-6, IL-10 and IL-13 (Parker 1993). T regulatory cells normally function to protect tissue from autoimmune disease and express CD4, CD25 and FOXP3 molecules (DeNardo and

Coussens 2007). Dendritic cells (DCs) influence the function of other immune cell functions by expression of transforming growth factor beta (TGF $\beta$ ) which has the ability to convert naive CD4 T cells to FOXP3 CD4 CD25 + Treg cells (Coombes, Siddiqui et al. 2007). Moreover, DCs express retinoic acid, which plays a critical role in the induction of Treg cells (Salagianni, Lekka et al. 2011). A recent study showed that interleukin (IL) - 10 produced by DCs is involved in tumour tolerance by promoting Treg cell development (Augier, Ciucci et al. 2010). CD25+CD4+ Treg cells have been used to suppress autoimmune reactions (Suri-Payer, Amar et al. 1998) and inflammatory bowel disease (Coombes, Robinson et al. 2005), while removal of CD25+CD4+ Treg cells results in enhanced resistance to tumours (Ko, Yamazaki et al. 2005), and increases the response to foreign antigens (Pasare and Medzhitov 2004). In fact, it has been proposed that depletion of Treg cells could be used as a therapeutic strategy for cancer (Salagianni, Lekka et al. 2011).

## **1.12 The role of the immune system in breast cancer**

In breast cancer, the role of the immune system is also paradoxical, being described both as pro-tumour and anti-tumor. Activation of different pathways results in a complex cascade of signalling which can affect the inflammatory response. Also these pathways are affected by environmental factors and other tumour derived stimuli. Immunohistochemical studies have shown that T lymphocyte infiltration is more extensive in higher grade DCIS and invasive carcinoma (Wong, Staren et al. 1998), while B cells were the dominant lymphocyte population in non-malignant breast lesions and in DCIS,

suggesting that a B-cell response may occur early in tumor development. (Coronella-Wood and Hersh 2003). In breast cancer the percentage of Treg cells, as evaluated by the presence of FOXP3, increases in parallel with cancer stage, from normal to DCIS and from DCIS to invasive carcinoma (Bates, Bellovin et al. 2005). The presence of large numbers of FOXP3 positive cells in invasive carcinoma is associated with poor relapse-free survival. The CD4+ CD25+ FOXP3+ Treg has the ability to inhibit CD4+ CD25- T cells, CD8+ T cells, natural killer cells and B cells in a cell-cell contact dependent manner (Chen 2006).

Infiltrating inflammatory cells are also involved in later stages of tumour progression where they are thought to play a role in promoting progression to invasion and metastasis. One mechanism by which this can occur is the induction of epithelial to mesenchymal transition (EMT) in breast cancer cells by infiltrating T lymphocytes (Santisteban, Reiman et al. 2009). A recent study has demonstrated a direct link between inflammation and breast tumourgenesis including an epigenetic switch induced by NF- $\kappa$ B and IL6 in tumour epithelial cells leading to an increasingly malignant phenotype (Iliopoulos, Hirsch et al. 2009). The study has shown the link between these molecules using MCF-10A cells as a model, and then subsequently demonstrating that the activation signature is also present in primary human breast tumours so implicating IL6-STAT3 signalling in breast cancer (Iliopoulos, Hirsch et al. 2009).

B-lymphocytes are recognized as contributing to anticancer immune responses via their secretion of antigen-specific immunoglobulin. Chronic activation of B cells may, paradoxically, play a role in potentiating carcinoma development.

During breast carcinogenesis, mature B cells (including naive cells and activated cells) can be found in secondary lymphoid tissues as well as in tumour-associated stroma. Furthermore, data from retrospective studies examining the percentage of B cells present in sentinel and axillary lymph nodes of breast cancer patients reveal that their presence and/or maturation immunoglobulin (IgG+) correlates with advanced disease stage and total tumour burden (Wernicke 1975, Morton, Ramey et al. 1986) . A study conducted by Urdiales- Viedma and his colleagues report the immunohistochemical detection of IgA, IgG and IgM in axillary lymph nodes from 50 unselected ductal breast carcinomas, and found that lymph nodes with IgG+ lymphoid follicles and/or metastatic lymph nodes with IgM+ lymphoid cells were significantly related to breast tumours of high histological grade and with more than three lymph node metastases (Urdiales-Viedma, Nogales-Fernandez et al. 1986). Also B cells present in breast tumour-associated stroma may have a role in disease progression. Approximately 20% of invasive breast cancers contain high numbers of B cells, and when present, these cells can comprise up to 60% of the neoplasia- associated lymphocyte population (Coronella, Telleman et al. 2001).

### **1.13 T lymphocytes**

T cells are a sub-group of lymphocytes involved in the immune response (Hahn and Kaufmann 1981). Their production begins in fetal life, and is maintained throughout adult life by the bone marrow, and they are mobilized to the thymus for differentiation (Guidos 2006, Schwarz and Bhandoola 2006). The differentiation process is continued in peripheral tissues and results in

production of various sub-groups of T lymphocytes that have different functions (Miller 1961) .

### **1.13.1 CD69 T cells**

CD69 is an early membrane receptor transiently expressed on activated T cells, not detected in resting lymphocytes, and selectively expressed in chronic inflammatory infiltrates (Sancho, Gomez et al. 2005). Its expression is associated with production of Th1 T cell cytokines, including IL-2, TNF- $\alpha$  and interferon- $\gamma$  (IFN $\gamma$ ) (Ziegler, Ramsdell et al. 1994, Rutella, Rumi et al. 1999). It also has been shown that CD69 cells can promote Transforming growth factor beta (TGF- $\beta$ ) production in CD4 and CD8 T cells, NK cells and macrophages (Esplugues, Sancho et al. 2003, Sancho, Gomez et al. 2003). Moreover, TGF- $\beta$  synthesis is dependent on extracellular-signal-regulated kinases (ERK) activation (Grewal, Mukhin et al. 1999), and CD69 mediates ERK activation (Zingoni, Palmieri et al. 2000).

#### **1.13.1.1 The role of CD69 T cells in malignancy**

CD69 antibody increases the cytotoxic activity of host NK cells, mediated by reduction of TGF $\beta$  (Esplugues, Vega-Ramos et al. 2005).

Moreover, CD69 antibody can stimulate the production of interleukin-2 (IL-2), which leads to T-cell proliferation (Cebrian, Yague et al. 1988, Testi, Phillips et al. 1989), and tumour necrosis factor-a (TNF-a) synthesis (Santis, Campanero et al. 1992, Sancho, Santis et al. 2000). Anti-CD69 increases secretion of nitric oxide (NO) by monocytes (De Maria, Cifone et al. 1994). CD69 also can trigger apoptosis in different types of cells including monocytes and eosinophils (Ramirez, Carracedo et al. 1996, Walsh, Williamson et al.

1996), and might mediate inhibitory signals to the IL-1 receptor (IL-1R) or on CD3 T cells proliferation (Cosulich, Rubartelli et al. 1987).

In lung cancer, a study has shown that accumulation of CD69+ve T cells is associated with the metastatic phenotype. (Wald, Izhar et al. 2006, Han, Guo et al. 2009). Thus, immune activation in tumour microenvironments may result in immune tolerance (Zhao, Kuang et al. 2012).

In contrast, lower numbers of CD69+ T cells are retrieved from the tumour-associated colonic mucosa compared to unaffected mucosa (Svensson, Olofsson et al. 2012). In addition, in ovarian cancer, the presence of CD69+ve cells is associated with an increase in survival (Yacyshyn, Poppema et al. 1995), and a study has shown that tumour-infiltrating activated CD4+CD69+ T cells are associated with a good prognosis in head and neck squamous cell carcinoma (Badoual, Hans et al. 2006).

### **1.13.1.2 Role of CD69+ cells in breast cancer**

Little is known about the role of CD69+ve cells in breast cancer, however, a positive correlation has been found between the presence of CD69+ cells and survival in patients with invasive breast cancer (Yacyshyn, Poppema et al. 1995).

### **1.13.2 CD4 T cells**

CD4 cells are a sub-group of T lymphocytes that are important for maintaining self-tolerance (Tai, Cowan et al. 2005). CD4 T cells are divided into two main categories: T helper 1 (Th1) and Th2 depending on the cytokines they produce in response to antigen activation. Th1 cells produce IL-2, IL-12 and IFN- $\gamma$  and

Th2 cells produce IL-4 and IL-5 (Swain, Bradley et al. 1991, O'Garra and Murphy 1994).

### **1.13.2.1 Role of CD4 T cells in immunity**

CD4 T cells play a key role in orchestrating the beginning and maintenance of the adaptive immune response (Gerlioni and Zanetti 2005). They have the ability to help antibody responses (Mitchison 1971) and they also help activation and expansion of CD8 cytotoxic cells (Keene and Forman 1982). CD4 T cells also regulate DCs to increase their ability to stimulate CD8 T cells (Bennett, Carbone et al. 1998, Ridge, Di Rosa et al. 1998, Schoenberger, Toes et al. 1998, Smith, Wilson et al. 2004): CD4 T cells release IL-2 that is critical to elicit the full response of CD8 T cells (Lai, Lin et al. 2009). Cytokines released by Th1 T cells regulate M1 macrophages, and subsequently enhance the cytotoxic activity of macrophages, whereas, Th2 cytokines stimulate the M2 macrophage phenotype is more frequently associated with solid tumors and thought to mediate an immunosuppressive effect (Leek, Hunt et al. 2000, Mantovani, Sica et al. 2007).

### **1.13.2.2 Role of CD4 T cells in cancer**

CD4 T cells play a dual role in tumour development and progression dependent on their phenotype, which is regulated both by the tumour and the tumour microenvironment (DeNardo, Barreto et al. 2009). They can act as tumour suppressive cells. Th1 cells repress tumour growth by release of IFN $\gamma$  and support cytotoxic T cells function, or as tumour promoting cells, including the function of Treg cells, that enhance tumour expansion by suppressing CD8 T cell and NK cell functions (Trzonkowski, Szmit et al. 2006). In sarcomas, one

study demonstrated that deficiency of CD4 T cells leads to enhanced tumour development (Koebel, Vermi et al. 2007).

In contrast, CD4 cells that express IL-17 regulate chronic inflammation and promote tumour progression when activated in the presence of TGF- $\beta$  and IL-6 or IL-23 (Dong 2008). Furthermore, a direct correlation has been demonstrated between the number of infiltrating CD4 T cells and shorter survival in renal cell carcinomas patients (Nakano, Sato et al. 2001).

### **1.13.2.3 Role of CD4 T cells in breast cancer**

In breast cancer, CD4 lymphocytes can directly enhance early tumour development by their expression of IL-13 (Aspord, Pedroza-Gonzalez et al. 2007). In addition, the extent of CD4 T cell infiltration in primary tumours has been shown to be associated with lymph node metastasis (Macchetti, Marana et al. 2006), and an unfavourable prognosis (Matkowski, Gisterek et al. 2009). Studies in mice have shown that IL-4 expression CD4 T cells promote invasion and metastasis of mammary adenocarcinoma to lung by regulating the phenotype and effector function of tumour-associated CD11b<sup>+</sup> Gr1-F4/80<sup>+</sup> macrophages, that in turn enhance metastasis through activation of epidermal growth factor receptor signalling in malignant mammary epithelial cells (DeNardo, Barreto et al. 2009).

This study also demonstrated that CD4 T cell in primary mammary carcinoma expressed Th2 cytokines such as IL-4 and IL-13 (DeNardo, Barreto et al. 2009). This is consistent with results of studies that have shown that CD4 T cells isolated from primary human breast cancer tissue produce high levels of cytokines of Th2 cell type including IL-4 and IL-13 (Aspord, Pedroza-



Gonzalez et al. 2007, Pedroza-Gonzalez, Xu et al. 2011). Tissue microarray analysis of primary breast cancer showed that high CD4 T cell density is associated with reduce overall survival of patients (DeNardo, Brennan et al. 2011).

### **1.13.3 FOXP3+ cells**

Forkhead box protein 3 (FOXP3) is a member of the forkhead family of transcriptional regulators and expressed by regulatory T cells (Treg cells) and plays a key role in regulating their immunosuppressive function (Fontenot, Gavin et al. 2003, Sakaguchi, Ono et al. 2006). FOXP3 is the only definitive marker of CD4+ CD25+ Treg cells (Hori, Nomura et al. 2003, Fontenot, Rasmussen et al. 2005). However, FOXP3 is not entirely specific for Treg cells since it can also be detected on tumour cells such as colorectal cancer (Kim, Grimmig et al. 2013), pancreatic cancer (Hinz, Pagerols-Raluy et al. 2007) and melanoma (Ebert, Tan et al. 2008).

#### **1.13.3.1 Role of FOXP3 T cells in cancer**

FOXP3-positive Treg cells have been identified in peripheral blood and in the tumours of patients with different types of cancer, including ovarian (Curiel, Coukos et al. 2004, Leffers, Gooden et al. 2009), pancreatic (Liyanage, Moore et al. 2002), gastric (Ichihara, Kono et al. 2003) and breast cancer (Bates, Fox et al. 2006). The abundance of FOXP3-positive Tregs in tumours has been positively correlated with poor prognosis (Curiel, Coukos et al. 2004, Bates, Fox et al. 2006). For example, Treg cells have been shown to be increased in tumour sites in non- small lung cancer and ovarian cancer and demonstrated to release TGF-  $\beta$  leading to inhibition of CD8 T cells in vitro (Woo, Chu et al.

2001). The presence of Treg cells in ovarian cancer is associated with reduced patient survival (Curiel, Coukos et al. 2004). However, some studies have reported that higher infiltration of Treg cells in tumour sites are a marker of good clinical outcome such as in colon (Correale, Rotundo et al. 2010) and ovarian (Leffers, Gooden et al. 2009) carcinomas. This contradictory evidence may be explained by differences in the size of the studies, with the latter being significantly larger.

### **1.13.3.2 Role of FOXP3+ cells in breast cancer**

High density of FOXP3 positive Treg cells in DCIS has been associated with increased risk of relapse, and in invasive breast cancer associated with both shorter relapse-free and overall survival (Bates, Fox et al. 2006). Furthermore, abundant FOXP3 positive cells in breast cancer were significantly correlated with high grade and large tumour size (Bohling and Allison 2008). In addition to their potential value in predicting tumour progression, FOXP3 expressing cells have been identified as a marker to monitor therapeutic response. For example, response to neoadjuvant chemotherapy in breast cancer is associated with the disappearance of tumour-infiltrating FOXP3 positive Treg cells (Ladoire, Arnould et al. 2008). Moreover, FOXP3 has been investigated as a therapeutic target, and it has been demonstrated that vaccination to eradicate FOXP3 positive cells in mice enhances tumour immunity (Nair, Boczkowski et al. 2007). Recently, tissue microarrays study has investigated the density of FOXP3+ve cells in tumour nests, in tumour-adjacent stroma, and in distant stroma of 1445 cases of well-characterised primary invasive breast carcinoma with long-term follow up. This demonstrated that the total number of FOXP3<sup>+</sup> cells was significantly correlated with higher tumour grade and ER

negativity. In addition, it showed that FOXP3 infiltration positively correlated with HER2 expression and basal phenotype subclass (Mahmoud, Paish et al. 2011).

### **1.13.4 CD8 T cells**

CD8 T lymphocytes mediate a central role of the immune system in protection against infection (Olson, McDonald-Hyman et al. 2013). The major cytokine pattern secreted by CD8 T cells is similar to Th1 set of cytokines (Kelso and Glasebrook 1984, Fong and Mosmann 1990). However, not all CD8 lymphocytes express Th1 like cytokines with some CD8 cells expressing both Th1 and Th2 cytokines (Paliard, de Waal Malefijt et al. 1988).

#### **1.13.4.1 Role of CD8 T cells in cancer**

Cytotoxic CD8 T cells have an important role in tumour specific cellular adaptive immunity that attacks tumour cells. They produce IFN $\gamma$  following interaction with their target tumour cells resulting in cell cycle inhibition, apoptosis, angiostasis and induction of macrophage tumouricidal activity (Dunn, Old et al. 2004, Smyth, Dunn et al. 2006).

Immunohistochemistry studies have shown that infiltration of CD8 T cell in the tumour microenvironment appears to have an anti-tumour effect as they are associated with good prognosis in tumours such as ovarian (Zhang, Conejo-Garcia et al. 2003, Sato, Olson et al. 2005), colon (Galon, Costes et al. 2006, Pages, Kirilovsky et al. 2009), oesophageal (Ashida, Boku et al. 2006), renal (Nakano, Sato et al. 2001), lung (Kawai, Ishii et al. 2008) and pancreatic (Fukunaga, Miyamoto et al. 2004) cancer.

#### **1.13.4.2 Role of CD8 T cells in breast cancer**

The infiltration of CD8 T cells has also been investigated in breast cancer. A retrospective cohort study of 1,334 patients with primary breast cancer diagnosed from 1987 to 1998 in the UK found that infiltration of CD8+ T cells was independently correlated with better survival (Mahmoud, Paish et al. 2011). Another study from Switzerland between 1985 and 1996 also reported an independent favorable prognostic effect of CD8 T cells, shown only with ER-negative breast cancer, while in ER-positive cases, CD8 T cells were associated with an unfavourable effect on outcome (Baker, Lachapelle et al. 2011). Furthermore, among 3403 breast cancer cases for which immunohistochemical results were obtained, CD8 T cells have shown to be an independent prognostic factor associated with better patients survival in basal-like breast cancer, but not in non-basal triple negative breast cancer or in other intrinsic molecular subtypes (Liu, Lachapelle et al. 2012).

#### **1.13.5 CD45RO+ cells**

CD45 leukocyte common antigen is a family of 180-220 KD transmembrane glycoproteins present in high abundance on the surface of all leukocytes (Thomas 1989). CD45 isoforms modulate lymphocyte activation, function and signal transduction in a variety of cell types, including NK cells (Mittler, Greenfield et al. 1987, Starling, Davidson et al. 1987), B cells (Mittler, Greenfield et al. 1987, Lin, Brown et al. 1992) and T cells (Ledbetter, Rose et al. 1985, Martorell, Vilella et al. 1987). The CD45RA and CD45RO isoforms identify functionally distinct "naive" and "memory" T cell subsets (Akbar, Salmon et al. 1991, Beverley 1992, Clement 1992).

T cells that express the RA phenotype are small, resting cells that release a limited repertoire of cytokines (Salmon, Kitas et al. 1989, Akbar, Salmon et al. 1991, Kristensson, Borrebaeck et al. 1992).

In contrast, T cells that express RO phenotype are larger, activated cells that express activation markers such as CD25 and secrete a wide repertoire of cytokines such as IL-2, IL-4, IL-5, IL-6, TNF and IFN- $\gamma$  (Akbar, Terry et al. 1988, Sanders, Makgoba et al. 1988, Salmon, Kitas et al. 1989, Wallace and Beverley 1990, Akbar, Salmon et al. 1991, Mackay 1991, Beverley 1992, Clement 1992, Kristensson, Borrebaeck et al. 1992, Plebanski, Saunders et al. 1992). CD45RO is considered as the most suitable single marker for memory T-cell populations in humans, which could represent the activation status of the T cells (Hotta, Sho et al. 2011). CD45RO T cells predominate in inflammation sites (Sterry, Bruhn et al. 1990), mucosal tissues (Harvey, Jones et al. 1989, Marathias, Preffer et al. 1991), and among the population of tumor infiltrating lymphocytes (Bukowski, Sharfman et al. 1991, Nguyen, Moy et al. 1993).

#### **1.13.5.1 Role of CD45RO+ cells in cancer**

In gastric and colorectal cancers, high density of CD45RO cells has been associated with an increased survival rate and acted as an independent prognostic factor (Pages, Berger et al. 2005, Galon, Costes et al. 2006, Lee, Chae et al. 2008, Pages, Kirilovsky et al. 2009). It also has been shown that the presence of CD45RO cells is significantly associated with improved prognosis, independent of pathologic and clinical parameters in colorectal cancer (Nosho, Baba et al. 2010).

### 1.13.5.2 Role of CD45RO+ cells in breast cancer

An immunohistochemistry study of 196 breast cancer cases has shown that the extent of CD45RO cells in invasive breast cancer is associated with an increased risk of recurrence and poor survival (Scholl, Pallud et al. 1994), and also has been shown to correlate with angiogenesis (Lee, Happerfield et al. 1997).

## 1.14 Macrophages

Macrophages are released into the circulation as monocytes, and within a few days they seed throughout the body tissues, including the spleen, which acts as a storage reservoir for immature monocytes (Geissmann, Manz et al. 2010). Macrophages are located throughout the body, where they ingest and process foreign materials, dead cells and debris and recruit additional macrophages in response to inflammatory signals (Murray and Wynn 2011). They are highly heterogeneous cells that can rapidly change their function in response to local microenvironmental signals (Murray and Wynn 2011).

Macrophages have been sub-classified into two categories, M1 and M2, or classically-activated and alternatively-activated cells (Gordon 2003, Mantovani, Sica et al. 2004, Mantovani, Sica et al. 2005). Interferon-gamma (IFN $\gamma$ ) is involved in induction of classical macrophage activation, which refers to the pro-inflammatory phenotype (M1), and is produced by activated Th1 T cells and NK cells (Schroder, Hertzog et al. 2004). The IL-12 produced by M1 macrophages can promote the differentiation of Th1 cells, which can in turn improve antigen phagocytosis (Benoit, Desnues et al. 2008, Cassol, Cassetta et al. 2010). M1 macrophages are strongly positive for Major

histocompatibility complex class II (MHC class II) and present antigen to T cells, and contribute to the killing of microorganisms and of tumour cells (Mantovani, Sica et al. 2004, Hao, Lu et al. 2012). This type is characterized by production of nitric oxide (Ho and Sly 2009), high level of IL-12 and IL-23 release but low levels of IL-10 (Gordon and Taylor 2005, Mantovani, Sica et al. 2005, Benoit, Desnues et al. 2008, Solinas, Germano et al. 2009)..

In contrast to M1 macrophages, the alternatively-activated phenotype releases anti-inflammatory molecules such as high levels of IL-10, with low levels of IL-12 and IL-23 (Condeelis and Pollard 2006, Solinas, Germano et al. 2009). In addition, IL-10 expressed by M2 macrophages can promote production of IL-4 and IL-13 by Th2 (Mantovani, Sica et al. 2009), and IL-4 is a major promoter of wound healing because it can activate arginase, which contributes to production of the extracellular matrix (ECM ) (Hao, Lu et al. 2012).

### **1.14.1 Macrophages in cancer**

Macrophages dominate tumour microenvironments where they play a key role in tumour growth (Balkwill, Charles et al. 2005). A body of research suggests that tumour associated macrophages (TAMs) are biased towards the M2 phenotype and exhibit pro-tumour functions, promoting tumour cell proliferation and survival (Mantovani, Sozzani et al. 2002, Biswas and Mantovani 2010).

The distribution of TAMs in most tumours such as breast, prostate, ovarian, cervical, lung carcinoma, and cutaneous melanoma is considered to be anti-inflammatory and is associated with poor prognosis (Hao, Lu et al. 2012).

Epidemiological studies have suggested that a macrophage-rich microenvironment will promote an aggressive tumour behaviour with a high metastatic potential (Nardin and Abastado 2008).

### **1.14.2 Macrophages in breast cancer**

Several studies, mainly focusing on invasive ductal breast carcinomas, have investigated the correlation between level of macrophage infiltration in the tumour microenvironment and disease progression. Clinical studies have reported a correlation between density of TAMs and poor prognosis for breast cancer (Goede, Brogelli et al. 1999, Leek, Landers et al. 1999, Leek, Hunt et al. 2000). High level of TAM infiltration is associated with a high tumour vascular density, suggesting a pro-angiogenic activity for TAM in invasive breast cancer (Leek, Lewis et al. 1996, Tsutsui, Yasuda et al. 2005). In addition, a high density of macrophage infiltration is positively correlated with poor prognostic features such as high tumor grade, low estrogen and progesterone receptor status and high mitotic activity (Volodko N 1998).

### **1.14.3 CD68+ macrophages**

CD68 expression increases markedly during differentiation of monocytes into macrophages (van der Kooij, von der Mark et al. 1997). CD68 is also expressed in cancer tissue such as melanoma and predicts a poor prognosis (Jensen, Schmidt et al. 2009).

#### **1.14.3.1 CD68 + macrophages in cancer**

In Hodgkin's lymphoma, high numbers of CD68+ macrophages have been correlated with a shortened progression-free survival and with increased disease relapse (Steidl, Lee et al. 2010). In addition, CD68+ macrophages



infiltration in melanoma is associated poor prognosis (Brocker, Zwadlo et al. 1988, Bernengo, Quaglino et al. 2000, Makitie, Summanen et al. 2001, Varney, Johansson et al. 2005).

### **1.14.3.2 CD68+ macrophages in breast cancer**

In breast cancers, high infiltration with CD68+ macrophages has been associated with higher tumour histological grade (Naukkarinen and Syrjanen 1990, Lee, Happerfield et al. 1997, Volodko N 1998), larger tumour size, necrosis and metastasis (Lee, Happerfield et al. 1997, Bolat, Kayaselcuk et al. 2006) and shown to predicate reduced relapse-free and overall survival (Leek, Lewis et al. 1996). Immunohistochemistry and tissue microarray studies have investigated the number, density and localization of CD68+ve macrophages in 1322 breast tumours. This demonstrated that the distant stromal macrophage count (infiltrating stroma away from the carcinoma, median count 14 cells) was higher than the intratumoural (median zero cells) and adjacent stromal macrophage count (median three cells). It also showed a significant association between the total number of macrophages and tumour grade, ER and PR negativity, HER-2 positivity and basal phenotype. In univariate survival analysis, density of CD68 macrophages was significantly associated with worse breast cancer-specific survival and shorter disease-free interval. However in multivariate model analysis, the CD68 macrophage number cannot be considered as an independent prognostic marker (Mahmoud, Lee et al. 2012).

### **1.14.4 CD74+ cells**

CD74 is a transmembrane glycoprotein that is associated with MHC class II and it regulates antigen presentation for the immune response (Zheng, Yang et al. 2012). It is expressed on antigen-presenting cells, including B cells, monocytes, dendritic cells and macrophages (Greenwood, Metodieva et al. 2012). CD74 acts as the high-affinity receptor for the pro-inflammatory cytokine macrophage migration inhibitory factor (MIF) (Leng, Metz et al. 2003).

#### **1.14.4.1 CD74+ cells in cancer**

CD74 expression has also been detected in some tumor cells. Its expression has been reported on malignant B-cells and the majority of cell lines derived from these cancers (Burton, Ely et al. 2004, Stein, Qu et al. 2004). It also has been observed in Multiple Myeloma plasma cells as well as multiple myeloma cell lines and it has been suggested that CD74 may be a novel and promising therapeutic target (Burton, Ely et al. 2004). Up-regulation of CD74 expression in gastric cancer has been reported and is associated with increasing clinical stage and again is suggested to offer an opportunity as novel gastric cancer chemoprevention and treatment approach. In pancreatic cancer, it also has been demonstrated that over-expression of CD74 is clearly associated with perineural invasion of pancreatic cancer and may be a useful prognostic factor (Nagata, Jin et al. 2009). CD74 expression also has been found in other tumours such as renal, thymic epithelial neoplasms and non-small lung cancer (Ioachim, Pambuccian et al. 1996, Young, Amin et al. 2001).

#### **1.14.4.2 CD74+ cells in breast cancer**

In invasive breast cancer, CD74 has been detected predominantly in triple negative cancers. Interestingly, its expression was significantly correlated with lymph node metastasis. In addition, CD74 expression was significantly related to a poor chemotherapy response in patients undergoing neoadjuvant chemotherapy (Tian, Zhang et al. 2012). Moreover, a study has shown that Stat1/CD74 positive triple- negative tumors are more aggressive and suggests this may be a targeted therapy for triple-negative breast cancer (Tian, Zhang et al. 2012).

#### **1.14.5 Macrophage inhibitory factor (MIF)**

MIF is a product of activated macrophages, which sustains macrophage survival and function (Mitchell, Liao et al. 2002). It regulates the expression of proinflammatory mediators by macrophages, and also is involved in T cell activation (Calandra, Bernhagen et al. 1994, Bacher, Metz et al. 1996). It is a proinflammatory cytokine and is expressed by several cells types such as T cells, B-lymphocytes, monocytes, macrophages, lung and gastrointestinal tissue (Calandra and Roger 2003).

##### **1.14.5.1 Role of MIF in cancer**

Overexpression of MIF has been reported in many types of tumours, including hepatocellular (Ren, Tsui et al. 2003), lung (Meyer-Siegler and Hudson 1996, White, Flaherty et al. 2003), cervical cancer (Ishigami, Natsugoe et al. 2001, Xu, Wang et al. 2008, McClelland, Zhao et al. 2009, Hertlein, Triantafillou et al. 2010, Cheng, Deng et al. 2011) prostate (Meyer-Siegler and Hudson 1996),

colorectal (He, Chen et al. 2009) and breast (Hagemann, Wilson et al. 2005) cancer.

Several studies have shown that MIF is linked to fundamental processes that control cell proliferation, differentiation, angiogenesis, tumor progression, and metastasis (Takahashi, Nishihira et al. 1998, Ogawa, Nishihira et al. 2000, Mitchell, Liao et al. 2002). For example, it has been reported that MIF can abolish the tumor suppressive activity of p53 (Hudson, Shoaibi et al. 1999). In colorectal cancer, the concentration of serum MIF was positively correlated with an increased risk of hepatic metastasis (He, Chen et al. 2009). In breast cancer, high MIF expression correlates with larger tumour size (Verjans, Noetzel et al. 2009).

#### **1.14.6 Arginase-positive macrophages**

The differential metabolism of L-arginine provides a means of distinguishing the two macrophage activation states (Hao, Lu et al. 2012) . In M1 cells, L-arginine is catabolised to nitric oxide ( NO) by up-regulation of inducible nitric oxide synthesis (iNOS) (Odegaard and Chawla 2008) , which is used to kill intracellular pathogens, while M2 macrophages produce arginase-1, which can metabolize arginine to ornithine and polyamines, which leads to collagen synthesis and cellular proliferation (Odegaard and Chawla 2008).

Interestingly, in an animal tumor model, the increase in NOS activity has been observed during tumor rejection, whereas the increase in arginase activity occurs during tumor growth (Mills, Shearer et al. 1992). These results suggest that L-arginine metabolism in macrophages at the tumor site, through the iNOS or arginase pathways, may have either pro-tumour or anti-tumour effects, based on which pathway is prevailing (Chang, Liao et al. 2001). This contention is

supported by the findings that the tumoricidal activity of macrophages is increased when transfected with the iNOS gene (Lorsbach, Murphy et al. 1993, Lala 1998, Xie and Fidler 1998). In addition, it was reported that arginase induction in macrophages can enhance tumor cell growth by providing them with polyamines and suppress tumor cytotoxicity by reducing NO production (Chang, Liao et al. 2001).

## **1.15 Apoptosis (programmed cell death)**

Cell death is a critical cellular process that has an important role in shaping tissues and organs during development and in regulating tissue homeostasis by eliminating unwanted or damaged cells. Cell death can be classified into regulated or un-regulated processes (Degterev and Yuan 2008). Regulated cell death is called apoptosis and reflects an active programme of cell death as result of specific cues and is executed by intrinsic cellular mechanisms (Degterev and Yuan 2008). The concept of apoptosis was described by plant biologists working on *Caenorhabditis elegans* in the early 1990s (Yuan and Horvitz 2004). In contrast, necrosis is a form of unregulated cell death that is caused by overwhelming stress that is incompatible with cell survival (Degterev and Yuan 2008). These two mechanisms have classically been considered as independent process (Zeiss 2003).

Apoptosis is an important phenomenon within biological systems and is the most common form of physiological cell death that can be initiated by exogenous and endogenous stimuli such as radiation, chemicals and oxidative stress, and defects in apoptosis have been implicated in diseases such as cancer, neurodegenerative and autoimmune disorders (figure 1.7) (Rastogi, Richa et al. 2009). It is an energy- dependent process that includes the activation of a set of

cysteine proteases (caspases) in a complex cascade of events. Apoptotic cells are morphologically characterised by cell shrinkage, nuclear fragmentation, chromatin and cytoplasmic condensation and cytoplasmic membrane blebbing with formation of apoptotic bodies (Majno and Joris 1995, Trump, Berezesky et al. 1997).

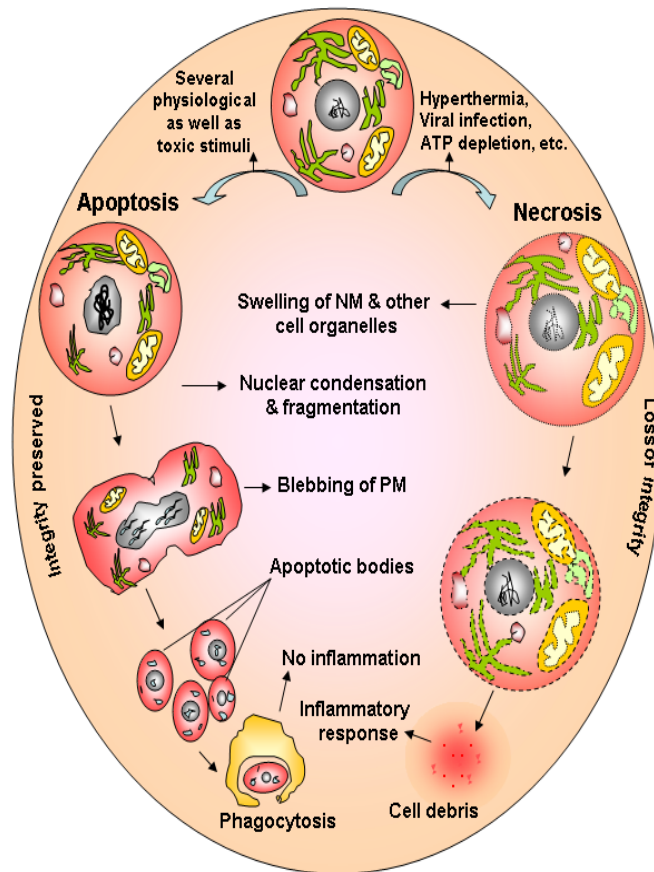


Figure 1.7 Key morphological changes exhibited in apoptosis and necrosis (Rastogi et al. 2009).

## 1.16 Mechanism of apoptosis

Apoptotic cell death is triggered by two signalling pathways; intrinsic (mitochondria-mediated) or extrinsic (receptor-mediated), both of which involve a number of different proteins (Rastogi, Richa et al. 2009).

### I. Extrinsic pathway

The extrinsic pathway is initiated by activation of cell surface death receptors such as TNF1 receptor, Fas, DR3, DR4 and DR5 (Haupt, Berger et al. 2003, Yan and Shi 2005, Elmore 2007). Ligands binding to these death receptors trigger the intra-cellular association of Fas associated death domain (FADD) with pro-caspase-8 forming the death-inducing signalling complex (DISC) (Boldin, Goncharov et al. 1996, Muzio, Chinnaiyan et al. 1996). This will result in activation of pro-caspase-8 (Walczak, Miller et al. 1999). Caspase-8 then activates the executioner caspases-3, -6 and -7 which are responsible for widespread proteolytic activity leading to the removal of the apoptotic cell by the immune system (Hengartner 2000).

### II. Intrinsic pathway

The signalling through this pathway of apoptosis is linked to permeabilization of the mitochondrial outer membrane (Green, Ferguson et al. 2009). The control and regulation of apoptotic mitochondrial events occurs through members of the Bcl-2 family of proteins (Cory and Adams 2002). The Bcl-2 super family act as sentinels of cell well-being that detect stress signals such as DNA damage, cytokine/growth factor withdrawal and anoikis (detachment induced cell death) (Borner 2003). They also ensure the completion of apoptosis by irreversible mitochondrial membrane damage (Newmeyer and

Ferguson-Miller 2003). The Bcl-2 family is classified into three functionally distinct groups governed by the number of BH domains present (Huang and Strasser 2000). The Bcl-2-like anti-apoptotic proteins (Bcl-2, Bcl-xL, Bcl-w, Mcl-1 and A1) contain BH 3 and 4 domains and protect cells from apoptosis by guarding the outer mitochondrial membrane (OMM) (Reed 1994)( Admas, 2003,Reed 1994). The BH3-only proteins (Bim, Bad, Bid/tBid, Bmf, Bik, Hrk and Noxa Puma) contain a single BH domain and when activated engage with specific pro-survival Bcl-2 partners neutralizing their pro-survival activity (Bouillet and Strasser 2002, Chen, Willis et al. 2005). The last group comprises the BH1–3 proteins (Bax, Bak and Bok) that regulate mitochondrial membrane permeability (Willis and Adams 2005, Dewson and Kluck 2009).

Once the mitochondrial outer membrane is disrupted, several proteins are released including cytochrome c, second mitochondrial activator of caspase (Smac), apoptosis inducing factor (AIF) and endonuclease G (Saelens, Festjens et al. 2005). Cytochrome c release is particularly important as it forms the apoptosome complex with apoptosis activating factor-1 (Apaf-1) and pro-caspase-9. Caspase- 9 can also activate caspases-3, -6 and -7 to further provoke the apoptosis response. These pathways and their interaction are summarised in Figure 1.8 (Desouza, Gunning et al.) .



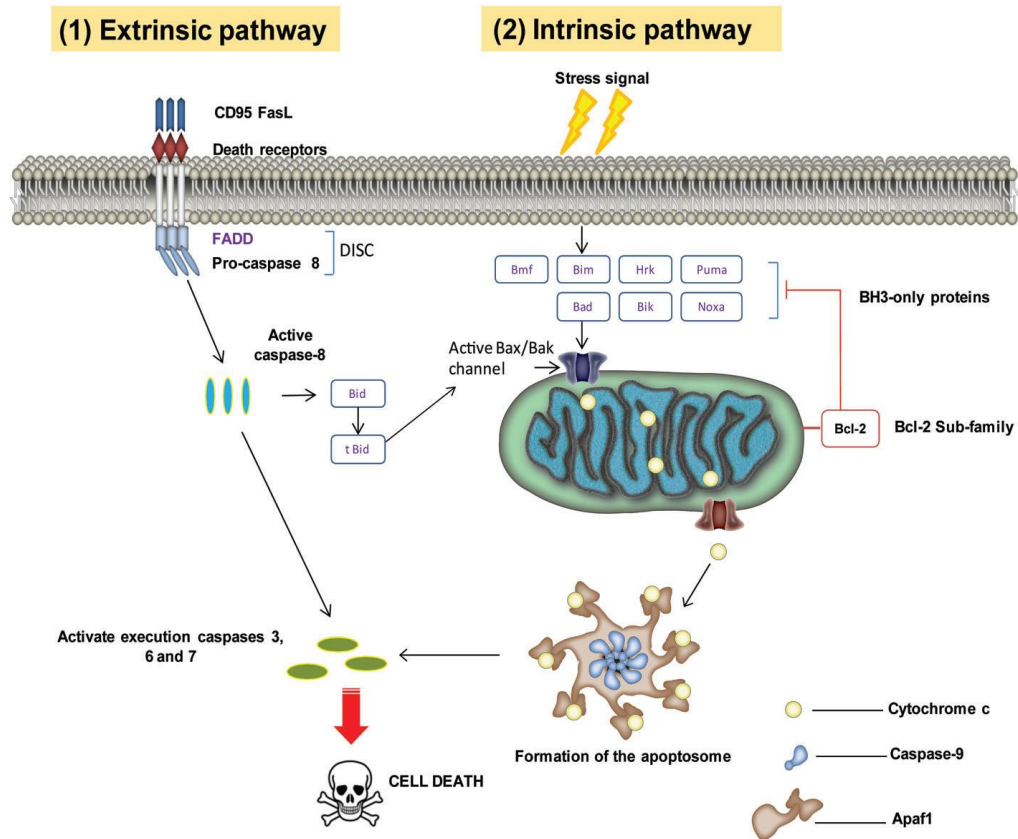


**Figure 1.8** The extrinsic and intrinsic apoptosis pathways (Desouza, Gunning et al. 2012)

(1) The extrinsic pathway is initiated by the ligation of TNF members to the surface receptors. This results in the formation of the death-inducing signalling complex (DISC) composed of FADD and pro-caspase 8. Caspase 8 activation also can activate the pro-apoptotic protein Bid which feeds into the intrinsic pathway. (2) The intrinsic pathway is chiefly mediated by the Bcl-2 super family. Inactivation of Bcl-2 pro-survival partners by BH3 group (pro-apoptotic proteins) leads to the release of Bax and Bak. Homo-oligomerization of Bax and Bak at the outer mitochondrial membrane results in the release of cytochrome c and activation of caspase-9. Both pathways converge to activate the executioner caspases leading to cell death.

## **1.17 Markers of apoptosis**

### **I. Cleavage of Poly (ADP-ribose) polymerase (PARP)**

PARP is a 116 KDa protein involved in the repair of DNA and in formation of chromatin structure (Lazebnik, Kaufmann et al. 1994). It also is important in maintaining cell viability, whilst the degradation of PARP facilitates disassembly of cells and is considered a marker of the apoptotic cell (Oliver, de la Rubia et al. 1998). During apoptotic cell death, PARP cleavage into its characteristic 89KDa fragment is mediated by caspase-3 (Le Rhun, Kirkland et al. 1998).

### **II. Cleavage of $\beta$ – actin**

The actin cytoskeleton is a structural network of proteins that is involved in many biological functions including cell contraction, cell motility, intracellular organization, vesicle trafficking, cytokinesis, endocytosis and apoptosis (Pollard and Cooper 1986, Khaitlina 2001, Yarar, Waterman-Storer et al. 2005, Franklin-Tong and Gourlay 2008). Actin is a 42 kDa globular protein (G-actin) that reversibly polymerizes to form filaments (F-actin). In muscle cells actin is a core component of the sarcomere that interacts with myosin filaments to enable force generation needed during muscle contraction (Huxley, 1969). In non-muscle cells, actin isoforms ( $\beta$  and  $\gamma$ ) perform a different range of functions that permit cell survival and adaptation to a changing environment (Cooper 1991, Hooek, Newcomb et al. 1991, Schevzov, Lloyd et al. 1992, Hill and Gunning 1993).

The actin cytoskeleton has been shown to be essential during the apoptosis process, with extensive changes in the organization of actin filaments

accompanying different stages of apoptosis (Laster and Mackenzie 1996, Hacker 2000) . Cell rounding, which involves the loss of focal contacts with the extra-cellular environment, requires the formation of a contractile cortex of myosin II arranged actin filaments (Charras, Hu et al. 2006). Retraction of the actin-myosin II cortex considerably alters membrane dynamics leading to formation of membrane blebs (Coleman and Olson 2002, Charras, Hu et al. 2006) .

There are also several lines of evidence that suggest a role for actin in signalling apoptosis (Suria, Chau et al. 1999, Yamazaki, Tsuruga et al. 2000, White, Williams et al. 2001, Bando, Miyake et al. 2002, Kim, Schwabe et al. 2002, Cabado, Leira et al. 2003). In some cells, induction of apoptosis is accompanied by caspase-dependent  $\beta$ -actin cleavage to 15 and 31 kDa fragments (Mashima, Naito et al. 1995, Kayalar, Ord et al. 1996, Mashima, Naito et al. 1997, Mashima, Naito et al. 1999, Nakazono-Kusaba, Takahashi-Yanaga et al. 2002, Cabado, Leira et al. 2003). Furthermore, ectopic expression of the 15 kDa actin fragment in HeLa and A431 cells has been shown to induce morphological changes resembling those in etoposide-induced apoptosis (Cabado, Leira et al. 2003). Exposing HeLa cells to etoposide treatment resulted in  $\beta$ -actin cleavage, but  $\beta$ -actin cleavage was not detected in TNF-treated L929 cells (Li, Li et al. 2004). Thus, it appears that at least in some cell systems, cleavage of  $\beta$ -actin may act as a marker of apoptosis.

## 1.18 Role of apoptosis in breast cancer

The balance between proliferation, differentiation and cell death in the mammary gland is important in normal development and homeostasis (Parton, Dowsett et al. 2001). Conditions that cause regulation of proliferation and downregulation of apoptosis may allow accumulation of mutations that can lead to development of breast cancer (Parton, Dowsett et al. 2001).

Many studies have focused on understanding the mechanism by which apoptosis may be disrupted in tumours. In the context of the current study, however, the focus is whether induction of apoptosis in myoepithelial cells could contribute to the disruption of the limiting barrier in DCIS, allowing progression to invasive disease.

## 1.19 TRAIL (APO-2L)

Tumour necrosis factor-related apoptosis-induced ligand (TRAIL) belongs to the TNF ligand family that induces apoptosis in a variety of cancer cell lines including breast cell lines (Keane, Ettenberg et al. 1999, Chinnaiyan, Prasad et al. 2000, Wendling, Walczak et al. 2000). TRAIL protein is expressed by peripheral T lymphocytes (Salehi, Vodjgani et al. 2007), including CD4 T cell (Sato, Niessner et al. 2006). TRAIL has been detected in a broad range of cells, in particular in activated T cells (Jeremias, Herr et al. 1998, Sato, Nuki et al. 2010) Furthermore, activated Treg cells express TRAIL in vivo (Ren, Wagner et al. 2004, Ren, Ye et al. 2007). Thus it is feasible that changes in the inflammatory microenvironment may expose both tumour cells and other host cell populations to a variety of pro-apoptotic signals. TRAIL binds to five different members of the TNF receptor family, TRAIL-R1/DR4, TRAILR-2/DR5/TRICK2/Killer, TRAIL-R3/TRID/DcR1/LIT, TRAIL-

R4/TRUNDD/DcR2 and osteoprotegerin (Locksley, Killeen et al. 2001). TRAIL-R1 and TRAIL-R2 mediate apoptosis and contain a death domain (Pan, Ni et al. 1997, Pan, O'Rourke et al. 1997, Walczak, Degli-Esposti et al. 1997) while TRAIL-R3, which lacks the death domain, is considered as a decoy receptor (Degli-Esposti, Smolak et al. 1997). TRAIL-R4 has an incomplete death domain (Degli-Esposti, Dougall et al. 1997). Osteoprotegerin receptor inhibits TRAIL-induced apoptosis (Emery, McDonnell et al. 1998). NF-KB prevents TRAIL induced apoptosis in human hepatoma (Kim, Schwabe et al. 2002).

## **1.20 Galectin-7 expression in tissue**

Galectins, previously known as S-type lectins, constitute one of several families of endogenous lectins and are named for their ability to bind  $\beta$ -galactosides (Barondes, Cooper et al. 1994). All galectins display a similar sequence in the carbohydrate recognition domain (CRD) which includes about 130 amino acids, and a globular tertiary structure making a groove for the binding of carbohydrate (Leffler, Carlsson et al. 2004). There are 15 forms of galectins, 11 of them are expressed in humans, known as galectin 1-4, 7,10 and 12-14 (Liu and Rabinovich 2005). In recent years, they have emerged as novel modulators in different aspects of cancer (Demers, Rose et al. 2010).

Galectin-7 was isolated by Madsen and colleagues in their attempt to identify new markers involved in the maintenance of the normal human epidermal phenotype (Madsen, Rasmussen et al. 1995). Galectin-7 is expressed in stratified epithelia, including cornea, oral cavity, esophagus, anorectal epithelium and epidermis (Magnaldo, Bernerd et al. 1995). Galectin-7 expression is up-regulated in mouse cornea during wound healing, and

recombinant galectin-7 stimulated re-epithelization of the cornea during healing (Cao, Said et al. 2003). Moreover, galectin-7 has been described both as pro-apoptotic and anti-apoptotic, in vivo and in vitro. An early report identified galectin-7 as one of the first genes responding to over-expression of the p53 tumour suppressor gene in human DLD-1 colon cancer cells (Polyak, Xia et al. 1997) . It also has been reported that galectin-7 expression is increased in apoptotic keratinocytes of human skin explants exposed to UVB light (Bernerd, Sarasin et al. 1999). In addition, ectopic expression of galectin-7 in HeLa and DLD-1 cells renders them more susceptible to apoptosis induced by actinomycin D and UVB (Kuwabara, Kuwabara et al. 2002). In contrast, exposure of skin of wt and galectin-7<sup>-/-</sup> adult mice to UVB has demonstrated a twofold increase in apoptotic cells in galectin-7<sup>-/-</sup> compared with wt epidermis at 6 h (Gendronneau, Sidhu et al. 2008). In the normal breast, Demer and his colleagues (2010) have shown that galectin-7 is highly expressed by the myoepithelial cell population. They also have shown that high-grade breast cancers express high levels of galectin-7 while low-grade cancers show none or minimal galectin-7 expression. Moreover, they found its over-expression to be associated with tumour metastasis to the lung and bone. It has been suggested that galectin-7 has the ability to render mammary epithelial cells more resistant to apoptosis (Demer et al 2010). It also has been revealed that intracellular galectin-7 may have a novel function as a transcriptional regulator whereby galectin -7 interacts with Smad3 to regulate its export from the nucleus, thereby inhibiting TGF $\beta$  signalling (Inagaki, Higashi et al. 2008). Given the privileged position of myoepithelial cells in DCIS, changes in the myoepithelial phenotype which may influence their response to apoptotic

stimuli may be of importance in defining the integrity of the myoepithelial-basement membrane interface and so disease progression. Changes in galectin-7 by breast myoepithelial cells have not, to our knowledge, been previously investigated.

## 1.21 Hypothesis

The microenvironment in DCIS is complex and the myoepithelial cell, which forms the major barrier between the epithelial and stromal compartments, may play a key role in disease progression. We previously have shown that myoepithelial cells in DCIS display an altered phenotype, with up-regulation of the integrin  $\alpha\beta 6$ , switching myoepithelial function from tumour suppressor to tumour promoter. However, the relationship between myoepithelial phenotype and the peri-ductal inflammatory infiltrate, and the influence of it on myoepithelial integrity have not been investigated.

Therefore, the hypothesis of the study is that changes in myoepithelial phenotype that occur during evolution of DCIS, including up regulation of integrin  $\alpha\beta 6$ , result in an altered peri-ductal inflammatory microenvironment contributing to a pro-tumour phenotype. A key step in progression of DCIS is loss of the myoepithelial cell layer. We hypothesise that one mechanism by which the inflammatory infiltrate may promote tumour progression is through induction of myoepithelial cell apoptosis, possibly through release of TRAIL. Since galectin-7, a molecule highly expressed by normal myoepithelial cells, has been shown in some situations to protect cells from apoptosis, we postulate that changes in galectin-7 in DCIS-associated myoepithelial cells may enhance their susceptibility to apoptosis: To investigate this hypothesis the aims are:

- To characterise the nature of the inflammatory cell infiltrate in the periductal environment of DCIS, and correlate this with myoepithelial phenotype as indicated by  $\alpha v\beta 6$  expression.
- To investigate the impact of myoepithelial cells on the inflammatory cell phenotype using co-culture systems and in-vivo Matrigel plug assays.
- To investigate the cytokine profile of normal and DCIS-modified myoepithelial cells, and whether this is influenced by inflammatory cells, using cytokine arrays.
- To study the sensitivity of  $\beta 4$  and  $\beta 6$  myoepithelial cells to apoptosis generated through release of inflammatory cell mediators (such as T cell-derived TRAIL) and investigate whether phenotypic alterations in myoepithelial cells, such as loss of Galectin-7, influenced their response. This will be done using knock-down and over-expression culture model systems.

Together, this should elucidate the functional relationship between the altered myoepithelial phenotype observed in DCIS and the nature of the inflammatory infiltrate, and indicate whether these changes impact on loss of the myoepithelial cell layer through apoptosis.



# Chapter 2: Materials & Methods

## Materials and Methods

---

### 2.1 Clinical materials

#### 2.1.1 Tissue samples

##### 2.1.1.1 UK tissue samples

Cases of DCIS were identified from The Barts Cancer Institute Breast Tissue Bank, covered by Research Tissue Bank Ethics Approval (10/H0308/49, Cambridge 2 Research Ethic Committee). These were sequential patients presenting to Barts Health Breast Unit during the period of 2007-2009 and who had consented for use of their tissues for research. Samples were linked-anonymised prior to use in this study. Forty-seven cases of DCIS of different grades were used in the study. Details of patient demographics and pathology are given in Table 2.1.

**Table 2.1** Details of patient demographics and pathology

DCIS grade	Age		Size mm		Invasive Number (%)		Total number (%)
	Mean	Range	Mean	Range	Present	Absent	
<b>Low</b>	56	54-59	14.2	6-19	0 (0%)	3 (100%)	3 (6%)
<b>Intermediate</b>	57	52-63	19.0	4-28	0 (0%)	8 (100%)	8 (17%)
<b>High</b>	46	39-54	32.9	9-47	0 (0%)	36 (100%)	36 (77%)

### 2.1.1.2 Netherland tissue samples

Through collaboration with Dr. Pieter Westenend (Laboratorium voor Pathologie, Dordrecht), sections from patients with a diagnostic core biopsy of DCIS were obtained for study. A total of 294 cases were received, all anonymised. Following analysis, data were returned to Dr. Westenend to be collated with clinicopathological information and then returned for statistical analysis. Details of patient demographics and pathology are given in Table 2.2.

**Table 2.2 Details of patient demographics and pathology**

DCIS grade	Age		Size mm		Invasive Number (%)		Total number (%)
	Mean	Range	Mean	Range	Present	Absent	
<b>Low</b>	61.6	44-77	11.1	2-60	5 (15%)	29 (85%)	34 (11.5%)
<b>Intermediate</b>	59.1	27-83	19.8	1-100	18 (27%)	48 (73%)	66 (22.5%)
<b>High</b>	57.1	45-88	26.7	3-90	46 (24%)	148 (76%)	194 (66%)

### **2.1.2 Tissue block selection**

For the Barts Cancer Institute samples, formalin-fixed paraffin embedded blocks were sectioned for Haematoxylin and Eosin (H&E) staining and representative blocks selected for the study by Professor Louise Jones (JLJ). Then, 4  $\mu$ M serial sections were obtained from these blocks for immunohistochemical staining for galectin-7,  $\alpha$ v $\beta$ 6 and inflammatory markers.

## **2.2 Origin of primary cells and cell lines**

Details of cells lines and primary cells used are summarized in Table 2.3. Primary breast myoepithelial cells were isolated from donors undergoing reduction mammoplasty surgery (section 2.1.3.1). Primary T lymphocytes were obtained from peripheral blood samples of healthy donors.

Table 2. 3 Source and Characteristics of cells used in *in vitro* experiments

Type of cells		Characteristics
Human Breast Myoepithelial cells	$\beta 4$	Origin: immortalised line initially derived from breast reduction tissue (O'Hare, Bond et al. 2001). Features: immortalized line of normal mammary myoepithelial cells positively selected for $\beta 4$ using magnetic beads.
	$\beta 6$	Origin: $\beta 6$ cell line was derived from $\beta 4$ cells in our lab by stable over-expression of $\beta 6$ . Features: Virally transfected with PBabepuro- $\beta 6$ to express high levels of $\beta 6$ integrin.
	Primary myoepithelial	Origin: normal human breast  Features: normal mammary myoepithelial cells isolated using CALLA-magnetic beads
Human T lymphocytes	Jurkat cell line	Origin: in 1970s isolated from the peripheral blood of a 14 year old boy with T cell leukemia.  Features: immortalized line of T lymphocyte cells.
	Primary T lymphocytes	Origin: peripheral blood from healthy donors.  Features: CD4/ CD8 positive.

## 2.2.1 Primary cells

### 2.1.3.1 Breast myoepithelial cells

Primary breast myoepithelial cells were obtained from donors undergoing reduction mammoplasty surgery at Barts Health NHS Trust. All donors were consented prior to Surgery. Ethical approval was obtained from Barts Cancer Institute Breast Tissue Bank (10/H0308/49, Cambridge 2 Research Ethic Committee). Cell isolation was carried out by Dr. Jenny Gomm (Gomm, Browne et al. 1995). Normal Breast tissue was minced into small pieces

(0.5cm), and then incubated in RPMI medium containing 10 % FBS, collagenase and hyaluronidase overnight at 37 °C. Following enzyme digestion the fat layer was removed and the remaining organoids and single cells centrifuged and washed 3 times in medium. To isolate the ductal elements from the stroma, sedimentation steps at 1g were employed for 30 minutes and repeated 3 times. Supernatant was removed and used for stromal cells. A loose pellet of the organoids was collected and used as the ductal fragment.

Purification of myoepithelial cells was performed using anti-CALLA (common acute lymphocytic leukaemia antigen)-labelled magnetic beads, as a specific cell membrane marker of myoepithelial cells (figure 2.1). This process was performed using immunomagnetic isolation with Dynabeads as described (section 2.8.9).

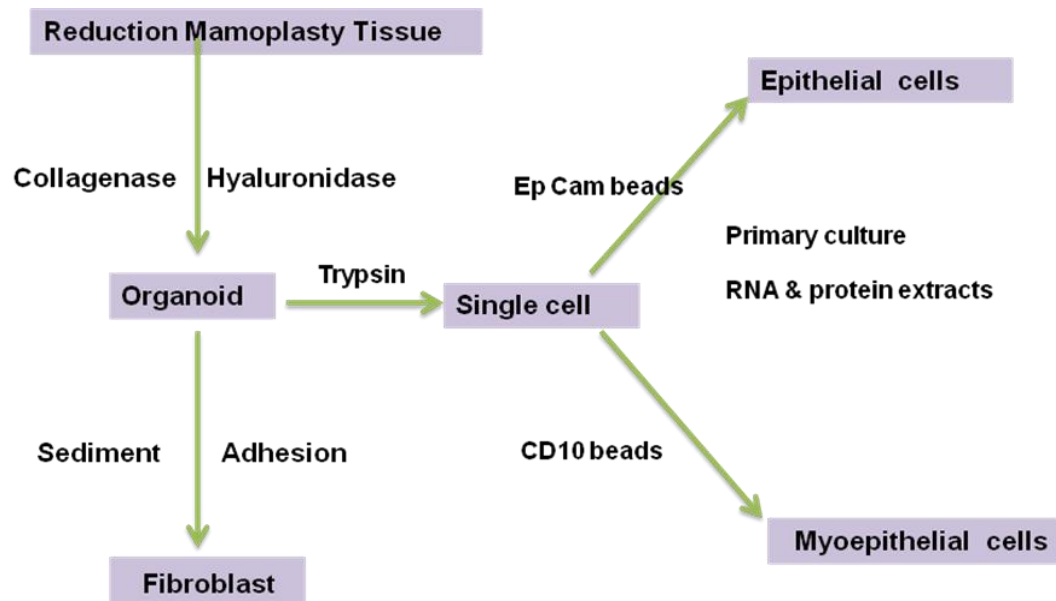


Figure 2.1 Scheme depicting preparation and purification of breast cell types (Gomm, Browne et al. 1995).

### **2.1.3.2 Primary T lymphocytes**

Primary T cells were obtained from peripheral blood samples from healthy donors at Barts Hospital. Cell isolation was undertaken in the Centre of Medical Oncology at Barts Cancer Institute and was a gift from Dr. Alan Ramsey.

## **2.3 Matrigel plug assays**

A group of 12 female C57/Blk6 normal mice, 4 weeks old were used in this study.  $\beta$ 4 cells and  $\beta$ 6 myoepithelial cells were suspended in Matrigel then injected separately into opposite flanks of the mice. B16 mouse melanoma cells were used as a positive control and Matrigel alone as a negative control. After 9 days when the tumours became palpable, the mice were sacrificed, and Matrigel with the surrounding tissue was extracted.

These Matrigel plugs were formalin-fixed and paraffin- embedded then sections cut and stained for inflammatory markers CD4, FOXP3 (Treg), CD8 (cytotoxic T cell), CD74 (macrophage inhibitory factor receptor) and arginase (M2 macrophage) (figure 2.2).

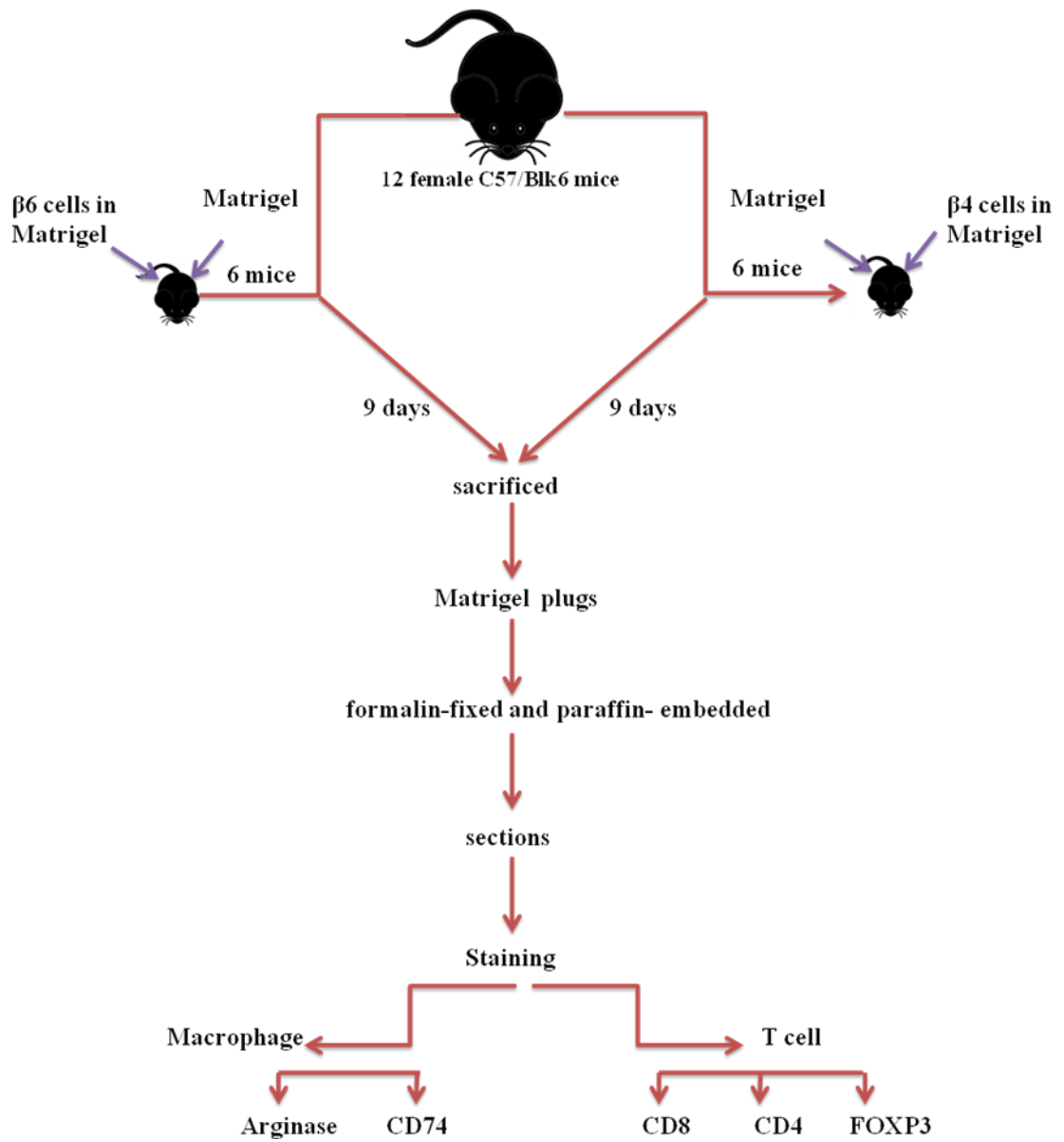


Figure 2.2 Scheme depicting investigation of the interaction between myoepithelial cells and the inflammatory infiltrate *in - vivo*.



## **2.4 Immunohistochemistry**

### **2.4.1 Slide preparation**

Formalin-fixed, paraffin-embedded breast tissue blocks including different grades and subtypes of DCIS were used in the study. Serial sections of 4µm thickness were cut and placed on positively charged microscope slides for immunohistochemical analysis.

### **2.4.2 Haematoxylin and eosin staining**

Sections were dewaxed through changes of xylene then rehydrated through graded alcohols (100%, 100%, 80%, 70%, and 50%). After washing in tap water, the sections were immersed in Haematoxylin for 90 seconds, washed in tap water, and then briefly dipped in Eosin. After washing in tap water the sections were dehydrated through graded alcohols (50%, 70%, 80%, 100%, 100%) and finally dipped in xylene. Finally the slides were drained in a rack and a drop of DPX mountant was spread over cover slips. All procedures that included xylene or alcohol-containing materials were carried out in a fume hood.

### **2.4.3 Immunohistochemistry technique**

Immunohistochemical staining is accomplished with antibodies that detect the target protein. Since antibodies are highly specific, the antibodies will bind only to the protein of interest in the tissue section. Then the antibody-antigen reaction is visualized using fluorescent detection, in which a fluorophore is conjugated to the antibody and visualized using fluorescence microscopy or by

chromogenic detection, in which an enzyme conjugated to the antibody cleaves a substrate to produce a coloured precipitate at the site of the target protein.

#### **2.4.4 Slide preparation for staining**

Sections were dewaxed in xylene and then rehydrated through graded alcohols as described. Endogenous peroxidase was blocked using a solution of hydrogen peroxide and methanol 3:200 for 10 minutes, followed by dipping in graded alcohols again for 2 minutes per solution.

#### **2.4.5 Antigen retrieval**

Antigen retrieval is a technique used to enhance the binding of antibody to antigen in tissue through unmasking of the antigenic site. It is usually used when a fixation or embedding method has caused changes which mask antibody binding.

Most antigen retrieval methods are based on microwave or pressure cooker treatment to heat the tissue sections to temperatures at 100-120 °C in the presence of metal solutions. Three approaches were tested in this study:

- i. Heat-induced: sodium citrate 10 mM, pH 6.0 at 100-120°C for 10 minutes
- ii. Heat-induced: Tris/EDTA pH 9.0 at 100-120°C for 10 minutes.
- iii. Enzymatic: trypsin, pepsin, or other protease.

After establishing the optimal antigen retrieval method, the antibody concentration can then be further optimized.

### **2.4.6 Blocking**

Sections were washed in distilled water. The sections were outlined using a PAP pen. Background was blocked for 10 minutes using 20% Normal Rabbit Serum (NRS) or 1.5% Normal Horse Serum, according to the nature of secondary antibody, made up in 0.2% bovine serum albumin (BSA) dissolved in phosphate buffered saline (PBS/BSA 0.2%).

### **2.4.7 Primary antibody**

Sections were drained and 200 µl of primary antibody, made up in 0.2% BSA to optimal concentration, was applied. The sections were incubated for 1 hour at RT. Details of antibodies used and optimal dilutions and antigen retrieval are provided below (Tables 2.4 and 2.5). FOXP3 and CD8 antibodies could not be optimized, therefore, in order to investigate expression of FOXP3 and CD8 in Matrigel plugs, they were replaced with alternative antibodies.

Table.2.4 Details of Antibodies for human tissue: working dilutions and antigen retrieval techniques

Antibody	Dilution	Antigen retrieval	Source	Positive control
<b>CD4</b>	1:25	EDTA pH 8.0	Leica	Tonsil
<b>CD68</b>	1:50	0.1M Tri-sodium citrate pH 6.0	Dako	Tonsil
<b>CD69</b>	1:100	EDTA pH 8.0	Leica	Tonsil
<b>Arginase-1</b>	1:75	EDTA pH 8.0	Sigma	Liver
<b>FOXP3</b>	1:50	0.1M Tri-sodium citrate pH 6.0	Abcam	Tonsil
<b>MHC-II</b>	1:1000	0.1M Tri-sodium citrate pH 6.0	Abcam	Tonsil
<b>CD8</b>	1: 300	0.1M Tri-sodium citrate pH 6.0	Dako	Tonsil
<b>CD45RO</b>	1:200	0.1M Tri-sodium citrate pH 6.0	Dako	Tonsil
<b>CD74</b>	1:200	0.1M Tri-sodium citrate pH 6.0	Leica	Tonsil
<b>Galectin-7</b>	1:750	0.1M Tri-sodium citrate pH 6.0	Epitomics	Skin Normal breast
<b>Caspase-3</b>	1:300	0.1M Tri-sodium citrate pH 6.0	Cell Signaling	Internal
<b>β 6 integrin</b>	1:300	Pepsin	Calbiochem	Skin

**Table 2.5** Details of Antibodies for mouse tissue: working dilutions and antigen retrieval technique

Antibody	Dilution	Antigen retrieval	Source	Positive control
CD4	1:25	EDTA pH 8.0	Leica	Spleen
Arginase-1	1:75	EDTA pH 8.0	Sigma	Liver
FOXP3	1:200	0.1M Tri-sodium citrate pH 6.0	Novus	Spleen
CD74	1:200	0.1M Tri-sodium citrate pH 6.0	Leica	Spleen
CD8	1:300	0.1M Tri-sodium citrate pH 6.0	Cell Signaling	Spleen

### 2.4.8 Secondary antibody

Sections were washed twice in PBS for 5 minutes. 200 µl of biotinylated secondary antibody at the appropriate concentration in 0.2% BSA was applied to each section, and incubated for 40 minutes at RT.

### 2.4.9 Avidin biotin complex (ABC)

Sections were washed twice in PBS for 5 minutes each before adding ABC solution (1:50 A and 1:50 B in PBS) which was made 30 minutes prior to application. The sections were incubated for 30 minutes at RT.

### 2.4.10 Detection

For light microscopy, horseradish peroxidase (HRP) is a commonly used label. Peroxide/DAB are the substrate and recommended chromogen for horseradish peroxidase. Sections were washed with PBS buffer twice for 5 minutes each before being developed with 3, 3-diaminobenzidine tetrahydrochloride (DAB)

for 2-5 minutes at RT and then washed with distilled water, counterstained with haematoxylin and finally washed with tap water.

### **2.4.11 Dehydration**

After washing with distilled water the sections were passed through graded alcohols for 2 minutes each and xylene for 5 minutes. They were mounted with a drop of DPX mountant.

## **2.5 Scoring of Immunohistochemistry**

### **2.5.1 Scoring of $\alpha\text{v}\beta\text{6}$ IHC staining**

Whole sections of DCIS were stained for  $\alpha\text{v}\beta\text{6}$  expression and the extent of staining on DCIS-associated myoepithelial cells was recorded by Professor Louise Jones (JLJ) and myself.

Cases that showed homogeneously positive or negative patterns of staining i.e. where all DCIS ducts showed myoepithelial cells positive or negative for  $\alpha\text{v}\beta\text{6}$ , were selected to further analyze the characteristics of the peri-ductal inflammatory infiltrate in DCIS, and its relationship to  $\alpha\text{v}\beta\text{6}$  expression.

### **2.5.2 Relationship between $\alpha\text{v}\beta\text{6}$ and galectin-7 expression**

The relationship between myoepithelial expression of  $\alpha\text{v}\beta\text{6}$  and expression of galectin-7 was analysed in two cohorts:

- (i) A set of 40 cases from the Barts Cancer Institute Breast Bank Tissues were analysed on a duct- by- duct basis. The stained sections were scanned using NDP Nanozoomer scanner. Cases were scored duct by duct for positive or negative staining for Galectin-7 and  $\alpha\text{v}\beta\text{6}$  in the myoepithelial cells independently by JLJ and myself, and the results compared. Where there

was disagreement, the images were viewed by both scorers and an agreed score made.

- (ii) A series of 294 core biopsies with a pre-operative diagnosis of DCIS were received from our collaborator Dr. Pieter Westenend, and stained for  $\alpha\beta6$  and galectin-7. The biopsies were scored by Professor Louise Jones (JLJ), Dr. Purnima Makhija and myself as the percentage of DCIS ducts showing myoepithelial positivity for each stain. Where there was discrepancy between the scorers, the cases were viewed on a double-headed microscope, and an agreed score made. The staining scores were returned to Dr. Pieter Westenend to reconcile with the clinical data, specifically whether the surgical excision showed pure DCIS, or had admixed invasive carcinoma.

## **2.5.3 Scoring of inflammatory cell infiltrate in DCIS**

### **2.5.3.1 Photography**

The DCIS cases classified as homogeneously positive or negative for  $\alpha\beta6$  were then stained with a series of antibodies to characterize the inflammatory cell infiltrate. The serial sections were scanned using an NDP Nanozoomer scanner, a minimum of 4 ducts from each case were captured. Each duct image was exported as a jpg at X5 or X10 magnification (figure 2.3).

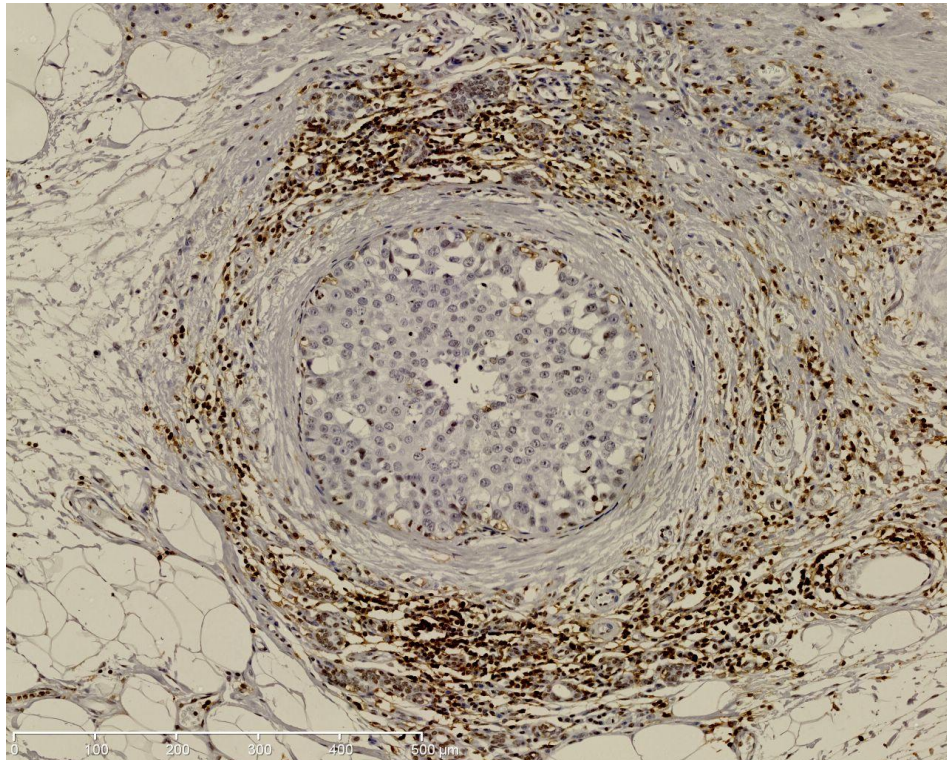


**Figure 2.3 NDP Image software**

A series of cases of DCIS homogenously positive or negative  $\alpha\beta6$  were stained for a panel of inflammatory markers and scanned using NDP Nanozoomer scanner. Each duct image was exported to jpg with X5 or X10 magnification.



### 2.5.3.2 Process Image program

To assess the relationship between  $\alpha\beta6$  staining of myoepithelial cells and the peri-ductal inflammatory environment, images of ducts were uploaded to Process Image software in order to score them. This software is a program that allows conversion of graphic files to editable forms that can be scored in co-operation with the freeware image manipulation program GNU image manipulation program (GIMP). It enables an image to be edited to calculate areas, lengths and marker counts. A region of 100 $\mu\text{m}$  from the edge of the duct was defined by this software and the number of cells positive for different inflammatory markers was counted in this area. The positive cells were manually highlighted, then the program was run to calculate them (figure 2.4).

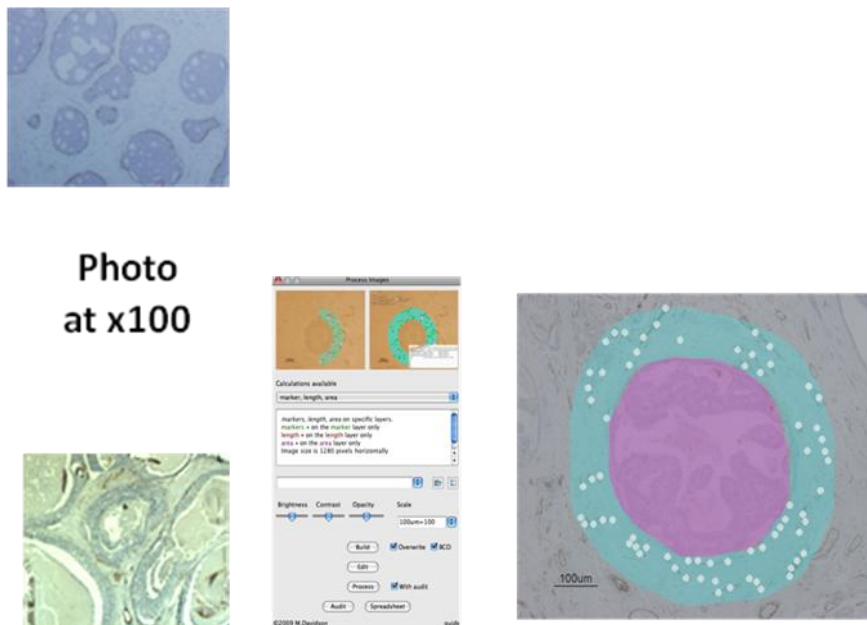


**Figure 2.4 Process Image Software.**

This software was used to score the inflammatory cells around each of the DCIS ducts. The number of inflammatory cells staining for each marker was counted in a region of 100 $\mu\text{m}$  from the edge of the duct.

## **2.5.4 Scoring of inflammatory cell infiltrate in Matrigel plugs**

### **2.5.4.1 Photography**

Immunohistochemically stained sections of Matrigel plugs were scanned using NDP Nanozoomer scanner. The numbers of positive cells for inflammatory cells markers were scored using Imagescope software.

### **2.5.4.2 Aperio Imagescope software**

Imagescope is a new image analysis solution for immunohistochemistry as part of the Aperio digital pathology system. Aperio's IHC image analysis algorithms are designed to assess staining of cell features (nuclei and membrane).

The scoring scheme parameters specify the staining intensity thresholds that determine the individual cell. The program classifies the intensity of staining as 0, 1+, 2+ and 3+. Cell staining is classified 0 when there is no staining, 1+ when there is weak staining, 2+ for moderate staining and 3+ for strong staining.

### **2.5.4.3 Quantitation of the inflammatory cell infiltrate in Matrigel plugs containing myoepithelial cells**

Whole sections of Matrigel plugs were scanned using NDP software and analysed using Imagescope software. Each section was opened in the Imagescope program, the scoring scheme parameters specifying the staining intensity threshold of each marker were set up based on intensity of staining, which is classified as 0 (negative), 1+ (weak), 2+ (positive) and 3+ (strong

positive), and the software was run to count the positive and negative cells for each inflammatory marker over the entire section. The result was exported to an Excel file and the number of positive cells per mm<sup>2</sup> was calculated, and plotted on a graph using prism software.

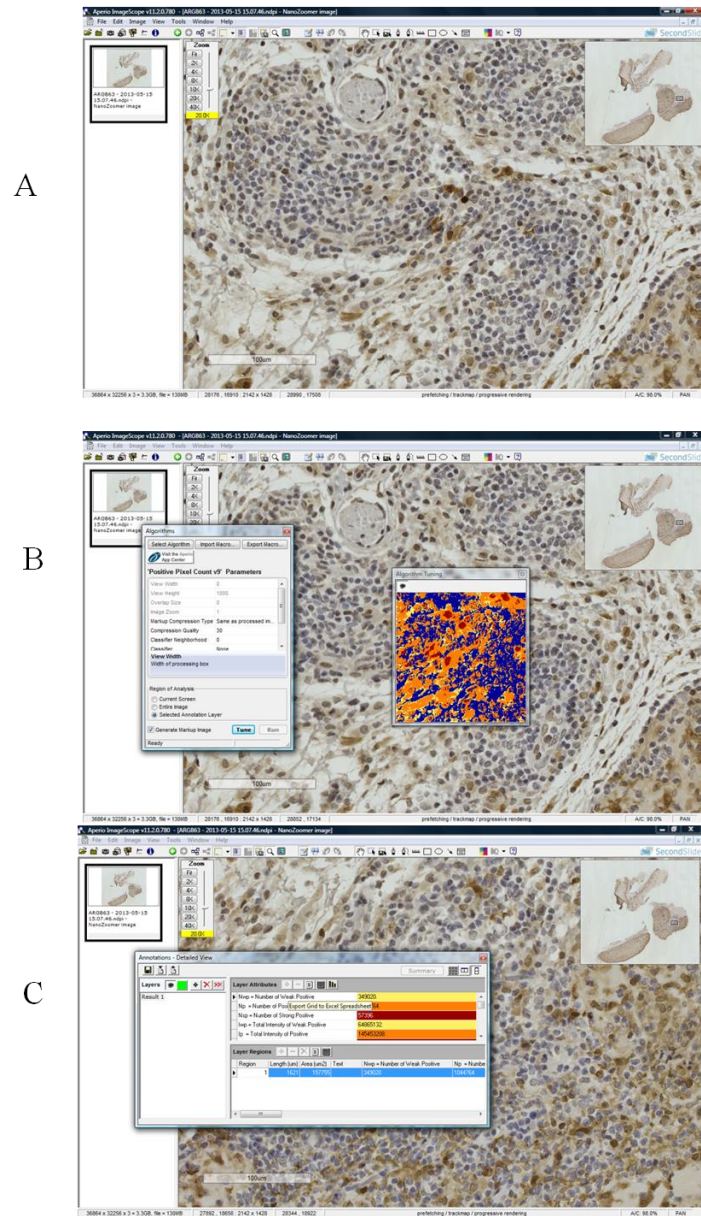


**Figure 2.5** Imagescope software

The program enabled an image to be edited to score intensity, area and marker-positive cell counts (A). Parameters of each marker were set up to avoid scoring background and based on intensity, staining is classified as 0 (negative, blue), 1+ (weak, yellow), 2+ (positive, orange) and 3+ (strong positive, red) (B). The software then calculated the define area, number of positive cells according to their intensity and number of negative cells. Data was exported into an Excel spread sheet (C).

## 2.6 Measuring of DCIS duct size

Differences in size of the DCIS ducts were observed whilst scoring the IHC staining for galectin-7 and  $\alpha\text{v}\beta 6$ . Therefore I measured the duct size and related it to IHC pattern to assess whether there is a correlation between the size of ducts and myoepithelial cell phenotype. The measurement was applied using NDP software after scanning the sections. Ducts were selected from 40 DCIS cases retrieved from the Barts Cancer Institute Tissue Bank. Ducts were measured in two diameters as they are not definitive spheres (Figure 2.6). The area of duct was calculated using using a mathematical formula derived by Dr.

Michael Allen to measure the area of ellipse (  $2\pi \left[ \sqrt{\frac{r_1^2+r_2^2}{2}} \right]$  ). A total of 617

ducts were analysed.

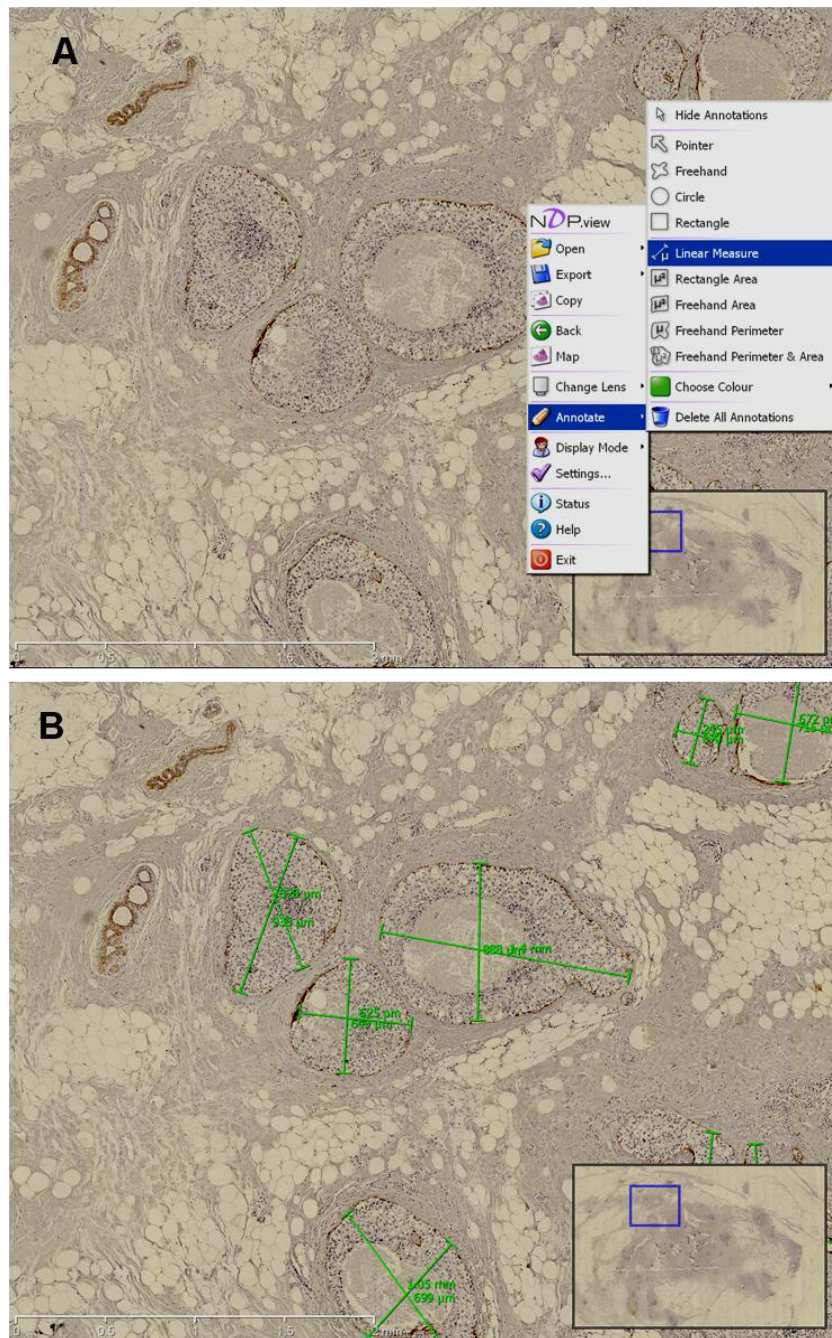


**Figure 2.6 Measuring DCIS duct size**

Each photo is opened in NDP software, and linear measure selected from the annotate menu (A). As DCIS ducts are not definite circles, they were measured in two directions using the linear measure (B).



## 2.7 Statistical analysis

Data has been analysed using the Mann Whitney test and one way ANOVA, and p values less than 0.05 were identified as statistically significant. Graphs were generated using GraphPad Prism software.

Data from the Netherland DCIS series were analysed by Professor Stephen Duffy, Wolfson Institute for Preventive Medicine, by Spearman's correlation using STATA software.

## 2.8 Cell culture

Primary cells and cell lines were regularly assessed for contamination with mycoplasma using RT-PCR protocol (section 1.1, appendix 1).

### 2.8.1 Myoepithelial cell line culture

$\beta$ 4 myoepithelial cells ( $\beta$ 4 myo) and its  $\beta$ 6 over-expressing counterpart, termed  $\beta$ 6 myo, were stored in liquid nitrogen in 10% Dimethyl sulphoxide (DMSO), 20% fetal calf serum (FCS) (Life Technologies) and 70% Ham's F12: DMEM (Dulbeccos MEM; Cancer Research UK). Cells were recovered quickly from liquid nitrogen storage by defrosting at 37°C and re-suspending in pre-warmed complete myoepithelial medium. Complete myoepithelial medium consisted of Ham's F12, 10% FCS (Life technologies), 2mM L-glutamine, 10 ng/ml epidermal growth factor (EGF), 5 $\mu$ g/ml insulin, 0.4  $\mu$ g/ml hydrocortisone (Invitrogen). After centrifugation at 1,200 rpm for 3 minutes the cell pellet was

resuspended in culture medium and transferred to culture flasks. Cells were usually cultured in T75 or T175 tissue culture flasks under standard conditions (37°C, 5% CO<sub>2</sub>), and the cells passaged on reaching 70% confluence (every 2-3 days) by trypsinizing with 10x Trypsin-EDTA for 2-5 minutes at 37°C. After the cells were detached from the flask surface, the trypsin is deactivated by adding 3 ml of culture medium followed by centrifugation at 1,200 rpm for 3 minutes to collect the cell pellet and then re-cultured in 1:3 split ratio.

### **2.8.2 Maintenance of myoepithelial cell line**

β4 and β6 cell lines show phenotypic drift over time, particularly down-regulation of α6 β4 integrin, a key characteristic of myoepithelial cells. Therefore, myoepithelial cell lines were re-sorted for high expression of β4 integrin expression, using magnetic beads (section 2.8.9). For the myo β4 cells, a population was positively selected using magnetic beads labeled with an antibody to β4 integrin. For β6 myos, cells were positively selected using beads labeled with β6 integrin.

### **2.8.3 Primary myoepithelial cell culture**

Primary myoepithelial cells were grown routinely in mammary epithelial growth medium (MEGM) containing 50μl EGF, 25 μl insulin, 50μl hydrocortisone (HC) and 10 μl gentamycin.

### **2.8.4 Jurkat cell line culture**

Jurkat cells were placed in suspension cultures at  $\sim 1 \times 10^5$  cells/ml in RPMI 1640 containing 2 mM L-glutamine and 10% FCS. Cells were split 1:4 every 3 days after reaching a density of  $\sim 1 \times 10^7$  cells/ml.



### **2.8.5 Primary T cell culture**

Primary T cells were recovered from liquid nitrogen storage by thawing at 37°C with 2 µl of DNAase added to avoid cell clustering. The cells were then resuspended in pre-warmed RPMI 1640 media containing 10% FCS, then centrifuged at 1500rpm for 5 minutes. The pellet was resuspended in 4 ml of complete T cell media. Cell counts were carried out as described in section 2.8.6. The viability of cells was determined using trypan blue. The cells were incubated overnight at 37°C to aid recovery, then counts and viability were assessed again ready for use in experiments.

### **2.8.6 Counting of cells**

Cell pellets were resuspended in 10 mls of medium in preparation for counting using a haemocytometer. 10µl of suspension was removed and transferred to the haemocytometer. Cells in the haemocytometer grid were viewed using a Zeiss Axiovert microscope. The number of cells in four of 4 X 4 grids was counted (number of cells  $\times 10^4$ / ml of cell suspension) and an average taken. Total cell count was determined and multiplied by a dilution factor (X 2). Viability of cells was assessed by trypan blue.

### **2.8.7 Cryopreservation of cells**

Freezing medium was prepared, comprising DMEM, 40% FCS and 10% dimethyl sulphoxide (DMSO). At 70-80% confluence, cells were washed with PBS, trypsinised when required, then centrifuged at 1200rpm for 3 minutes.

The pellet was resuspended in 1ml of freezing medium, then slowly frozen in a -80°C freezer. The next day vials were transferred to liquid nitrogen. When needed, cells were thawed quickly in a water bath at 37°C and pipetted slowly into a 15ml falcon tube containing 4 mls of complete cell medium.

### **2.8.8 Generation of condition medium**

To generate myoepithelial cell conditioned medium (CM),  $7 \times 10^4$  myoepithelial cells were seeded into each well of a 6 well plate and grown in general cell medium for 24hrs, to establish the culture. The next day the medium was replaced by 2 ml of serum free medium (SFM) and incubated for 48 hrs to generate condition medium (CM). This was aspirated, centrifuged and the supernatant aliquoted into 15 ml falcon tubes before freezing at -20°C.

### **2.8.9 Magnetic activated cell sorting**

A cell suspension was prepared and counted. An aliquot of cells at the desired concentration was added to 1ml of ice-cold SFM and transferred to an eppendorf tube and 5 µl of β6 antibody added and mixed gently. The eppendorf then was placed on a rotating wheel at 4°C for 20 minutes. Cells were centrifuged at 1200rpm for 3 minutes and washed with ice-cold SFM. This process was repeated twice. Rabbit anti-mouse IgG Dyanbeads were added to 1ml of the cell suspension at 1:1 bead to cell ratio. This was incubated for 20 minutes at 4°C on a rotating wheel. The eppendorf was then placed into a magnetic bead concentrator to separate the labeled cells.

For positive selection, medium was carefully aspirated, a further 1ml of SFM was added and the eppendorf gently shaken. This was placed again in the magnetic bead concentrator and repeated 3 times. For negative selection, the

aspirated medium was transferred to a separate eppendorf and placed in the magnetic bead concentrator. This process was repeated 5 times. Sorted cells were resuspended in complete medium and plated out into a T25 flask or stored in liquid nitrogen to maintain cell stocks (section 2.8.7).

### **2.8.10 Co-culture of myoepithelial cells with T cells**

Myoepithelial cells ( $7 \times 10^4$ ) were plated in the wells of a 6 well plate and incubated overnight in complete myoepithelium medium (figure 2.7A). The following day, the medium was removed and replaced with 2ml of serum free medium (SFM) followed by incubation overnight (figure 2.7B). Jurkat T cells or primary T cells were spun down and re-suspended in SFM.  $3 \times 10^5$  T cells per well were aliquoted, centrifuged and medium discarded. Then, these cells were re-suspended in 2ml of the myoepithelial medium and seeded back into the plates containing myoepithelial cells (figure 2.7C). These co-cultures were incubated for 24, 48 and 72 hrs then the floating T cells (Jurkat or primary T cells) were collected for flow cytometry or harvested and protein isolated. The attached myoepithelial cells were harvested and protein isolated.

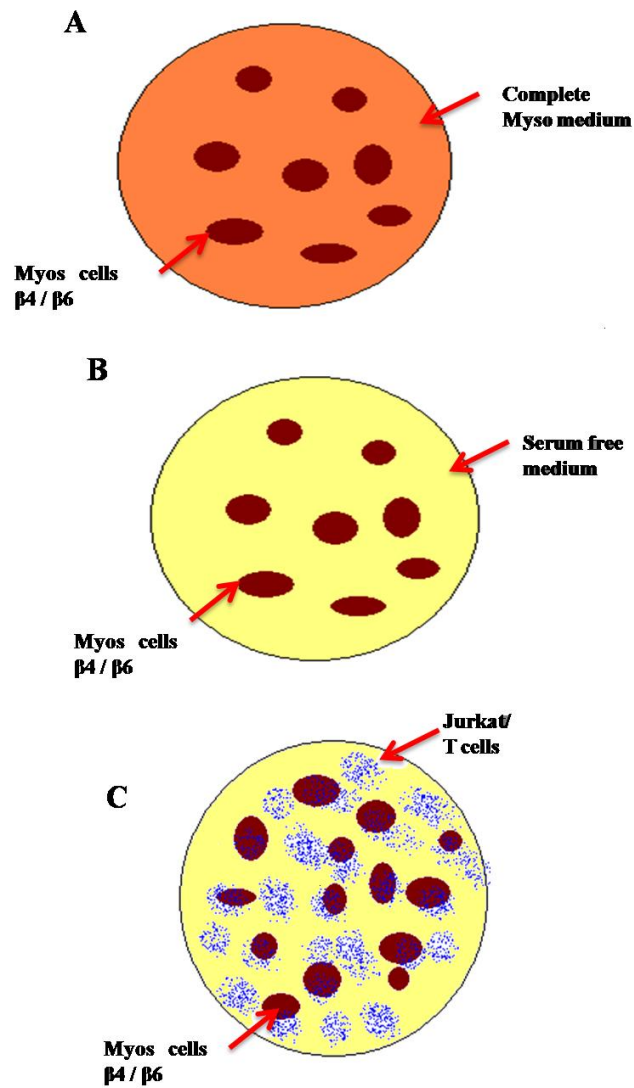


**Figure 2.7 Co-culture of myoepithelial cells with Jurkat or Primary T cells**

$7 \times 10^4$  myoepithelial cells were plated into each well of a 6 well plate and incubated overnight (A). Then the myoepithelial cell medium was replaced with SFM (B). Jurkat/T cells were counted, suspended in the condition medium from the myoepithelial cells and placed back into the wells with the myoepithelial cells to form the co-culture (C).

## 2.9 Cell treatment

$5 \times 10^5$  myoepithelial cells, either  $\beta 4$  or  $\beta 6$  myoepithelial cell lines, were seeded into T25 flasks, with 5 ml of complete myoepithelial medium. The cells were allowed to attach overnight then the medium was replaced with medium containing 500ng/ml of recombinant TRAIL (Peprotech) and the cells cultured for 2, 4 and 8 hrs before protein was extracted for Western blot. In separate flasks, as a control, both cell lines were also exposed to etoposide chemotherapy (1 $\mu$ M/ml) (Sigma) for 4, 6, 8 and 48 hrs to induce apoptosis. A similar experiment was performed using the myoepithelial cell lines following knockdown of galectin-7 (section 2.11), and the cells were then treated with recombinant TRAIL or etoposide at the same concentrations and incubated for the same time course before being harvested. All experiments were performed a minimum of 3 times in duplicate.

## 2.10 Western blotting

### 2.10.1 Preparation of whole cell lysates

Cell pellets were washed with cold PBS and spun at 10,000 rpm, 4°C for 2 minutes twice. 200  $\mu$ L of cold Radio Immune Precipitation Assay (RIPA) buffer (section 1.2, appendix 1) containing protease inhibitor cocktail (Calbiochem) at 1:100 was added to the cells and incubated for 15 minutes on ice. Cells were then centrifuged at 4°C at 13000 rpm for 5 minutes. The cell lysate supernatants were collected and stored at -20° C.

### **2.10.2 Estimation of protein concentration**

Bovine serum albumin (BSA) standards (0.1mg/ml to 5mg/ml) were made up using serial dilutions of a 5mg BSA solution (diluted in PBS). Then, 5 µl of each sample and the BSA standards were loaded into a 96-well plate in triplicate. Measurement of protein concentration was performed using the BioRad Dc protein assay kit (Reagent A, Reagent B, Reagent S) according to manufacturer's protocols. 20µl of A and S mixture (1000:25) was added to each well followed by 200µl of B reagent. After incubation at RT for 10 minutes, the color change was assessed using an ELISA plate reader set up to read the protein assay at an absorbance of 630nm. A standard curve was generated, which was used to determine the protein concentration of the experimental samples.

### **2.10.3 Immunoblotting**

A 1.5 ml acrylamide gel cassette was filled with 12% or 8% SDS-polyacrylamide resolving gel (section 1.3, appendix 1). 1ml of distilled water was added to cover the gel, which was left to set for 30 minutes. The distilled water was removed using filter paper and a stacking gel (section 1.4, appendix 1) was pipetted on the top of the resolving gel. A tooth-comb was inserted and the gel left to set for 30 minutes. The gel cassette was placed in an electrophoresis apparatus and surrounded by running buffer (section 1.5, appendix 1). 10 µl of molecular weight marker (Thermo Fisher Scientific) was loaded into the first well of the gel. Each sample (40µg protein) of the whole cell extract was mixed with 4 x Laemmli buffer containing Bromophenol Blue (Epigentic).

The samples were then denatured at 95°C for 5 minutes and vortexed before being loaded into the gel. The gels were run at 125V for one and half hours until adequate separation was obtained. The proteins were then transferred onto nitrocellulose membrane (Amersham), using a wet blotting system (Biorad) and transfer buffer (section 1.6, appendix1) was added. A constant voltage of 30V was applied until sufficient transfer of proteins had been achieved. The membrane was removed and stained with 0.1% Ponceau S solution to visualize the total protein bands.

#### **2.10.4 Antibody detection**

The membrane was blocked with 5% milk in PBS with 0.1% Tween 20 for 20 minutes at room temperature.

Specific primary antibodies were diluted in 0.1% Tween –PBS with 5% milk. Details of the antibodies and optimal dilutions used in this study are summarized in Table 2.6. Incubation of the membranes with the primary antibodies was performed overnight with shaking at 4°C. After that the membranes were washed 3 times with 0.1% Tween- PBS for 5 minutes each then incubated with mouse or rabbit secondary antibody conjugated to horseradish peroxidase for 1hr at room temperature. To detect the bound antibody, the membranes were washed 3 times for 5 minutes each and incubated in ECL solution (Amersham) for 1 minute. Then they were placed in the film cassette boxes with an X-ray film and developed with an automated developing system.

Table 2.4 Details of antibodies used in Western blot

<b>Antibody species</b>	<b>Dilution</b>	<b>Source</b>
<b>Primary antibody</b>		
<b>Galectin-7</b>	1:1000	Epitomics
<b><math>\beta</math>- Actin</b>	1:5000	Santa Cruz
<b>Cleaved PARP</b>	1:1000	Santa Cruz
<b>HSC70</b>	1: 5000	Santa Cruz
<b><math>\beta</math>6</b>	1:1000	Santa Cruz
<b>CD3</b>	<b>1:1000</b>	Novus
<b>Secondary antibody</b>		
<b>Anti-rabbit-HRP (Goat)</b>	1:1000	Dako
<b>Anti-mouse-HRP (Goat)</b>	1:1000	Dako
<b>Anti-Goat –HRP (Mouse)</b>	1:1000	Dako

### 2.10.5 Blotting for $\beta$ -actin/HSC70

Detection of  $\beta$ -actin or HSC70 was used as a loading control to ensure that the samples were equally loaded. This involved stripping the membrane after detection of the antibody of interest, then washing with TBS/0.05Tween-20 three times for 5 minutes each. The membrane was re-blotted with either  $\beta$ -actin or HSC70 antibody at the appropriate concentration (section 2.10.4) for 1 hr at RT on a rotator. The remainder of the procedure was as described for the primary antibodies (section 2.10.4).



## 2.11 siRNA Transfection

Gene knock down of galectin-7 was conducted using DharmaFECT transfection reagent (Thermo Fisher Scientific) following the manufacturers protocols. For this experiment,  $7 \times 10^4$  cells per-well were plated into 6-well plates and cultured overnight in complete myoepithelial medium. Transfection mixture consisting of 3.3  $\mu$ l of siRNA galectin-7 (L-001719-00, Dharmacon) or 3.3 ml of siRNA non targeting (D-001206-14, Dharmacon), 24  $\mu$ l of interferen (Bioscience) and 1200  $\mu$ l of serum free medium was vortexed for 10 seconds. Cells were incubated with transfection mixture for 10 minutes at room temperature. Cells in each well were supplemented with 2 ml of complete medium and 200  $\mu$ l of siRNA mixture then incubated at 37°C for 48 hrs. Knockdown was confirmed by Western blotting as described in section 2.10.

## 2.12 Detection of apoptosis

Apoptosis was detected in TRAIL- treated cells by Western blot for cleaved PARP (89 KDa) as described in section 2.10.

## 2.13 RNA extraction

RNA extraction from primary cells and cell lines was performed using Quick RNA Miniprep kit (Zymo Research) according to the manufacturer's protocol (section 1.7, Appendix 1).

## 2.14 Quantitation of RNA

All samples were diluted 1: 100 in PCR-grade water. The spectrophotometer was blanked with PCR-grade water and absorbance reading for each sample was recorded at 260nm and the amount of RNA in  $\mu\text{g}/\mu\text{l}$  calculated.

## 2.15 Complementary DNA (cDNA) synthesis

2  $\mu\text{g}$  of isolated RNA was diluted with 12  $\mu\text{L}$  of nuclease free water (NFW). Then, 2  $\mu\text{L}$  of random hexamer primer was added and the mixture was heated at 70°C for 5 minutes and chilled on ice for 4 minutes. 5  $\mu\text{L}$  of 5x first-strand buffer, 5  $\mu\text{L}$  of 0.25 mM dNTP and 1  $\mu\text{L}$  of Molony Murine Leukemia Virus Reverse Transcriptase (M-MLV-RT) were mixed with the RNA, and incubated at room temperature for 10 minutes, followed by 50 minutes at 40°C. Finally, the mix was adjusted with NFW to a final volume of 100  $\mu\text{L}$ . cDNA samples were stored at -20°C until further use. All the chemicals used to generate the cDNA were obtained from Promega.

## 2.16 Polymerase chain reaction (PCR)

Polymerase chain reaction was performed using 2  $\mu$ l of cDNA in a 20 $\mu$ l reaction volume. The PCR mixture used is described in Table 2.7

**Table 2.5 Recipe for the PCR mixture**

Components	Volume ( $\mu$ l)	Source
<b>Megamix</b>	16.5	Sigma
<b>NFW</b>	0.5	Sigma
<b>Forward primer</b>	1	Sigma
<b>Reverse primer</b>	1	Sigma
<b>cDNA</b>	1	
<b>Total</b>	20	

PCR was carried out to determine the expression of galectin-7 in  $\beta$ 4 and  $\beta$ 6 myoepithelial lines. Primary mammary myoepithelial and luminal epithelial cells (isolated by Dr. Jenny Gomm, section 2.1.3.1) were used as positive and negative controls respectively. The cDNA amplification programme used is outlined in Table 2.8.

Table 2.6 cDNA amplification programme

Step	Temperature	Time
<b>Initial denaturation</b>	95°C	5 min
<b>35 cycles</b>		
<b>Denaturation</b>	95°C	45 sec
<b>Primer annealing</b>		45 sec
<b>Galectin-7</b>	65°C	
<b>β6</b>	64.3°C	
<b>DR4</b>	56.8°C	
<b>DR5</b>	55.7°C	
<b>Elongation</b>	72°C	2 min
<b>Final elongation</b>	72°C	10 min
<b>Chilling</b>	4 °C	Infinite

Primer sequences were as follows:

GAPDH forward: CAT CAT CCC TGC CTC TAC TG,

GAPDH reverse: TTG GCA GGT TTT TCT AGA CG

Galectin-7 forward primer: ATG TCC AAC GTC CCCCAC AAG

Galectin-7 reverse primer: TGA CGC GAT GAT GAG CAC CTC

DR4 forward primer: ACAGCAATGGGAACATAGCC

DR4 reverse primer, GTCACTCCAGGGCGTACAAT.

DR5 forward primer, TGCAGCCGTAGTCTTGATTG

DR5 reverse primer, GCACCAAGTCTGCAAAGTCA.

The PCR product was detected by running the reaction product on a 1 % agarose gel in Tris-Acetate-EDTA (TAE) buffer and visualised using ethidium bromide staining.

## 2.17 qPCR

The reaction was performed using the ABI One Plus according to the manufacture's protocol. Each reaction contained 7 $\mu$ l of Sybr Green PCR Master Mix, 300nM of each forward and reverse primer and the equivalent 1 $\mu$ l of cDNA. Conditions for the reaction were 2 minutes at 50°C, 10 minutes at 95°C and then 40 cycles, each consisting of 15 seconds at 95°C, and 1 minute at 60°C.

### 2.17.1 Relative expression level

The threshold level (Ct) is the point at which the fluorescence can be detected. The average Ct value for the triplicates of the samples and GAPDH was calculated and the difference between the two values was determined ( $\Delta$ Ct).

The reference cell line (control)  $\Delta Ct$  was subtracted from the other samples ( $\Delta\Delta Ct$ ). The values were put into the equation  $2^{-\Delta\Delta Ct}$  to give the fold change in expression. The fold change of the reference sample equals 1, so any reduction in the gene expression will be  $<1$  and any increase in the gene expression will be  $>1$ .

## 2.18 Proteome Profiler

All reagents were prepared at room temperature. Array membranes (R&D System) contain 36 different cytokine antibodies were incubated in 2ml of buffer 4 (blocking buffer) for one hr on a rocking platform. 1ml of each sample was added to 0.5 ml of buffer 4 in separate tubes. Then, 15  $\mu$ l of reconstituted Cytokine Array Panel A Detection Antibody Cocktail was added to each prepared sample. The samples were mixed and incubated at RT for one hr. The buffer 4 was aspirated from each membrane, and incubated with the mixture overnight at 2-8°C on a rocking platform. The membrane was washed with 20 ml of the washing buffer for 10 minutes x 2 on a rocking platform shaker. The membrane was then incubated with secondary antibody for 30 minutes, followed by three washes in buffer. The membrane was then incubated in ECL solution (Amersham) for 1 minute after which the membrane was placed in the film cassette boxes with an X-ray film and developed with an automated developing system.

## 2.19 Flow cytometry

Cells were trypsinised and counted.  $4 \times 10^4$  cells were suspended in 1 ml of FACS buffer (DMEM + 1% BSA). An aliquot of 50 $\mu$ l of cell suspension was pipetted into each flow cytometry tube. 50 $\mu$ l of primary antibody at the optimized concentration (Table 2.9) was added and incubated for 45 minutes at 4°C in the dark room.

**Table 2.7 Primary antibodies used for Flow cytometry**

Primary antibody	Dilution	Source
CD3 Alexa fluor <sup>®</sup> 488	1:20	BD
CD4 Alexa fluor <sup>®</sup> 488	1:20	BD
CD8a APC	1:20	BD

Two wash steps with 2ml of FACS buffer were performed, centrifuging the samples at 1200rpm for 5 minutes between washes. Cells were resuspended in 500 $\mu$ l of FACS buffer before being analyzed on the flow cytometry (BD FACS Caliber) using Cell quest program. A negative control, using matched isotype antibody instead of the primary antibody, was used in each run.

When analyzing data, forward scatter and side scatter were plotted, to allow gating of the live cell population. Dead cells were gated out, based either on the appearance of the plot or using the viability stain, propidium iodide (PI), which was added prior to analysis. In order to quantify live cells, a dot plot was set up which plotted the fluorescence of the labeled cells against cell count.

## 2.20 TRAIL ELISA

Both myoepithelial cell lines ( $\beta 4 / \beta 6$ ) were co-cultured with Jurkat or primary T cells for 48 hrs as described in section 2.8.10. Lysates from Jurkat and primary T cells from 3 independent experiments were collected and assayed for TRAIL by ELISA (R & D Systems) according to the manufacturer's protocol.

A protein assay was performed on each of the samples (section 2.10.2). 100  $\mu$ l of protein from each sample was pipetted into an eppendorf and diluted to 400  $\mu$ l with buffer and vortexed. TRAIL standards were prepared with PBS using TRAIL supplied with the Quantikine immunoassay to make concentrations: 1000 pg/ml, 500 pg/ml, 250 pg/ml, 125 pg/ml, 62.5 pg/ml, 31.2 pg/ml, 15.6 pg/ml and distilled water only. The protocol supplied with each kit was then followed. 100  $\mu$ l of assay diluent RD1S was added to each well of the supplied microplate, pre-coated with a monoclonal antibody specific for TRAIL.

50  $\mu$ l of either standard or Sample was added to each well. The sample wells were set up in duplicate and incubated at RT for 2 hours on a shaker. Samples were then aspirated and the wells washed with 200  $\mu$ L of the supplied washing buffer three times. 200  $\mu$ L of Conjugate solution, containing an enzyme-linked polyclonal antibody specific for TRAIL was then added to the wells and incubated at RT for 2 hours on the shaker. Samples were then aspirated and the plate washed with the washing buffer three times. 200  $\mu$ L Substrate Solution was added to each well and the plate covered with foil and incubated for 30 minutes at RT.



The observed colour change is proportional to the amount of TRAIL in the initial sample. 50  $\mu$ L of Stop Solution was added to each well and intensity of the colour change read on an ELISA reader at 450nm with a wavelength correction at 540nm. A standard curve was generated from the TRAIL standards, plotting mean absorbance for each standard against concentration. This was used to derive the absolute values of TRAIL for the samples, which were corrected for the total number of cells in the flask. Throughout, pipette tips were used only once and plate sealers were used during incubation periods.

## **Chapter 3: Inflammatory cell infiltrate in DCIS**

## 3.1 Introduction

---

### 3.1.1 Role of Inflammatory cells in cancer

The inflammatory tumour microenvironment (iTME) contributes significantly to the biological behaviour of cancer (Hanahan and Weinberg 2011). Accordingly, the inflammatory cell infiltrate in the cancer microenvironment can be negatively associated with prognosis, such as with CD68-positive macrophages in Hodgkin's lymphoma (Steidl, Lee et al. 2010) and Ewing's sarcoma (Fujiwara, Fukushi et al. 2011), or be associated with a favourable clinical course as shown for CD8-positive lymphocytes in colon cancer (Fridman, Galon et al. 2011, Galon, Pages et al. 2012). Accumulating evidence has emphasised that the development of cancer and its progression are dependent on a complex interaction of the tumour and the host inflammatory response (Coussens and Werb 2002, de Visser, Eichten et al. 2006, DeNardo and Coussens 2007, Colotta, Allavena et al. 2009, Hanahan and Weinberg 2011), and better characterisation of this interaction should facilitate the use of the immune infiltrate as a prognostic factor and raise strategies for targeting immune cells in the treatment of cancer. A recent review of evidence for the role of inflammatory cells in breast cancer has concluded that despite the large number of published studies, the relationship between different aspects of the inflammatory cell infiltrate and outcome of primary operable breast cancer remains unclear (Mohammed, Going et al. 2012).

Out of a total of 24 studies, 13 showed an association between the inflammatory cell infiltrate and improved survival, 4 studies showed no association and 7 studies concluded that the inflammatory cell infiltrate correlated with poor prognosis. The review suggests that the inconsistencies between published studies is, in large part, due to the absence of methodological validation, underpowered studies (small size of the samples, heterogeneity of tumour subtypes and insufficient follow-up) and the absence of independent validation (Mohammed, Going et al. 2012). Overall, published data on the prognostic value of the inflammatory cell infiltrate in breast cancer remains unclear (Mohammed, Going et al. 2012), emphasising the need for improved analysis of the inflammatory cell infiltrate in stage-specific breast cancer (Kruger, Wemmert et al. 2013).

## 3.2 Rationale for investigation

---

Work in our lab has shown that one of the most consistent changes in myoepithelial cells in DCIS is up-regulation of the integrin  $\alpha v \beta 6$ . Normal myoepithelial cells do not express this integrin, but it is induced in ~60% of DCIS cases with no evidence of invasion, and in >90% of cases of DCIS associated with established invasion (Allen, Thomas et al. 2014). Previous studies have suggested that the extent of inflammatory infiltrate is related to behaviour of DCIS (Lee, Happerfield et al. 1996).

We hypothesised that the changes in myoepithelial phenotype that occur during evolution of DCIS, including up regulation of integrin  $\alpha v \beta 6$ , result in an altered peri-ductal inflammatory microenvironment, the characteristics of which contribute to a pro-tumour phenotype.

The aim of this chapter was to analyse human tissue samples to characterise the extent and nature of the inflammatory cell infiltrate in the DCIS microenvironment, and to relate this to the myoepithelial phenotype. A further aim was to use an in-vivo model to address more directly whether myoepithelial phenotype influences the nature of the inflammatory infiltrate.

### **To address these aims, the approaches used were:**

- Immunohistochemical analysis of a series of DCIS cases of known  $\alpha v \beta 6$  status, using a range of antibodies to characterise and quantitate the peri-ductal inflammatory cell infiltrate.

- In-vivo Matrigel plug assays incorporating  $\alpha\beta6^{+ve}$  and  $\alpha\beta6^{-ve}$  myoepithelial cells then characterised for the nature of inflammatory infiltrate.

### **3.3 Selection of inflammatory cell markers**

To determine the phenotype of infiltrating inflammatory cells, a series of markers was used to identify key immune cell populations. T cell markers used include CD4 and FOXP3 as markers of T regulatory cells, CD8 for cytotoxic T lymphocytes, CD69 expressed on activated T cells, CD45RO identifying activated T cells and also expressed by Treg cells, macrophage markers including CD74 and MHCII, recognising M1 classically activated macrophages, and arginase recognising M2 alternatively activated macrophages.

## 3.4 Methods and Materials

---

### 3.4.1 Immunohistochemistry

Paraffin-embedded sections were stained for  $\alpha\beta6$  and inflammatory markers as described in section 2.4.

### 3.4.2 Scoring of $\alpha\beta6$ IHC staining

Scoring of the extent of  $\alpha\beta6$  staining on DCIS-associated myoepithelial cells has showed that some cases were homogenous positive or negative for  $\alpha\beta6$  and other were heterogenous. Cases that were homogeneously positive or negative for  $\alpha\beta6$  were selected to be stained for the inflammatory cell markers.

### 3.4.3 Scoring of inflammatory cell infiltrate in DCIS

In order to investigate the relationship between  $\alpha\beta6$  expression and inflammatory cell infiltrate, the sections were scanned and scored using Process Image software as described in section 2.5.3.

### 3.4.4 Matrigel assay

A group of C57/Blk6 normal mice were used in this study.  $\beta4$  cells and  $\beta6$  myoepithelial cells were suspended in Matrigel then injected separately into opposite flanks of the mice. B16 mouse tumour was used as positive control. After 9 days when the tumour became palpable the mice were sacrificed and Matrigel with the surrounding tissue was extracted. The Matrigel plugs were processed for staining for the inflammatory cell markers as described in section 2.3.

### **3.4.5 Scoring of inflammatory cell infiltrate in Matrigel plugs**

The numbers of cells positive for different inflammatory cells markers were scored using Imagescope software (section 2.5.4).



## 3.5 Results

### 3.5.1 Selection of DCIS cases

To investigate the relationship between myoepithelial expression of  $\alpha\beta6$  and inflammatory cell profile in the DCIS microenvironment, 47 cases of DCIS were stained for  $\alpha\beta6$ . Sixteen cases of  $\alpha\beta6$ -positive and 15 cases of  $\alpha\beta6$ -negative DCIS were selected for characterisation of the inflammatory cell infiltrate (figure 3.1).

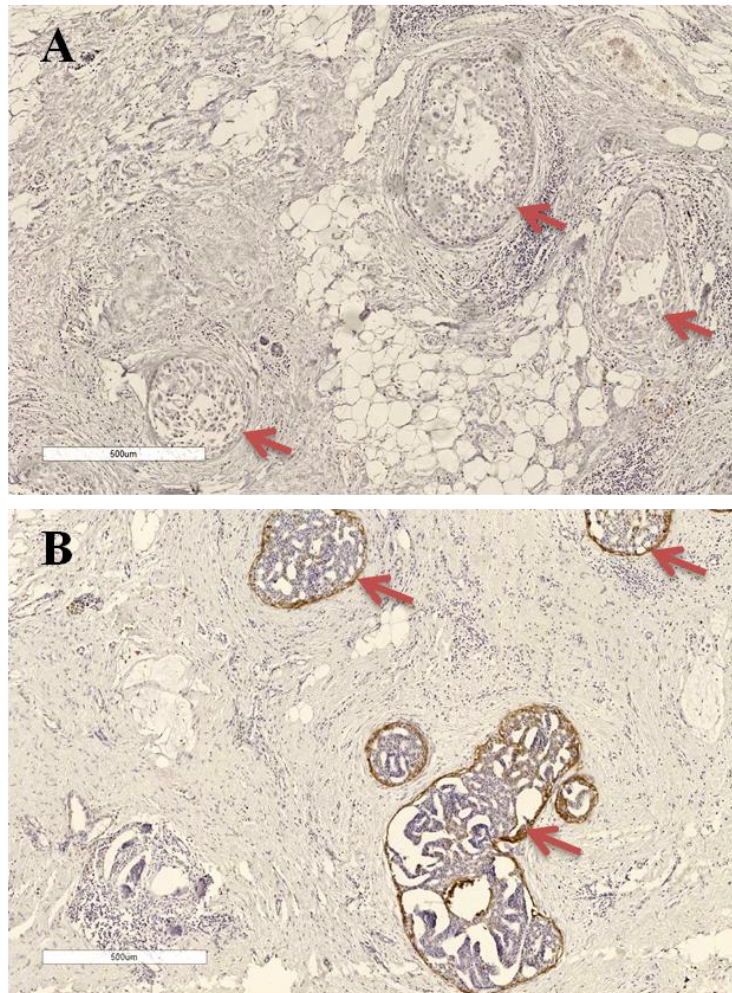


**Figure 3.1** Representative images of DCIS with myoepithelial cells homogeneously negative (A) or positive (B) for  $\alpha\beta6$  integrin.

These cases were selected for staining for inflammatory cells markers.

## **3.5.2 Inflammatory cell infiltrate in DCIS in relation to altered myoepithelial cell phenotype**

### **3.5.2.1 CD69+ve cells in DCIS in relation to $\alpha\beta6$ expression**

CD69 is a membrane receptor transiently expressed on activated T lymphocytes and not detected in resting lymphocytes (Sancho, Gomez et al. 2005). CD69 antibody was first optimised for use on human tonsil tissue as a positive control and when specific staining was achieved, the antibody was applied to the DCIS tissue samples. Immunohistochemistry staining for CD69 antigen was performed on 15 cases of DCIS where the myoepithelial compartment was homogenously positive for  $\alpha\beta6$  and 15 cases homogenously negative for  $\alpha\beta6$ , but only 4 cases of  $\alpha\beta6$ -negative and 14 cases of  $\alpha\beta6$ -positive were scored as other cases had insufficient peri-ductal stroma around the DCIS for evaluation. The cases were scored on a duct-by-duct basis. Images of whole ducts were scanned using NDP software, exported to JPG image format, and analysed using Process Image software (section 2.8.2). At least 4 ducts in each case were analysed, counting the number of cells in a 100 $\mu$ m perimeter around each duct, and the relationship between density of CD69+ve cells and myoepithelial  $\alpha\beta6$  status was determined using the Mann Whitney test. CD69+ve cells were distributed around the ducts in the stroma, within ducts and at the edge of the ducts. The purpose of this study was to investigate the peri-ductal inflammatory cell infiltrate, therefore, only CD69+ve cells around the ducts were counted. The number of CD69+ve cells around the ducts varied between 0 and 47 in both groups of DCIS cases.

However, DCIS ducts positive for  $\alpha\beta6$  showed significantly higher numbers of CD69 +ve cells compared to  $\alpha\beta6$ -ve cases ( $p=0.0001$ ) (figures 3.2 & 3.3).

This suggests that T cell infiltrate in  $\alpha\beta6$  +ve DCIS is more activated.

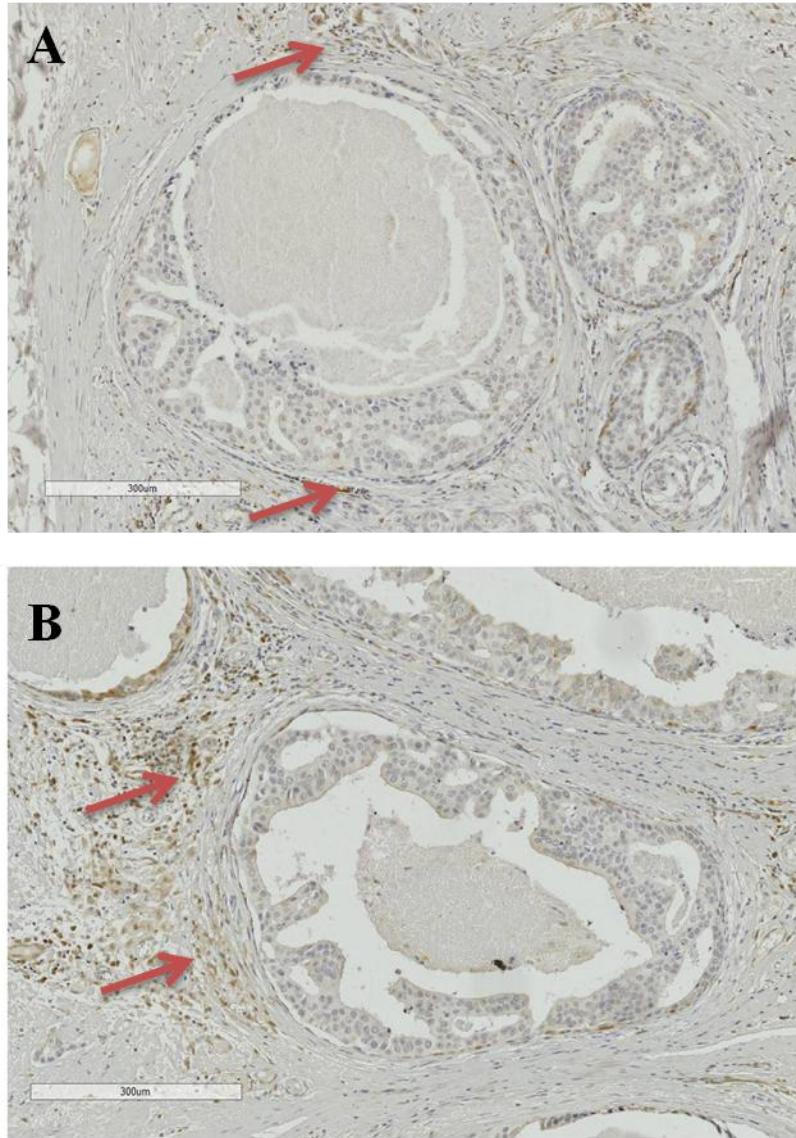


**Figure 3.2 Representative images of CD69 staining in DCIS cases**

DCIS cases homogenously positive or negative for  $\alpha\beta6$  were stained for CD69 and the number of CD69+ve cell around each duct in a 100µm perimeter was quantitated. Higher cell density was detected in the peri-ductal areas of  $\alpha\beta6$ -positive ducts (B) compared to  $\alpha\beta6$ -negative ducts (A).

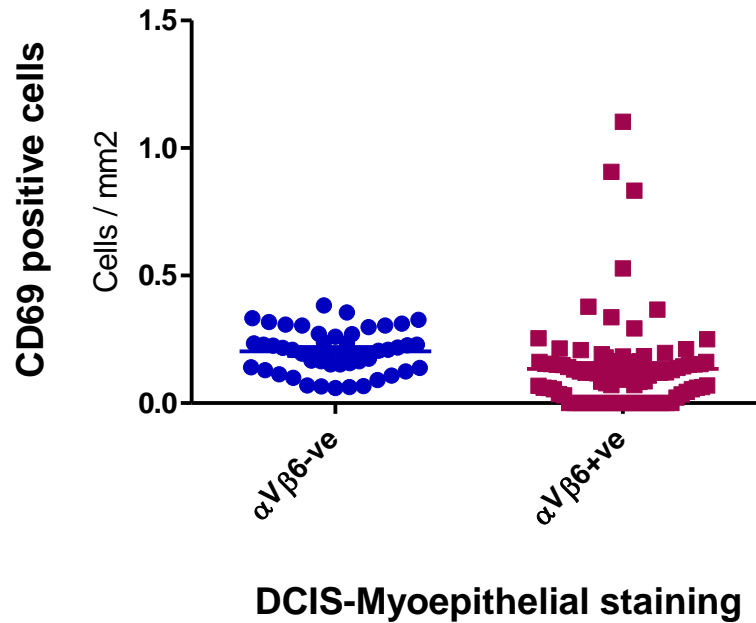


**Figure 3.3** CD69+ve cells in DCIS in relation to myoepithelial  $\alpha\text{V}\beta\text{6}$  status

DCIS cases where the myoepithelial compartment was either homogenously positive or negative for  $\alpha\text{V}\beta\text{6}$  were stained for CD69. Cells positive for CD69 were counted in a region of  $100\mu\text{m}$  around the duct. A total of 4 ducts for each case were scored. Significantly more CD69+ve cells were present around ducts positive for  $\alpha\text{V}\beta\text{6}$  ( $p=0.0001$ ). The four ducts that showed the highest number of CD69 positive cells are derived from two different cases. However, the both cases also include ducts with very low CD69 counts. This suggests the nature of the peri-ductal environment is locally determined varying between ducts in the same case.

### 3.5.2.2 CD4+ve cells in DCIS microenvironment

The same series of DCIS samples was stained for CD4 and human tonsil tissue was used as a positive control. Nine cases of  $\alpha\beta6$ -negative and 12 cases of  $\alpha\beta6$ -positive DCIS had sufficient peri-ductal stroma for scoring. CD4+ve cells were also scattered within the ducts, around the ducts and at the edge of the ducts and only the number of the positive cells around the ducts was counted. In each case, at least 4 ducts have been analysed using Process Images software, counting the number of cell in a 100  $\mu\text{m}$  perimeter around each duct. The number of CD4+ve cells in  $\alpha\beta6$ -positive cases ranged from 0 to 207 and in  $\alpha\beta6$ -negative cases ranged from 0 to 160. However, a higher number of CD4 positive cells was detected around ducts positive for  $\alpha\beta6$  compared to the negative ducts ( $p < 0.01$ ) (figures 3.4 & 3.5).



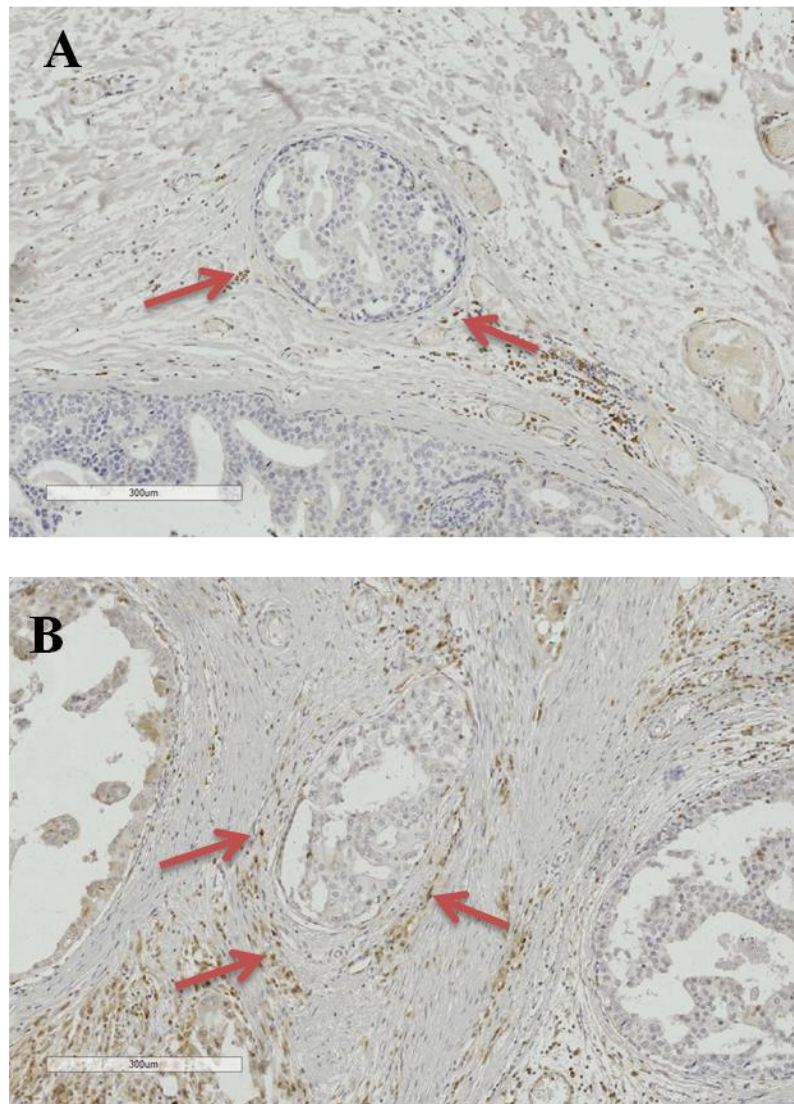


**Figure 3.4 Representative images of CD4 staining in DCIS cases**

DCIS cases positive or negative for  $\alpha\beta6$  were stained for CD4. Positively stained cells are indicated by arrows. A higher infiltrate was present around  $\alpha\beta6$ -positive ducts (B) compared to  $\alpha\beta6$ -negative ducts (A).

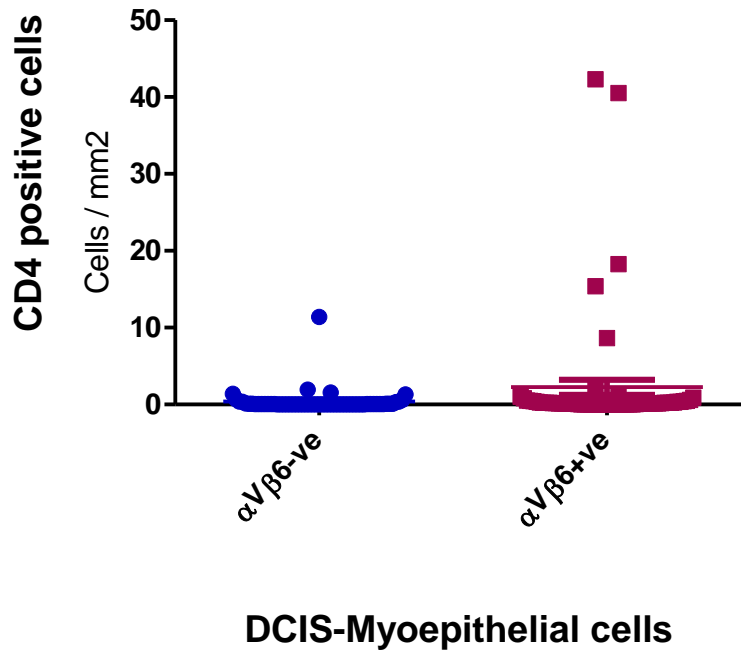


**Figure 3.5 Quantification of CD4+ve cells around DCIS ducts in relation to  $\alpha\text{V}\beta\text{6}$  expression**

The number of CD4 positive cells in a 100 $\mu\text{m}$  perimeter around DCIS ducts positive or negative for  $\alpha\text{V}\beta\text{6}$  was quantitated. This showed significantly higher number of CD4+ve cells in  $\alpha\text{V}\beta\text{6}$ -positive DCIS cases ( $p < 0.01$ ). The five highest scoring datapoints in  $\alpha\text{V}\beta\text{6}$ -positive samples are all derived from a single case. However, this case also contained many ducts with low scoring counts, again indicating the very heterogeneous nature of the samples, even within a case.

### 3.5.2.3 FOXP3+ve cells in DCIS microenvironment

Since FOXP3+ve Treg cells have been implicated as having a role in the progression of breast cancer, their presence in DCIS was investigated. 15 cases of  $\alpha\beta6$  positive and 15 cases of  $\alpha\beta6$  negative DCIS were stained with monoclonal antibody to FOXP3 antigen, using human tonsil tissue as a positive control. Three cases of  $\alpha\beta6$ -negative and 14 cases of  $\alpha\beta6$ -positive DCIS had sufficient peri-ductal stroma for scoring. At least 4 ducts in each case were analysed, counting the number of cells in a 100 $\mu$ m perimeter around each duct using Process Image software. FOXP3+ve cells were also scattered inside the ducts, around the ducts and at the edge of the ducts, but only peri-ductal cells were counted. The level of FOXP3+ve cells varied between  $\alpha\beta6$ -negative cases and  $\alpha\beta6$ -positive cases. The number of FOXP3+ve cells in the peri-ductal area of  $\alpha\beta6$ -negative cases ranged from 0 to 13 while in  $\alpha\beta6$ -positive cases ranged from 0 to 57. However,  $\alpha\beta6$  negative cases showed a lower density of FOXP3+ve cells compared to  $\alpha\beta6$  positive cases (figure 3.6). The positive correlation between  $\alpha\beta6$  +ve myoepithelial cells and the number of FOXP3+ve cells was significant ( $p < 0.01$ ) (figure 3.7).



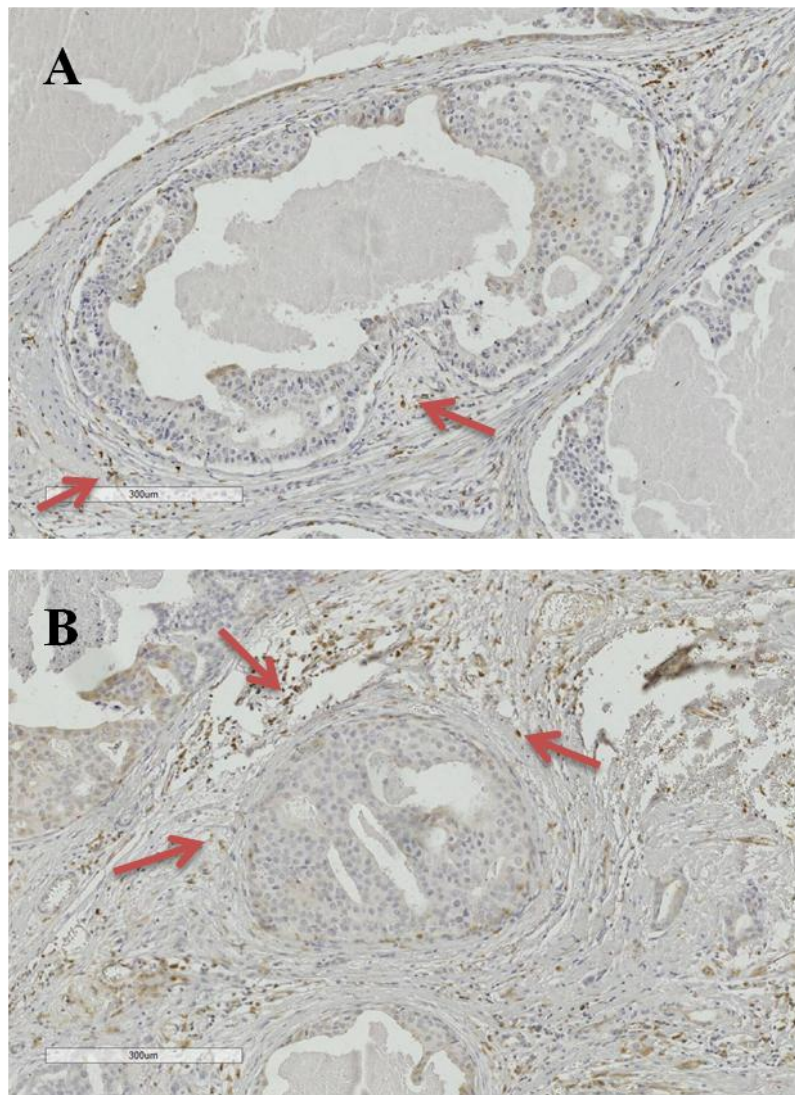


**Figure 3.6 Representative images of FOXP3+ve cells in DCIS cases**

DCIS samples with myoepithelial cells positive or negative for  $\alpha\text{v}\beta\text{6}$  were stained for FOXP3. This demonstrated a higher number of FOXP3+ve cells around ducts positive for  $\alpha\text{v}\beta\text{6}$  (B) compared to those negative for  $\alpha\text{v}\beta\text{6}$  (A). Positively stained cells are indicated by arrows.

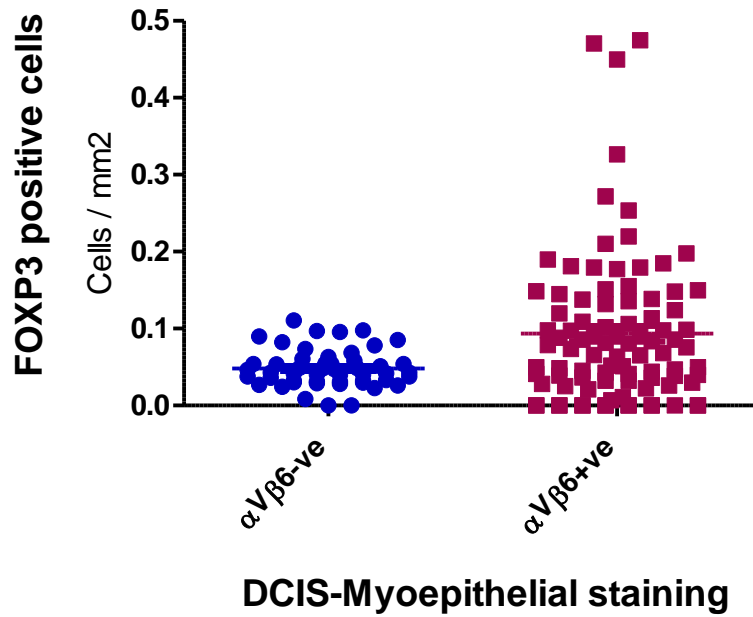


**Figure 3.7 FOXP3+ve cell density in DCIS microenvironment in relation to  $\alpha V\beta 6$  expression**

The number of FOXP3+ve cells in a 100 $\mu$ m perimeter of DCIS ducts positive or negative for  $\alpha V\beta 6$  was quantitated and showed significantly more FOXP3+ve cells in  $\alpha V\beta 6$ -positive cases ( $p < 0.01$ ).

#### 3.5.2.4 CD8 cytotoxic T cell density in DCIS cases

CD8 antibody was tested for use on human tonsil tissue as a positive control and when specific staining was achieved, the antibody was applied to DCIS samples. Three cases of  $\alpha\text{v}\beta 6$ -negative and 7 cases of  $\alpha\text{v}\beta 6$ -positive DCIS had sufficient peri-ductal stroma to allow scoring. At least 4 ducts per cases were analysed using Process Image software. The number of CD8+ve cells varied from 0 to 74 in both groups of DCIS cases. However, the analysis demonstrated a lower number of CD8 positive cells around ducts positive for  $\alpha\text{v}\beta 6$  compared to the negative ducts ( $p=0.0003$ ) (figures 3.8& 3.9).

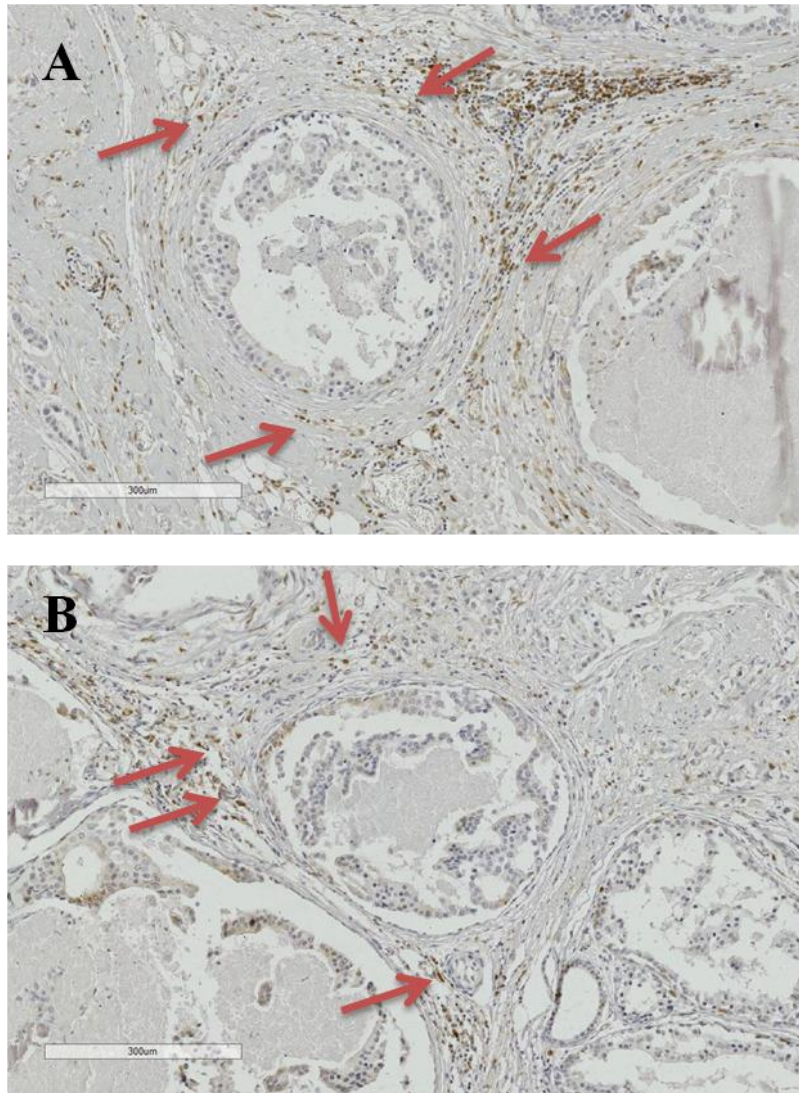


**Figure 3.8 Representative IHC images of CD8+ve cells in DCIS**

DCIS cases with myoepithelial cells positive or negative for  $\alpha v\beta 6$  were stained with CD8 antibody. Positive cells are indicated with arrows. This showed a higher number of CD8+ve cells around ducts negative for  $\alpha v\beta 6$  (A) compared to those positive for  $\alpha v\beta 6$  (B)

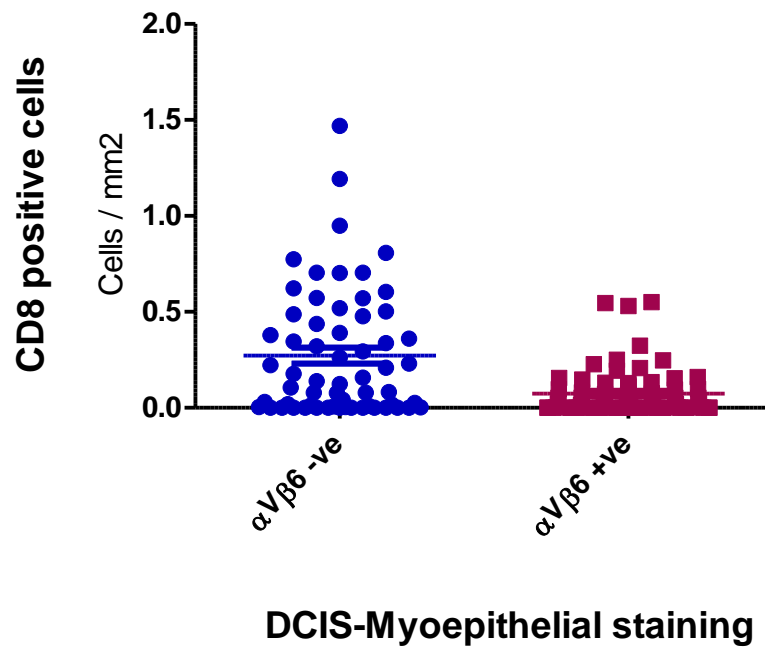


**Figure 3.9 CD8+ve cell density in DCIS in relation to  $\alpha\text{V}\beta\text{6}$  expression**

The number of CD8 positive cells in a 100 $\mu\text{m}$  perimeter around DCIS ducts positive or negative for  $\alpha\text{V}\beta\text{6}$  was quantitated. This showed significantly lower numbers of CD8 +ve cells in  $\alpha\text{V}\beta\text{6}$ -positive DCIS samples ( $p=0.0003$ ).

### 3.5.2.5 DCIS-associated CD45RO+ve cells

CD45RO antibody was optimised for use on human tonsil tissue as a positive control and when the specific staining was achieved, the antibody was applied to DCIS samples. Five cases of  $\alpha\beta6$ -negative and 5 cases of  $\alpha\beta6$ -positive DCIS contained sufficient peri-ductal stroma for scoring. At least 4 ducts in each case were analysed using Process Image software. The number of positive cells in a region of 100  $\mu\text{m}$  around the duct was counted and the proportion ranged from 0 to 145 in both groups of the DCIS cases. Comparing the density of CD45RO+ve cells, no difference was identified between the two groups of DCIS cases ( $p=0.2$ ) (figures 3.10 & 3.11).



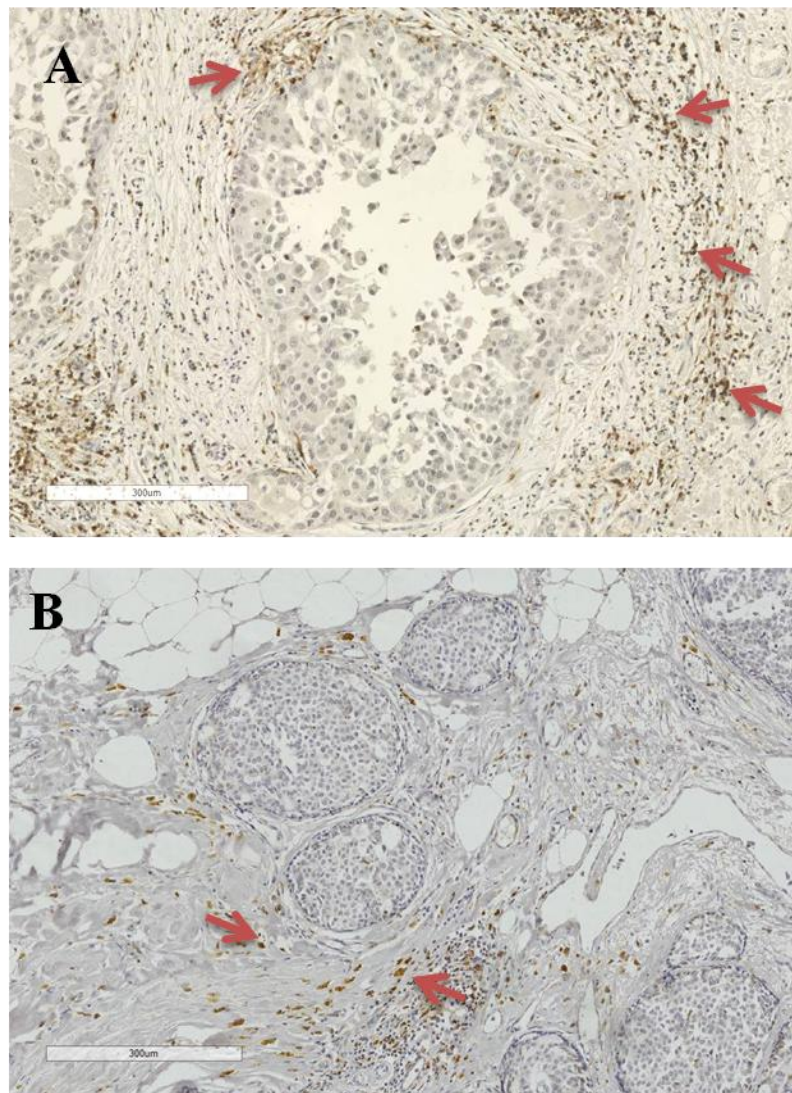


**Figure 3.10 Representative IHC images of CD45RO in DCIS**

A series of cases of DCIS with myoepithelial cells homogenously positive or negative for  $\alpha\beta6$  were stained for CD45RO. Positive cells are indicated by the arrows. The microenvironment of  $\alpha\beta6$  positive (B) and  $\alpha\beta6$  negative (A) cases showed no difference in the number of CD45RO + cells.

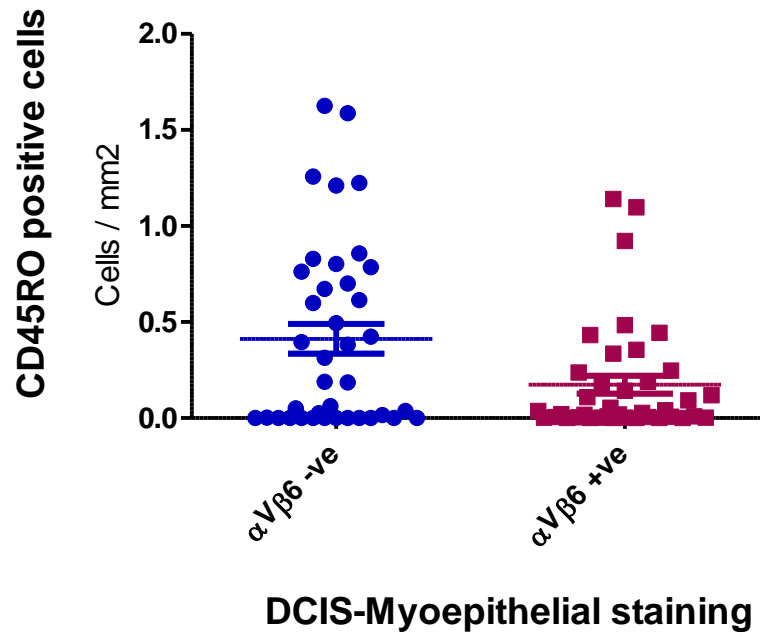


**Figure 3.11 CD45RO+ve cell density in DCIS microenvironment in relation to  $\alpha\text{v}\beta\text{6}$  status**

The number of positive cells in a 100 $\mu\text{m}$  perimeter around DCIS ducts positive or negative for  $\alpha\text{v}\beta\text{6}$  was quantitated. Comparing the proportion of CD45RO+ve cells, no difference was identified between the two groups of DCIS cases ( $p=0.2$ ).



### 3.5.2.6 MHC-II+ve cells in DCIS

Macrophages dominate tumour microenvironments where they play a key role in tumour growth (Balkwill, Charles et al. 2005). Typically, the M1 macrophage phenotype is associated with up-regulation of MHC class II (Quiding-Jarbrink, Raghavan et al. 2010).

In order to investigate the presence of M1 macrophages in DCIS stroma in relation to  $\alpha\beta6$  expression, the same DCIS samples with myoepithelial cells positive or negative for  $\alpha\beta6$  were stained for MHC-II. The antibody was tested on human tonsil as a positive control. Five cases of  $\alpha\beta6$ -negative and 15 cases of  $\alpha\beta6$ -positive DCIS were analysed. At least 4 ducts in each case were analysed using Process Image, and the number of positive cells in a region of 100 $\mu$ m around the duct was counted. The level of MHC-II+ve cells varied between  $\alpha\beta6$ -positive cases and  $\alpha\beta6$ -negative cases. The number of MHC-II+ve cells in  $\alpha\beta6$ -positive cases ranged from 0 to 33 while in the  $\alpha\beta6$ -negative cases was from 0 to 87. This demonstrated a higher number of MHC-II+ve cells around ducts negative for  $\alpha\beta6$  compared to the positive ducts ( $p = < 0.0001$ ) (figures 3.12 & 3.13).

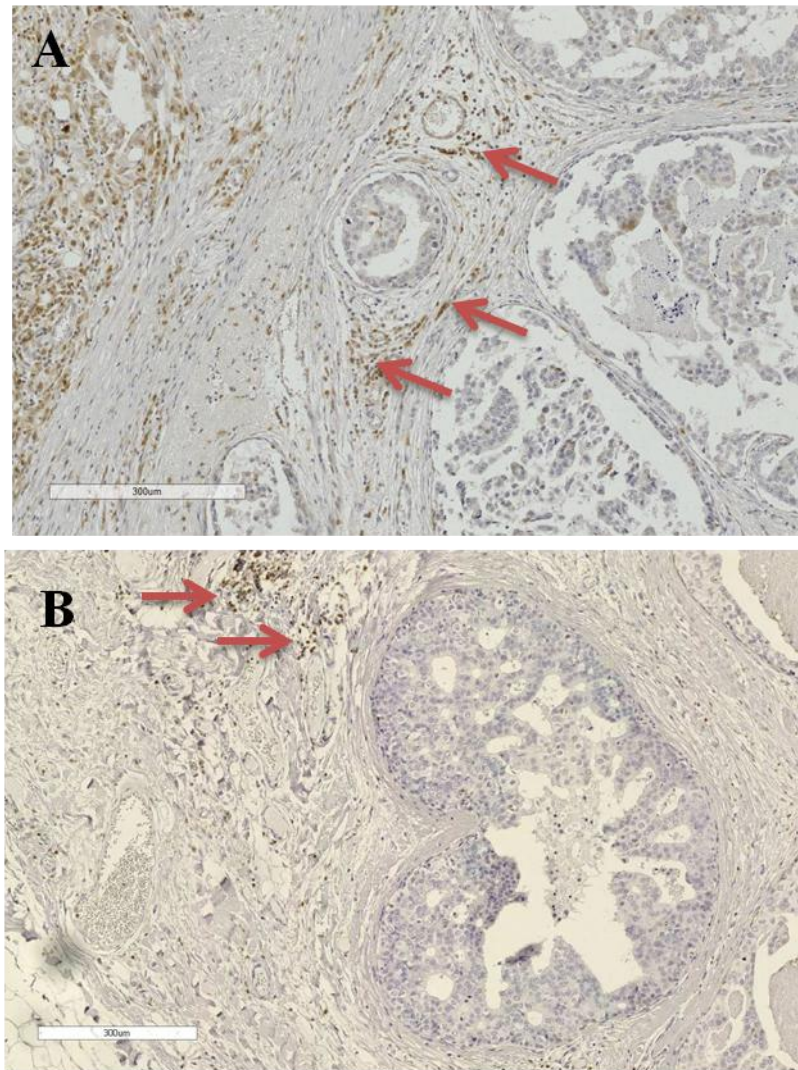


**Figure 3.12 Representative images of MHCII+ve cells in DCIS microenvironment in relation to  $\alpha v \beta 6$  status**

DCIS cases where the myoepithelial compartment was either homogenously positive or negative for  $\alpha v \beta 6$  have been stained with MHC-II antibody. Positive cells are indicated by arrows. A higher infiltrate was present around  $\alpha v \beta 6$  negative ducts (A) compared to  $\alpha v \beta 6$  positive ducts (B).

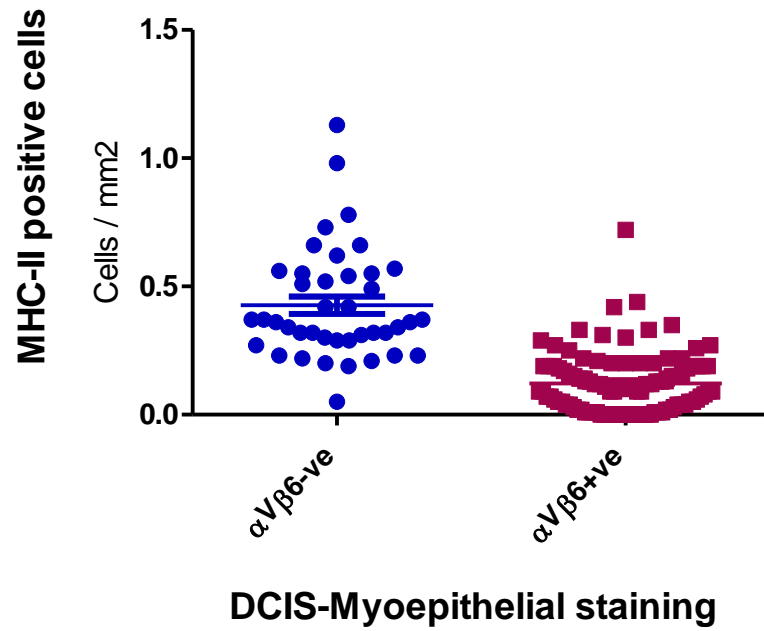


**Figure 3.13 MHC-II+ve cell in DCIS microenvironment in relation to  $\alpha\text{v}\beta\text{6}$  status**

A series of DCIS cases homogenously positive or negative  $\alpha\text{v}\beta\text{6}$  were stained for MHC class II antigen and the number of positive cells in the peri-ductal region was counted. This showed significantly more MHC-II+ve cells around ducts negative for  $\alpha\text{v}\beta\text{6}$  ( $p < 0.0001$ ).

### 3.5.2.7 CD74+ve cell infiltrate in DCIS microenvironment

CD74 is expressed on antigen-presenting cells, including B cells, monocytes, dendritic cells and macrophages (Greenwood, Metodieva et al. 2012). CD74 acts as the high-affinity receptor for the pro-inflammatory cytokine macrophage migration inhibitory factor (MIF) (Leng, Metz et al. 2003).

CD74 was optimised for use on human tonsil tissue and when specific staining was achieved, the antibody was applied to DCIS samples, with three cases of  $\alpha\beta6$ -negative and 5 cases of  $\alpha\beta6$ -positive DCIS being appropriate for scoring. Whole sections were scanned using NDP scanner, and each duct image exported to JPG format. CD74+ve cells were distributed within the ducts, around the ducts and at the edge of the ducts, but only peri-ductal cells were counted. At least 4 ducts in each case were analysed using Process Image software, and the number of positive cells in a region of 100  $\mu\text{m}$  around the duct was counted. The number of positive cells ranged between 0-44 in both groups of DCIS cases, with no significant difference between  $\alpha\beta6$ -positive and negative ducts ( $p=0.1$ ) (Figures 3.14 & 3.15).

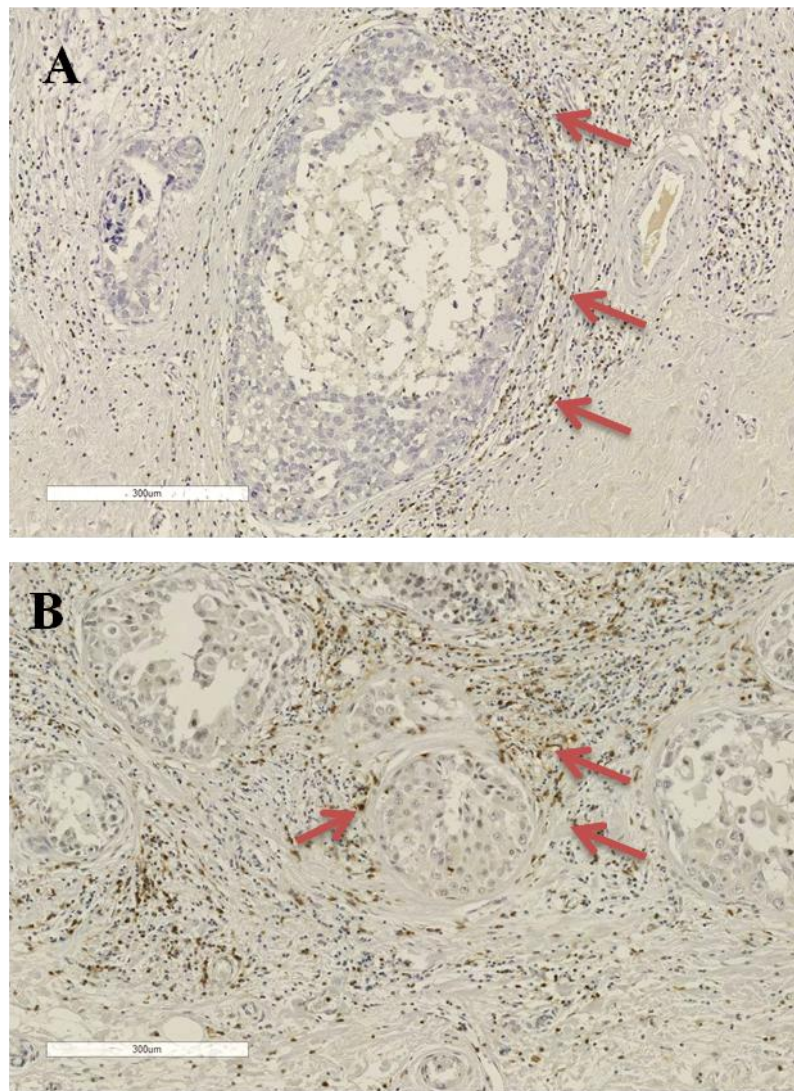


**Figure 3.14 Representative images of CD74+ve cell in DCIS cases**

DCIS cases where myoepithelial cells are homogenously positive or negative for  $\alpha\beta6$  were stained for CD74. Positive cells are indicated by arrows. The microenvironment of  $\alpha\beta6$  positive and  $\alpha\beta6$  negative cases showed no difference in the number of CD74+ve cells.



### 3.5.2.8 CD68+ve cells in DCIS cases

The presence of CD68+ve macrophages in breast cancer has been associated with higher tumour histological grade (Naukkarinen and Syrjanen 1990, Lee, Happerfield et al. 1997, Volodko N 1998). To investigate the relationship with altered myoepithelial phenotype, the CD68 antibody was tested on human tonsil tissue as a positive control and when specific staining was achieved, the antibody was applied to the same series of DCIS cases positive or negative for  $\alpha\text{v}\beta\text{6}$ . Five cases of  $\alpha\text{v}\beta\text{6}$ -negative and 13 cases of  $\alpha\text{v}\beta\text{6}$ -positive DCIS had sufficient peri-ductal stroma for analysis. At least 4 ducts in each case were analysed using Process Image, and the positive cells in a 100 $\mu\text{m}$  perimeter were quantitated. The number of CD68+ve cells ranged between 0 and 110 in the peri-ductal area of  $\alpha\text{v}\beta\text{6}$ -negative cases while in  $\alpha\text{v}\beta\text{6}$ -positive cases ranged between 0 and 270. Comparing the number of CD68+ve cells, no difference was detected between  $\alpha\text{v}\beta\text{6}$  positive and  $\alpha\text{v}\beta\text{6}$  negative cases ( $p=0.5$ ) (figures 3.16 & 3.17).



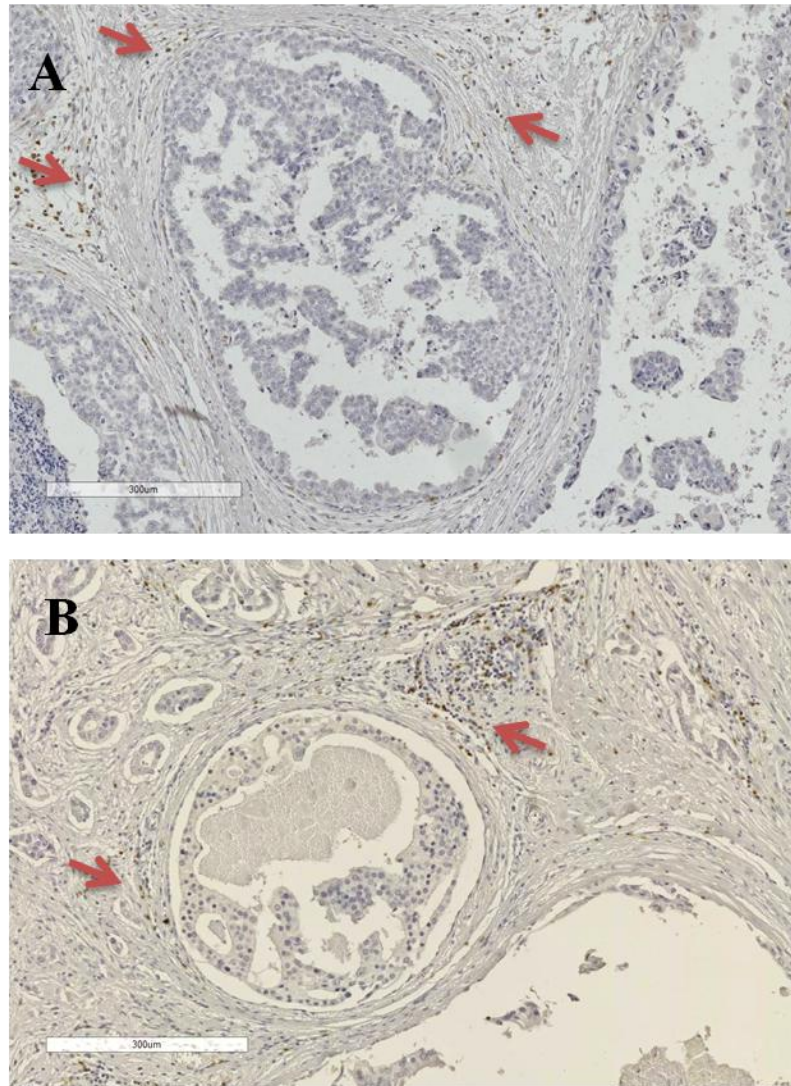


**Figure 3.16 Representative images of CD68+ve cells in DCIS stroma in relation to  $\alpha\beta 6$  status**

The microenvironment of  $\alpha\beta 6$  positive and  $\alpha\beta 6$  negative cases showed no difference in the number of CD68+ve cells. Positively stained cells were indicated by arrows.



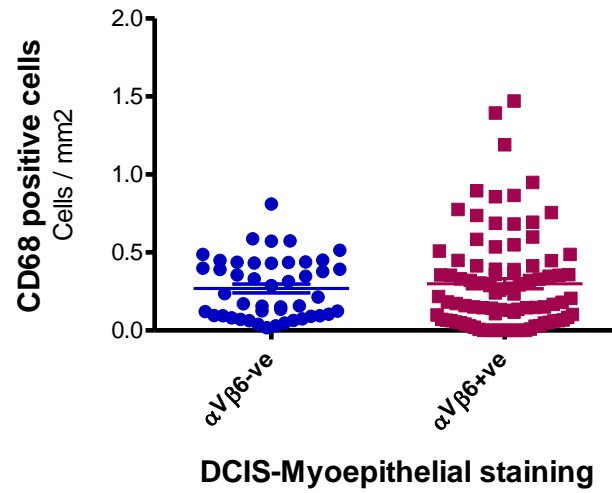


**Figure 3.17 CD68+ve cells in DCIS microenvironment in relation to  $\alpha\text{v}\beta\text{6}$  expression**

A series of DCIS cases homogeneously positive or negative for  $\alpha\text{v}\beta\text{6}$  were stained for CD68 antigen and the number of positive cells in the peri-ductal region was counted as described. . Comparing the proportion of CD68+ve cells, no difference was identified between the two groups of DCIS ( $p=0.5$ ).

### 3.5.2.9 Arginase-1+ve cells in DCIS microenvironment

It has been reported that M2 macrophages express arginase-1 (El Kasmi, Qualls et al. 2008), therefore, in order to investigate M2 macrophages in DCIS stroma in relation to  $\alpha\text{v}\beta\text{6}$  status, arginase-1 antibody was optimised on normal human liver as a positive control and when specific staining was achieved, the antibody was applied to the same series of DCIS cases. Seven cases of  $\alpha\text{v}\beta\text{6}$ -negative and 12 cases of  $\alpha\text{v}\beta\text{6}$ -positive DCIS were appropriate for analysis. Whole sections were scanned using NDP scanner, and each duct image exported to JPG format. At least 4 ducts per case were analysed using Process Image, and the number of arginase-1 positive cells in a 100 $\mu\text{m}$  perimeter around the duct was counted. The number of arginase-1+ve cells ranged between 0 and 47 in  $\alpha\text{v}\beta\text{6}$ -positive cases and between 0 and 10 in  $\alpha\text{v}\beta\text{6}$ -negative cases. Interestingly, the peri-ductal microenvironment in  $\alpha\text{v}\beta\text{6}$  +ve cases showed a higher number of arginase-1 +ve cells compared to the  $\alpha\text{v}\beta\text{6}$ -ve cases ( $p=0.0001$ ) (figures 3.18 & 3.19), suggesting that  $\alpha\text{v}\beta\text{6}$  expression in DCIS is associated with M2 macrophage infiltration.

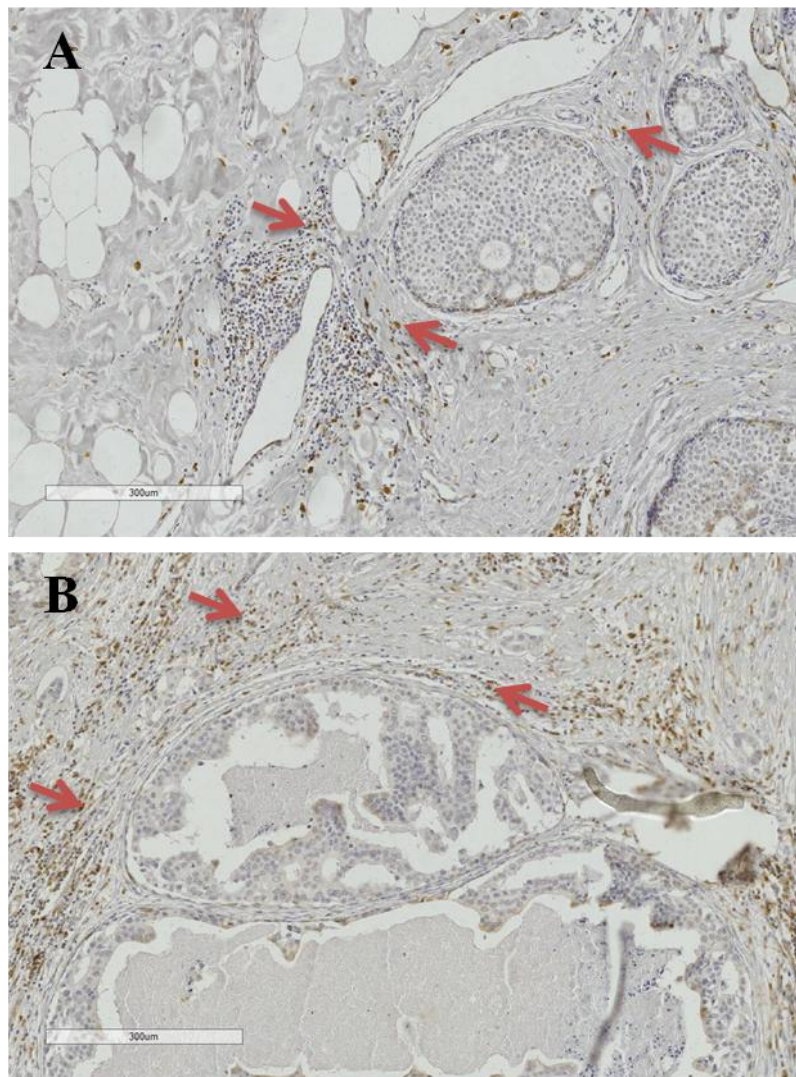


**Figure 3.18 Representative images of arginase-1+ve cells in DCIS stroma in relation to  $\alpha\beta6$  status**

The microenvironment of  $\alpha\beta6$  positive DCIS cases (B) showed a higher number of arginase-1+ve cells compared to the negative cases (A). Positive cells are indicated by arrows.

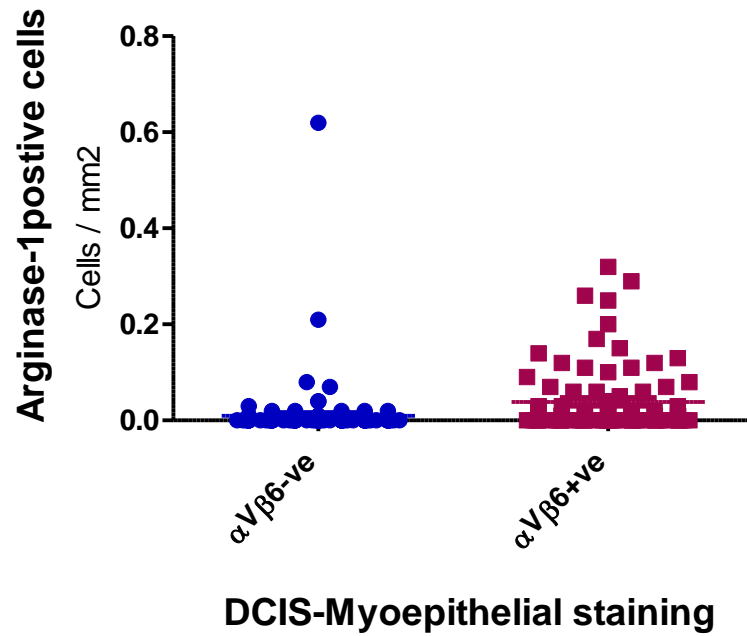


**Figure 3.19 Arginase-1+ve cells in DCIS microenvironment in relation to  $\alpha v\beta 6$  expression**

The number of arginase-1 positive cells in a region of 100 $\mu$ m around DCIS ducts was counted. This demonstrates significantly higher numbers of arginase-1+ve cells in  $\alpha v\beta 6$ -positive DCIS cases compared to the  $\alpha v\beta 6$ -negative ducts ( $p=0.0001$ ).

### 3.5.3 Inflammatory cell profile in relation to $\alpha\beta6$ status

In order to gain a picture of the relative levels of the different inflammatory cell types in  $\alpha\beta6$ -positive and  $\alpha\beta6$ -negative DCIS, the mean of each cell type in all the  $\alpha\beta6$  positive ducts and  $\alpha\beta6$  negative ducts was calculated, and then the different cell types were expressed as a percentage of the total inflammatory infiltrate (figure 3.20). This demonstrated that CD4+ve cells were the most dominant cell in  $\alpha\beta6$ -positive DCIS cases while MHC-II+ve cells were the dominant population in  $\alpha\beta6$ -negative DCIS cases (figure 3.20 A& B). Although the relative number of FOXP3+ve cells was small, they made up 3% of the population in  $\alpha\beta6$ -positive cases and only 2% in  $\alpha\beta6$ -negative cases. In contrast, CD8+ve cell number was nearly three-fold in the cases negative for  $\alpha\beta6$  compared to  $\alpha\beta6$ -positive cases (figure 3.20 A).

CD45RO+ve cells were the second dominant cell type in the microenvironment of  $\alpha\beta6$  negative cases (figure 3.20 A), while they represent only 5% of inflammatory cell infiltrate in  $\alpha\beta6$  positive DCIS cases (figure 3.20 B). FOXP3+ cells and arginase-1 + cells represent a minor component of the inflammatory cell population in both groups of DCIS cases (figure 3.20 A).

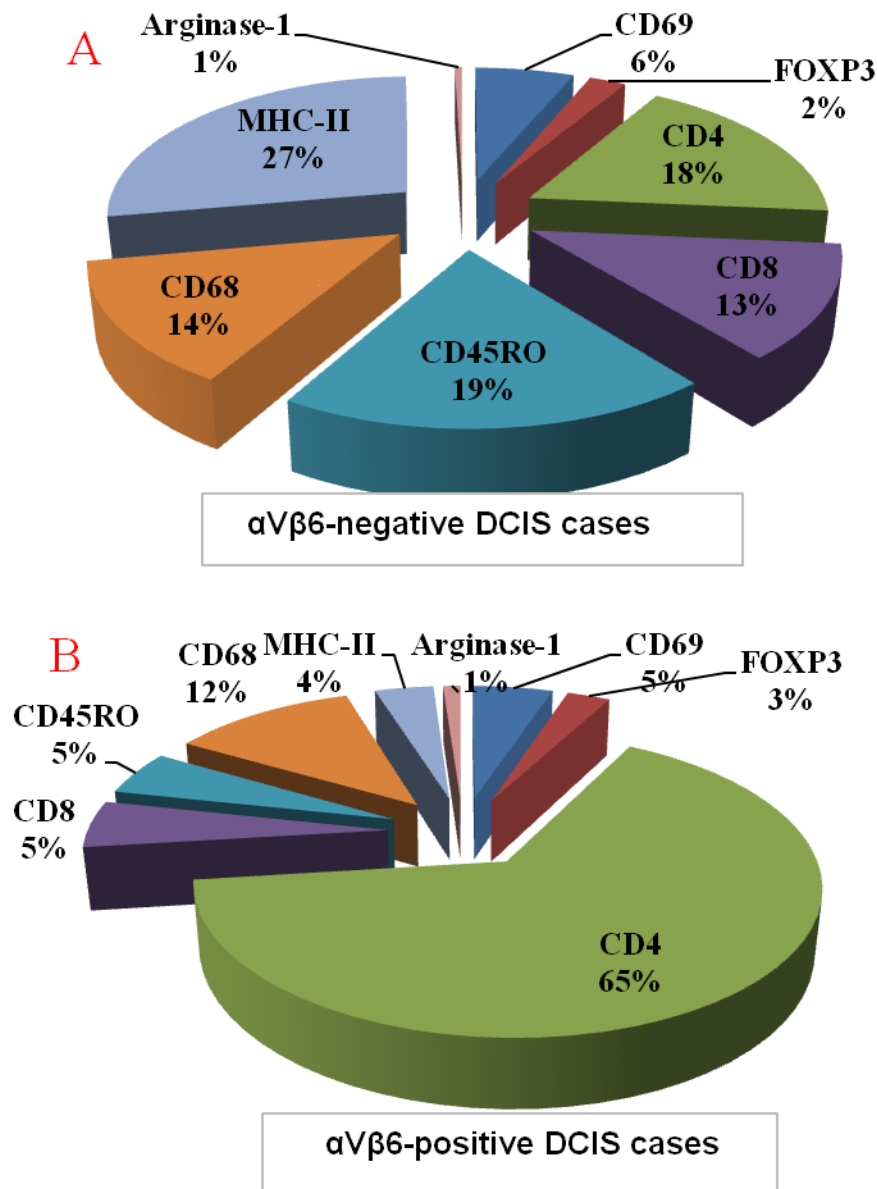


**Figure 3.20 Percentage of inflammatory cell populations in the peri-ductal microenvironment of DCIS in relation to  $\alpha\text{V}\beta\text{6}$  status**

CD4 + cells are the dominant cell in  $\alpha\text{V}\beta\text{6}$ -positive DCIS cases while MHC-II+ve cells are the dominant population in  $\alpha\text{V}\beta\text{6}$ -negative DCIS cases. CD8+ cells represent 13% in negative cases (A) and 5% in positive cases (B). FOXP3+ cells and arginase-1 + cells are a minor population in both DCIS groups. Numbers of CD45RO +ve cells are very low in the  $\alpha\text{V}\beta\text{6}$ -positive cases (B), but represent the second dominant population in the  $\alpha\text{V}\beta\text{6}$ -negative cases (A).

### **3.5.4 Analysis of the inflammatory cell infiltrate in relation to myoepithelial $\alpha\beta6$ status *in-vivo***

The immunohistochemical analysis of DCIS samples for peri-ductal inflammatory cell infiltrate suggests that expression of  $\alpha\beta6$  in DCIS-associated myoepithelial cells correlates with a higher Treg cell and M2 macrophage infiltrate. To test this more directly, the second part of this chapter aimed to study the relationship between  $\alpha\beta6$  status and the inflammatory cell infiltrate using an *in-vivo* assay.

Matrigel plugs containing either  $\beta6$  ( $\alpha\beta6$ -positive) or  $\beta4$  ( $\alpha\beta6$ -negative) myoepithelial cells were injected into the flanks of 6 mice. B16 mouse melanoma cells were used as a positive control. After 9 days when the tumours became palpable, the mice were sacrificed, and Matrigel with the surrounding tissue was extracted. The gels were formalin fixed and paraffin embedded and sections were stained for inflammatory cell markers. Matrigel plugs without myoepithelial cells were used as negative controls.

#### **3.5.4.1 Quantitation of CD4<sup>+</sup>ve T cells in Matrigel plug assays**

CD4 antibody was optimised on normal mouse spleen tissue and when specific staining was achieved, the antibody was applied to Matrigel plugs containing either  $\beta4$  or  $\beta6$  myoepithelial cells (section 2.3). Whole sections were scanned using NDP software and analysed using Imagescope software (section, 2.9.2.1). The scoring scheme parameters specifying the staining intensity threshold of CD4 were set up and the software was run to count the cells positive for CD4 over the entire section. The result was exported to an Excel

file and the number of CD4+ve cells per mm<sup>2</sup> was calculated, and plotted on graph using prism software. This showed a higher number of CD4+cells in Matrigel plugs containing  $\beta$ 6 cells compared to Matrigel plugs containing  $\beta$ 4 cells (p=0.005) (figures 3.21 & 3.22).

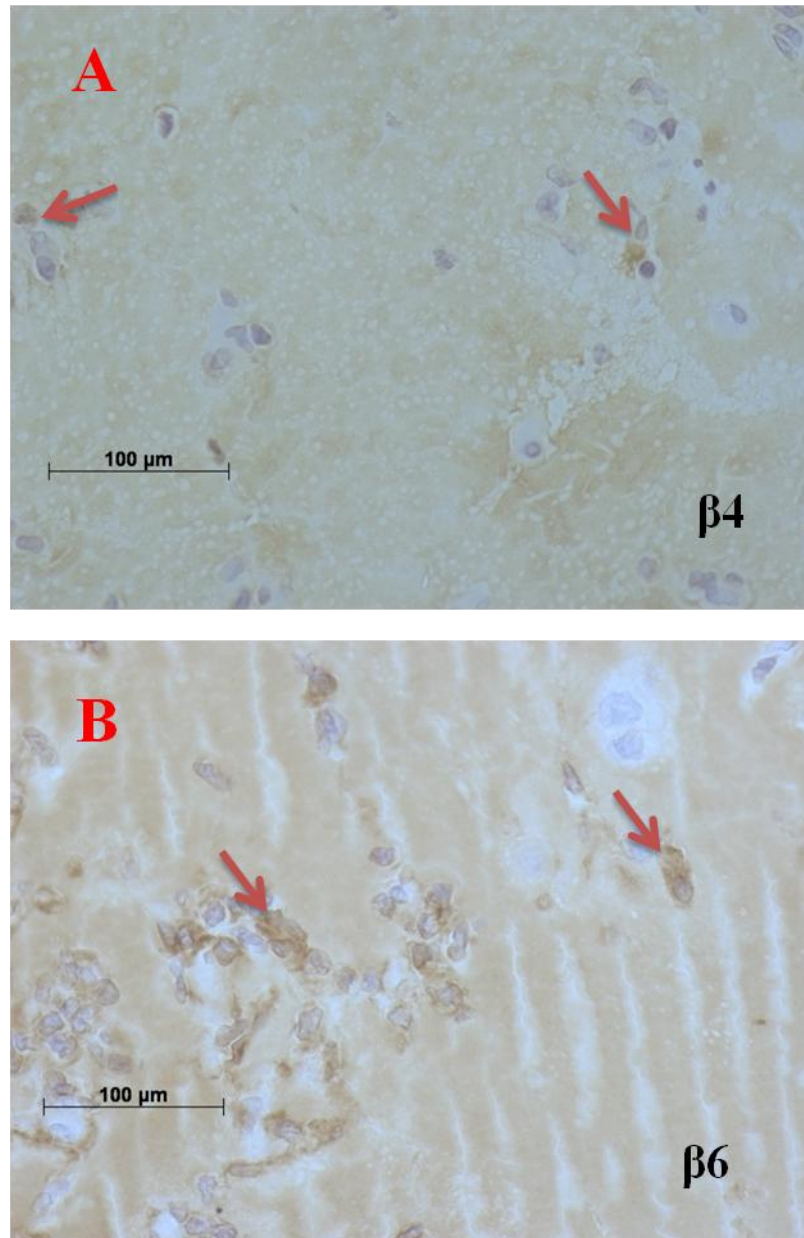


**Figure 3.21 Representative images of CD4+ve cells in Matrigel plugs**

The number of CD4+ve cells in Matrigel plugs containing either  $\beta$ 4 or  $\beta$ 6 cells was analysed using Imagescope software. Matrigel plugs containing  $\beta$ 6 cells (B) showed a higher number of CD4+ve cells per unit area compared to those plugs containing  $\beta$ 4 cells (A). Positively stained cells are indicated by arrows.



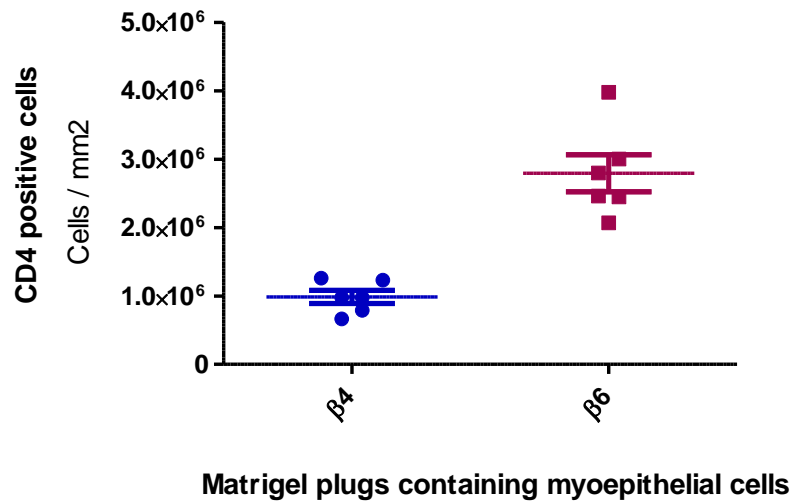


**Figure 3.22 CD4+ve cells in Matrigel plugs containing myoepithelial cells**

The number of CD4+ve cells in Matrigel plugs containing either β4 or β6 myoepithelial cells was analysed as described. This showed more CD4+ve cells were present in Matrigel plugs containing β6 cells compared to Matrigel plugs containing β4 cells ( $p=0.005$ ).

#### **3.5.4.2 Density of FOXP3+ve cell in Matrigel plugs**

The same series of Matrigel plugs containing myoepithelial cells were stained for FOXP3 and normal mouse spleen tissue was used as a positive control. Whole sections of Matrigel plugs were scanned using NDP and the number of FOXP3+ve cells was analysed using Imagescope software. Appropriate scoring parameters detecting the specific staining of FOXP3 were set up and the Imagescope software was run to count cells positive for FOXP3 over the entire section. The result was exported to an Excel file and the number of FOXP3+ve cells per mm<sup>2</sup> was calculated and plotted on a graph. This demonstrated a higher number of FOXP3+ ve cells in Matrigel plugs containing  $\beta$ 6 cells compared to Matrigel plugs containing  $\beta$ 4 cells (p=0.007) (figures 3.21 & 3.22).

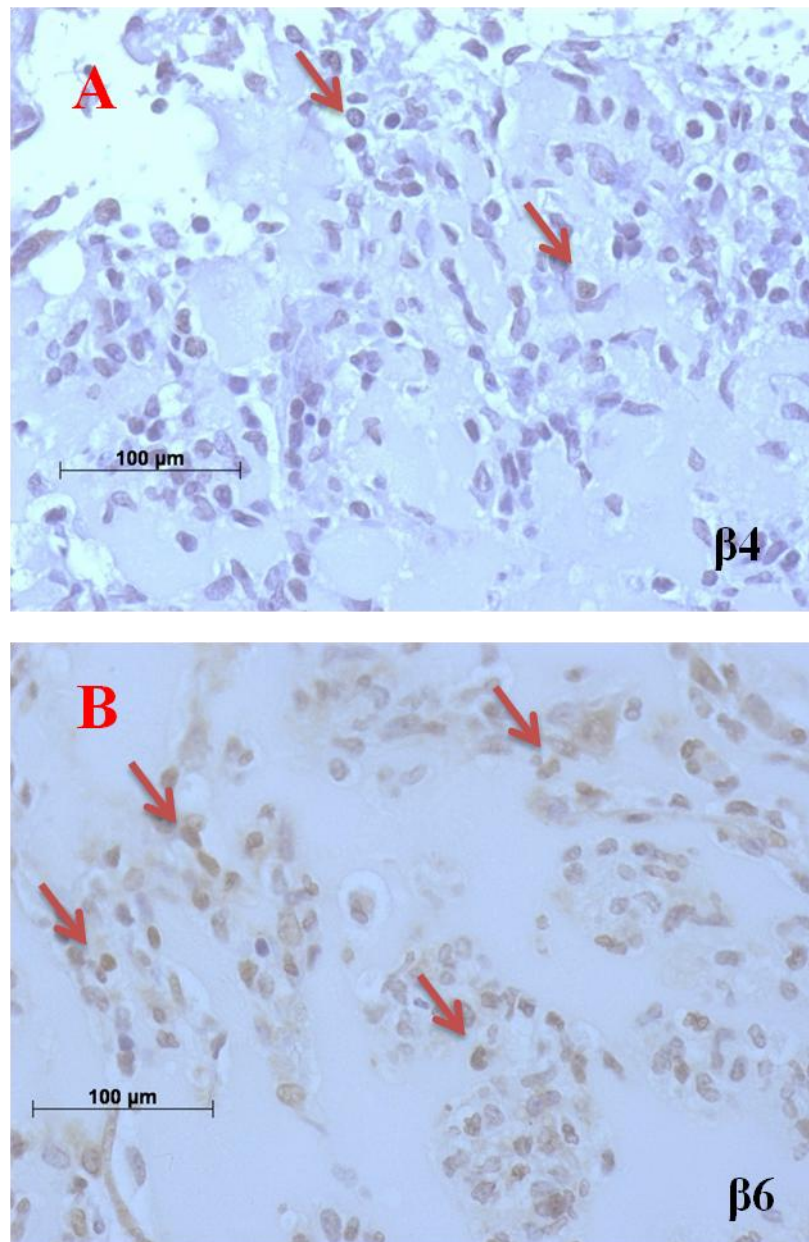


**Figure 3.23 Representative images of FOXP3+ve cells in Matrigel plugs**

The same series of the Matrigel plugs containing myoepithelial cells were stained for FOXP3. Positive cells are indicated by arrows. FOXP3+ve cells were counted using Imagescope software and significantly more FOXP3+ve cells were present in Matrigel plugs containing β6 cells (B) compared to those plugs containing β4 cells (A).

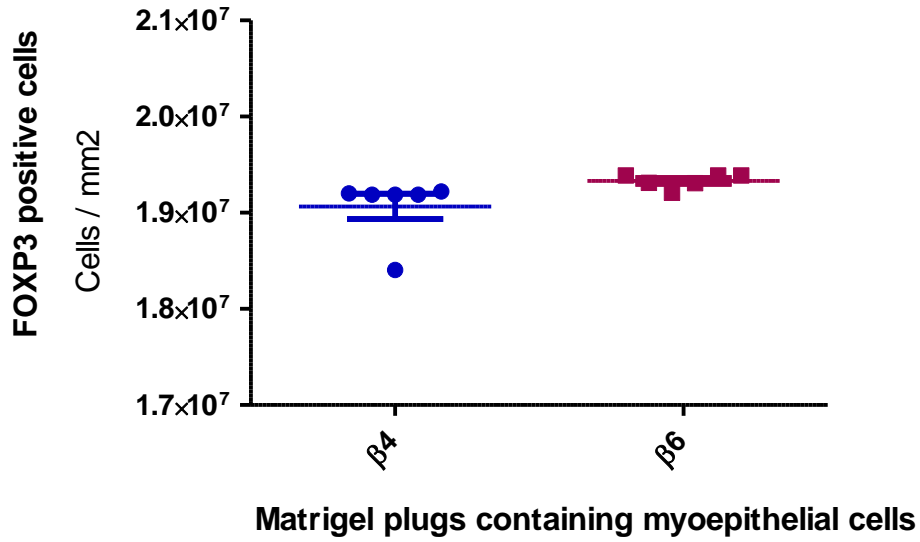


**Figure 3.24 Distribution of FOXP3+ve cells in Matrigel plugs containing myoepithelial cells**

The number of FOXP3+ve cells in Matrigel plugs containing either  $\beta 4$  or  $\beta 6$  myoepithelial cells was analysed using Imagescope software. Significantly more FOXP3+ve cells were present in Matrigel plugs containing  $\beta 6$  cells compared to the Matrigel plugs containing  $\beta 4$  cells ( $p=0.007$ ).

### 3.5.4.3 Density of CD8+ve T cells in Matrigel plugs

CD8 antibody was optimised for use on normal mouse spleen tissue as a positive control and when specific staining was achieved, the antibody was applied to the same series of Matrigel plugs containing myoepithelial cells. The sections from Matrigel plugs were scanned using NDP software and the number of CD8+ve cells was analysed using Imagescope software. The scoring scheme parameters detecting the specific staining of CD8 were set up and the Imagescope software was run to count cells positive for CD8 over the entire section. The result was exported to an Excel file and the number of CD8+ve cells per mm<sup>2</sup> was calculated and plotted on a graph using prism software. Comparing the number of CD8+ve cells, no difference was identified between Matrigel plugs containing  $\beta$ 4 cells and Matrigel plugs containing  $\beta$ 6 myoepithelial cells ( $p=0.6$ ) (figures 3.25 & 3.26).

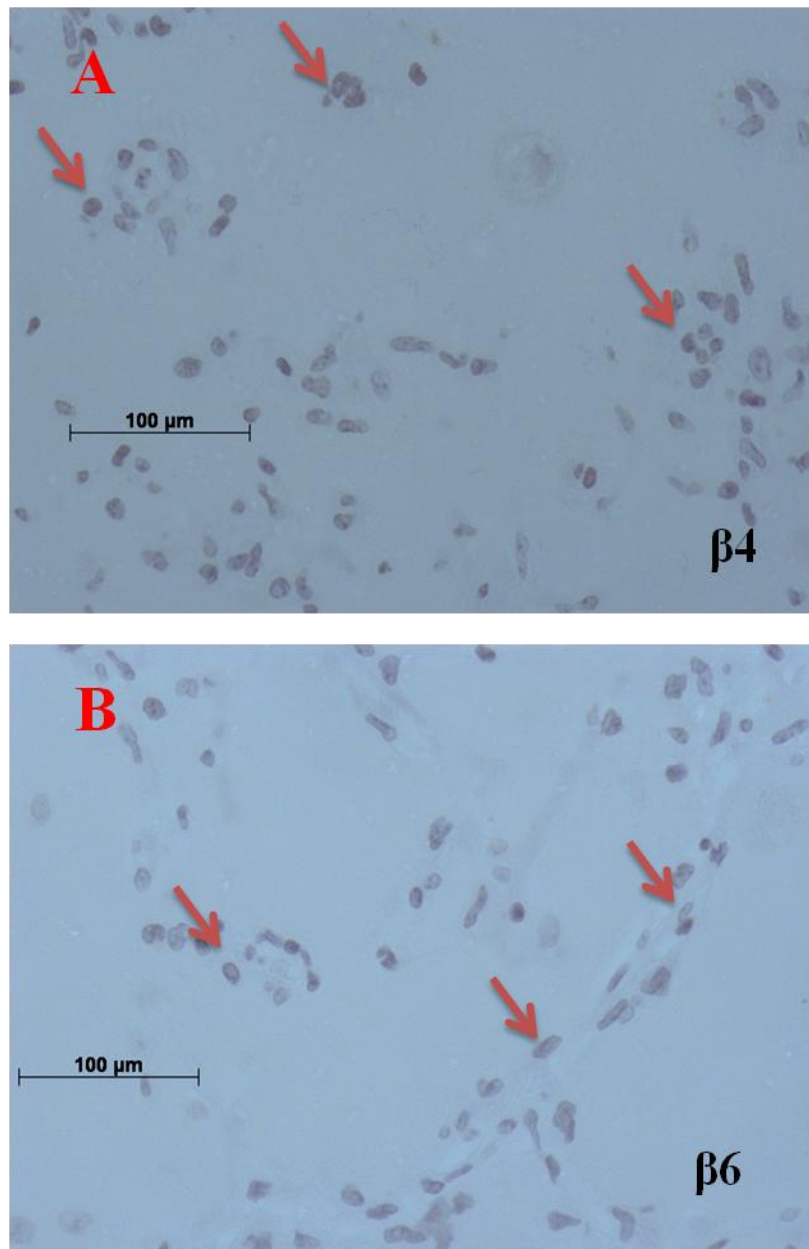


**Figure 3.25 Representative images of CD8+ve cells in Matrigel plugs**

The same series of Matrigel plugs containing myoepithelial cells was stained for CD8. The number of CD8+ve cells was quantitated using ImageScope software. This demonstrated no difference between the number of CD8+ve cells in Matrigel plugs containing β4 cells (A) and Matrigel plugs containing β6 cells (B). Positive cells indicated by arrows.

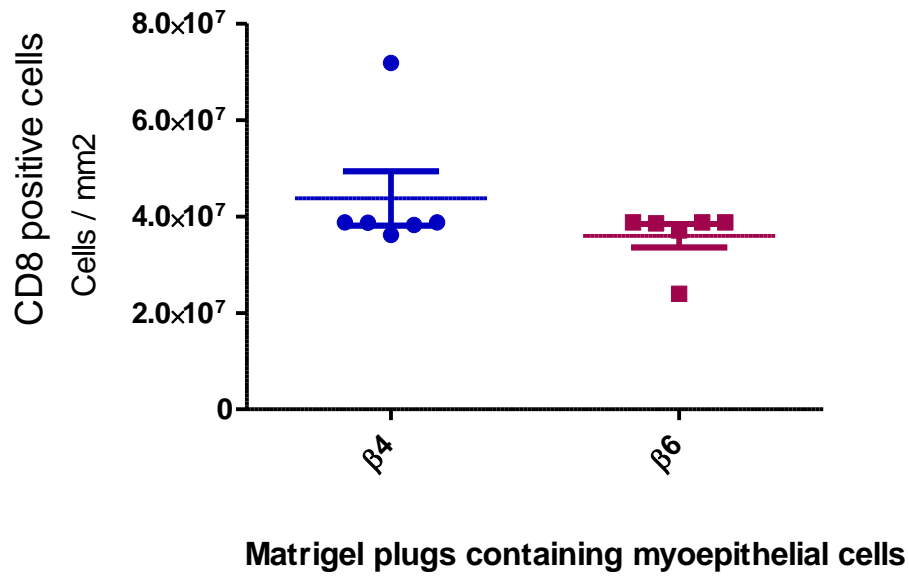


**Figure 3.26** Distribution of CD8+ve cells in Matrigel plugs

The number of CD8+ve cells in Matrigel plugs containing either  $\beta 4$  or  $\beta 6$  myoepithelial cells was counted using ImageScope software. This showed no difference between the two groups of Matrigel plugs ( $p=0.6$ ).

#### **3.5.4.4 Quantitation of CD74+ve cells in Matrigel plugs**

The same series of Matrigel plugs containing myoepithelial cells was stained for CD74 and normal mouse spleen tissue was used as a positive control. The slides were scanned using NDP software. Each section from the Matrigel plugs was opened in Imagescope software, appropriate scoring parameters to detect the specific staining of CD74 in the cells were set up and the software was run to count the cells positive for CD74 in the total area of the section. The result was exported to an Excel file and number of CD74+ve cells per mm<sup>2</sup> was calculated, and plotted on a graph using prism software. This showed no difference between Matrigel plugs containing  $\beta$ 4 cells and Matrigel plugs containing  $\beta$ 6 myoepithelial cells (p=0.9) (figures 3.27 & 3.28).



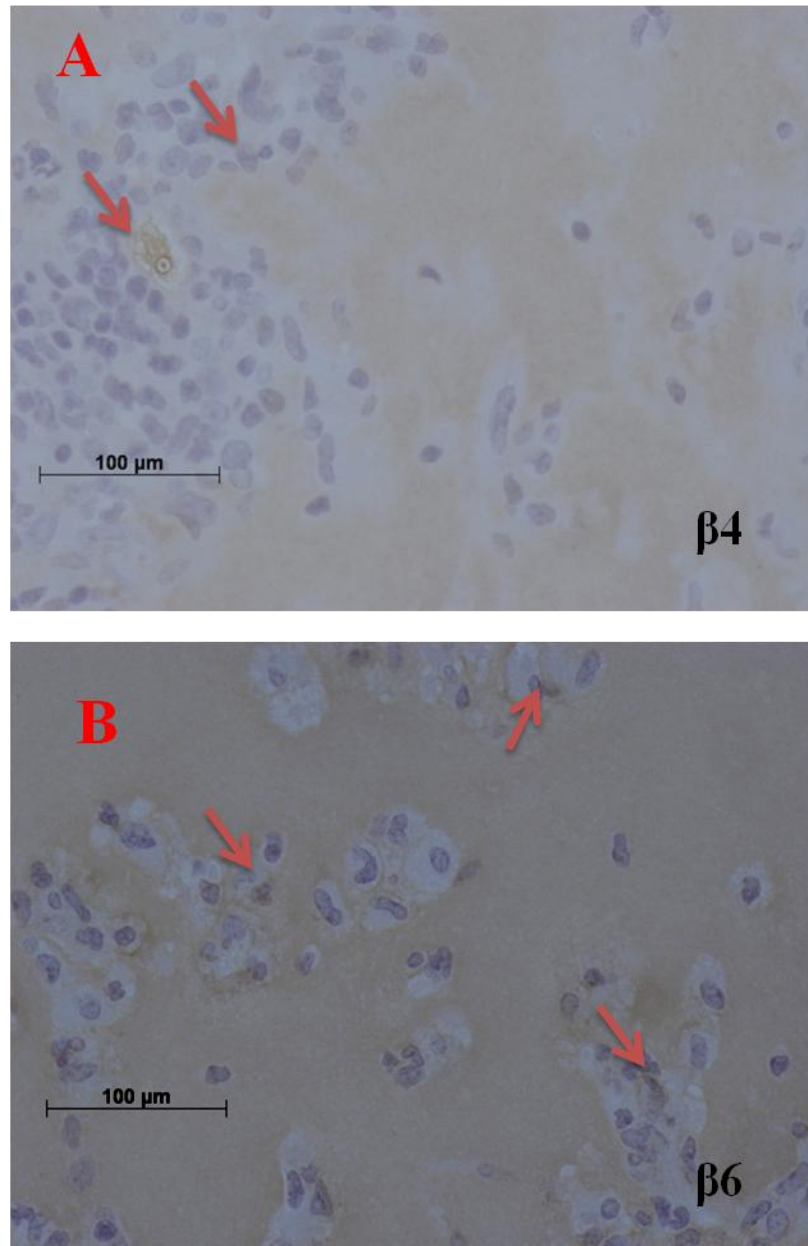


**Figure 3.27 Representative images of CD74+ve cells in Matrigel plugs assays**

The same series of Matrigel plugs containing either  $\beta 4$  or  $\beta 6$  myoepithelial cells was stained for CD74. The number of CD74+ve cells was counted using Imagescope software. This showed no difference between the number of CD74+ve cells in Matrigel plugs containing  $\beta 4$  cells (A) and Matrigel plugs containing  $\beta 6$  cells (B). Positive cells are indicated by arrows.

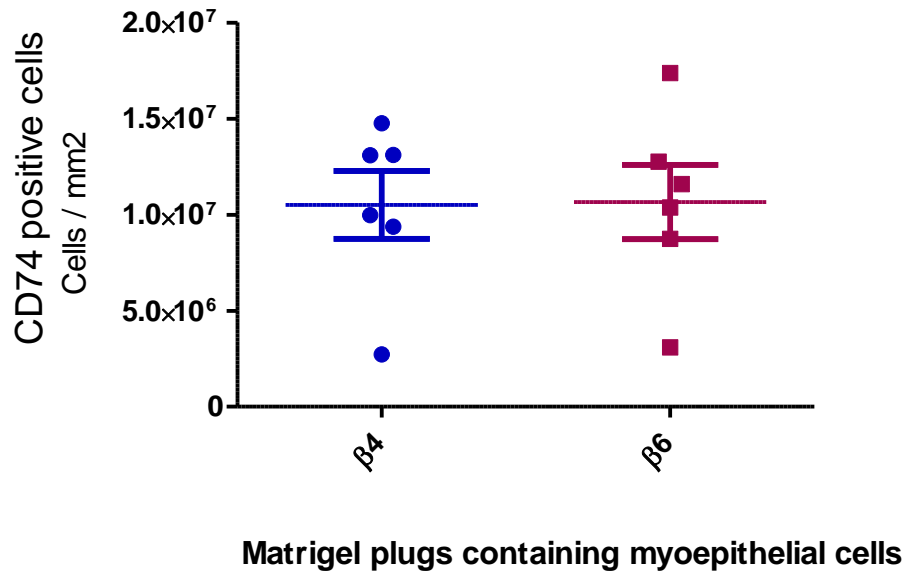


**Figure 3.28 Density of CD74+ve cell in Matrigel plugs**

Matrigel plugs containing either  $\beta 4$  or  $\beta 6$  myoepithelial cells were stained for CD74 and the number of CD74+ve cells was scored using Imagescope software as described. Comparing the proportion of CD74+ve cells, no difference was identified between the two groups of Matrigel plugs containing myoepithelial cells ( $p=0.9$ ).

### **3.5.4.5 Distribution of Arginase-1+ve cells in Matrigel plugs assays**

Arginase-1 antibody was optimised for use on normal mouse liver tissue and when specific staining achieved, the antibody was applied to the same series of Matrigel plugs containing myoepithelial cells. The sections were scanned using NDP software. Each section from the Matrigel plugs was opened in Imagescope software, appropriate scoring parameters to detect the specific staining of arginase-1 set up and the software was run to count cells positive for arginase-1 in the total area of the section. The result was exported to an Excel file and number of arginase-1+ve cells per mm<sup>2</sup> was calculated, and plotted on a graph using prism software. Comparing the number of arginase-1+ve cells, no difference was detected between Matrigel plugs containing  $\beta$ 4 and Matrigel plugs containing  $\beta$ 6 myoepithelial cells (p=0.4) (figures 3.29 & 3.30).

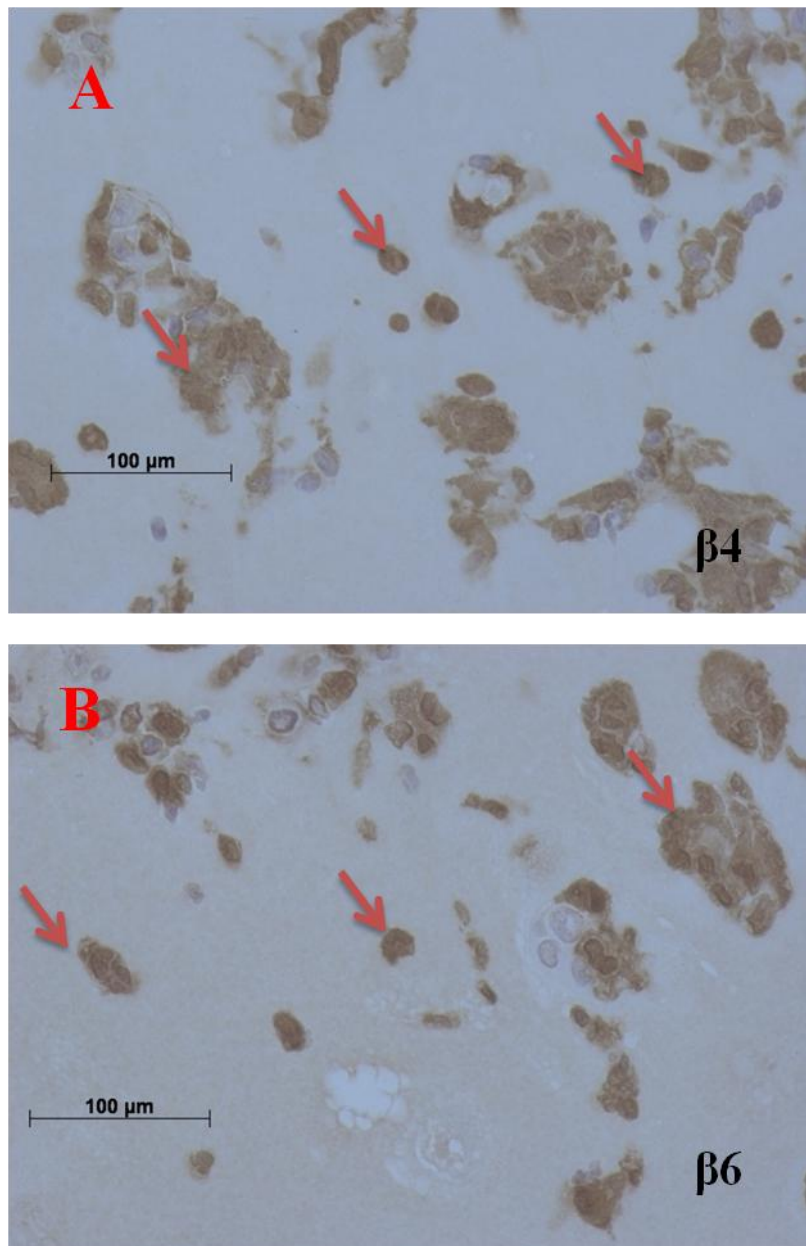


**Figure 3.29 Representative images of arginase-1+ve cells in matrigel plugs**

The same series of Matrigel plugs containing either  $\beta$ 4 or  $\beta$ 6 myoepithelial cells were stained for arginase-1. The number of positive cells was quantitated using ImageScope software. This showed no difference between the two groups of Matrigel plugs. Positively stained cells indicated by arrows.

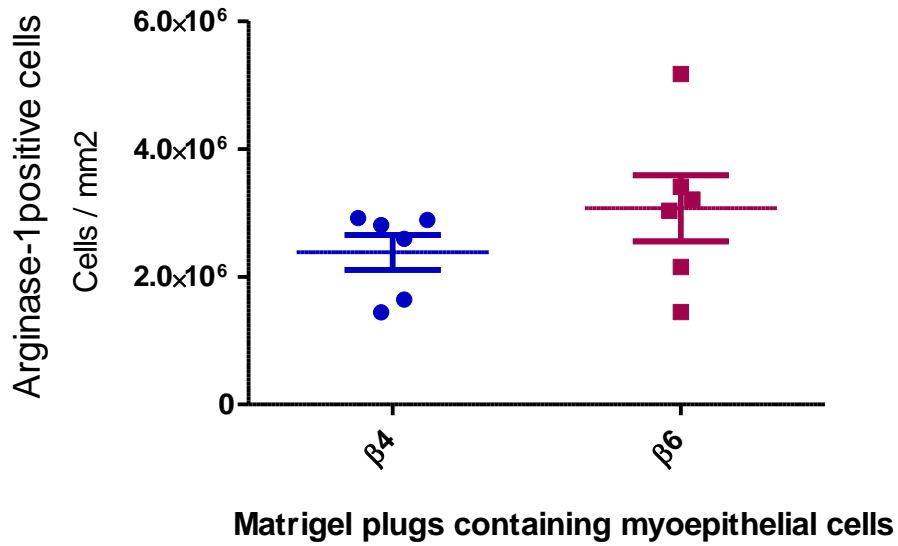


**Figure 3.30 Density of arginase+ve cell in Matrigel plugs**

The number of arginase+ve cells in Matrigel plugs containing myoepithelial cells was counted using Imagescope. No difference was identified between the two groups of Matrigel plugs ( $p=0.4$ ).

## 3.6 Discussion

---

There is growing evidence for a role of the microenvironment in modulating tumour cell behaviour. In DCIS, the microenvironment is complex with myoepithelial cells forming a unique component. Myoepithelial cells play a role in suppression of breast cancer cell growth, invasion and angiogenesis through expression of protease inhibitors and other factors (Alpaugh, Lee et al. 2000), though it is not clear if this function is retained in DCIS. In fact, Allinen et al (2004) showed that myoepithelial cells in DCIS exhibit multiple changes in gene expression, with loss of anti-angiogenic factors and up-regulation of certain chemokines (Allinen, Beroukhi et al. 2004). The epithelial-specific integrin  $\alpha\beta6$  is not normally detected on normal adult epithelia but is highly expressed during tissue remodelling including wound healing and carcinogenesis (Breuss, Gallo et al. 1995). We previously identified de novo up-regulation of  $\alpha\beta6$  on myoepithelial cells in a subset of DCIS with almost universal expression in DCIS associated with invasive disease (Allen, Thomas et al. 2014). In addition,  $\alpha\beta6$  appears to play a critical role in the induction of tumour tolerance as a recent study has shown that there is a direct relationship between the number of infiltrating Treg cells and the level of  $\alpha\beta6$  expression in colorectal cancer (Yang, Du et al. 2012).  $\alpha\beta6$  integrin also can convert the precursor TGF $\beta$  to the active form of TGF $\beta$  in dendritic cells (DCs), which converts immature DCs to tolerogenic DCs (Chen, Yao et al. 2011). In turn, tolerogenic DCs generates Treg cells (Li, Guo et al. 2008).

Moreover, down-regulation of  $\alpha\beta6$  results in inflammation by impairing the immune-suppressive activity of Treg cells (Munger, Huang et al. 1999). Suppression of the  $\beta6$  integrin in mice results in down regulation of inflammation in skin and respiratory tract (Huang, Wu et al. 1996).

Together, these data imply a relationship between  $\alpha\beta6$  and the inflammatory environment. We therefore hypothesised that this altered myoepithelial phenotype, with up-regulation of  $\alpha\beta6$ , may also modulate the inflammatory infiltrate in the DCIS microenvironment and so contribute to disease progression. To address this, the relationship between the peri-ductal inflammatory infiltrate in DCIS and myoepithelial expression of  $\alpha\beta6$  integrin was analysed by immunohistochemistry, quantitating the peri-ductal infiltrate on a duct-by-duct basis. This demonstrated significantly higher infiltration of Treg cells, as determined by CD4 and FOXP3 expression, in  $\alpha\beta6$ -positive DCIS cases as compared to  $\alpha\beta6$ -negative cases ( $P=0.01$ ). CD69, a marker of activated T cells was detected at a higher level in  $\alpha\beta6$ -positive cases compared to the  $\alpha\beta6$ -negative cases ( $p<0.0001$ ). Higher levels of arginase expression, a marker of tumour associated macrophages (TAMs), also was identified in  $\alpha\beta6$ -positive DCIS compared to  $\alpha\beta6$ -negative DCIS cases ( $P=0.0001$ ), whereas a higher number of M1 macrophage, as detected by MHC-II was present in  $\alpha\beta6$ -negative cases compared to  $\alpha\beta6$ -positive cases ( $P<0.0001$ ).

TAMs and Treg cells have been shown to exert a tumour-promoter action, and these data suggest therefore that expression of  $\alpha\beta6$  on myoepithelial cells in DCIS may be associated with a more tumour-promoter inflammatory infiltrate.

In invasive breast cancer, the number of CD45RO +ve cells is associated with an increased risk of recurrence and poor survival (Scholl, Pallud et al. 1994). However, this study demonstrated that the microenvironment of  $\alpha\beta6$  positive and  $\alpha\beta6$  negative showed no difference in the number of CD45RO +ve cells. This may reflect the difficulties of using a single marker, which is not specific to one cell type, since it will not adequately reflect more subtle differences in immune cell populations, or may be a consequence of study size. Expanding the number of cases analysed may help clarify this.

In addition, CD4+ve cells are the dominant inflammatory cell population in  $\alpha\beta6$ -positive DCIS microenvironment and MHC-II+ve cells are the dominant population in the  $\alpha\beta6$ -negative DCIS microenvironment. FOXP3+ve cells and arginase-1+ve cells were the least abundant inflammatory cell population in DCIS microenvironments.

To investigate the hypothesis *in vivo*, a group of 12 female C57/Blk6 normal mice, 4 weeks old were used in this study.  $\beta4$  cells and  $\beta6$  cells were suspended in Matrigel then injected into mice flanks separately. B16 mouse Lewis lung cancer cells were used as a positive control and Matrigel alone as a negative control. After 9 days mice were sacrificed, and Matrigel with the surrounding tissue was extracted. These Matrigel plugs were formalin-fixed and paraffin-embedded then sections stained for inflammatory markers CD4, FOXP3 (Treg), CD8 (cytotoxic T cell), CD74 (MIF receptor) and arginase (M2 macrophage). It was difficult to quantify the positive cells in the Matrigel plugs sections because of the level of background staining, and care was taken to apply stringent thresholds on the software to identify what represented true staining over background levels.



Within the limitations of the study and confidence of interpretation, the in vivo assays demonstrated a positive correlation between  $\beta 6^{+ve}$  myoepithelial cells and CD4<sup>+</sup>ve cells (p=0.005) and FOXP3<sup>+</sup>ve cells (P=0.007). This confirms the human tissue study and further supports the concept that the altered myoepithelial phenotype can directly modulate the nature of the inflammatory cell infiltrate.

## 3.7 Conclusion

---

These studies have shown a correlation between the inflammatory infiltrate in DCIS and expression of  $\alpha\beta6$  integrin by myoepithelial cells. This work has demonstrated higher infiltration of regulatory T cells, as determined by CD4 and FOXP3, in  $\alpha\beta6$ +ve DCIS cases as compared to  $\alpha\beta6$ -negative cases. It also has shown that the  $\beta6$ +ve DCIS cases are associated with higher numbers of TAMs compared to  $\beta6$ -ve DCIS cases.

Overall, DCIS tissue data also have suggested that the DCIS microenvironment contains high infiltration of CD4+ve T cells. The number of FOXP3 + cells and arginase-1+ cells indicates they are a minor inflammatory cell population in DCIS, whilst MHCII cells numbers are very low in  $\alpha\beta6$  +ve cases but represents the second dominant cell population in  $\alpha\beta6$  -ve cases. Despite difficulties with interpretation, the *in-vivo* study is valuable in demonstrating a more direct link between myoepithelial phenotype and inflammatory infiltrate and showed a positive correlation between the numbers of CD4 and FOXP3 cells and up-regulation of  $\alpha\beta6$ . In conclusion, this work indicates that there is variation in the extent and nature of the inflammatory infiltrate in DCIS and this is influenced by myoepithelial cell phenotype.

# **Chapter 4: Role of T cells in progression of DCIS**

## 4.1 Introduction

---

### 4.1.1 Progression of DCIS to invasive disease

There are major limitations in understanding the natural history of progression DCIS to invasive breast cancer. One study by Page et al, reports on the follow-up of a group of women in whom the diagnosis of DCIS was missed, such that these women received no treatment following biopsy. In the most recent report, extended follow-up data are provided on the original cohort of 28 women over a total of 46 years, with a median follow-up of 31 years for women who did not develop carcinoma. (Sanders, Schuyler et al. 2005). This demonstrated that eleven of 28 women developed invasive breast carcinoma (IBC), all in the same breast and quadrant from which their low-grade DCIS biopsy was taken (Sanders, Schuyler et al. 2005). Whilst clearly this study is very much biased towards low grade disease, it does indicate that not all DCIS will progress to invasive disease, even over a very extended time period.

A major diagnostic factor that can be used to distinguish DCIS from invasive breast cancer is the presence of an intact basement membrane and myoepithelial cell layer (Polyak and Kalluri 2010). The importance of myoepithelial cells in DCIS progression is supported by several lines of evidence. Toussaint et al analyzed the expression profile of DCIS with clinical follow-up and demonstrated that decreased expression of CD10, a differentiated myoepithelial cell marker, was associated with decreased disease-free survival (Toussaint, Durbecq et al. 2010).

Work in our laboratory has identified a novel and functionally relevant change in DCIS-associated myoepithelial cells: up-regulation of the integrin  $\alpha\beta6$ . We show that this leads to a switch in myoepithelial cell function from tumour suppressor to tumour promoter (Allen, Thomas et al. 2014). We previously have shown that normal myoepithelial cells can influence breast fibroblast function (Jones, Shaw et al. 2003) but the potential impact of  $\alpha\beta6$ -modified myoepithelial cells on the peri-ductal microenvironment has not been explored.

## 4.2 Hypothesis

---

In chapter 3, this study has shown that expression of  $\alpha\beta6$  on DCIS-associated myoepithelial cells is associated with an altered peri-ductal inflammatory microenvironment that would contribute to a pro-tumour phenotype. A key step in progression of DCIS is loss of the myoepithelial cell layer. We hypothesise that one mechanism by which the inflammatory infiltrate may promote tumour progression is through induction of myoepithelial cell apoptosis, possibly through release of tumour necrosis factors (TNF). Since the immunohistochemical analysis suggests that  $\alpha\beta6$  expression correlates with increased Treg cells, and a key cytokine released by these cells is the pro-apoptotic molecule TRAIL, we hypothesise that loss of the myoepithelial layer could be mediated by TRAIL-induced apoptosis, and that  $\alpha\beta6$ -positive myoepithelial cells may be more susceptible to this effect than their negative counterparts.

The objectives are to:

- Co-culture primary T cells and Jurkat T cells with  $\beta4$  myoepithelial cells or  $\beta6$  myoepithelial cells and measure induction of TRAIL.
- Analyse expression of the TRAIL receptors, DR4 & DR5, in myoepithelial cells by RT-PCR, Western blot and flow cytometry.
- Analyse directly the sensitivity of myoepithelial  $\beta4$  and myoepithelial  $\beta6$  cell populations to TRAIL-induced apoptosis using recombinant TRAIL.

- To further substantiate the clinical relevance of apoptosis in DCIS tissues using caspase-3 as a marker.

## 4.3 Methods and Materials

---

### 4.3.1 Measuring TRAIL levels in T cells

Primary T cells and Jurkat T cells were co-cultured with  $\beta 4$  and  $\beta 6$  myoepithelial cells for 48 hrs (section 2.8.10). After this, T cells were harvested and protein isolated and assayed for TRAIL by ELISA as described in section 2.20.

### 4.3.2 Measuring TRAIL receptors in myoepithelial cells

The levels of DR4 and DR5 TRAIL receptors in  $\beta 4$  and  $\beta 6$  myoepithelial cell lines were analysed by qPCR (section 2.17). Western blot and Flow cytometry techniques to measure the protein level of both receptors was unsuccessful as the antibodies could not be optimised.

### 4.3.3 Analysing the susceptibility of myoepithelial cell lines to apoptosis

- $\beta 4$  and  $\beta 6$  myoepithelial cells were treated with recombinant TRAIL for 2,4 and 8 hrs (section 2.9) then the level of cleaved PARP (apoptosis marker) was detected by Western blot as described in section 2.10.

- Both myoepithelial cell lines were treated with etoposide chemotherapy for 4, 6, 8 and 48 hrs to induce apoptosis (section 2.9). Serial images of the cells were taken during the treatment time course in order to assess morphological changes relating to apoptosis.

#### **4.3.4 Detection of apoptosis in DCIS-associated myoepithelial cells by immunohistochemistry**

A set of DCIS cases positive for  $\alpha\text{v}\beta 6$  and showing high infiltration with Treg cells was stained with cleaved caspase-3 antibody as described in section 2.4.



## 4.4 Results

---

### 4.4.1 Impact of myoepithelial cells on T-cell derived TRAIL

Primary T cells and Jurkat T cells were co-cultured with  $\beta$ 4 or  $\beta$ 6 myoepithelial cells for 48 hrs, and then levels of TRAIL in primary T cell and Jurkat T cell lysates measured by ELISA (Enzyme-Linked Immunosorbent Assay) (section 2.20). The co-culture experiment was repeated a minimum of three times (section 2.8.10). Lysates of primary T cells and Jurkat T cell from the three independent experiments were loaded, in duplicate, onto the ELISA plate.

At the 48hrs time point, there was no difference in TRAIL levels in Jurkat T cells co-cultured with either  $\beta$ 4 myoepithelial cells or  $\beta$ 6 myoepithelial cells (figure 4.1,  $p=0.1$ ). However, at the same time point, higher levels of TRAIL were detected in primary T cells following co-culture with  $\beta$ 6 myoepithelial cells compared to T cells co-cultured with  $\beta$ 4 myoepithelial cells (figure 4.1,  $p=0.02$ ).

There was no significant proliferation of either Jurkat T cells or primary T cells following co-culture with myoepithelial cells, as determined by cell counts at the endpoint of the experiment.

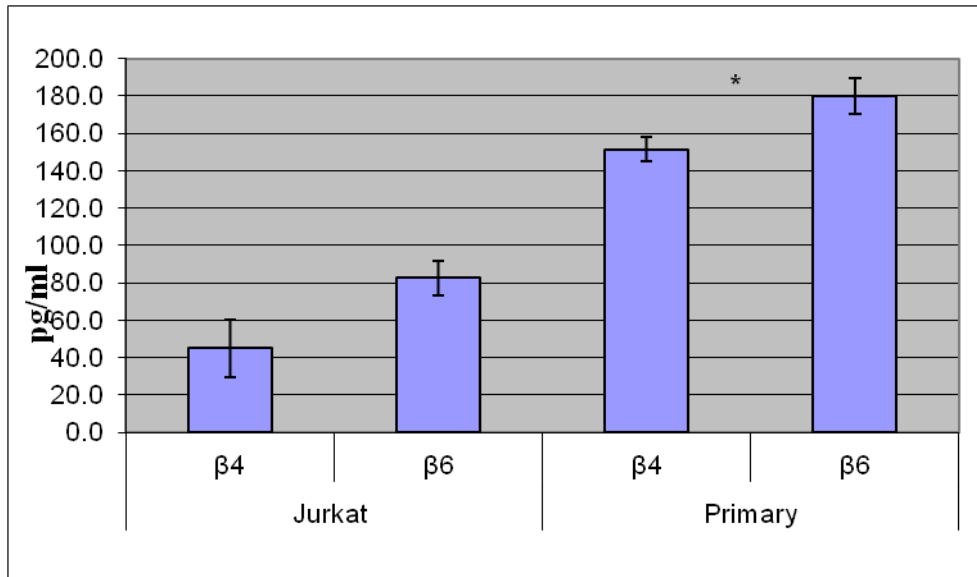


**Figure 4.1** Measurement of TRAIL levels in Jurkat T cells and primary T cells co-cultured with  $\beta 4$  or  $\beta 6$  myoepithelial cells for 48 hrs

Both T cells populations (primary and Jurkat cells) were co-cultured with  $\beta 4$  or  $\beta 6$  myoepithelial cells for 48 hrs and lysates of T cells then harvested and TRAIL levels measured by ELISA. Jurkat cells co-cultured with  $\beta 6$  cells show no significant difference in TRAIL levels compared to those cultured with  $\beta 4$  myoepithelial cells ( $p=0.1$ ). However, primary T cells co-cultured with  $\beta 6$  myoepithelial cells show higher levels of TRAIL compared to those co-cultured with  $\beta 4$  myoepithelial cells ( $p=0.02$ ). Results represent three independent experiments.

#### **4.4.2 Expression of TRAIL receptors DR4 & DR5 in myoepithelial cell populations**

Expression of DR4 and DR5 RNA was analyzed in myoepithelial cell populations using RT-PCR. GAPDH was used to normalize DR4 and DR5 expression levels. HeLa cells were used as a positive control for TRAIL receptors. This demonstrated  $\beta 6$  myoepithelial cells express higher levels of DR4 RNA compared to  $\beta 4$  myoepithelial cells (figure 4.2,  $p=0.002$ ).  $\beta 6$  myoepithelial cells also express higher levels of DR5 RNA compared to  $\beta 4$  myoepithelial cells (figure 4.3,  $p=0.03$ ). Using HeLa cells as a positive control DR4 and DR5 monoclonal antibodies failed to be optimised in order to investigate expression of DR4 and DR5 at the protein level in myoepithelial cells by Western blot. FITC conjugated antibodies to DR4 and DR5 were also tested in flow cytometry but this was unsuccessful as the antibodies could not be optimised.

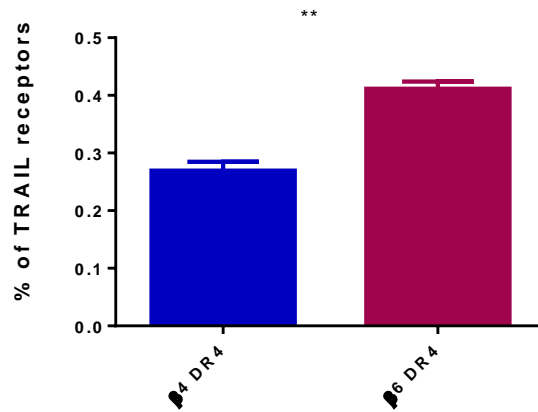


**Figure 4.2 RNA expression of DR4 in myoepithelial cells**

RT-PCR showed  $\beta 6$  myoepithelial cells express higher levels of DR4 RNA compared to  $\beta 4$  myoepithelial cells ( $p=0.002$ ). Error bars=SD. Bars represent the mean of triplicate experiments.

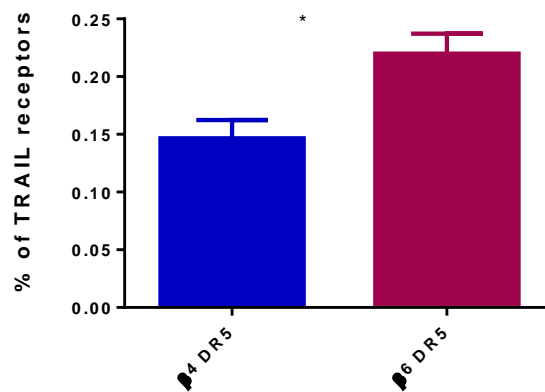


**Figure 4.3 RNA expression of DR5 in myoepithelial cells**

DR5 RNA levels were analysed by RT-PCR. This demonstrated  $\beta 6$  myoepithelial cells express higher levels of DR5 RNA compared to  $\beta 4$  myoepithelial cells ( $p=0.03$ ). Error bars=SD. Bars represent the mean of triplicate experiments.

### **4.4.3 Detection of apoptosis in TRAIL-treated myoepithelial cell lines**

#### **(i) Detection of cleaved PARP**

Apoptosis was assessed in TRAIL-treated  $\beta 4$  and  $\beta 6$  myoepithelial cells by Western blot using an antibody to cleaved PARP.  $\beta 4$  and  $\beta 6$  myoepithelial cells were exposed to recombinant TRAIL at 500ng/ml concentration for 2, 4 and 8 hrs (Figure 4.4A). Cells were grown under control conditions (vehicle only) over the same time periods (Figure 4.4 B). At the appropriate time point the cells were harvested, protein extracted and Western blot carried out for cleaved PARP to determine the level of apoptosis. Experiments were repeated a minimum of three times.  $\beta 4$  myoepithelial cells showed very low levels of cleaved PARP at all the time points (Figures 4.4 A&B). However,  $\beta 6$  myoepithelial cells exhibited stronger bands for cleaved PARP compared to  $\beta 4$  myoepithelial cells, with maximum levels being observed between 4-8 hrs (Figures 4.4 A&B). This suggests that  $\beta 6$  myoepithelial cells may be more sensitive to TRAIL-induced apoptosis compared to  $\beta 4$  myoepithelial cells.

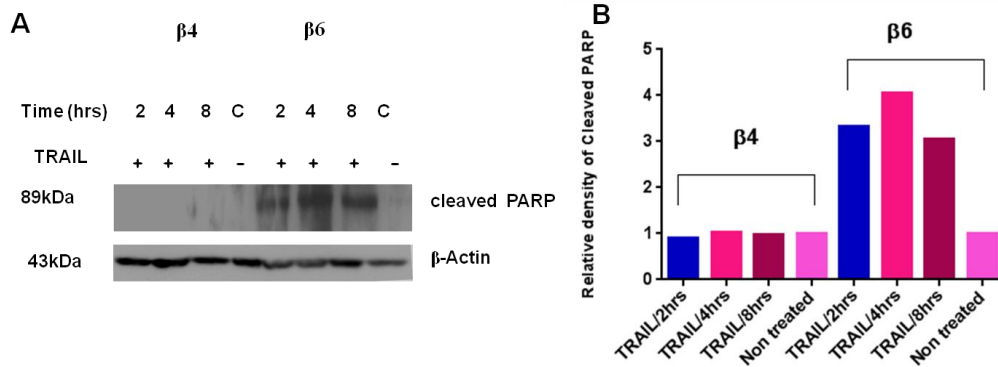


**Figure 4.4 A: Detection of apoptosis by cleaved PARP in β4 and β6 myoepithelial cells exposed to TRAIL**

β4 and β6 myoepithelial cells were treated with recombinant TRAIL (500ng/ml) at 37 °C for 2, 4 and 8hrs. Apoptosis was analysed by immunoblotting for the presence of cleaved PARP. β6 myoepithelial cells exhibit higher levels of cleaved PARP compared to β4 myoepithelial cells at all time points (A). β- actin was used as a loading control. The results also were analysed via ImageJ integrated density (B). Relative density of Cleaved PARP for non-treated β4 cells versus β4 cells treated with TRAIL for 2, 4 and 8 hrs was 1:0.90, 1:1 and 1: 0.97, respectively. While, relative density of Cleaved PARP for non-treated β6 cells versus β6 cells treated with TRAIL for 2, 4 and 8 hrs was 1: 3.3, 1:4 and 1:3, respectively.

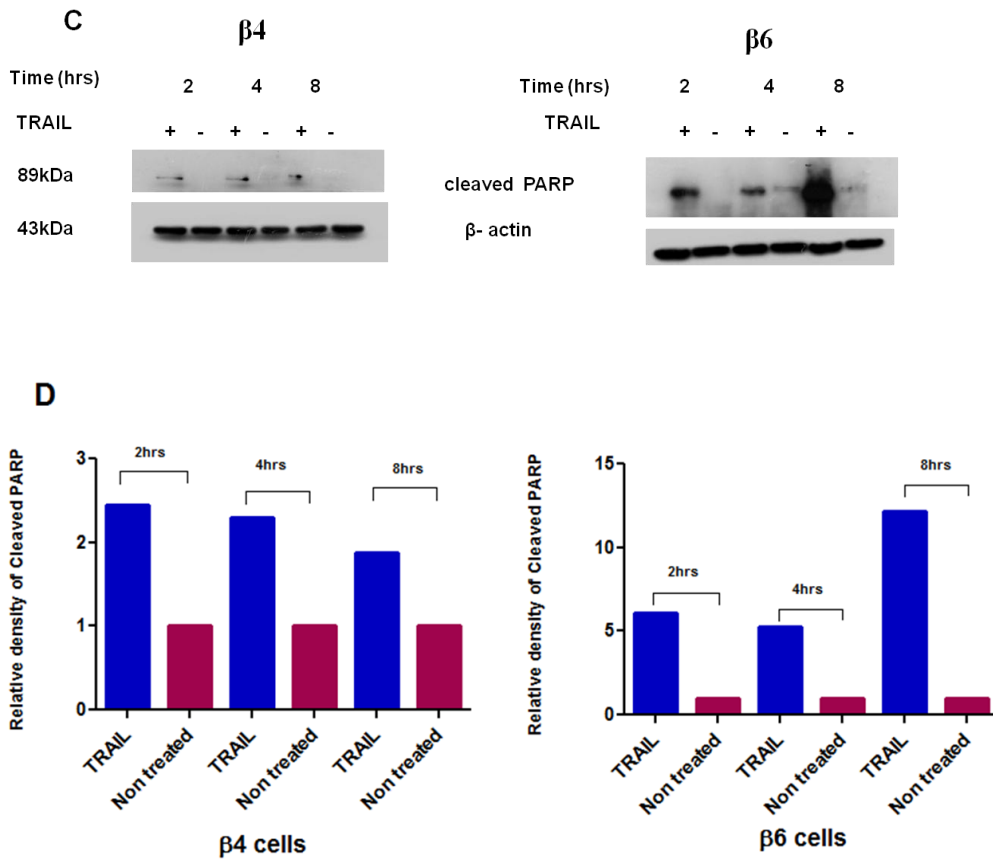


**Figure 4. 4 B: Detection of apoptosis by cleaved PARP in β4 and β6 myoepithelial cells exposed to TRAIL**

β4 and β6 myoepithelial cells were treated with recombinant TRAIL (500ng/ml) at 37 °C for 2, 4 and 8 hrs. Apoptosis was analysed by immunoblotting for the presence of cleaved PARP. β4 myoepithelial cells showed low level of cleaved PARP compared to β6 myoepithelial cells (C), and β6 myoepithelial cells exhibit the highest level after 4 hrs (C). β- actin was used as a loading control. The results also were analysed via ImageJ integrated density (D). Relative density of Cleaved PARP for β4 cells treated with TRAIL for 2, 4 and 8 hrs versus β4 cells were grown under control conditions (vehicle only) over the same time periods was 2.4:1, 2.2:1 and 1.8: 1, respectively. While, relative density of Cleaved PARP β6 cells treated with TRAIL for 2, 4 and 8 hrs versus non treated β6 cells were grown over the same time periods was 6:1, 5.2:1 and 12.1:1, respectively.

**(ii) Morphological changes**

In order to investigate susceptibility to apoptosis in both myoepithelial cell lines, the lines were exposed to etoposide chemotherapy (1 $\mu$ M/ml) for 4, 6, 8 and 48 hrs. After 4, 6 and 8 hrs, neither cell line showed a response to the treatment (figure 4.5A), however, by 48hrs  $\beta$ 6 myoepithelial cells started to display changes in morphology with reduction in the cell number. The cells showed contraction, blebbing of the cell membrane and phase bright appearance (Figure 4.5B & C). In contrast, the majority of  $\beta$ 4 myoepithelial cells look healthy with just occasional cells becoming phase bright (Figure 4.5B).

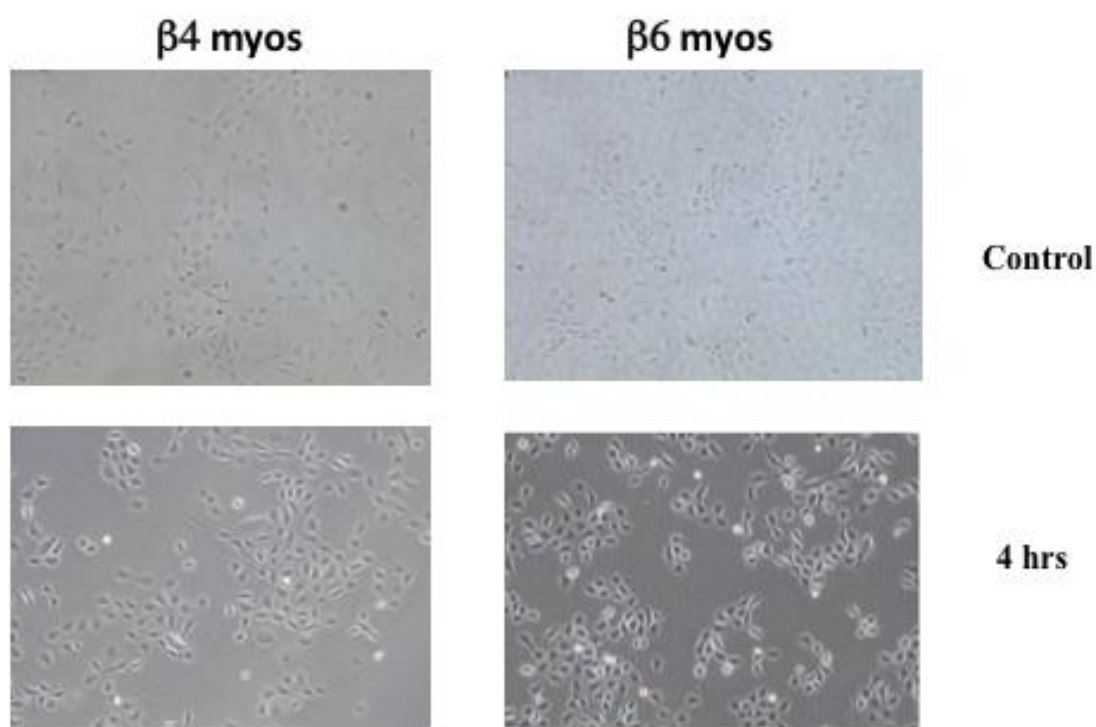


**Figure 4.5 A: Induction of morphological changes in  $\beta$ 4 and  $\beta$ 6 myoepithelial cell lines on exposure to etoposide chemotherapy**

Control cells, exposed to vehicle only, appear healthy, and both cell lines remained healthy at 4 hrs post-treatment.



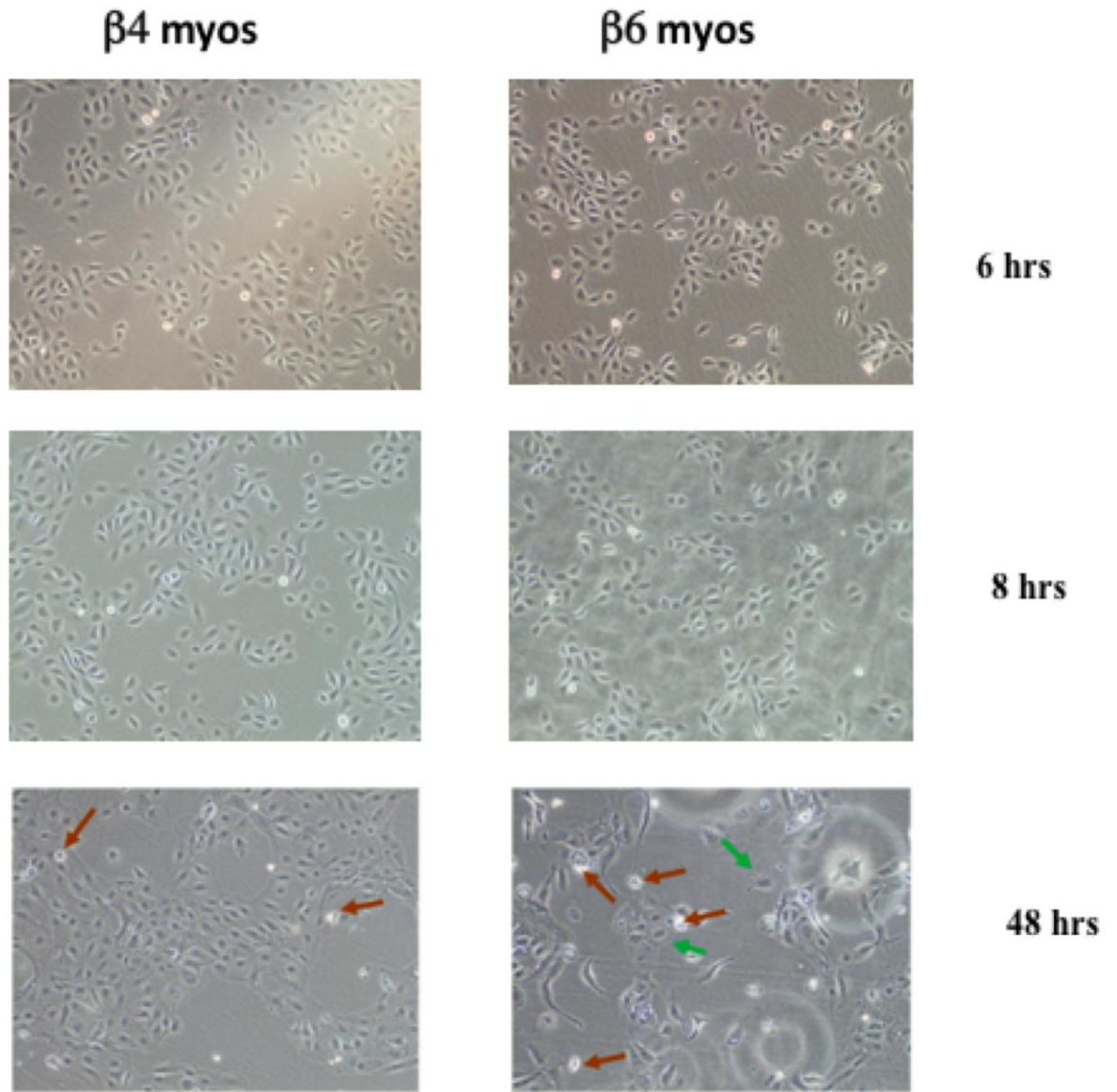


**Figure 4.5B: Induction of morphological changes in  $\beta 4$  and  $\beta 6$  myoepithelial cell lines on exposure to etoposide chemotherapy**

Both cell lines remained healthy at 6hrs and 8 hrs after treatment. However, by 48hrs, whereas  $\beta 4$  myoepithelial cells (left panel) still look healthy with only occasional cells becoming phase bright (late stage, brown arrow),  $\beta 6$  myoepithelial cells (right panel) showed a change in morphology, with reduced cell numbers. The cells displayed extensive plasma membrane blebbing (green arrows), contracted morphology (early stage, red arrow) and phase-bright appearance (late stage, brown arrow).

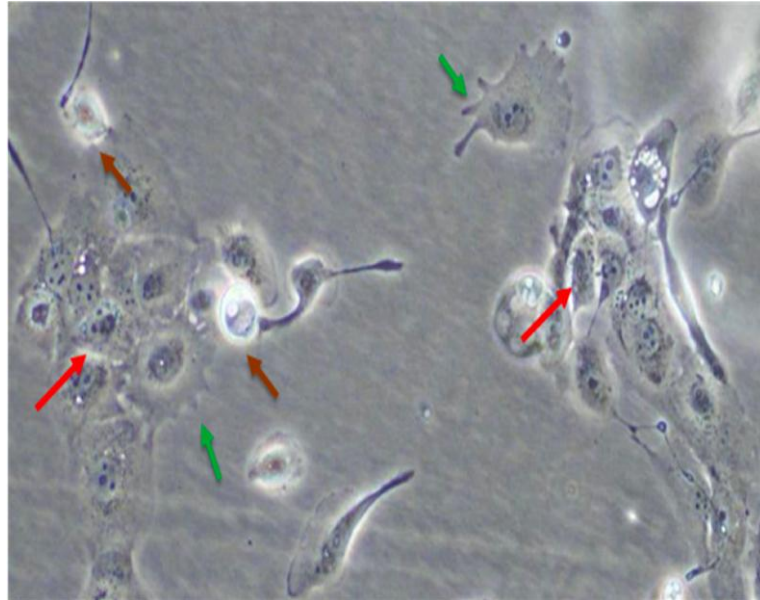


**Figure 4. 5 C Induction of morphological changes in  $\beta 6$  myoepithelial cell lines on exposure to etoposide chemotherapy.**

Both cell lines were treated with  $1\mu\text{M}/\text{ml}$  etoposide for different time periods as indicated. After 48 hrs,  $\beta 6$  myoepithelial cells showed changes in their morphology, with a reduced cell number and extensive plasma membrane blebbing (green arrows), contracted (early stage, red arrow) and phase-bright (late stage, brown arrow) morphology.

#### **4.4.4 Detection of cleaved caspase-3 as a marker of apoptosis in DCIS**

The above data suggests that acquisition of  $\alpha v \beta 6$  by myoepithelial cells in DCIS may make them more susceptible to apoptosis and contribute to their loss in DCIS.

In this study we propose that myoepithelial cells may be lost through apoptosis generated by signals from inflammatory cell mediators. To investigate the hypothesis that myoepithelial cell apoptosis may be taking place in-vivo, a preliminary analysis of 6 cases of DCIS positive for  $\alpha v \beta 6$  and showing high infiltration with Treg cells were selected and stained for cleaved caspase-3. Immunohistochemistry demonstrated staining for cleaved caspase-3 in myoepithelial cells in some of the DCIS ducts (Figure 4.6.). This provides some support for the hypothesis that myoepithelial cells may be lost through apoptosis however further work is needed to provide definitive evidence.

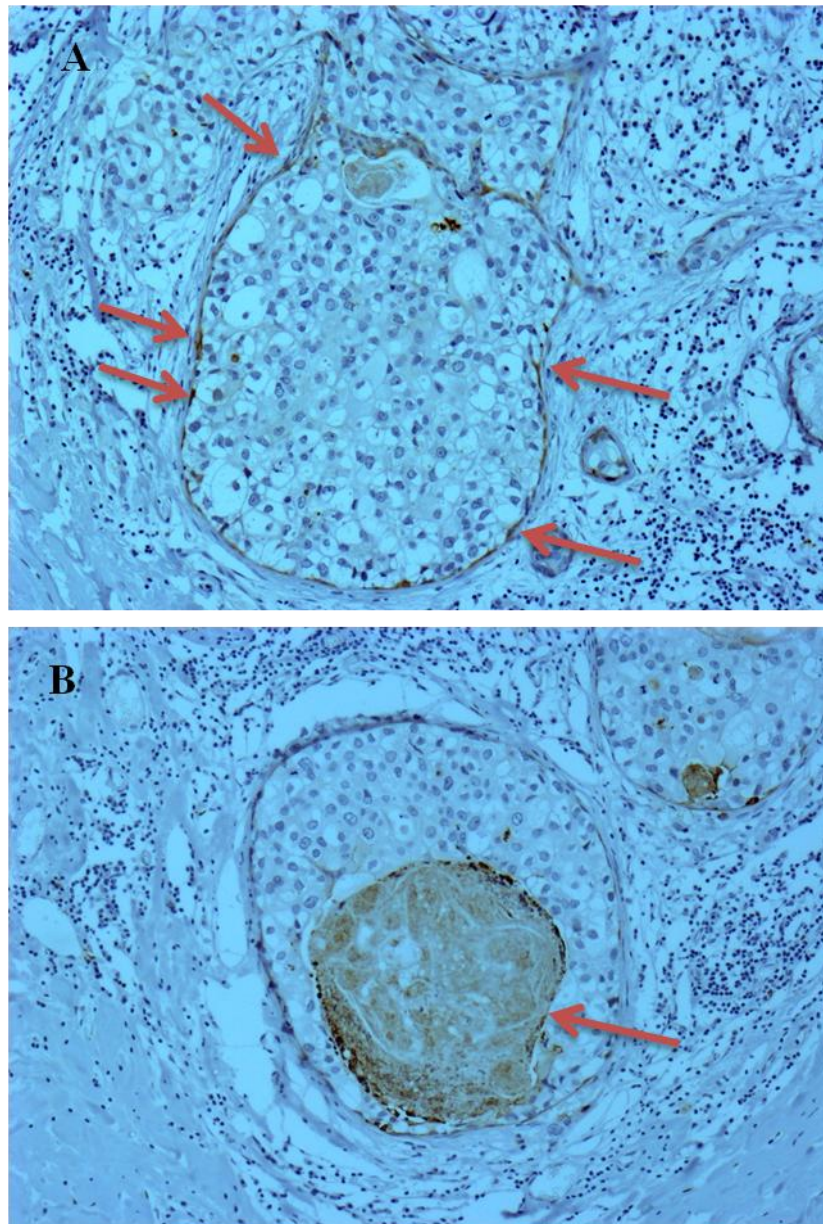


**Figure 4.6 Representative example of caspase-3 immunohistochemistry staining in  $\alpha v \beta 6$  +ve DCIS case with high peri-ductal infiltration of Treg cells.**

Staining for cleaved Caspase-3 was evident in myoepithelial cells of DCIS, as indicated by arrows (A). Apoptotic tumour cells (together with necrotic debris) inside the ducts of DCIS showed strong positive staining with caspase-3 and served as an internal positive control, as indicated by arrow (B).

## 4.5 Discussion

---

It is well documented that disruption of the myoepithelial layer (ME) and basement membrane (BM) is a prerequisite for breast cancer invasion (Clarke, Brunner et al. 1989, Sheikh, Garcia et al. 1994). Moreover, it has been shown that the stromal tissue surrounding mammary ducts that exhibit disruption of the ME layer is often highly vascular and highly infiltrated with inflammatory cells (WBCs) when compared to the stroma around ducts with an intact ME layer (Man, Tai et al. 2003). White blood cells (WBCs) release proteolytic enzymes that are capable of degrading the BM and alter host cells in vivo and in vitro (Zhang, Schiller et al. 1998, Yakirevich, Izhak et al. 1999). In addition, WBCs can freely cross over the ME and BM barrier, (Chen, Yang et al. 1997, Correa, Plunkett et al. 2003), and tumours with or without WBC infiltration have been shown to have a different clinical course and outcome (Menard, Tomasic et al. 1997, Hartveit 1998). Yousefi and his colleagues demonstrated that mammary ducts with focal disruption of the myoepithelial cell layer showed a higher frequency of WBC infiltration than ducts without myoepithelial cell layer disruption. They also pointed out that WBCs were often located at or close to the centre of myoepithelial cell layer disruptions, raising the possibility that inflammatory cells may be involved in disruption of myoepithelial cell layer (Yousefi, Mattu et al. 2005). Furthermore, a study has reported that patients with a lymphocytic infiltrate at the tumour edge have a significantly poorer short-term prognosis compared to patients with lymphocytic infiltration in other locations (Hartveit 1998), suggesting a direct interaction between tumour



cell behaviour and inflammatory cells. Tumour necrosis factor- related apoptosis-induced ligand (TRAIL) is expressed by peripheral T lymphocytes (Salehi, Vodjgani et al. 2007) and induces apoptosis in a variety of cancer cell lines, including breast cell lines (Keane, Ettenberg et al. 1999, Walczak, Miller et al. 1999, Chinnaiyan, Prasad et al. 2000). Furthermore, activated Treg cells express TRAIL in vivo (Ren, Ye et al. 2007) but whether this may be involved in mediating loss of myoepithelial cells in DCIS has yet to be established.

WBCs may have a direct or indirect influence on the integrity of the structure of ME cells and the BM layer, and therefore play a key role in mediating the transition of DCIS to invasive disease. Since a positive correlation was identified between myoepithelial expression of  $\alpha\text{v}\beta\text{6}$  and peri-ductal Treg cell infiltration, the study aimed to address two main questions: firstly, to develop an in-vitro model system to determine whether expression of  $\alpha\text{v}\beta\text{6}$  on myoepithelial cells actually induces higher levels of TRAIL in T cells, and secondly to investigate whether TRAIL can disrupt the myoepithelial cells barrier through induction of myoepithelial cells apoptosis.

We first have examined the levels of TRAIL in Jurkat and primary T cell populations following co-culture with  $\beta\text{4}$  or  $\beta\text{6}$  myoepithelial cells for 48 hrs. Primary T cells, but not Jurkat T cells, were found to express higher levels of TRAIL when they were co-cultured with  $\beta\text{6}$  myoepithelial cells than when co-cultured with  $\beta\text{4}$  myoepithelial cells. The lack of response in the established cell line may be a reflection of its immortalisation, and the lack of 'plasticity' in a cell line, in comparison to primary cells. TRAIL has been shown to be induced in activated T cells (Jeremias, Herr et al. 1998, Sato, Nuki et al. 2010).

CD69 is considered to be an early marker of T cell activation (Sancho, Gomez et al. 2005), and in the immunohistochemical study on DCIS tissues, we demonstrated higher numbers of CD69-positive T cells in the peri-ductal environment of  $\alpha\beta6$ -positive myoepithelial cells compared to  $\alpha\beta6$ -negative ducts. Thus, it is possible that up-regulation of  $\alpha\beta6$  can lead to T cell activation. Co-culture studies followed by a detailed phenotypic analysis of T cells could address this. Similar studies in our laboratory have shown that  $\alpha\beta6$ -positive myoepithelial cells can modulate macrophage phenotype and activation (M Allen, personal communication), making this a plausible theory.

TRAIL mediates its actions through specific TRAIL receptors, DR4 and DR5. These receptors have been detected on breast cancer cells and high DR5 expression is strongly correlated with decreased survival (McCarthy, Sznol et al. 2005). The aim, therefore, was to measure the levels of TRAIL receptors (DR4& DR5) in the myoepithelial cell populations. Both DR4 and DR5 were detected on the myoepithelial cell lines, with significantly higher levels of mRNA expression for both receptors in the  $\beta6$  myoepithelial cells compared to  $\beta4$  myoepithelial cells. Unfortunately attempts to measure DR4 and DR5 at the protein level were unsuccessful as the antibodies could not be optimised.

To investigate more directly the effect of TRAIL on ME apoptosis,  $\beta6$  and  $\beta4$  myoepithelial cells were treated with recombinant TRAIL for 2, 4 and 8 hrs, after which the cells were analysed for expression of cleaved PARP, as a marker of apoptosis.

This demonstrated enhanced apoptosis in the  $\beta 6$ +ve myoepithelial cell line compared to the  $\beta 6$ -ve myoepithelial cells at each time point. The results also showed that apoptosis reached peak levels at 4hrs post- treatment in both cell lines. This provides early evidence that ME positive for  $\beta 6$  integrin may be more susceptible to the effect of Treg cells, but this requires further investigation. In addition, exposure of both myoepithelial cell lines to Etoposide-induced apoptosis has shown that  $\beta 6$ +ve myoepithelial cells were more susceptible to apoptosis compared to  $\beta 6$ -ve myoepithelial cells. Therefore, the effect is not specific to TRAIL.

As a preliminary approach to evaluate the clinical relevance of these findings, a small series of DCIS samples was assessed for the presence of apoptosis, specifically relating to the myoepithelial compartment. A set of DCIS cases showing  $\alpha \nu \beta 6$ +ve myoepithelial cells and high levels of infiltration with Treg cells were stained with an antibody against caspase-3 antigen, as a marker of apoptosis. Immunohistochemistry demonstrated staining for caspase-3 in myoepithelial cells in some of the DCIS ducts. This provides some support for the hypothesis that myoepithelial cells may be lost through apoptosis however further work is needed to provide definitive evidence, including analysis of DCIS ducts negative for  $\alpha \nu \beta 6$ , and normal breast ducts, as a comparison.



## 4.6 Conclusion

---

Up-regulation of  $\beta 6$  in DCIS-associated myoepithelial cells influence primary T cells to express higher levels of TRAIL, and  $\beta 6$  myoepithelial cells express higher levels of TRAIL receptor mRNA compared to  $\beta 6$ -ve myoepithelial cells. Furthermore, expression of  $\beta 6$  by myoepithelial cells appears to increase their sensitivity to TRAIL induced apoptosis.

This may represent one mechanism whereby the myoepithelial cell population in DCIS may be lost, so promoting progression to invasive disease.

# Chapter 5: Galectin-7 in relation to $\alpha v \beta 6$

## 5.1 Introduction

---

### 5.1.1 Galectin-7 expression in myoepithelial cells

In the normal breast, it has been shown that galectin-7 is highly expressed by the myoepithelial cells (Demers, Rose et al. 2010). In breast cancer, High expression levels of galectin-7 were restricted to high-grade breast carcinoma (Demers, Rose et al. 2010). Its over-expression has been shown to be associated with metastasis to the lung and bone. It has been suggested that galectin-7 has the ability to render mammary epithelial cells more resistant to apoptosis (Demers, Rose et al. 2010).

Moreover, galectin-7 has been described both as pro-apoptotic (Bernerd, Sarasin et al. 1999, Kuwabara, Kuwabara et al. 2002), and anti-apoptotic (Gendronneau, Sidhu et al. 2008, Demers, Rose et al. 2010).

## 5.2 Hypothesis

---

Galectin-7 is a molecule highly expressed by normal myoepithelial cells and is down-regulated in low-grade invasive breast cancer and up-regulated in high grade invasive cancer. Evidence suggests that galectin-7 modulates cellular apoptotic response, but in some situations it appears to protect against apoptosis and others promote apoptosis. The expression of galectin-7 in DCIS has not previously been reported, however, given the multiple phenotypic changes in DCIS-associated myoepithelial cells, we hypothesise that this important regulatory protein may also be altered in DCIS, and this may alter the susceptibility of myoepithelial cells to apoptotic signals.

### 5.2.1 Aims of this chapter

- To determine the expression of galectin-7 in DCIS-associated myoepithelial cells.
- Analyse its relationship with  $\alpha\text{v}\beta\text{6}$  expression.
- Analyse the relationship between galectin-7 and  $\alpha\text{v}\beta\text{6}$  with clinical characteristics of DCIS
- Investigate expression and relationship of galectin-7 and  $\alpha\text{v}\beta\text{6}$  in myoepithelial cell lines and primary populations
- To examine the influence of galectin-7 expression on myoepithelial apoptosis using recombinant TRAIL.

## 5.3 Methods and Materials

---

### 5.3.1 Investigation of galectin-7 and $\alpha\text{v}\beta\text{6}$ expression in DCIS

Galectin-7 and  $\alpha\text{v}\beta\text{6}$  antibodies were applied to 47 cases of DCIS and a series of 294 core biopsies with a pre-operative diagnosis of DCIS (section 2.4).

### 5.3.2 Analysis of the relationship between galectin-7 and $\alpha\text{v}\beta\text{6}$ in DCIS

47 cases of DCIS were scored duct-by-duct for expression of galectin-7 and  $\alpha\text{v}\beta\text{6}$  as described in section 2.5. The core biopsies were scored for overall amount of staining for both markers and not on a duct-by-duct basis (section 2.5).

### **5.3.4 Measurement of galectin-7 in myoepithelial cells**

Protein and mRNA levels of galectin-7 in  $\beta 4$  and  $\beta 6$  myoepithelial cells were measured using Western blot and PCR as described in sections 2.10 and 2.16.

### **5.3.5 Knockdown of galectin-7 in primary myoepithelial cells and $\beta 4$ myoepithelial cell line**

In order to investigate the impact of knockdown of galectin-7 on  $\alpha\beta 6$  expression, primary myoepithelial cells were treated with galectin-7 siRNA or control siRNA for 24, 48 and 72hrs as described in section 2.11, and galectin-7 and  $\beta 6$  expression was measured by Western blot. In addition, galectin-7 was knocked down in  $\beta 4$  cells then cells were exposed to TRAIL or etoposide (section 2.9) to study the effect on apoptosis by measurement of cleaved PARP by Western blot (2.10).

### **5.3.6 Measuring duct size**

Duct size was measured in 47 cases of DCIS and related to expression of galectin-7 and  $\alpha\beta 6$  using NDP software as described in section 2.6.

## 5.4 Results

---

### 5.4.1 Expression of galectin-7 in control tissues

The Galectin-7 antibody was first optimised for use on normal breast tissue and skin tissue as positive controls and when specific staining of the appropriate cell compartment was achieved, the antibody was applied to the breast tissue samples. Initial staining of normal human breast tissue sections showed staining of cytoplasm and nuclei of myoepithelial cells with sparing of the luminal cell population (Figure 5.1A), consistent with the previous study reporting galectin-7 as a marker of myoepithelial cells (Demers, Rose et al. 2010). In skin there was extensive staining of the epidermis (Figure 5.1C) as has been reported in previous studies describing galectin-7 as a marker of stratified epithelium (Madsen, Rasmussen et al. 1995, Magnaldo, Bernerd et al. 1995).

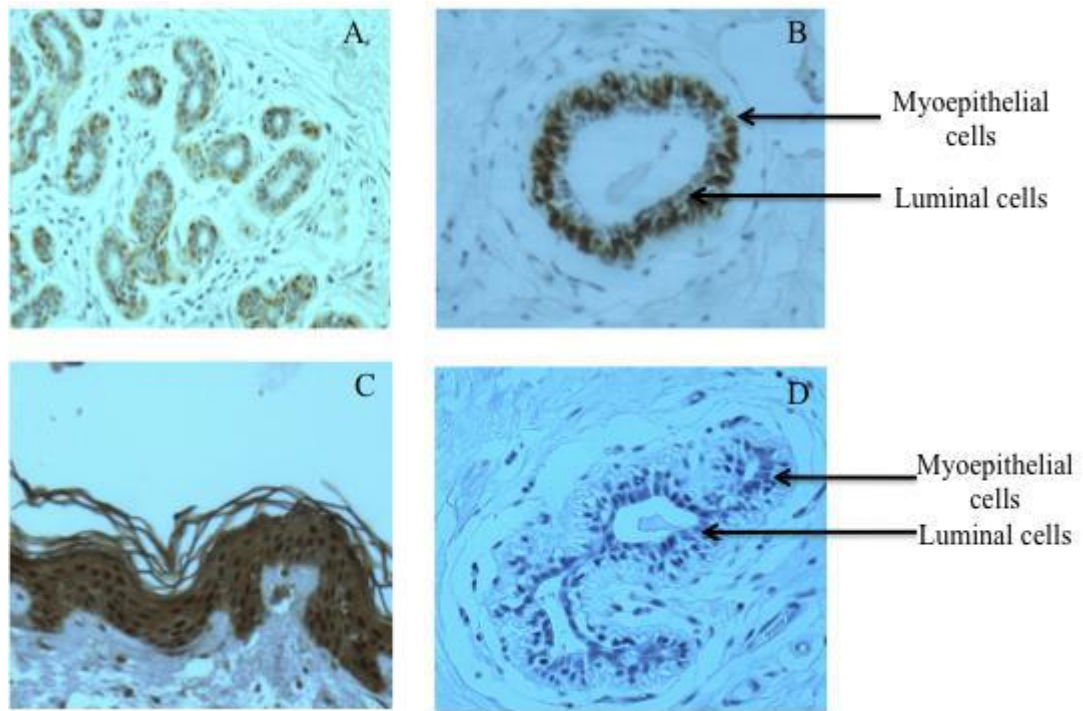


**Figure 5. 1** Galectin-7 expression in normal mammary gland and skin tissue

Immunohistochemical analysis of human normal tissues demonstrates specific expression of galectin-7 in myoepithelial cells. Luminal epithelial cells and stroma are clearly negative (panels **A & B**), and strong positive staining is seen in stratified epithelium of skin (panel **C**). Normal mammary myoepithelial cells show no staining with rabbit IgG, which was used as negative control (panel **D**). (Magnification A&C 5X; B&D 20X).

### **5.4.2 Galectin-7 expression in DCIS cases and its correlation with $\alpha\beta 6$**

To examine the expression of galectin-7 in DCIS and its relationship to  $\alpha\beta 6$  expression, paraffin-embedded tissue sections were selected from 47 patients with DCIS and stained for both markers. Rabbit IgG was used as negative control. After staining, the sections were scanned using Nanozoomer software and then scored on a duct-by-duct basis for each marker on serial sections.

The number of ducts positive for the two markers varied greatly between samples. The majority of ducts positive for  $\alpha\beta 6$  were negative for galectin-7, with 70% of galectin-7 positive ducts being  $\beta 6$  negative compared to 30% being  $\beta 6$  positive (Figure 5.2 & 5.3). This demonstrated an inverse relationship between the two proteins ( $p= 0.001$ ). In some cases, myoepithelial cells were positive for both proteins or negative for both markers, though this was less common (Figure 5.2 & 5.3).



**Galectin-7**

**$\alpha\text{v}\beta\text{6}$**

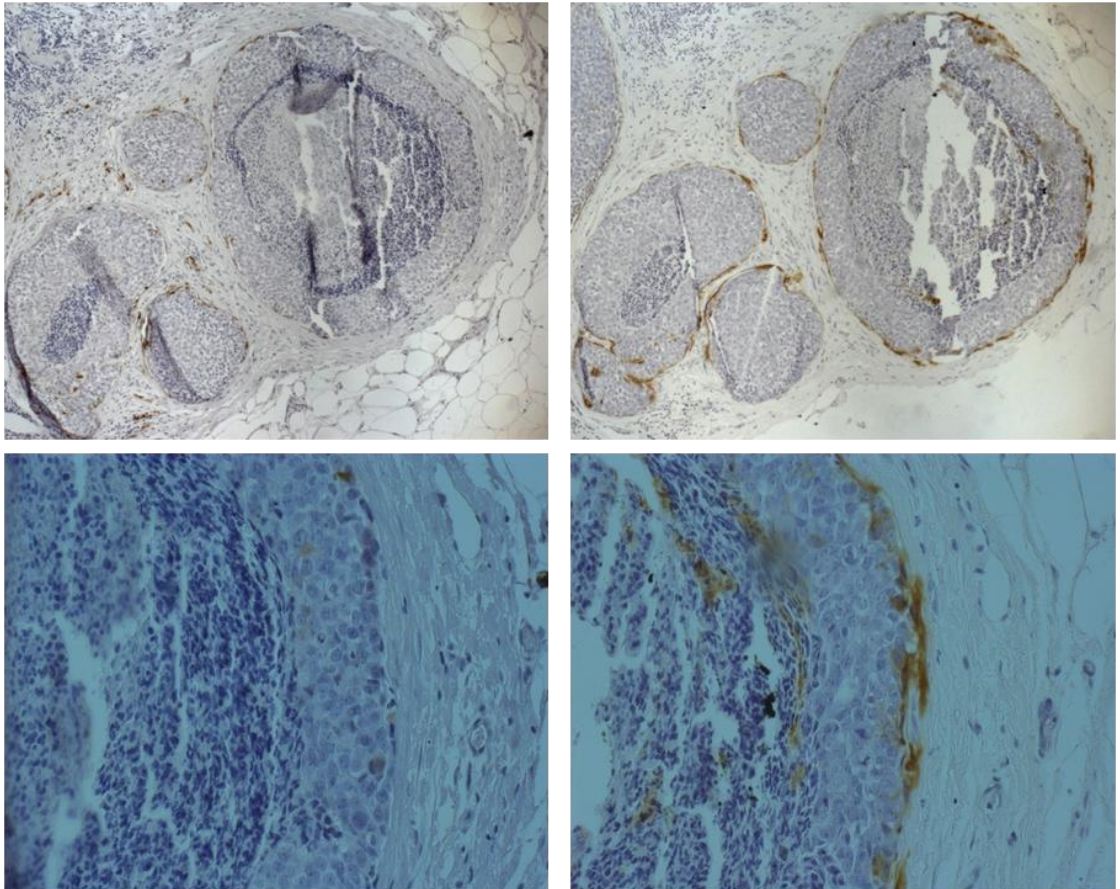


**Figure 5. 2 Immunohistochemical staining of DCIS for Galectin 7 and  $\alpha\text{v}\beta\text{6}$**

Paraffin-embedded sections from DCIS specimens were stained with antibodies to galectin-7 and  $\alpha\text{v}\beta\text{6}$ . The specimens have been scored duct by duct for galectin-7 and  $\alpha\text{v}\beta\text{6}$  expression. The study showed that the majority of ducts of DCIS that express  $\alpha\text{v}\beta\text{6}$  are negative for galectin-7.

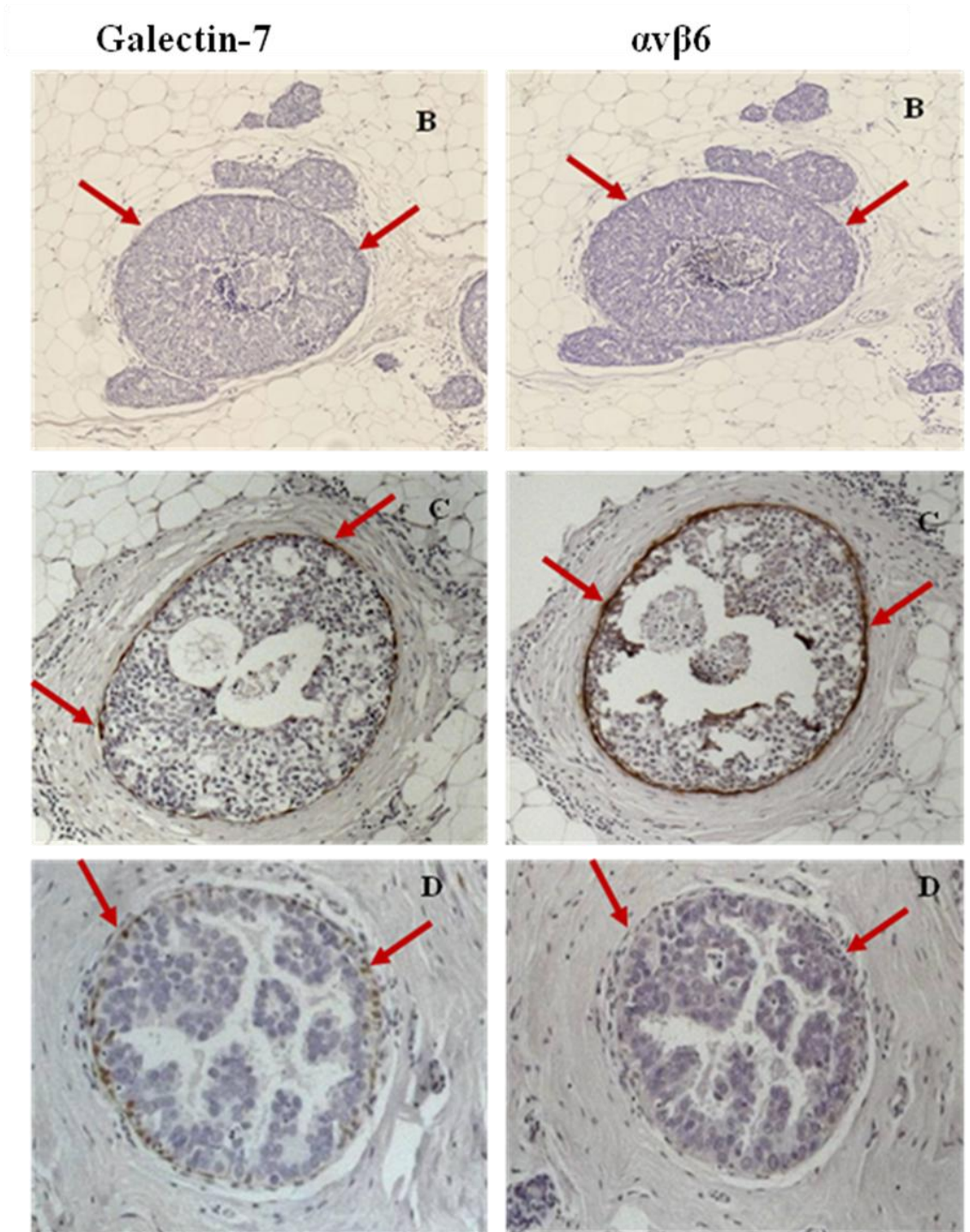


**Figure 5. 3 Immunohistochemical staining of DCIS for Galectin 7 and  $\alpha v\beta 6$**

The pattern of staining varied between cases and in a minority of cases myoepithelial cells were negative for both markers (panel B) or were positive for both markers (panel C). Some cases were positive for galectin-7 and negative for  $\alpha v\beta 6$  (D).

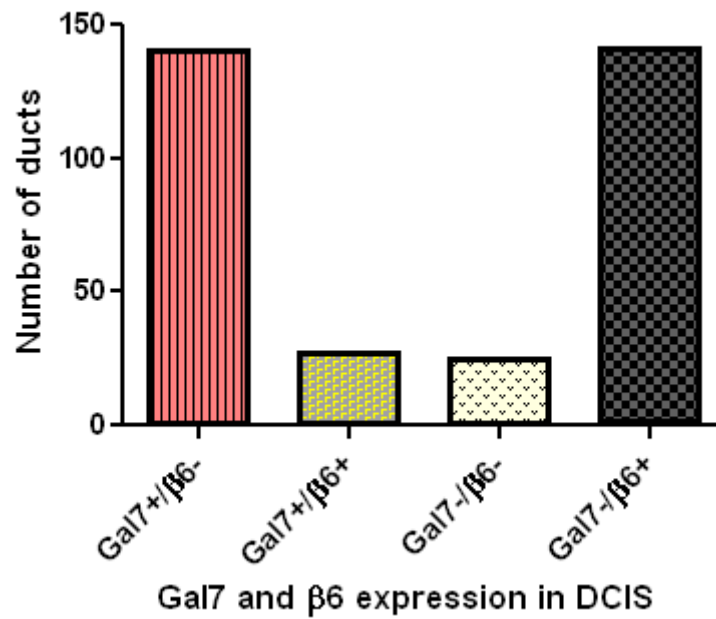


**Figure 5.4** Analysis of galectin-7 and  $\alpha\beta 6$  expression in DCIS cases

There was a significant inverse relationship between expression of  $\beta 6$  and Galectin-7 in DCIS-associated myoepithelial cells, with 70% of Galectin-7 positive ducts being  $\beta 6$  negative compared to 30% being  $\beta 6$  positive ( $p=0.001$  using one way ANOVA test). It can also be seen that a minority of DCIS ducts showed expression of both markers or were negative for both Galectin-7 and  $\alpha\beta 6$ .

### 5.4.3 Galectin- 7 expression in myoepithelial breast cell lines

To determine the levels of galectin-7 in relation to  $\alpha\beta6$  expression in myoepithelial cells, and to provide the basis for future functional studies, two cell lines have been selected;  $\beta4$  myoepithelial cells that are negative for  $\alpha\beta6$ , and  $\beta6$  myoepithelial cells that over-express  $\beta6$  integrin. The level of galectin-7 protein and mRNA in both cell lines was analysed by Western blot and PCR, respectively.  $\beta4$  myoepithelial cells exhibited higher levels of expression of galectin-7 protein compared to  $\beta6$  myoepithelial cells (Figure. 5.5A). Similarly, mRNA expression analysis demonstrated that galectin-7 is expressed at higher levels in  $\beta4$  myoepithelial cells compared to  $\beta6$  myoepithelial cells (Figure 5.5C). The MDA MB 468 breast cancer cell line was used as a positive control for Western blot (Figure 5.5A), while primary myoepithelial cells were used as positive control and primary luminal epithelial cells as negative control for PCR (Figure 5.5C).

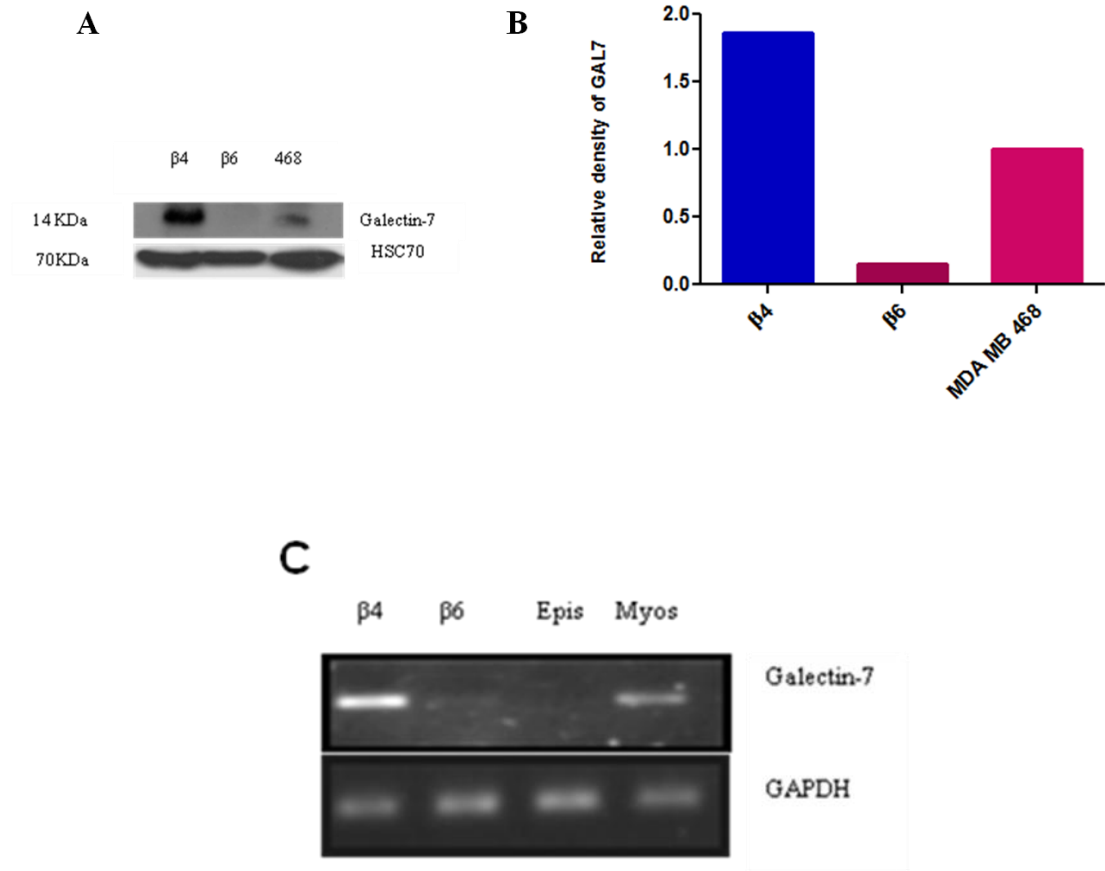


**Figure 5. 5 Analysis of Galectin- 7 in myoepithelial cell lines**

(A) Western blot analysis for galectin-7 in  $\beta 4$  and  $\beta 6$  myoepithelial breast cell lines.  $\beta 4$  myoepithelial cells show a higher level of galectin-7 (14 KDa) compared to  $\beta 6$  myoepithelial cells. HSC70 was used as a loading control. MDA MB 468 breast cancer cell line was used as positive control. (B) The results also were analysed via ImageJ integrated density and show relative density of galectin-7 for  $\beta 4$  myoepithelial cells versus MDA MB 468 cells was 1.86:1. The relative density of  $\beta 6$  cells versus MDAMB 468 cells was 0.14: 1. (C) Galectin-7 mRNA level in  $\beta 4$  and  $\beta 6$  myoepithelial cell lines was determined by PCR relative to the steady-state expression of GAPDH.  $\beta 6$  myoepithelial cells expressed very low levels of galectin-7 mRNA compared to  $\beta 4$  myoepithelial cells. Primary myoepithelial cells were used as positive control and primary luminal epithelial cells as a negative control for the PCR.



### 5.4.4 Impact of galectin-7 knockdown on $\alpha\beta 6$ expression

Immunohistochemical analysis of DCIS tissues demonstrated an inverse correlation between myoepithelial galectin-7 and  $\alpha\beta 6$  expression. In order to investigate this further, galectin-7 was knocked down in the  $\beta 4$  myoepithelial cell line and in primary myoepithelial cells for 24, 48 and 72 hrs, and  $\beta 6$  expression was measured by Western blot. Galectin-7 knockdown in primary myoepithelial cells was achieved at both 24 hrs and 48 hrs time points (figure 5.6 & 5.7) as detected by Western blot. Western blot on these cells for  $\beta 6$  demonstrated up-regulation of  $\beta 6$  in myoepithelial cells treated with galectin-7 siRNA for 48hrs compared to those treated with Control siRNA for the same time point (figure 5.8). The experiments were repeated on the  $\beta 4$  myoepithelial cell line and whilst knockdown of galectin-7 was achieved, there was no change in the level of  $\beta 6$  expression (data not shown).

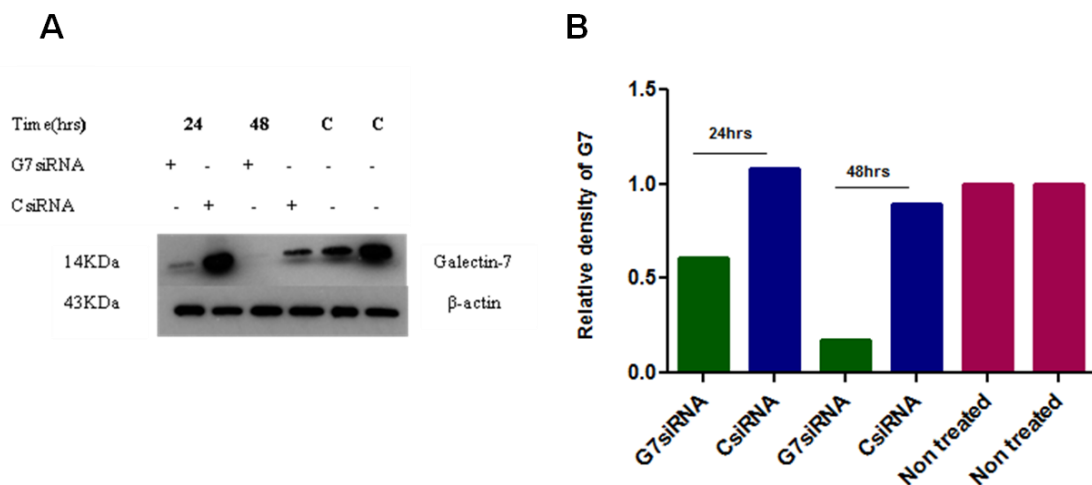


**Figure 5. 6 Knockdown of galectin-7 in primary myoepithelial cells**

(A) Galectin-7 knockdown in primary myoepithelial cells was achieved at both 24 hrs and 48 hrs time-point as detected by Western blot. Two samples of non-treated myoepithelial cells were used as controls. (B) The results also were analysed via ImageJ integrated density. The relative density of in gal-7 siRNA 24hrs versus CsiRNA for same time point was 0.61:1.2 respectively. The relative density of gal-7 siRNA 48hrs versus CsiRNA at 48 hrs was 0.17: 0.89.

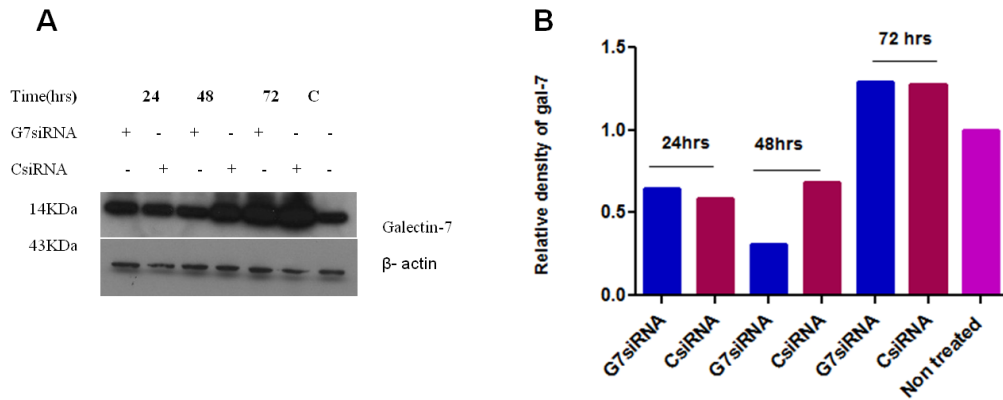


**Figure 5.7 Knockdown of galectin-7 in primary myoepithelial cells at extended time-points**

(A) Galectin-7 knockdown in primary myoepithelial cells was achieved at 48 hrs time as detected by Western blot. Non-targeting siRNA (CsiRNA) and non-treated myoepithelial cells were used as controls. The cells were also analysed following 72hrs knockdown, however, no difference in the level of galectin-7 was evident. (B) The results also were analysed via ImageJ integrated density. The relative density for galectin-7 in cells treated with gal-7 siRNA for 24hrs versus cells treated with CsiRNA at the same time point was 0.64:0.58. The relative density for gal-7 in cell treated with siRNA for 48hrs versus CsiRNA treated cells at the same time point was 0.30: 0.68. At 72 hrs the relative density for gal-7 in cells treated with siRNA for 72hrs versus CsiRNA treated cells at the same time point was 1.2: 1.2.

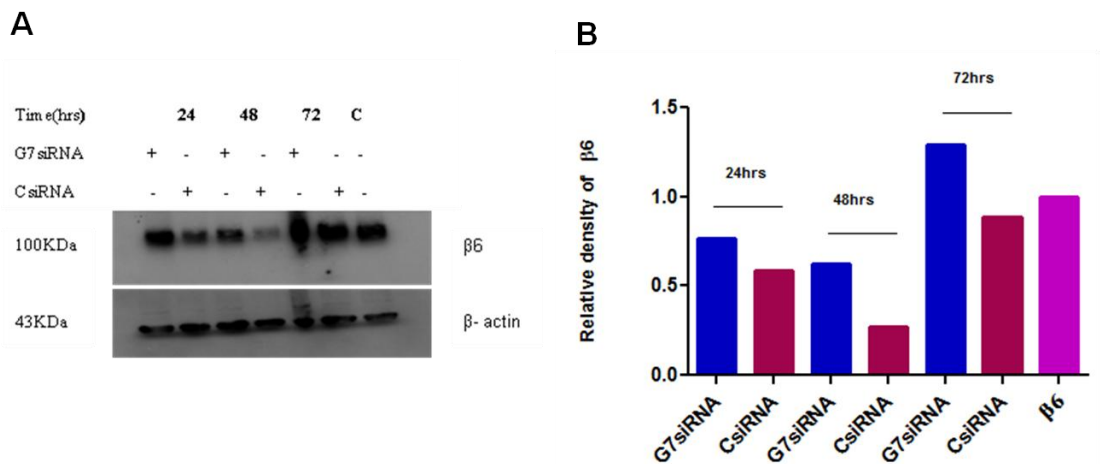


**Figure 5.8 Analysis of  $\beta 6$  expression following knockdown of galectin-7 in primary myoepithelial cells**

(A) Galectin-7 knockdown in primary myoepithelial cells was achieved at 24 hrs and 48 hrs time-points.. Western blot for  $\beta 6$  was carried out on these cell lysates and demonstrates up-regulation of  $\beta 6$  in myoepithelial cells treated with gal-7 siRNA for 48hrs compared to those treated with CsiRNA at the same time point. (B) The results also were analysed via ImageJ integrated density. The relative density for  $\beta 6$  in cells treated with gal-7 siRNA for 24hrs versus CsiRNA for the same time point was 0.76:0.58. The relative density for  $\beta 6$  in cells treated with gal-7 siRNA for 48hrs versus CsiRNA for the same time point was 0.62: 0.27. At 72 hrs the relative density for  $\beta 6$  in gal-7 siRNA treated cells versus CsiRNA treated cells was 1.2: 0.88.

### 5.4.5 Relationship between Galectin-7 expression and apoptotic response

#### (i) Detection of cleavage PARP

In earlier experiments, treatment of myoepithelial cells with TRAIL led to induction of apoptosis in  $\beta 6$  cells but not in  $\beta 4$  cells. Furthermore, we demonstrated an inverse relationship between  $\beta 6$  expression and galectin-7 in human DCIS tissues. Galectin-7 has been implicated in apoptosis, having both pro-apoptotic and anti-apoptotic functions. We therefore investigated whether loss of galectin-7 in  $\beta 4$  cells would make these cells more sensitive to TRAIL-induced apoptosis. Thus, we knocked down Galectin-7 in  $\beta 4$  myoepithelial cells. RT-PCR for galectin-7 RNA and immunoblotting for galectin-7 protein was undertaken to assess knockdown efficiency (Figure. 5.9, 5.10, 5.11 and 5.12). Optimal knockdown was reached by 48 hrs. Galectin-7 knockdown cells and non-targeting control cells were then exposed to recombinant TRAIL for 2, 4 and 8 hours. Apoptosis was assessed by detection of cleaved PARP by Western blot. Knockdown of Galectin-7 appeared to enhance apoptosis in  $\beta 4$  myoepithelial cells. The time-course study indicates that there is no difference in cleaved PARP levels between the non-targeting control cells and galectin-7 knockdown cells after 2 hrs of treatment, whereas high levels of cleaved PARP were detected after 4 hrs of exposure to TRAIL in  $\beta 4$  galectin-7 knock down cells compared to control cells. By 8 hrs, the same level of cleaved PARP was detected in galectin-7 knockdown cells and non-targeting control cells (Figure 5.13).



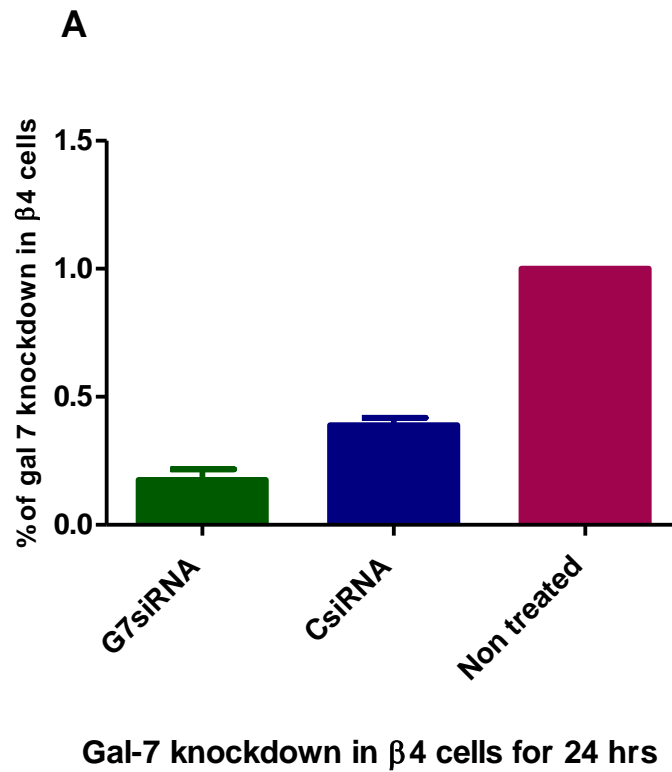


**Figure 5.9 Knockdown of galectin-7 in  $\beta 4$  cells for 24hrs**

RT-PCR results showed significant down-regulation of galectin-7 RNA in gal -7 knockdown  $\beta 4$  cells at the 24 hrs time point compared to CsiRNA and non-treated counterparts ( $p=0.0001$ ). There also was reduction of galectin-7 RNA in CsiRNA cells compared to non-treated controls. Error bars=SD. Bars represent triplicate experiments.

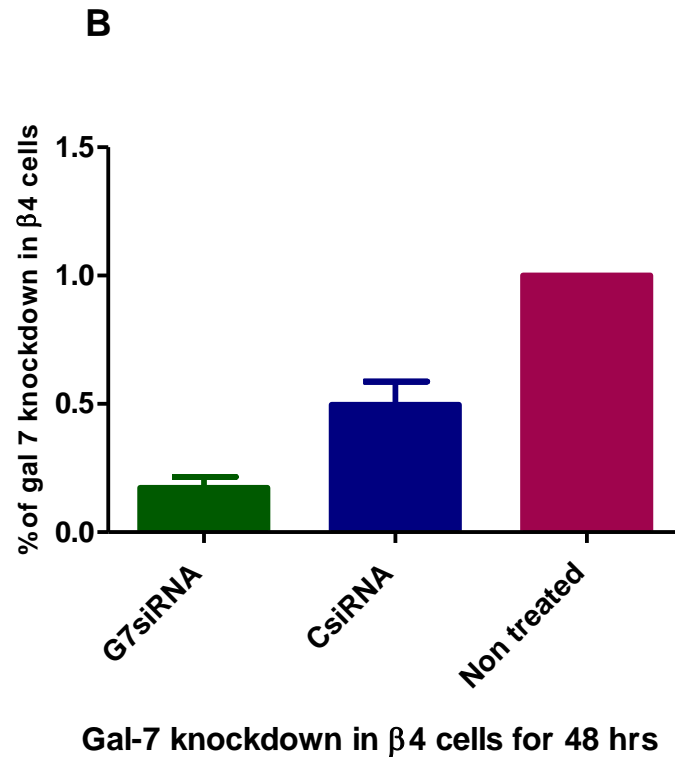


**Figure 5.10 Knockdown of galectin-7 in  $\beta\text{4}$  cells for 48hrs**

Galectin-7 was knocked down in  $\beta\text{4}$  myoepithelial cells for 48 hrs. This showed significant down-regulation of galectin-7 RNA in  $\beta\text{4}$  cells treated with Gal-7siRNA compared to the cells treated with CsiRNA and non treated cells ( $p=0.0002$ ). Error bars=SD. Bars represent triplicate experiments.

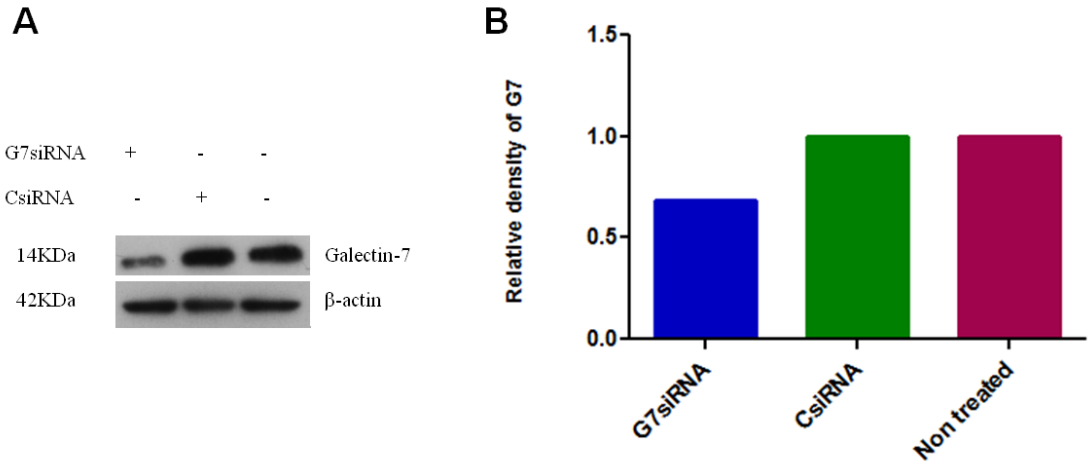


**Figure 5.11** Knockdown of galectin-7 in  $\beta 4$  myoepithelial cells at 24 hrs

(A) Galectin-7 knockdown  $\beta 4$  in myoepithelial cells was achieved at 24 hrs as detected by Western blot. Both CsiRNA and non-treated  $\beta 4$  myoepithelial cells were used as controls. (B) The results also were analysed via ImageJ integrated density. The relative density for galectin-7 in cells treated with gal-7 siRNA for 24hrs versus cells treated with CsiRNA for the same time was 0.68:1.

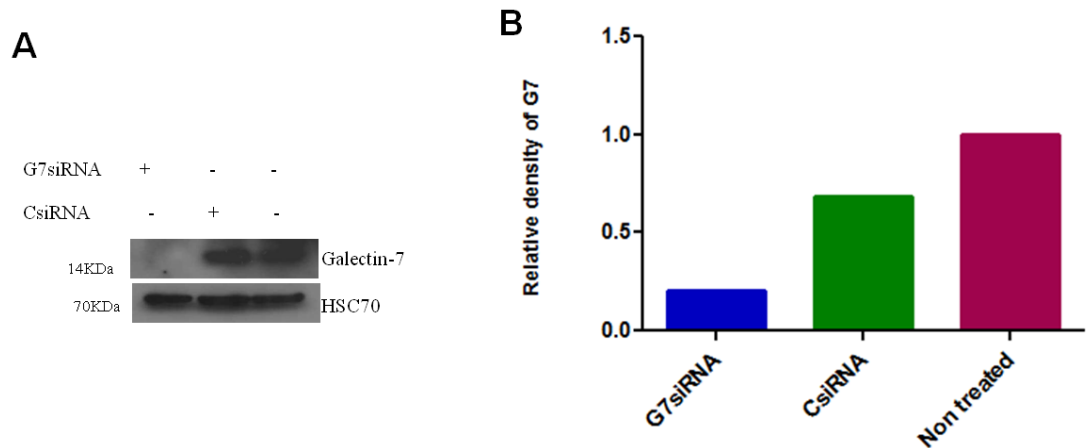


**Figure 5.12** Knockdown of galectin-7 in  $\beta 4$  myoepithelial cells at 48 hrs

(A) Optimal knockdown of galectin-7 in  $\beta 4$  myoepithelial cells was reached by 48 hrs as detected by Western blot. Cells treated with CsiRNA and non-treated  $\beta 4$  myoepithelial cells were used as controls. (B) The results also were analysed via ImageJ integrated density. The relative density for galectin-7 in cells treated with gal-7 siRNA for 48hrs versus cells treated with CsiRNA treated cells was 0.30:0.89.

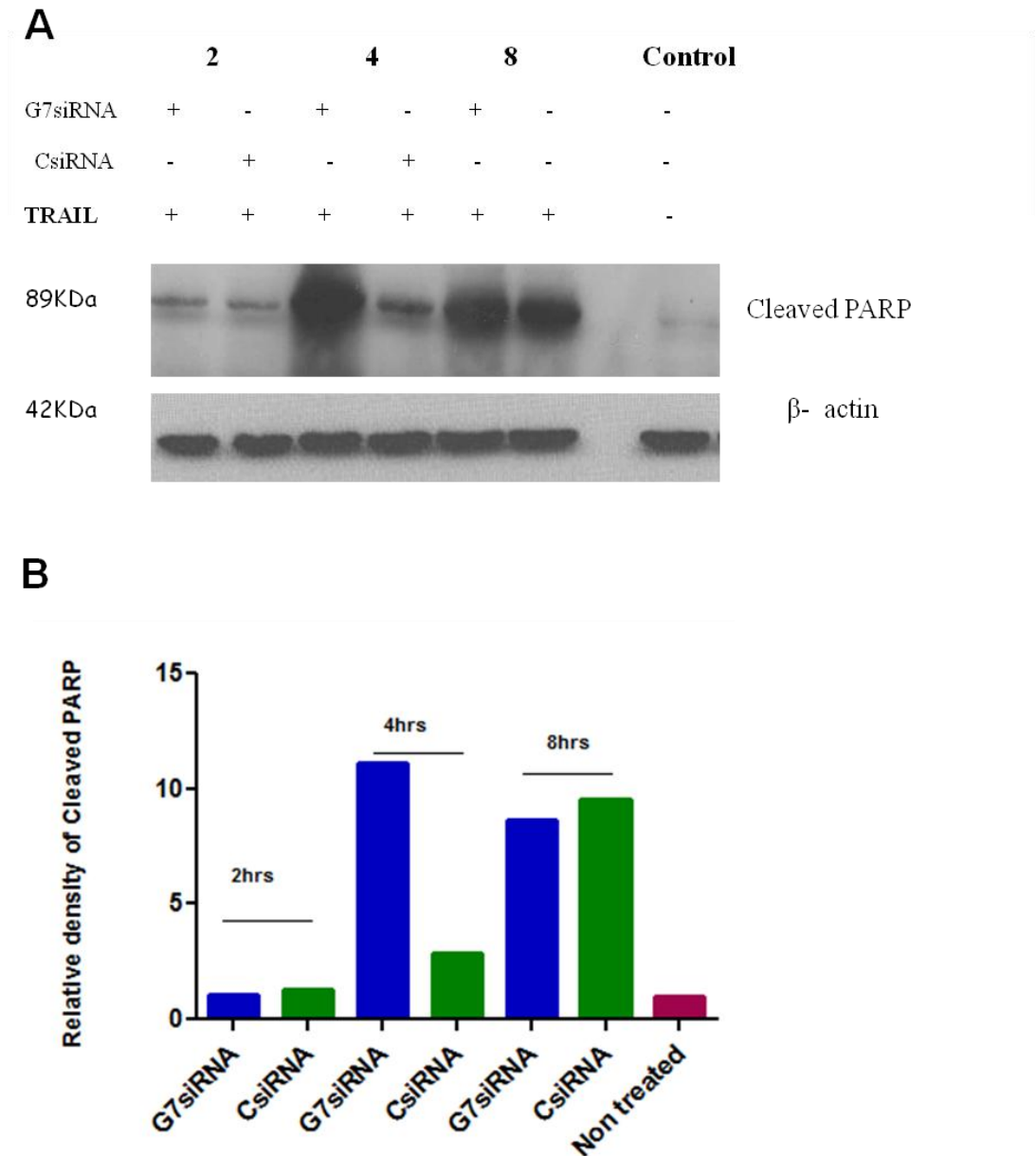


**Figure 5. 13** Detection of apoptosis by cleaved PARP in  $\beta4$  cells exposed to TRAIL following knockdown of galectin-7

(A) Cells treated with non-targeting siRNA or galectin-7 siRNA were exposed to recombinant TRAIL at 500 ng/ml for 2, 4 and 8 hrs. Apoptosis was analysed by Western blot using an antibody to cleaved PARP. By 4 hrs, galectin-7 knockdown  $\beta4$  cells exhibit increased PARP cleavage compared to non-targeting control cells. There is no difference in cleaved PARP between galectin-7 knockdown  $\beta4$  cells and non-targeting control cells at 2 hrs or 8 hrs post-treatment. (B) The relative density of cleaved PARP in gal-7 siRNA cells treated with TRAIL for 2 hrs versus CsiRNA cells at the same time point was 1:1.2. In contrast, the relative density of cleaved PARP in gal-7 siRNA cells treated with TRAIL for 4 hrs versus CsiRNA cells at the same time point was 11: 2.8. The relative density of cleaved PARP in gal-7 siRNA cells treated with TRAIL for 8 hrs versus CsiRNA cells at the same time point was 8.6: 9.5.

**(ii) Morphological changes**

To further investigate whether loss of galectin-7 enhances apoptosis in myoepithelial cells,  $\beta\text{4}$  cells treated with control siRNA (CsiRNA) or galectin-7 siRNA (G7siRNA) were exposed to etoposide chemotherapy at  $1\mu\text{M}/\text{ml}$  for 48 hrs. After 48 hrs, galectin-7 knockdown cells showed morphological changes suggestive of early apoptosis such as blebbing of the cell membrane, contraction and bright phase appearance, compared to the non-targeting control cells (Figure 5.14).

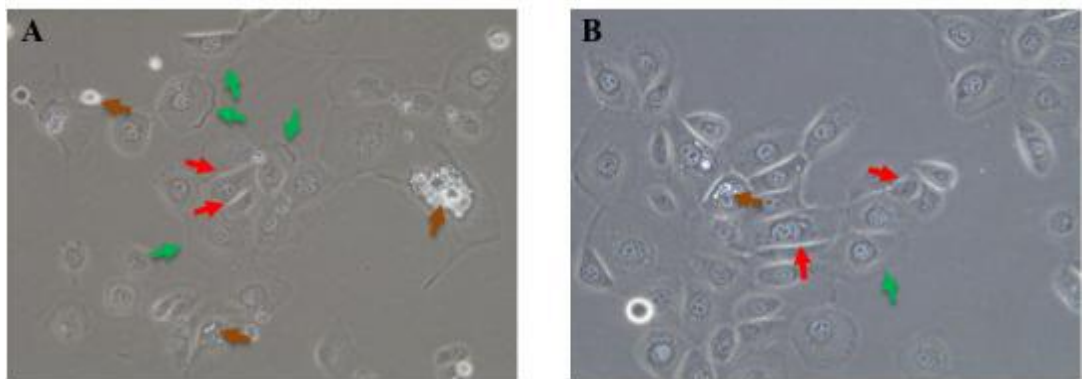


**Figure 5.14 Induction of morphological changes in  $\beta\text{4}$  cells treated with G7 siRNA (A) or control siRNA (B) on exposure to etoposide**

$\beta\text{4}$  cells were treated with G7siRNA or CsiRNA and exposed to  $1\mu\text{M}/\text{ml}$  etoposide for 48 hrs. (A) Galectin-7 knockdown cells exhibit morphological changes suggestive of early apoptosis indicated by plasma membrane blebbing (green arrows), contracted morphology (early stage, red arrow) and phase-bright appearance (late stage, brown arrow). (B) Less marked changes are seen in  $\beta\text{4}$  cells treated with control siRNA.

### 5.4.6 Relationship between galectin-7 and $\alpha\text{v}\beta\text{6}$ expression and DCIS duct size

On analysis of DCIS tissues it was clear that the size of involved ducts was variable. It may be postulated ducts become more expanded by neoplastic cells as the disease progresses. In order to assess whether there is a correlation between DCIS duct size and myoepithelial cell phenotype, the DCIS ducts were measured using NDP software (section 2.6). In the 47 cases of DCIS analysed, 268 ducts were positive for galectin-7 and 206 ducts were negative for galectin-7, and 521 ducts positive for  $\alpha\text{v}\beta\text{6}$  and 69 ducts negative for  $\alpha\text{v}\beta\text{6}$ . Data was plotted on a graph using prism software. Two-tailed T- test was used to measure the p value.

In general, the size of galectin-7 positive ducts was significantly smaller than the negative ducts ( $p=0.0001$ ) (figure 5.15). Whereas, the size of  $\alpha\text{v}\beta\text{6}$  positive ducts was larger compared to the  $\alpha\text{v}\beta\text{6}$  negative ducts ( $p=0.0006$ ) (figure 5.16). The ducts positive for galectin-7 and negative for  $\alpha\text{v}\beta\text{6}$  were significantly smaller than ducts positive for both markers ( $p<0.0001$ ), ducts negative for both ( $p=0.02$ ) and ducts negative for galectin-7 and positive for  $\alpha\text{v}\beta\text{6}$  ( $p<0.0001$ ) (figure 5.17).

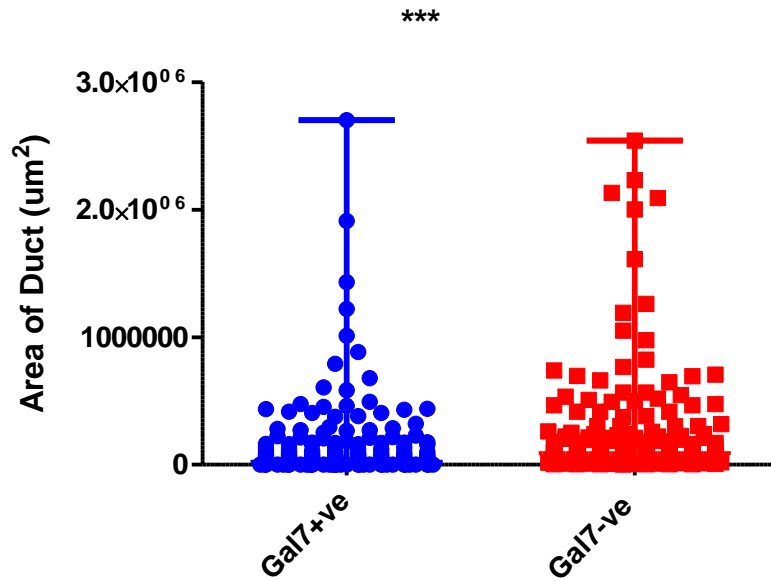


**Figure 5.15** Measurement of the area of ducts in DCIS cases where the ducts are positive or negative for galectin-7

47 DCIS cases were stained for galectin-7 and  $\alpha\beta 6$ . 268 ducts positive for galectin-7 and 206 ducts negative for galectin-7 were measurable in these cases. The size of the ducts was measured using NDP software. DCIS ducts negative for galectin-7 was significantly larger than the galectin-7 positive ducts ( $p=0.0001$ ).

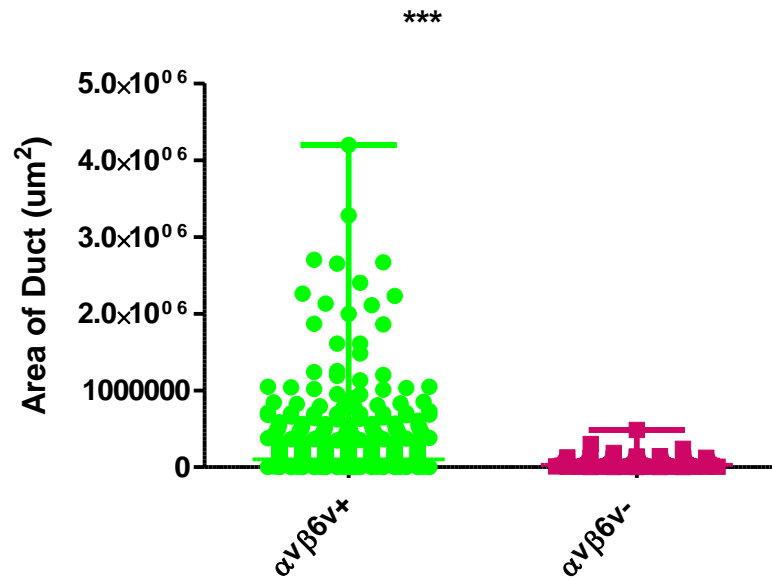


**Figure 5.16 Measurement of area of ducts in DCIS cases where the ducts are positive or negative for  $\alpha\beta 6$**

From 47 DCIS cases, 521 ducts positive for  $\alpha\beta 6$  and 69 ducts negative for  $\alpha\beta 6$  were measurable. The size of the ducts was measured using NDP software. DCIS ducts negative for  $\alpha\beta 6$  were significantly smaller compared to the  $\alpha\beta 6$  positive ducts ( $p=0.0006$ ).



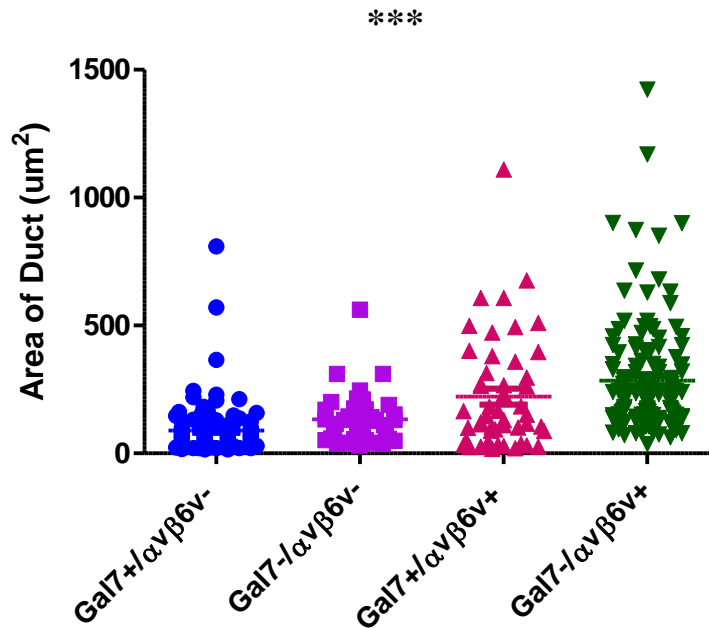


**Figure 5.17 Measurement of size of ducts in DCIS cases where the ducts are positive or negative for both galectin-7 and  $\alpha\beta6$  or positive for one and negative for the other**

From 47 cases ducts where they are positive or negative for both Galectin-7 and  $\alpha\beta6$  or positive for one marker and negative for the other one were measured for the size of ducts. This demonstrated that the size of ducts positive for galectin-7 and negative for  $\alpha\beta6$  is significantly smaller than the ducts are negative for both ( $p=0.02$ ), ducts positive for both markers ( $p<0.0001$ ) and ducts negative for galectin-7 and positive for  $\alpha\beta6$  ( $p=0.0001$ ).

### 5.4.7 Relationship between galectin-7 and $\alpha\beta6$ expression and clinical outcome

In order to address whether expression of  $\alpha\beta6$  and galectin-7 could act as predictors of progression to invasion, a second cohort of samples were analysed. This cohort included tissues from pre-operative diagnostic core biopsies showing DCIS in 294 patients, some of whom had invasive disease present on their surgical excision specimen. These samples were therefore stained and scored for galectin-7 and for  $\alpha\beta6$  integrin. This was done blind of the final histology and the scores returned to Prof Westenden to reconcile with clinical data. Some of the core biopsies showed invasive disease and these were excluded from the analysis, resulting in interpretable staining being available on 225 cases. The clinical and pathological features of these cases is summarised in Table 2.2.

**Table 5.1: Summary of case numbers with interpretable staining and other continuous attributes**

Factor	Number with known status	Mean (SD)
Size of DCIS (mm)	141	24 (20)
ER %	215	69 (44)
Galectin 7 hscore	225	93 (95)
$\alpha\beta6$ hscore	224	75 (85)

**Table 5.2 : Categorical pathological data relating to core biopsies with interpretable staining**

Factor	Category	No (%)
Grade of core	1	26 (11)
	2	47 (21)
	3	132 (59)
	NK	20 (9)
Invasive tumour present?	No	55 (24)
	Yes	170 (76)

There was no significant positive or negative association between galectin-7 hscore and  $\alpha\text{v}\beta\text{6}$  hscore (Spearman correlation coefficient = 0.08,  $p=0.2$ ). No significant association with presence of invasion was noted for either galectin-7 ( $p=0.4$ ) or  $\alpha\text{v}\beta\text{6}$  ( $p=0.5$ ). The only significant association with galectin-7 was with grade of core biopsy, with increasing galectin-7 levels with poorer grade ( $p=0.002$ ; data not shown). The only significant associate of  $\alpha\text{v}\beta\text{6}$  was ER status ( $p=0.001$ ), with decreasing  $\alpha\text{v}\beta\text{6}$  levels with increasing ER score- that is,  $\alpha\text{v}\beta\text{6}$  is associated with ER negativity (Table 5.3)

Table 5.3 Relationship between  $\alpha\beta 6$  and ER

ER	Mean (SD) $\alpha\beta 6$ hscore
<b>0</b>	102 (97)
<b>&gt;0, &lt;50</b>	123 (97)
<b>50-90</b>	76 (84)
<b>&gt;90</b>	61 (74)
<b>Missing</b>	57 (100)

## 5.5 Discussion

---

The results in chapter 4 provide early evidence that myoepithelial cells positive for  $\beta\text{6}$  integrin may be more susceptible to the effect of T-cells, though this requires further investigation in co-culture models. Many changes could influence the response of myoepithelial cells to TRAIL. It has been shown that normal myoepithelial cells express galectin-7 and its expression is altered during breast cancer progression (Demers, Rose et al. 2010). One of the major biological roles played by galectin-7 relates to its modulatory effects on apoptosis; while it seems to display pro-apoptotic activity in some tumour cell lines (Bernerd, Sarasin et al. 1999, Kuwabara, Kuwabara et al. 2002), other studies have suggested that galectin-7 may display anti-apoptotic effects (Gendronneau, Sidhu et al. 2008, Demers, Rose et al. 2010). With respect to the pro-apoptotic roles played by galectin-7, the Kuwabara group reported that ectopic expression of Galectin-7 in HeLa cells and in the colon carcinoma cell line DLD-1 renders them more susceptible to apoptosis induced by actinomycin D and UVB (Kuwabara, Kuwabara et al. 2002). Similarly, an increase in galectin-7 expression has been demonstrated in apoptotic keratinocytes of human skin explants exposed to UVB (Bernerd, Sarasin et al. 1999). In contrast, exposure of skin from wild type (wt) or galectin-7<sup>-/-</sup> adult mice to UVB revealed a twofold increase in apoptotic cells in galectin-7<sup>-/-</sup> compared with wt epidermis at 6 hrs (Gendronneau, Sidhu et al. 2008). A study by Demers and colleagues suggests that galectin-7 has the ability to render mammary cells more resistant to apoptosis. They demonstrated that the mouse breast cancer cell line 4T1, when transfected with galectin-7, become more resistant to apoptosis when exposed to epigallocatechin galatte, a

pharmacological agent known to induce apoptosis in 4T1 cells (Demers, Rose et al. 2010). Thus, it appears from the literature that galectin-7 certainly has a role in apoptosis, and whereas most evidence suggests it is pro-apoptotic some models suggest it may be anti-apoptotic, and this is context-dependent. The next aim therefore was to determine whether there was any change in galectin-7 expression in DCIS-associated myoepithelial cells, and whether this could influence their response to apoptosis-inducing stimuli.

Therefore, galectin-7 expression was examined in a series of DCIS tissue samples, in conjunction with  $\alpha\beta 6$  expression in order to investigate the relationship between these molecules. In keeping with previous reports galectin-7 expression was found to be limited to myoepithelial cells in normal breast. In DCIS cases there was more variable expression of galectin-7. Some ducts entirely lacked expression, others retained myoepithelial cell expression whilst in others the pattern of staining was heterogeneous. When compared to  $\alpha\beta 6$  status, there was an inverse relationship between the two markers, thus positivity for  $\alpha\beta 6$  on myoepithelial cells was associated with loss of galectin-7 ( $p= 0.001$ ). To further investigate the relationship between  $\alpha\beta 6$ , galectin-7 and susceptibility to apoptosis,  $\beta 4$  and  $\beta 6$  myoepithelial cells were examined for expression of galectin-7. This showed reduced expression of galectin-7 in the  $\beta 6$  cells. To determine whether galectin-7 has the ability to protect myoepithelial cells from apoptosis, galectin-7 was knocked down in  $\beta 4$  cells, which were then exposed to recombinant TRAIL and the level of apoptosis measured using cleaved PARP. This demonstrated that the  $\beta 4$  cells appeared to be more sensitive to TRAIL when galectin-7 levels were reduced compared to non-target control cells.

In order to investigate whether galectin-7 and  $\alpha\beta 6$  could be used to predict progression to invasive disease, a cohort of DCIS core biopsies was analysed, and expression related to final surgical pathology, where some cases were pure DCIS and others had areas of invasion. This analysis did not show a significant relationship between galectin-7 expression and  $\alpha\beta 6$ , and was not related to the presence or absence of invasive disease in the final surgical excision. It is not clear why the inverse relationship between galectin-7 and  $\alpha\beta 6$  identified on the initial DCIS set was not evident in this larger sample series. However, it may relate to the method of analysis of the staining. In the original DCIS sample set, staining for each marker was assessed on a duct-by-duct basis, whereas in the core biopsy series, a score of percentage staining for each marker was made. This may be too coarse a method of analysis to capture the relationship between the two markers, however time precluded the much more labour-intensive duct-by-duct analysis on the core biopsies, though this will be done as future work. It also is possible that the level of heterogeneity within a sample makes analysis on core biopsy too unreliable. The relationship between presence of myoepithelial  $\alpha\beta 6$  and negative ER status of DCIS cells is interesting and may reflect the more advanced stage of  $\alpha\beta 6$ -positive DCIS.

## 5.6 Conclusion

---

The work in this chapter has shown that  $\alpha\beta 6$  expression in myoepithelial cells is associated with lower levels of galectin-7 expression *in vitro* and *in vivo*. Furthermore, it demonstrates that knockdown of galectin-7 expression in myoepithelial cells *in vitro* results in enhanced susceptibility to TRAIL-induced apoptosis.



# Chapter 6: Myoepithelial- T cell interaction

## 6.1 Introduction

---

### 6.1.1 Cytokines expressed in normal breast and breast cancer

There is evidence for a change in cytokine profile in both invasive and pre-invasive DCIS. An early report showed that the cytokine High in normal- 1 (HIN-1) expression is significantly down regulated in 94% of human breast carcinomas and 95% of pre-invasive lesions, such as DCIS (Krop, Sgroi et al. 2001).

In contrast, IL-1 $\alpha$  is highly expressed in DCIS and invasive breast cancer compared to benign tumours (Kurtzman, Anderson et al. 1999), and promotes tumour growth (Kumar, Kishimoto et al. 2003). Moreover, IL-5 is inducing CD4 T cells (Hogan, Koskinen et al. 1998). IL-16 has a role in recruitment of Treg cells (McFadden, Morgan et al. 2007).

Since we have demonstrated a relationship between altered myoepithelial cell phenotype and inflammatory infiltrate it is possible that the altered phenotype results in an altered cytokine signature to influence the inflammatory population.

## 6.2 Hypothesis

---

The immunohistochemical analysis in this study demonstrates a correlation between the nature of the inflammatory cell infiltrate and myoepithelial cell phenotype. It is unclear from this tissue study whether there is a functional interaction between myoepithelial cells and the inflammatory infiltrate.

Therefore, this chapter aimed to study the interaction between myoepithelial cells and inflammatory cells *in vitro* using the Jurkat T cell line and primary T cells. The specific aims are to:

- Co-culture Jurkat and primary T cells with  $\beta 4$  ( $\alpha\beta 6$ -ve) or  $\beta 6$  ( $\alpha\beta 6$ +ve) myoepithelial cells and measure the levels of CD4 and CD8 in the T cells.
- Investigate the profile of cytokines released by both myoepithelial cell populations ( $\beta 4$  &  $\beta 6$ ) using condition medium.
- Investigate how myoepithelial cell – T cell interactions may impact on cytokine release by co-culture of Jurkat T cells with both  $\beta 4$  and  $\beta 6$  myoepithelial cell lines.

## **6.3 Methods and Materials**

---

### **6.3.1 Co-culture of myoepithelial cells with T cells**

$\beta$ 4 and  $\beta$ 6 myoepithelial cells were co-cultured with primary T cells and Jurkat T cells for 24, 48 and 72 hrs as described in section 2.8.10.

### **6.3.2 Measurement of CD4 and CD8 in T cells co-cultured with myoepithelial cells**

Levels of CD4 and CD8 were measured in primary T cells and Jurkat T cells co-cultured with  $\beta$ 4 or  $\beta$ 6 myoepithelial cells using flow cytometry technique (section 2.19).

### **6.3.3 Investigation of cytokine levels in myoepithelial cells**

Cytokines released and expressed by  $\beta$ 4 and  $\beta$ 6 myoepithelial cells were measured using cytokine profile arrays, as described in 2.18.

## 6.4 Results

### 6.4.1 Analysis of CD3 expression in Jurkat T cells

The Jurkat T cell line was assessed for CD3 expression prior to use to confirm their validity as a model of T cells. Jurkat cells were stained with Alexa Fluor 488 anti-human CD3 antibody and analysed on FACS Calibur (BD) using Cellquest software. At least 10000 cells were analysed and mouse IgG isotype was used as a negative control. The data acquisition threshold was set on a forward channel to exclude dead cells and debris with very low size. This revealed the percentage of CD3 expression in Jurkat T cells is 84.4% (figure 6.1 A). Jurkat cells were also investigated for expression of CD3 by Western blot, and were positive (figure 6.1, B).

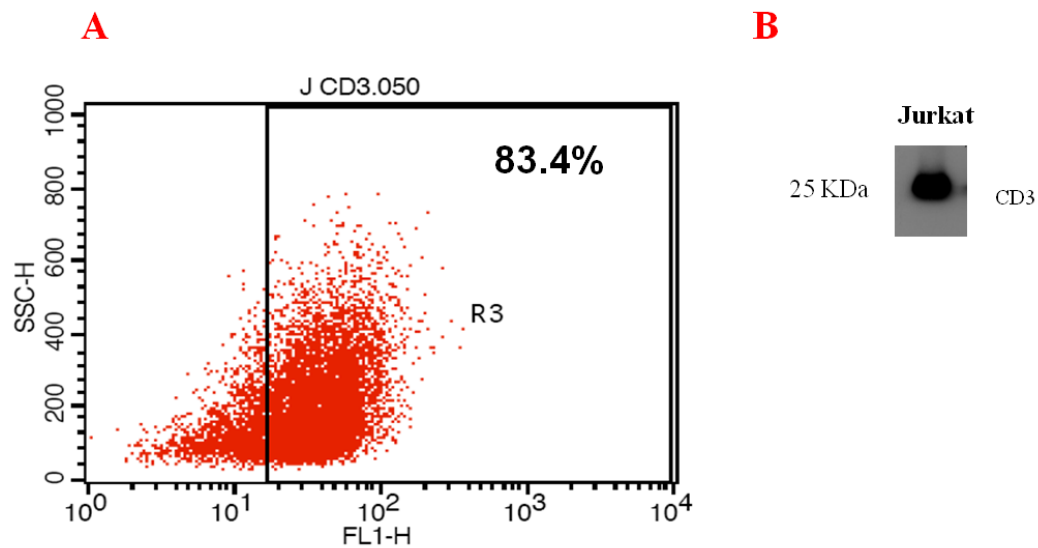


**Figure 6.1 Expression of CD3 in Jurkat T cells**

Flow cytometry analysis of expression of CD3 in Jurkat T cells showed 83.4% of Jurkat T cells were positive (A) and Western blot analysis also demonstrate Jurkat cells were positive for CD3 expression (B).

### 6.4.2 Analysis of CD3 expression in primary T cell

Primary T cells isolated from Peripheral blood mononuclear cell (PBMC) of healthy donors were also stained for CD3. Levels of CD3 were measured by flow cytometry. At least 10000 cells were analyzed using Cellquest software. This demonstrates that primary T cells were 74.4% positive for CD3 (figure 6.2).

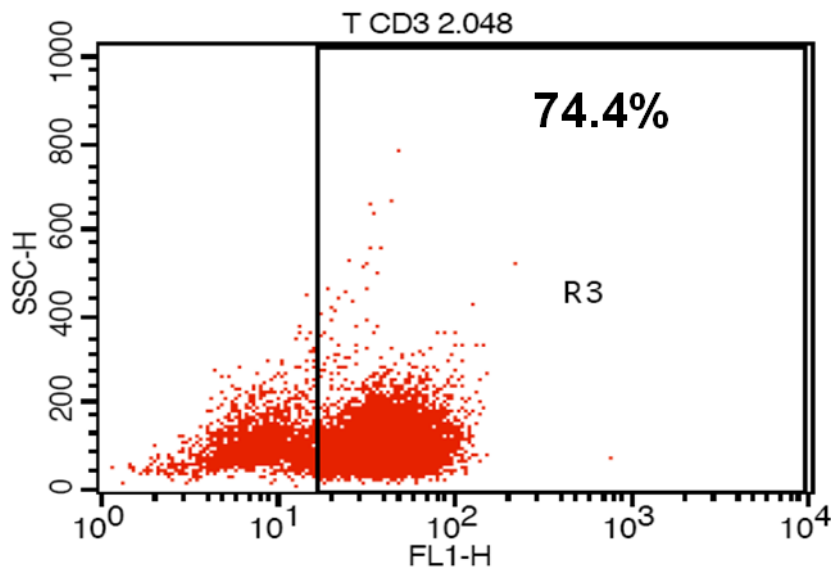


**Figure 6.2 Representative dot plot of CD3 expression in primary T cells**

Expression of CD3 in the primary T cells was measured by flow cytometry. Cells stained with isotype IgG control were used to set up the gate and at least 10000 cells were analyzed using Cellquest software. Primary T cells showed 74.4% positivity for CD3 expression.

### 6.4.3 Analysis of CD4 expression in primary T cells and Jurkat T cells

Primary T cells isolated from Peripheral blood mononuclear cell (PBMC) of healthy donors and Jurkat T cells were analysed for expression of CD4 by flow cytometry. Both cell types were stained with Alexa Fluor 488 anti-human CD4 antibody. Cells stained with mouse IgG isotype were used to set up the gates. At least 10000 cells were quantified using Cellquest software. This revealed that 45% of the primary T cells were positive for CD4 (figure 6.3), while 49.4% of Jurkat cells were positive for CD4 (figure 6.4).

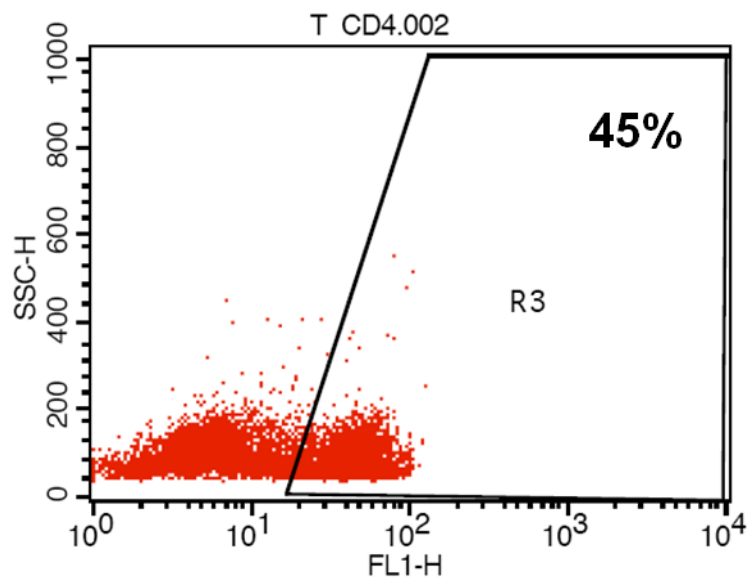


**Figure 6.3** Expression of CD4 in the primary T cells

Levels of CD4 expression was measured by FACS. Cells stained with matched isotype control were used to set up the gates and at least 10000 cells were analyzed using Cellquest software. Primary T cells showed 45% positivity for CD4 expression.

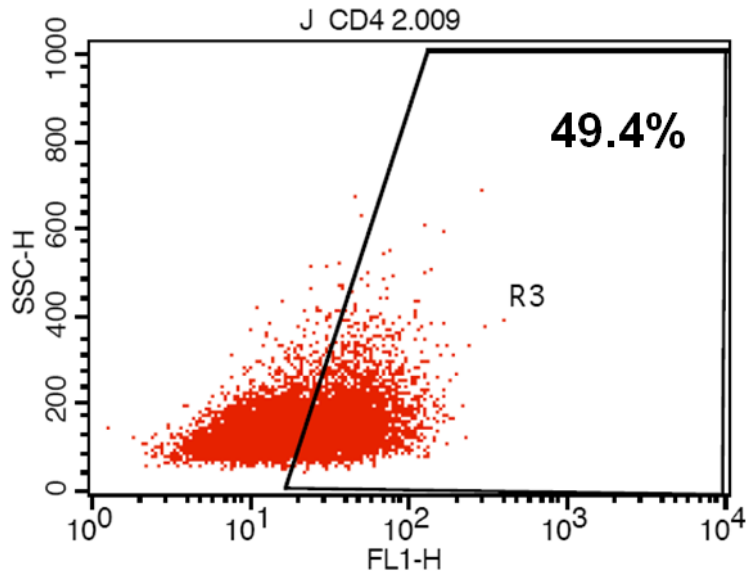


**Figure 6.4 Representative dot plot of CD4 expression in Jurkat T cells**

Jurkat T cells were measured for expression of CD4 by flow cytometry. The gates were set up using cells stained with mouse IgG isotype. At least 10000 cells were analyzed using Cellquest software. Jurkat T cells showed 49.4% positivity for CD4.



### 6.4.4 Analysis of CD8 expression in primary T cells and Jurkat T cells

Primary T cells and Jurkat T cells were analysed for expression of CD8 by FACS. Cells labelled with matched isotype control were gated on, and at least 10000 cells were quantified using Cellquest software. This revealed that 37.4% of primary T cells were positive for CD8 expression (figure 6.5) and 7.8% of Jurkat T cells were positive for CD8 expression (figure 6.6).

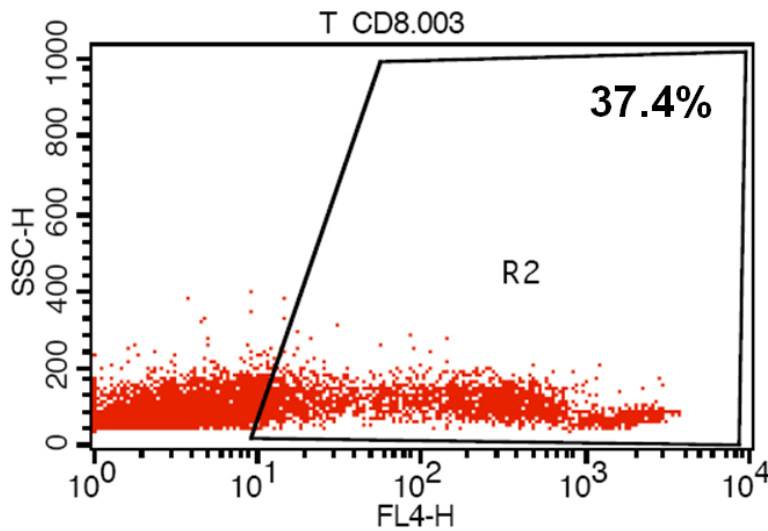


**Figure 6.5** Expression of CD8 in primary T cells

CD8 levels were measured in primary T cells by FACS. At least 10000 cells analyzed using Cellquest software. Primary T cells showed 37.4% of positivity for CD8 expression.

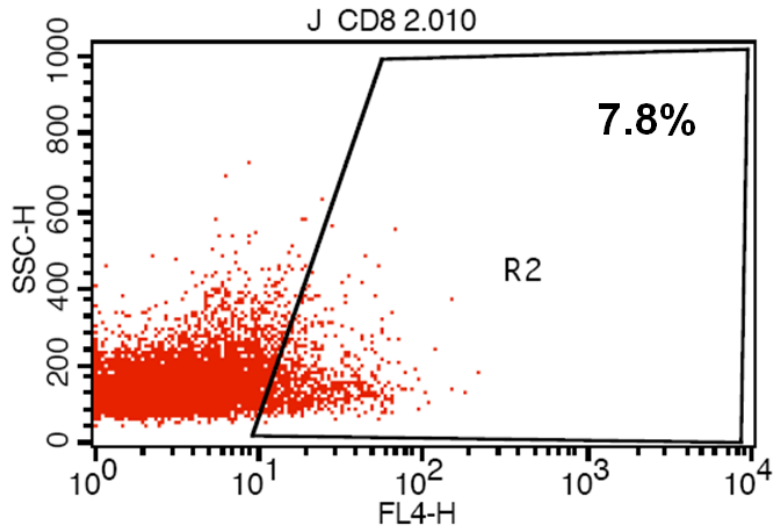


**Figure 6.6 Expression of CD8 in Jurkat T cells**

CD8 expression was measured in Jurkat T cells by flow cytometry. The same number of the cells was quantified using Cellquest software. This demonstrated 7.8% of Jurkat cells were positive for CD8.

### **6.4.5 Effect of myoepithelial cells on expression of CD4 in primary T cells**

Immunohistochemical analysis of DCIS tissues demonstrated lower numbers of CD4+ve cells and higher numbers of CD8+ve cells in ducts with  $\alpha\beta6$ -negative myoepithelial cells compared to those with  $\alpha\beta6$ -positive myoepithelial cells. This suggests that  $\alpha\beta6$  expression in myoepithelial cells may play a role in driving T cells towards CD4+ve phenotype. To investigate this, primary T cells were co-cultured with  $\beta4$  myoepithelial cells or  $\beta6$  myoepithelial cells, and the level of CD4 expression measured by flow cytometry.

Primary T cells were co-cultured with  $\beta4$  cells or  $\beta6$  cells for 24, 48 and 72 hrs (see 2.8.10). Primary T cells were stained with anti-CD4 antibody and matched isotype was used as a negative control for each run. At least 10000 cells were evaluated for expression of CD4 using Cellquest software.

At 24 hrs time point, CD4 level in primary T cells co-cultured with  $\beta4$  cells was 51.7% while its level was 52.4% in those co-cultured with  $\beta6$  myoepithelial cells (figure 6.7), and after 48 hrs, T cells co-cultured with  $\beta4$  cells showed 55.2% positivity for CD4 expression and 52.3% positivity in those co-cultured with  $\beta6$  cells (figure 6.8). At 72 hrs time point, CD4 levels were 52.9% and 52% with  $\beta4$  and on  $\beta6$  myoepithelial cells, respectively (figure 6.9). Thus, no significant difference was seen between the two myoepithelial cell lines. CD4 levels were up-regulated in primary T cells following co-culture under all conditions compared to T cells cultured without  $\beta4$  or  $\beta6$  cells (45%).

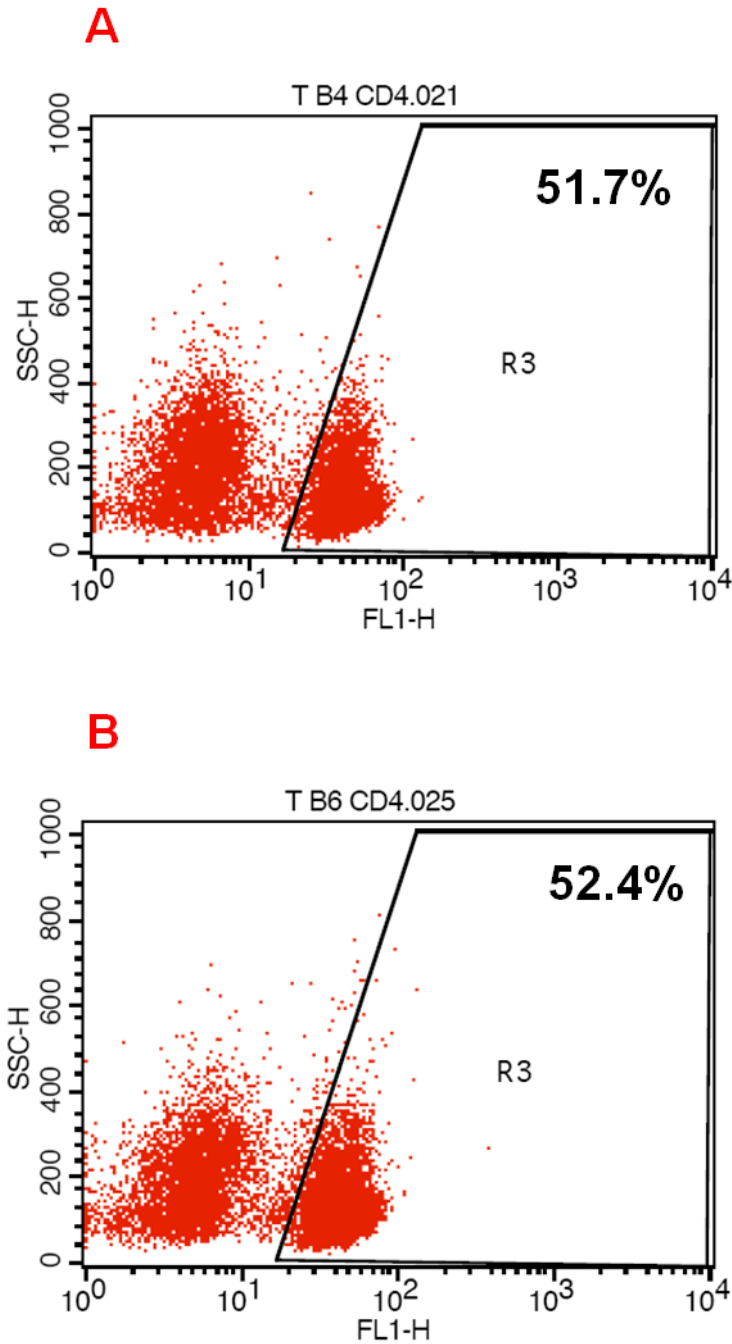


**Figure 6.7 Representative dot plots of CD4 expression in primary T cells co-cultured with  $\beta$ 4 or  $\beta$ 6 myoepithelial cells for 24hrs**

Primary T cells were co-cultured with  $\beta$ 4 or  $\beta$ 6 myoepithelial cells for 24hrs. The primary T cells were then collected and stained for CD4. At least 10000 of cells were evaluated using Cellquest software. Matched isotype control was used instead of the primary antibody as a negative control. 51.7 % of primary T cells co-cultured with  $\beta$ 4 cells were positive for CD4 (A), and when co-cultured with  $\beta$ 6 myoepithelial cells 52.4% were positive for CD4 (B).

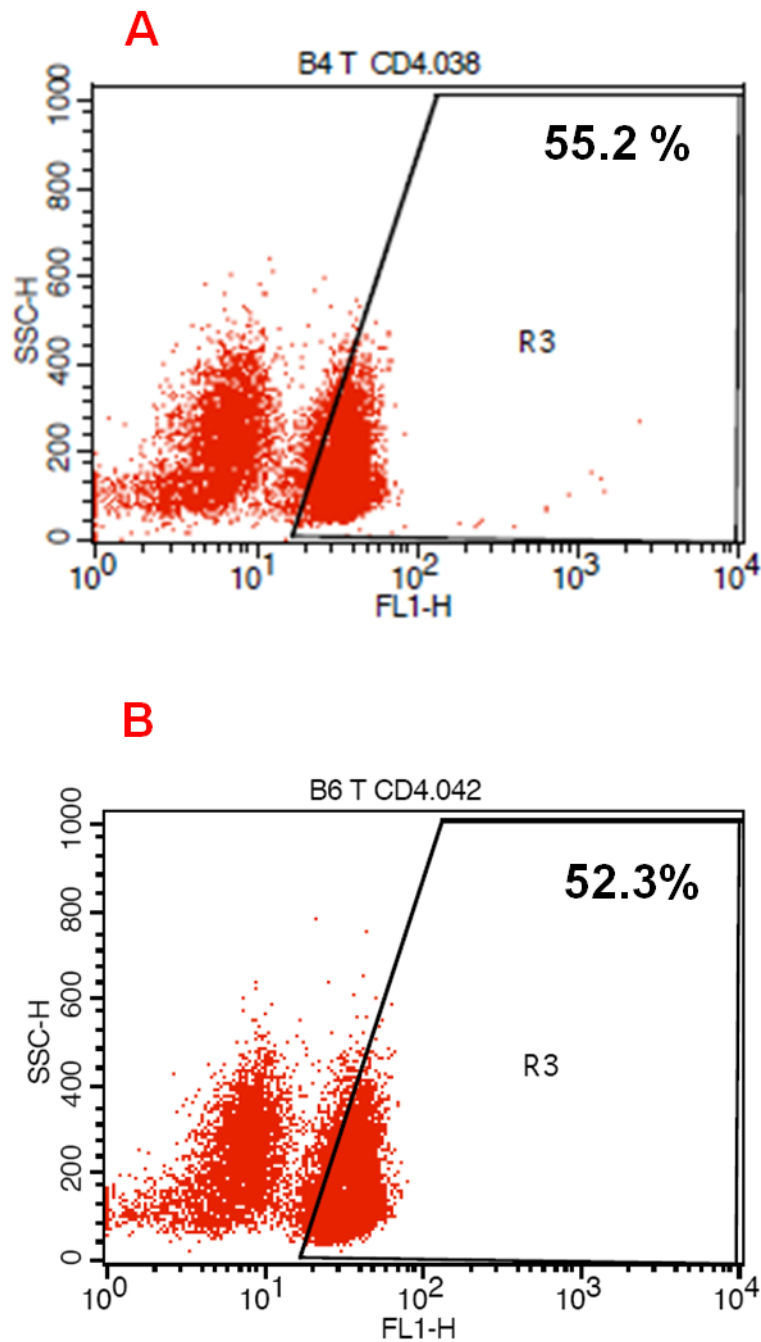


**Figure 6.8** Expression of CD4 in primary T cells co-cultured with  $\beta$ 4 or  $\beta$ 6 cells for 48 hrs

Primary T cells were co-cultured with  $\beta$ 4 or  $\beta$ 6 myoepithelial cells for 48 hrs. Primary T cells were collected and stained for CD4. At least 10000 cells were quantified using Cellquest software. This showed 55.2 % of primary T cells co-cultured with  $\beta$ 4 cells were positive for CD4 (A) and 52.3% were positive for CD4 when co-cultured with  $\beta$ 6 cells (B).

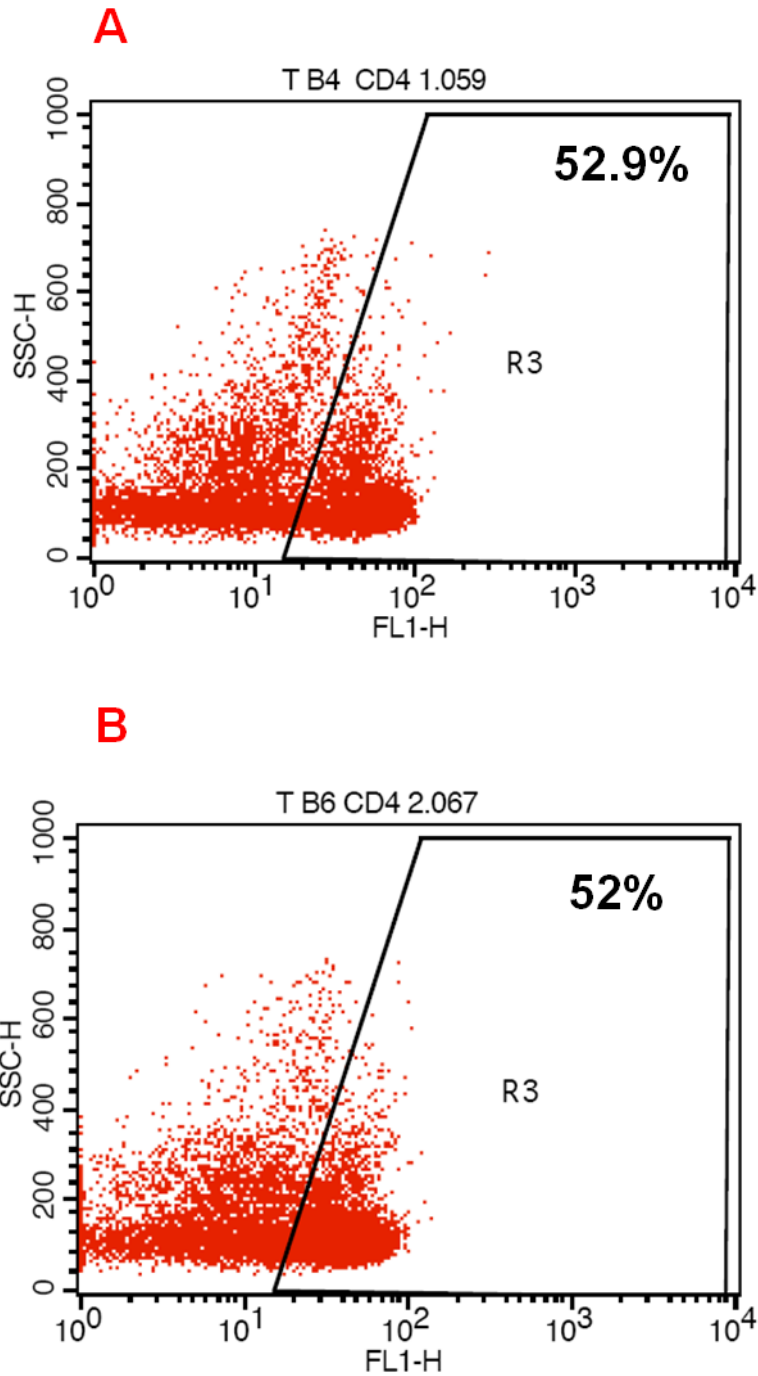


**Figure 6.9** Expression of CD4 in primary T cells co-cultured with  $\beta 4$  or  $\beta 6$  cells for 72 hrs

Primary T cells were co-cultured with  $\beta 4$  or  $\beta 6$  myoepithelial cells for 72 hrs. Gates were set up based on the cells labelled with IgG isotype control. At least 10000 cells were quantified using Cellquest software. T cells co-cultured with  $\beta 4$  cells showed 52.9 % positivity for CD4 (A) and T cells co-cultured with  $\beta 6$  cells showed 52% positivity for CD4 (B).

### **6.4.6 Effect of myoepithelial cells on expression of CD4 in Jurkat T cells**

Jurkat T cells were also co-cultured with  $\beta$ 4 or  $\beta$ 6 myoepithelial cells for the same time points as described above (24, 48 & 72hrs) (section 2.8.10). After each time point, CD4 expression in Jurkat T cells was measured by flow cytometry.

Jurkat cells labelled with matched isotype control instead of the primary antibody were used for each run to set up the gates. The same number of cells was analyzed using Cellquest software. CD4 expression level in Jurkat cells co-cultured with  $\beta$ 4 cells for 24 hrs was 32.3%, while in those co-cultured with  $\beta$ 6 cells was 33.8% (figure 6.10).

After 48 hrs a gradual decrease in the level of CD4 expression in Jurkat cells was observed in both groups of co-culture compared to non co-cultured cells: Jurkat cells co-cultured with  $\beta$ 4 cells showed 20.4% positivity for CD4 and those co-cultured with  $\beta$ 6 cells showed 21.8% positivity (figure 6.11). At 72 hrs time point, CD4 levels in Jurkat cells co-cultured with  $\beta$ 4 or  $\beta$ 6 cells were 31.8% and 32.7%, respectively (figure 6.12). Thus, no significant difference was seen between the two myoepithelial cell lines. The level of CD4 expression in Jurkat cells was 49.4% without co-culture.

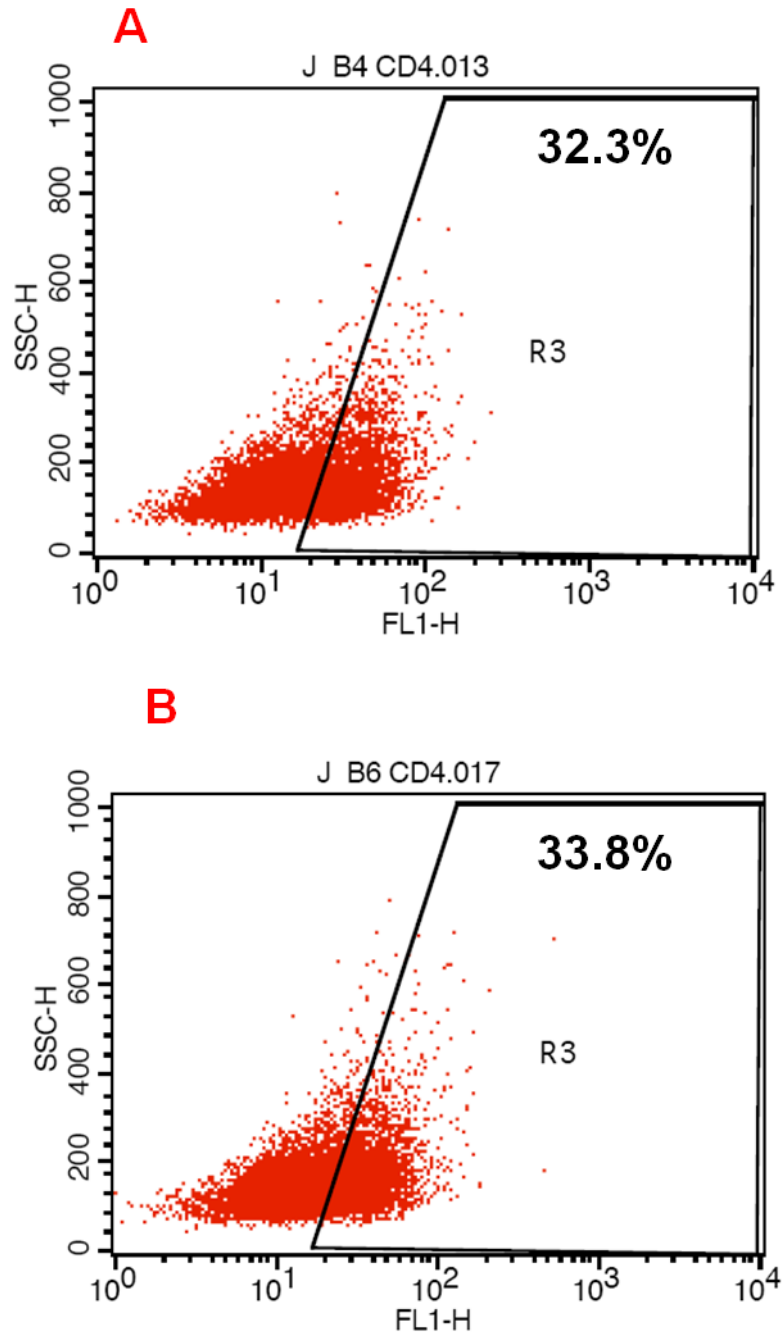


**Figure 6.10 Representative dot plots of CD4 expression in Jurkat T cells co-cultured with  $\beta$ 4 or  $\beta$ 6 myoepithelial cells for 24hrs**

Jurkat T cells were co-cultured with  $\beta$ 4 or  $\beta$ 6 myoepithelial cells for 24 hrs. Cells labelled with matched IgG isotype were used to set up the gates. At least 10000 cells were analyzed using Cellquest software. This demonstrated that CD4 level in Jurkat cells co-cultured with  $\beta$ 4 cells is 32.3% (A) and in Jurkat cells co-cultured with  $\beta$ 6 cells is 33.8% (B).



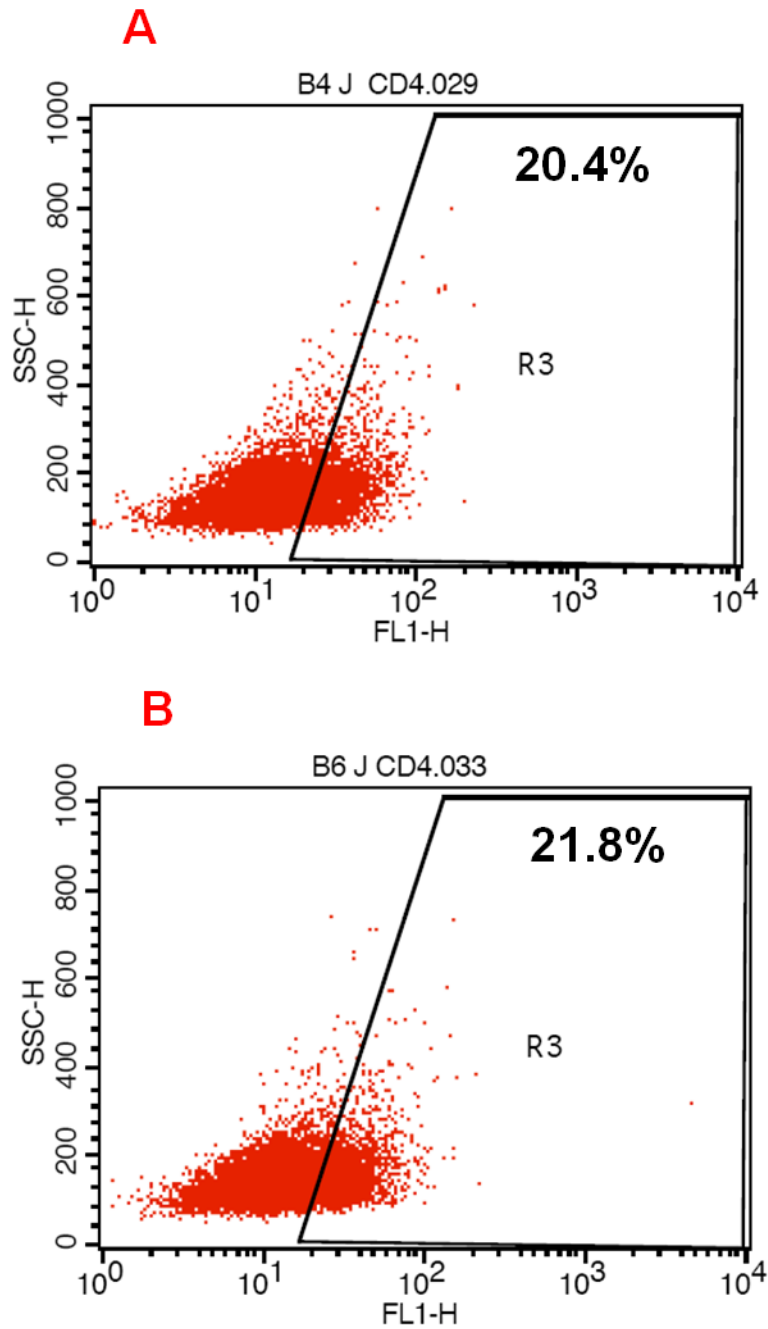


**Figure 6.11 Expression of CD4 in Jurkat T cells co-cultured with  $\beta$ 4 or  $\beta$ 6 myoepithelial cells for 48 hrs**

Jurkat T cells co-cultured with  $\beta$ 4 or  $\beta$ 6 myoepithelial cells for 48 hrs were collected and stained for CD4. At least 10000 cells were evaluated using Cellquest software. This demonstrated CD4 expression in Jurkat cells co-cultured with  $\beta$ 4 cells was 20.4% (A), and in those co-cultured with  $\beta$ 6 cells were 21.8% (B).

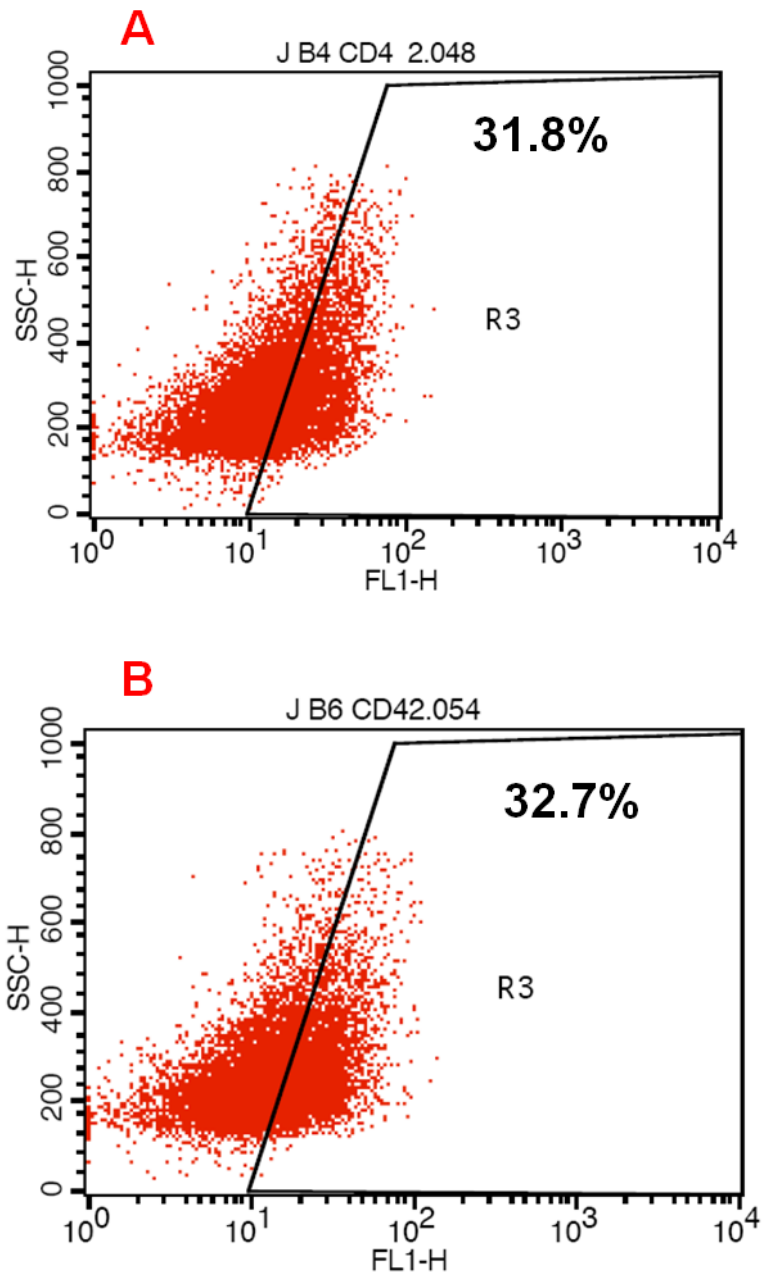


**Figure 6.12 Expression of CD4 in Jurkat T cells co-cultured with  $\beta 4$  or  $\beta 6$  myoepithelial cells for 72 hrs**

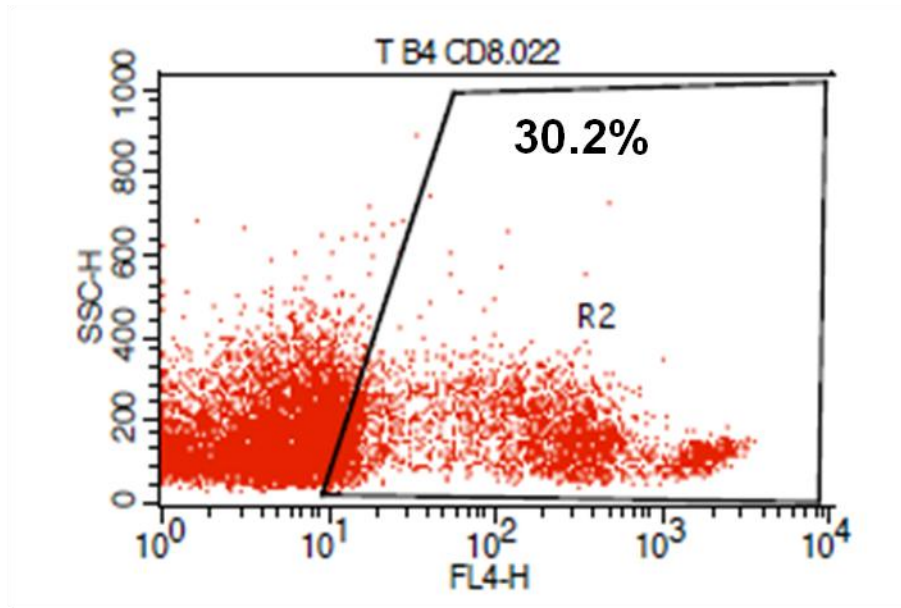
Jurkat T cells co-cultured with  $\beta 4$  or  $\beta 6$  myoepithelial cells for 48 hrs were collected and stained for CD4. Cells labelled with matched isotype control were used to gate on, and at least 10000 cells were evaluated using Cellquest software. This showed the levels of CD4 expression in Jurkat cells co-cultured with  $\beta 4$  cells was 31.8 % (A) and in those co-cultured with  $\beta 6$  cells was 32.7% (B).

### **6.4.7 Impact of myoepithelial cells on expression of CD8 in primary T cells**

CD8 expression was analyzed in primary T cells co-cultured with  $\beta$ 4 or  $\beta$ 6 myoepithelial cells for 24, 48 and 72 hrs (2.8.10) by FACS. A negative control using matched isotype antibody instead of the primary antibody was used for each run. At least 10000 cells were quantified using Cellquest software.

At 24hrs time point, comparing the levels of CD8 in primary T cells co-cultured with  $\beta$ 4 or  $\beta$ 6 cells showed no difference between the two groups, at 30.2%, and 30% respectively (figure 6.13). After 48 hrs of co-culture, CD8 expression in primary T cells was slightly up-regulated but with no striking difference between the two groups, with 34.2 % positivity in those exposed to  $\beta$ 4 cells and 31.9% positivity in those exposed to  $\beta$ 6 cells (figure 6.14). At 72 time point, the level of CD8 expression was 32% in T cells co-cultured with  $\beta$ 4 cells and 31% in those co-cultured with  $\beta$ 6 cells (figure 6.15). Each time point of the co-culture experiments was repeated at least three times. CD8 expression in primary T cells without co-culture was 37.4%.

**A**



**B**

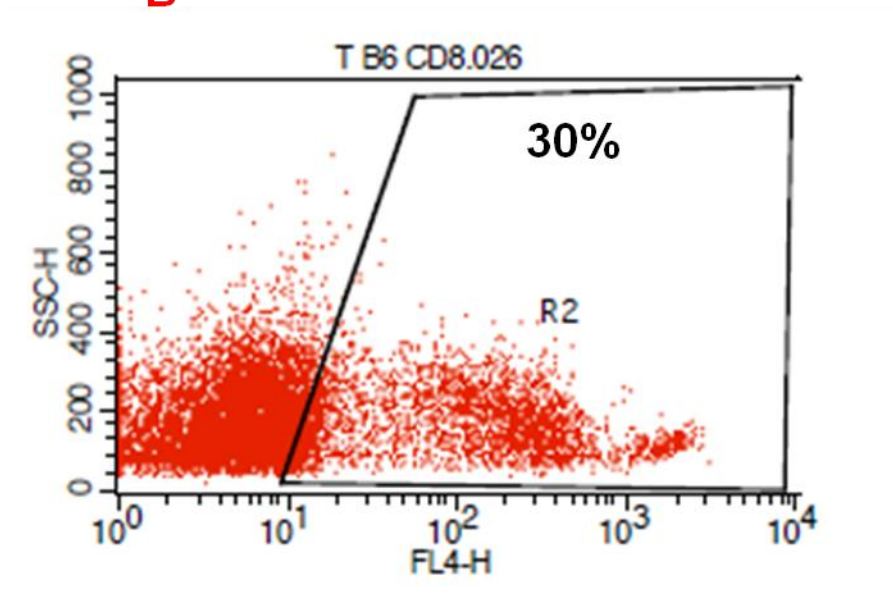


**Figure 6.13** Representative dot plots for expression of CD8 in primary T cells co-cultured with  $\beta$ 4 or  $\beta$ 6 myoepithelial cells for 24 hrs

Primary T cells were co-cultured with  $\beta$ 4 and  $\beta$ 6 myoepithelial cells for 24 hrs then collected and stained for CD8. At least 10000 cells were evaluated using Cellquest software. This showed CD8 level in T cells co-cultured with  $\beta$ 4 cells is 30.2% (A) and 30 % when co-cultured with  $\beta$ 6 cells (B).

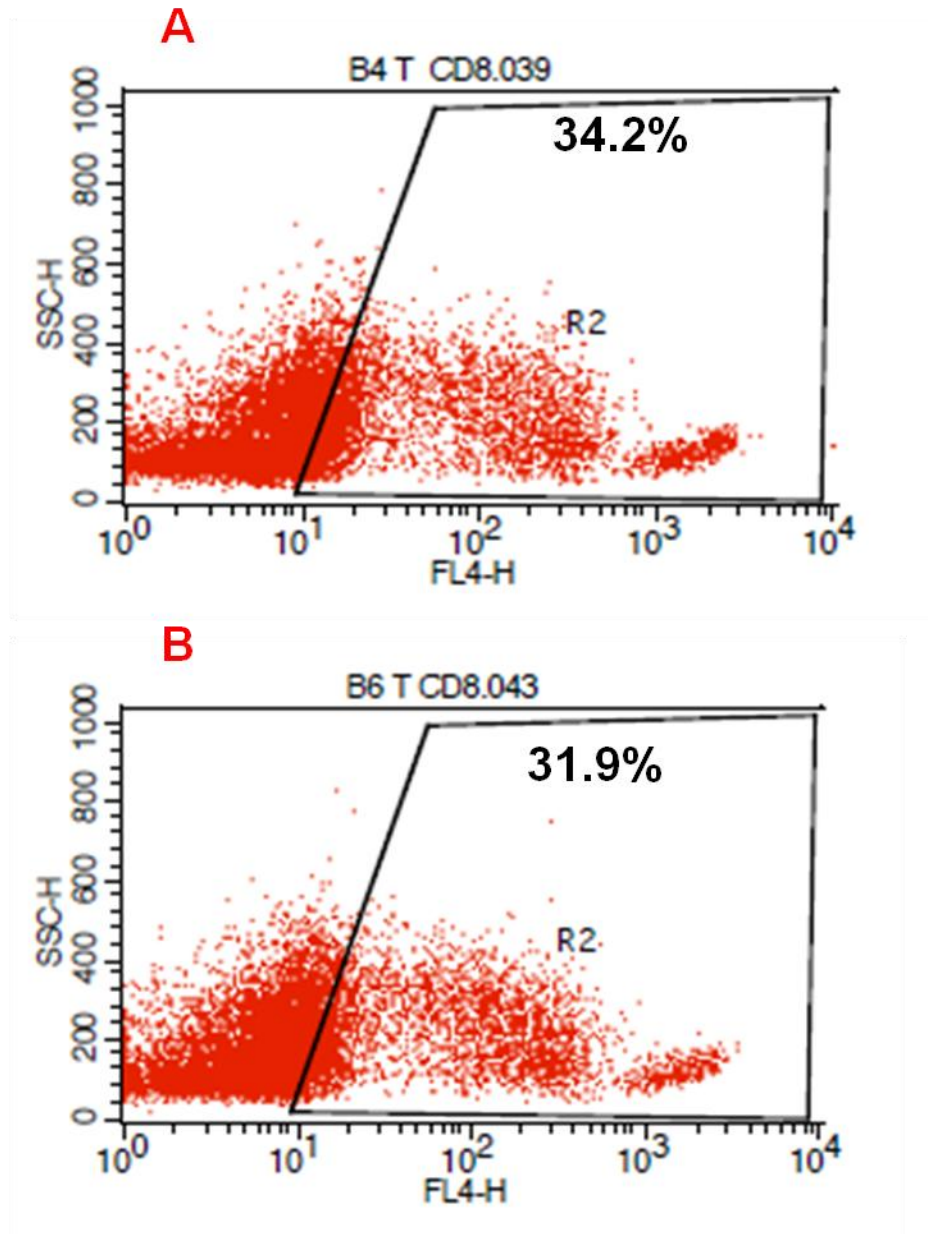


**Figure 6.14** Representative dot plots for expression of CD8 in primary T cells co-cultured with  $\beta 4$  or  $\beta 6$  myoepithelial cells for 48 hrs

Primary T cells were co-cultured with  $\beta 4$  and  $\beta 6$  myoepithelial cells for 48 hrs then collected and stained for CD8. At least 10000 cells were analyzed using Cellquest software. This showed no difference between the two groups; 34% CD8 positivity in the presence of  $\beta 4$  cells (A) and 31.9 % in those co-cultured with  $\beta 6$  cells (B).

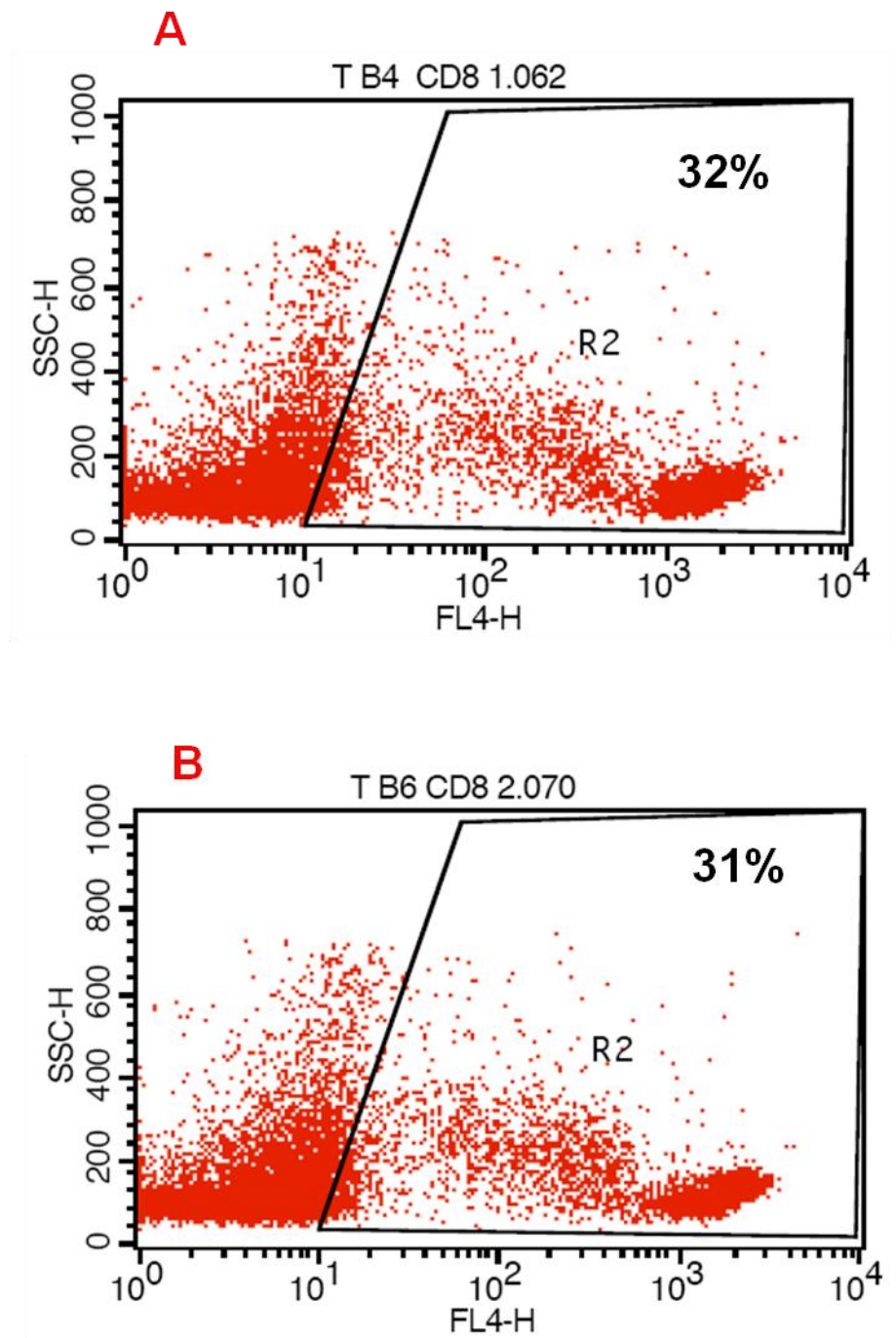


**Figure 2.15** Representative dot plots for expression of CD8 in primary T cells co-cultured with  $\beta$ 4 or  $\beta$ 6 myoepithelial cells for 48 hrs

Primary T cells were co-cultured with  $\beta$ 4 or  $\beta$ 6 cells for 48 hrs and analyzed for CD8 expression. This demonstrated 32% of T cells co-cultured with  $\beta$ 4 cells are positive for CD8 (A), while 31% of T cells co-cultured with  $\beta$ 6 cells are positive for CD8 (B).

### **6.4.8 Impact of myoepithelial cells on expression of CD8 in Jurkat T cells**

Levels of CD8 expression were also measured in Jurkat T cells by flow cytometry following co-culture with  $\beta$ 4 and  $\beta$ 6 myoepithelial cells for 24, 48 and 72 hrs (section 2.8.10). At each time point Jurkat cells were collected and stained for CD8. Cells labelled with matched isotype control were used to gate on, and at least 10000 cells were quantified using Cellquest software.

At 24hrs time point, the levels of CD8 in Jurkat T cells co-cultured with  $\beta$ 4 or  $\beta$ 6 cells showed no difference between the groups, at 12%, and 12.1 respectively (figure 6.16), and at 48 hrs there was 10.1% positivity in those cultured with  $\beta$ 4 cells and 10.7% positivity in those cultured with  $\beta$ 6 cells group (figure 6.17).

At 72 hrs time point, the levels of CD8 expression showed a slight decline, however, still there is no difference between the two groups. Jurkat cells co-cultured with  $\beta$ 4 cells showed 8.5% positivity for CD8 and Jurkat cells co-cultured with  $\beta$ 6 cells showed 7.1% positivity (figure 6.18).



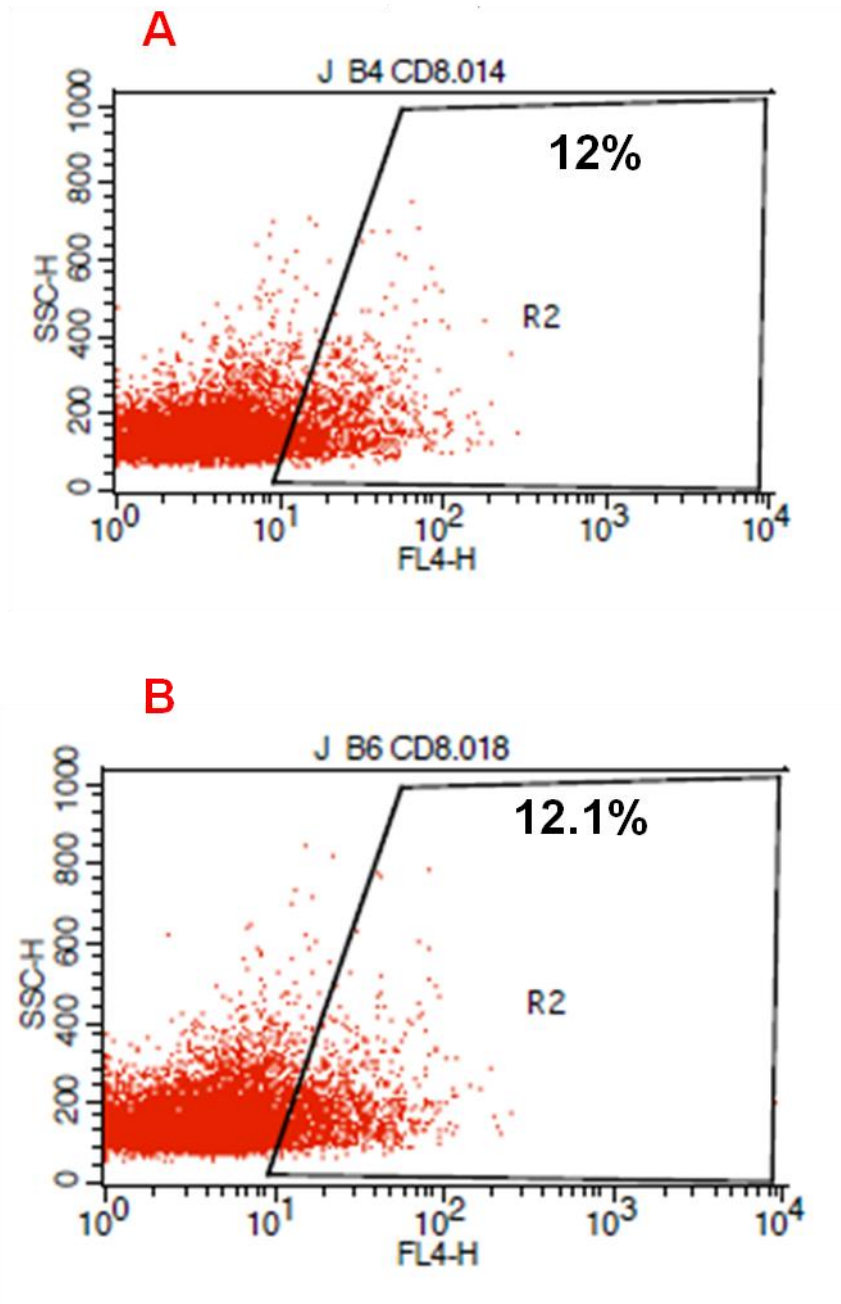


**Figure 6.16 Expression of CD8 in Jurkat T cells co-cultured with  $\beta$ 4 or  $\beta$ 6 myoepithelial cells for 24 hrs**

Jukat T cells were co-cultured with  $\beta$ 4 and  $\beta$ 6 myoepithelial cells for 24 hrs and then collected and stained for CD8. Cells labelled with isotype control were used to gate on, and at least 10000 cells were evaluated using Cellquest software. This demonstrated CD8 level in T cells co-cultured with  $\beta$ 4 cells at 12% (A) and 12.1% in those co-cultured with  $\beta$ 6 cells (B).



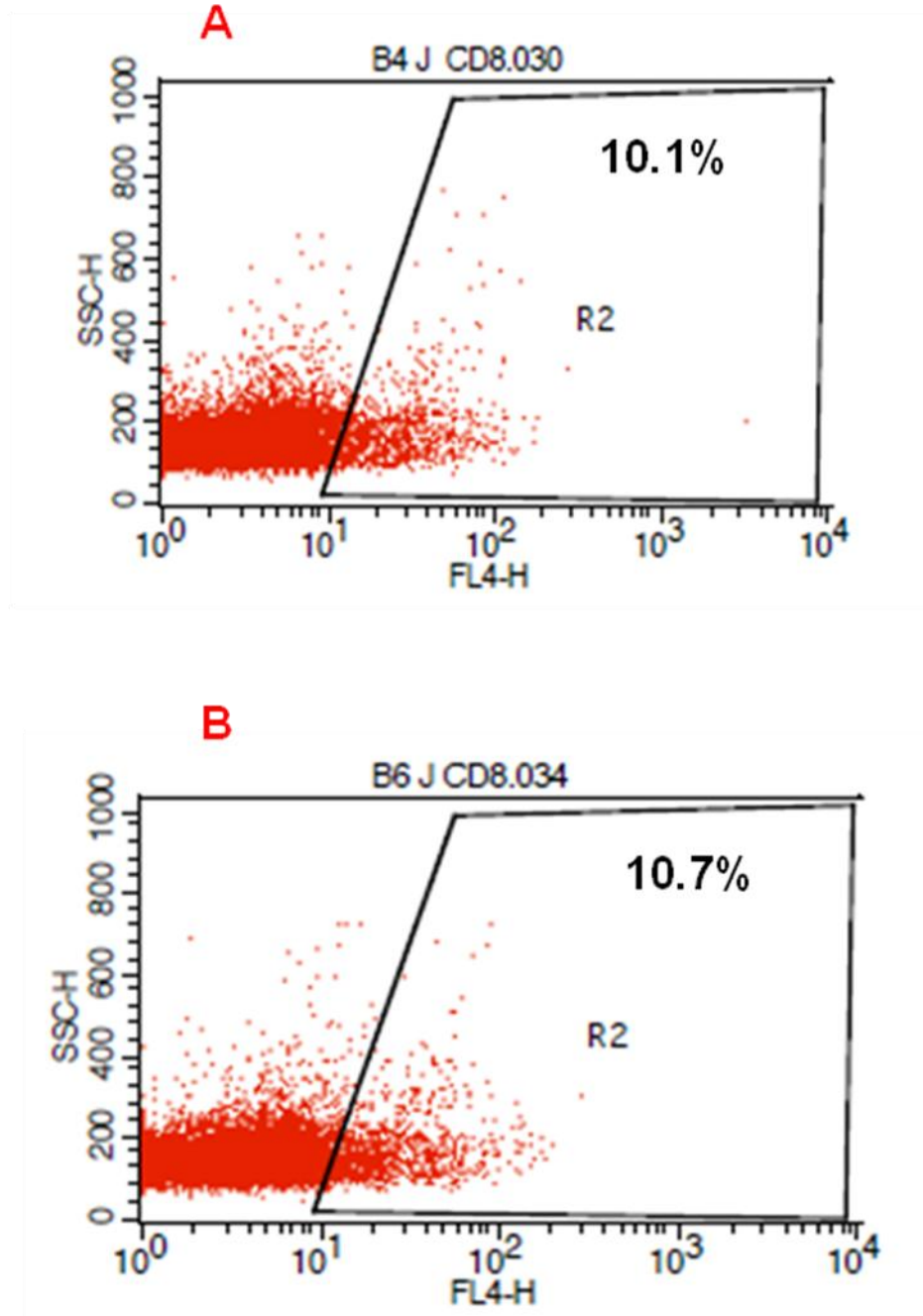


**Figure 6.17** Expression of CD8 in Jurkat T cells co-cultured with  $\beta 4$  or  $\beta 6$  myoepithelial cells for 48 hrs

CD8 levels were measured by FACS in Jurkat T cells co-cultured with  $\beta 4$  or  $\beta 6$  myoepithelial cells for 48 hrs. At least 10000 cells were evaluated using Cellquest software. This showed CD8 level in T cells co-cultured with  $\beta 4$  cells of 10.1% (A) and 10.7% in those they co-cultured with  $\beta 6$  cells (B).

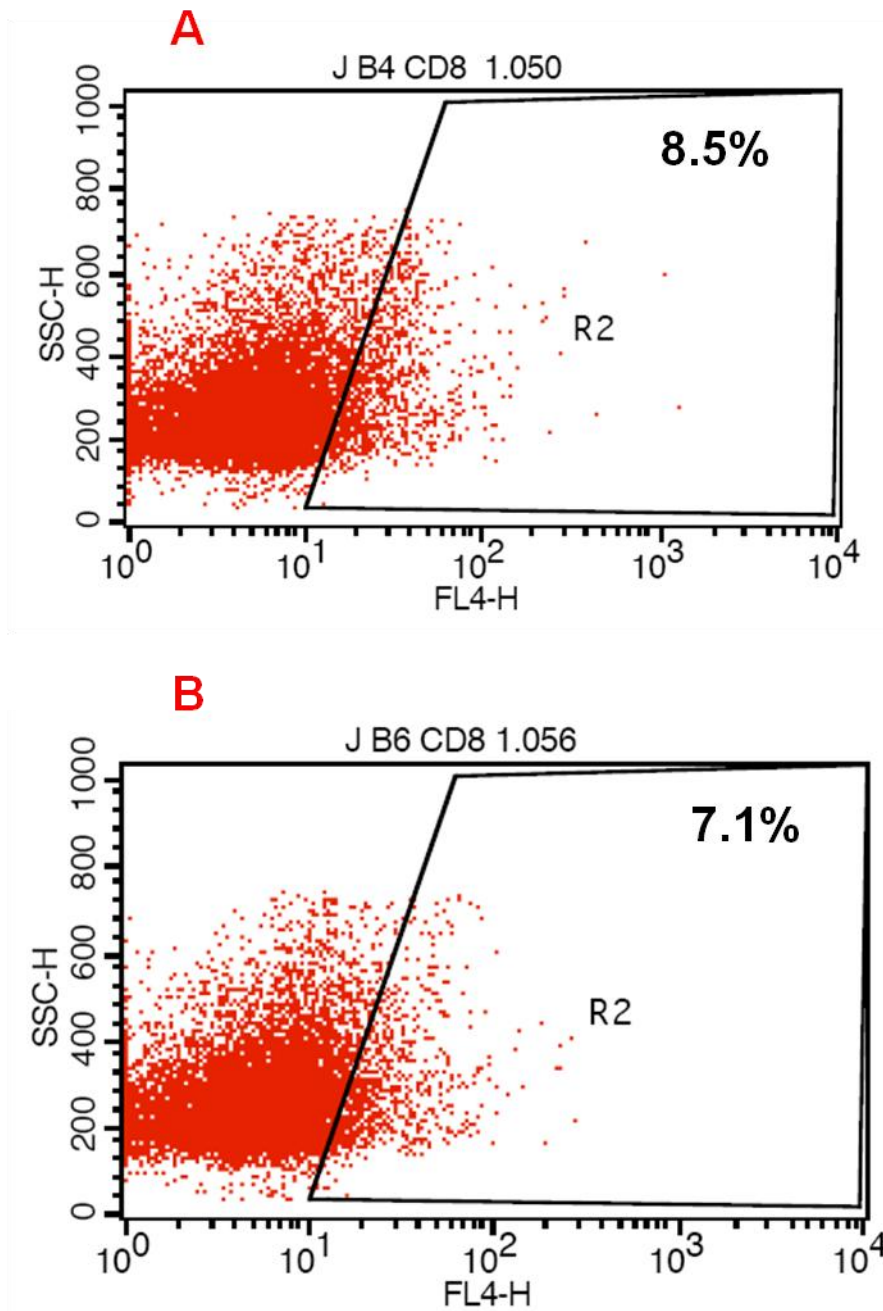


**Figure 6.18** Representative dot plots of expression of CD8 in Jurkat T cells co-cultured with  $\beta 4$  or  $\beta 6$  myoepithelial cells for 72 hrs

T cells were co-cultured with  $\beta 4$  or  $\beta 6$  myoepithelial cells for 72 hrs and analyzed for CD8 expression by FACS using Cellquest software. T cells co-cultured with  $\beta 4$  cells showed 8.5% positivity for CD8 (A), with 7.1% of positivity for CD8 when co-cultured with  $\beta 6$  cells (B).

### 6.4.9 Cytokine profile of myoepithelial cells

Cells lysates from  $\beta 4$  and  $\beta 6$  myoepithelial cells were collected as described in section, 2.10.1. Cytokine profile arrays for both cells types were performed (section 2.18). the expression of each cytokine is represented by two dots on the membrane. The densities of these dots were analyzed by Image J software and then plotted on a graph using Microsoft Office Excel 2007. This demonstrates that  $\beta 4$  and  $\beta 6$  myoepithelial cells express 20 of the cytokines present on the arrays, including C5/C5a, CD40L , G-CSF, GM-CSF, GRO $\alpha$ , I-309, SICAM-1, IFN  $\gamma$ , IL-1 $\alpha$ , IL-1 $\beta$ ,IL-1ra, IL-5, IL-13, IL-16, IL-23, IL-25,MIF, MIP-1 $\alpha$ , SerpinE1 and RANTES (figure 6.19).  $\beta 6$  myoepithelial cells were shown to express relatively higher levels of interleukins including IL-1 $\alpha$ , IL-1 $\beta$ , IL-5, IL-13, IL-16, IL-23 and IL-25 compared to  $\beta 4$  myoepithelial cells (figure 6.19). IL-1ra is expressed more highly by  $\beta 4$  myoepithelial cells (figure 6.19). Moreover,  $\beta 6$  myoepithelial cells showed relatively higher levels of MIF, Serpin E1 and C5/C5a compared to  $\beta 4$  myoepithelial cells.

These observations suggest that up-regulation of  $\alpha v\beta 6$  expression on myoepithelial cells during DCIS may have an influence on the cytokine profile of myoepithelial cells, which may in turn influence their effect on the microenvironment.

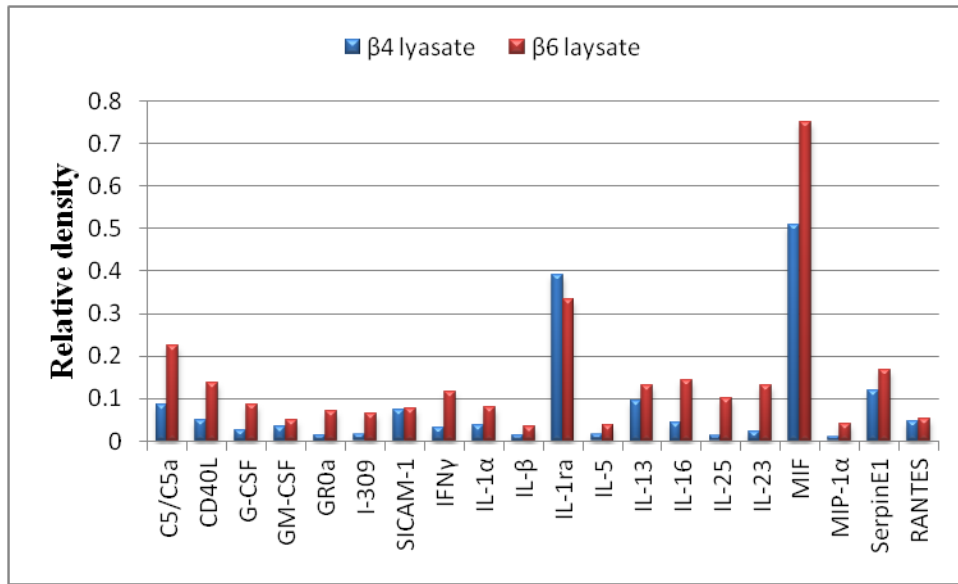


**Figure 6.19** Cytokines expressed in  $\beta 4$  and  $\beta 6$  myoepithelial cells

Lysates of  $\beta 4$  and  $\beta 6$  myoepithelial cells were collected and cytokine arrays were performed. Each cytokine is represented by two dots on the array blot. Densities of each cytokine dots was quantified using Image J software. Then, the relative densities were plotted on a graph using Microsoft Office Excel 2007. This shows that  $\beta 6$  myoepithelial cells express relatively higher levels of IL-1 $\alpha$ , IL-1 $\beta$ , IL-5, IL-13, IL-16, IL-23, IL-25, MIF, Serpin E1 and C5/C5a compared to  $\beta 4$  myoepithelial cells. In contrast, IL-1ra is expressed more by  $\beta 4$  cells compared to  $\beta 6$  myoepithelial cells.

#### **6.4.10 Cytokines released by myoepithelial cells**

Condition media (CM) from  $\beta 4$  and  $\beta 6$  myoepithelial cells were collected as described in section, 2.8.8. The CM were incubated with cytokine array membranes to investigate the cytokine profile released from  $\beta 4$  and  $\beta 6$  myoepithelial cells. As described, each type of cytokine is representative by two dots on the membrane, and the densities of the dots were quantified using Image J software. The relative density of signal was plotted on a graph using Microsoft office Excel 2007. This demonstrated that  $\beta 4$  myoepithelial cells released 10 types of cytokine including, GM-CSF, GRO $\alpha$ , SiCAM-1, IL-1 $\alpha$ , IL-1ra, IL-6, IL-8, MIF, serpinE1 and RANTES (figure 6.20 ) while  $\beta 6$  cells released 16 of the cytokines present on the array, including G-CSF, GM-CSF, GRO $\alpha$ , I-309, SiCAM-1, IFN $\gamma$ , IL-1 $\alpha$ , IL-1ra, IL-6, IL-8, IL-10, IL-13, MCP-1, MIF, serpinE1 and RANTES ( figure 6.20 ).  $\beta 4$  myoepithelial cells released higher levels of IL-8 and RANTES compared  $\beta 6$  myoepithelial cells. Whereas GM-CSF, GRO $\alpha$ , SiCAM-1, IL-1 $\alpha$ , IL-1ra, IL-6, MIF and serpin E1 are released at higher levels by  $\beta 6$  myoepithelial cells compared to  $\beta 4$  cells. In addition, G-CSF, I-309, IL-10 and IL-13, IFN $\gamma$ , and MCP-1 were detected only in CM from  $\beta 6$  myoepithelial cells. These findings support the suggestion that up-regulation of  $\alpha v \beta 6$  integrin on myoepithelial cells influences the profile of cytokines released.

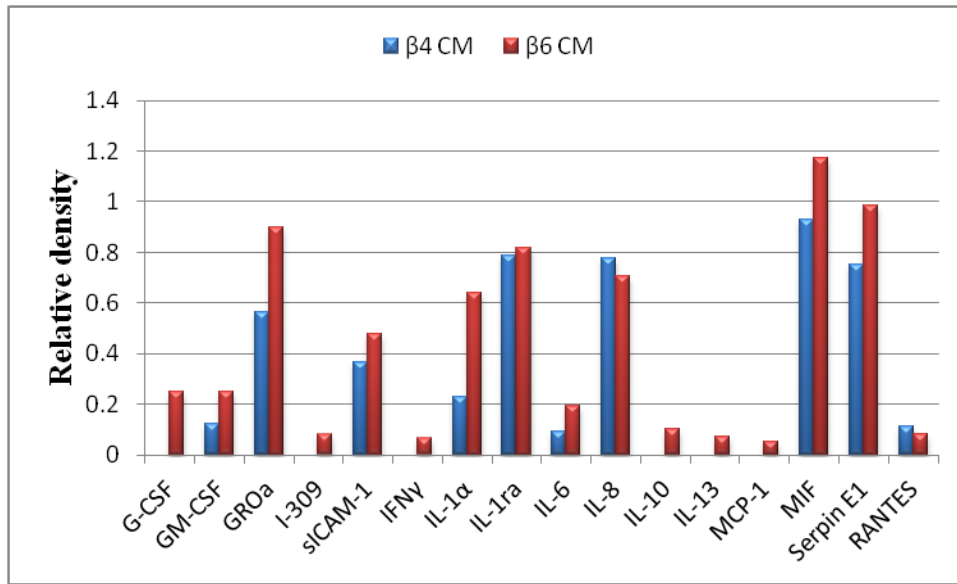


**Figure 6.20 Cytokine profile released by  $\beta$ 4 and  $\beta$ 6 myoepithelial cells**

Cytokine array profiles were run for the condition media collected from  $\beta$ 4 and  $\beta$ 6 myoepithelial cells. Each cytokine is representative by two dots on the array membrane, and the density of the signal from these dots was measured by Image J software and plotted on a graph using Microsoft Office Excel 2007. This demonstrates that some cytokines are released only by  $\beta$ 6 myoepithelial cells, including G-CSF, I-309, IL-10 and IL-13, IFN $\gamma$ , and MCP-1. Moreover, GM-CSF, GROa, SiCAM-1, IL-1 $\alpha$ , IL-6, MIF and serpin E1 are released at a higher level  $\beta$ 6 cells compared to  $\beta$ 4 cells.

### **6.4.11 Influence of T cells on myoepithelial cytokine expression**

To determine the influence of T cells on myoepithelial cell cytokine expression, Jurkat cells were used as a model of T cells and were co-cultured with either  $\beta$ 4 or  $\beta$ 6 myoepithelial cell types for 24 hrs as described in section, 2.8.10. Myoepithelial cell lysates were then collected and cytokine arrays were performed (section, 2.18).

$\beta$ 4 and  $\beta$ 6 myoepithelial cell cytokine profiles changed following co-culture with Jurkat T cells. They lost most of their cytokines expression after they were co-cultured with Jurkat cells. In addition, levels of  $\text{IFN}\gamma$ ,  $\text{IL-1}\beta$ ,  $\text{IL-1ra}$ , MIF and serpinE1 were expressed relatively more in  $\beta$ 4 cells compared to  $\beta$ 6 cells (figure, 6.21).

These observations suggest that T cells may have a role in changing of myoepithelial cells cytokines profile in DCIS disease. However, this suggestion needs further investigations.

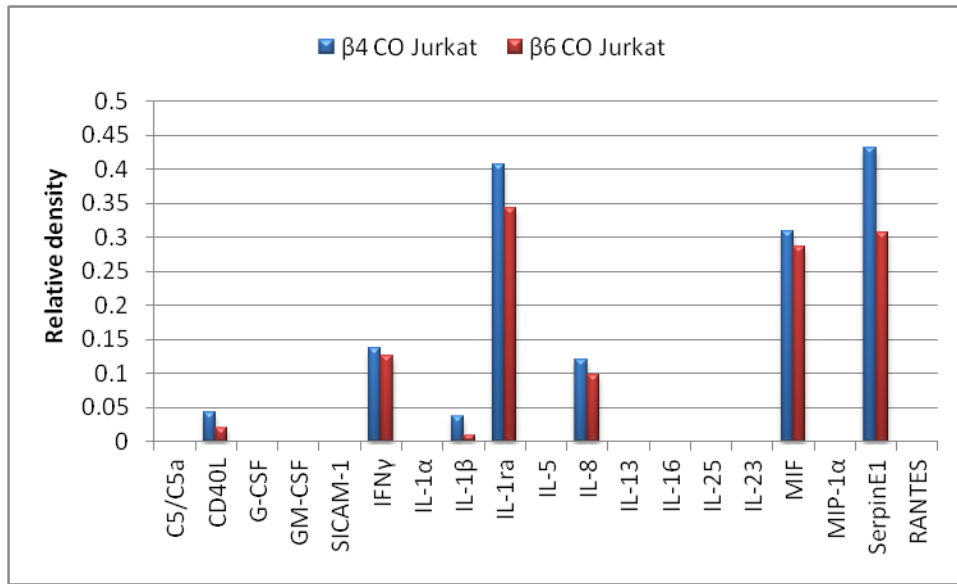


**Figure 6.21 Influence of jurkat T cells on cytokines express on myoepithelial cells**

Cytokines profiles have investigated in  $\beta 4$  and  $\beta 6$  cells co-cultured with jurkat T cells for 24hrs. Cytokines expressed on both myoepithelial cells changed after co-cultured with jurkat T cells as they lost the most of thier cytokines. Moreover,  $\beta 4$  cells relatively express more levels of of IFN $\gamma$ , IL-1 $\beta$ , IL-1ra, MIF and serprinE1 compared to  $\beta$  cells.



## 6.5 Discussion

---

Many studies have shown that inflammatory cell infiltrate may play a role in cancer cells behaviour in DCIS, it has demonstrated that myoepithelial cells exhibit multiple changes in gene expression and up-regulation of certain types of chemokines (Allinen, Beroukhi et al. 2004). We previously have shown that up-regulation of  $\alpha\beta6$  on myoepithelial cells in a subset of DCIS which is associated with invasive disease (Allen, Thomas et al. 2014).

We also have observed in this study that there is a correlation between certain types of inflammation cell infiltrate in DCIS with the expression of  $\alpha\beta6$  on myoepithelial cells. In DCIS microenvironments, expression of  $\alpha\beta6$  on myoepithelial cells is associated with a higher level of CD4+ve cells and a lower level of CD8+ cells. Therefore, this chapter was aimed to investigate the influence of  $\alpha\beta6+$  myoepithelial cells on the phenotype of inflammatory cells, also to investigate influence of T cells on myoepithelial cell cytokines.

$\beta6$  myoepithelial cells were used as a model of  $\alpha\beta6+$ ve myoepithelial cells and  $\beta4$  cells were used as a model of  $\alpha\beta6-$ ve myoepithelial cells. Both types of myoepithelial cells were co-cultured with primary T cells and Jurkat T cells for 24, 48 and 72 hrs and the levels of CD4 and CD8 expression were measured in primary T cells and Jurkat T cells by flow cytometry. This demonstrated the levels of CD4 expression in two types of T cells showed no difference between T cells co-cultured with  $\beta4$  cells and those co-cultured with  $\beta6$  cells at all time points. Also there was no difference in the levels of CD8 expression in both types of T cells between T cells co-cultured with  $\beta4$  cells and those co-cultured with  $\beta6$  cells for all time points.

This is not consistent with the observations from the tissue study but is probably a limitation in the study design, since in-vitro there is no new recruitment of T cell populations. *In-vivo* study has shown that Matrigel plugs containing  $\beta 6$  cells associated with higher numbers of CD4+ve cells compared to the Matrigel plugs containing  $\beta 4$  cells, and this supports the idea that the environment of  $\beta 6$ +ve myoepithelial cells leads to effects on recruitment of T cell populations.

In order to elucidate mechanisms that myoepithelial cells could effect the phenotypes of inflammatory cells infiltrate in DCIS stroma, cytokines of both phenotypes of myoepithelial cells were investigated with or without co-culture with T cells.

DCIS and invasive breast cancer express higher level of IL-1 $\alpha$  compared to benign tumours (Kurtzman, Anderson et al. 1999) and promotes tumour growth (Kumar, Kishimoto et al. 2003). This is consistent with the cytokines array results that show  $\beta 6$  myoepithelial cells relatively expressed a higher level of IL-1 $\alpha$  compared to  $\beta 4$  cells. In addition,  $\beta 6$  cells expressed higher level of IL-5 compared to  $\beta 4$  cells which induces CD4 T cells (Hogan, Koskinen et al. 1998).  $\beta 6$  cells also expressed more of IL-16 which has a role in induction recruitment T reg cells (McFadden, Morgan et al. 2007).

Therefore, upregulation of IL-5 and IL-16 in  $\beta 6$  cells is likely to be the explanation for the higher numbers of CD4+ve T and FOXP3+ve cells in  $\alpha\beta 6$  positive DCIS cases. However, cytokines arrays results need to be validated.

## 6.6 Conclusion

---

Expression of  $\alpha\beta6$  integrin in myoepithelial cells in DCIS has an effect in the cytokines expressed and released by myoepithelial cells. T cells may have also impact in types of cytokines expressed by myoepithelial cells.

# Chapter 7 Final discussion

## 7.0 Discussion

---

### 7.1 Overview of the study aims

The transition of DCIS to invasive disease is a critical stage in the progression of breast cancer and is characterised by penetration and eventual loss of the myoepithelial cell layer and basement membrane. Myoepithelial cells play an important role in the regulation of normal breast function and have been shown to exhibit potent tumour suppressor function (Jones, Shaw et al. 2003). However, DCIS-associated myoepithelial cells appear to have an altered phenotype (Zhang men et al 2003), including up-regulation of the tumour-promoting integrin  $\alpha\beta 6$ . The DCIS microenvironment is complex, composed of ECM and varied stromal cells types, including fibroblasts, blood vessels, adipocytes and immune cells (Polyak and Kalluri 2010). Inflammatory cells in breast cancer have been described as having both pro-tumour and anti-tumour effects. The aim of this project was to investigate the influence of the change in myoepithelial phenotype that occurs during DCIS on the inflammatory microenvironment, and to characterize the inflammatory cell infiltrate in ductal carcinoma in situ (DCIS) and its potential role in DCIS progression using a combination of immunohistochemistry, in-vitro and in-vivo techniques.

## 7.2 $\alpha\nu\beta 6$ positive DCIS-associated myoepithelial cells and the inflammatory cell infiltrate

In an immunohistochemical study, de-novo expression of  $\alpha\nu\beta 6$  on myoepithelial cells was confirmed in a subset of cases of DCIS.

Different types of inflammatory cells populations were identified in the DCIS microenvironment, including CD4+ve, CD8+ve, CD45RO+ve, CD69+ve, FOXP3+ve, MHCII+ve, CD68+ve and arginase+ve cell types. The presence of  $\alpha\nu\beta 6$  on the myoepithelial cells was significantly correlated with higher levels of CD4+ve, FOXP3+ve, CD69+ve and arginase+ve cells, and with low numbers of MHCII+ve and CD8+ve cells. Together, these observations suggest that  $\alpha\nu\beta 6$  expression by DCIS-associated myoepithelial cells may play a role in modifying the immune infiltrate, driving it towards a Treg and M2 macrophage phenotype.

To investigate the potential influence of myoepithelial cell expression of  $\alpha\nu\beta 6$  on the inflammatory cell phenotype, two myoepithelial cell lines were used in a series of *in-vivo* and *in-vitro* models:  $\beta 4$  ( $\alpha\nu\beta 6$ -ve) and  $\beta 6$  ( $\alpha\nu\beta 6$ +ve) myoepithelial cells. Matrigel plug assays were used in female C57/Blk6 normal mice to assess the inflammatory infiltrate in response to  $\beta 4$  or  $\beta 6$  myoepithelial cells. Immunohistochemical analysis of these tissues showed that  $\beta 6$  myoepithelial cells were associated with higher levels of CD4+ve cells, compared to  $\beta 4$  myoepithelial cells ( $p=0.007$ ). The number of FOXP3+ve cells was also higher in plugs containing  $\beta 6$  cells compared to  $\beta 4$  cells ( $p=0.005$ ), supporting the findings in human tissue samples.

### **7.3 Role of T cells in progression of DCIS**

Man and his colleagues (2007) have suggested that inflammatory cells play a role in transition of DCIS to invasive disease. They suggest that internal or external injuries such as trauma, inflammation or exposure to some chemicals results in disruption of the myoepithelial cell layer with subsequent infiltration of inflammatory cells. Thus, these inflammatory cells can lead to further degeneration of the myoepithelial cells and basement membrane, resulting in a gap that allows direct contact between the tumour tissue and stromal cells (Man 2007), however the mechanisms by which myoepithelial cells may be lost is unclear. The current study has shown that expression of  $\alpha\text{v}\beta\text{6}$  on DCIS-associated myoepithelial cells is associated with an altered peri-ductal inflammatory microenvironment that would contribute to a pro-tumour phenotype. One potential mechanism of myoepithelial cell loss could be through apoptosis. Therefore, this study hypothesised that loss of the myoepithelial layer could be mediated by T-cell derived TRAIL-induced apoptosis, and that  $\alpha\text{v}\beta\text{6}$ -positive myoepithelial cells may be more susceptible to this effect than their negative counterparts.

### **7.4 Increased expression of TRAIL**

TGF- $\beta$  has been shown to up-regulate TRAIL expression in primary human hepatocytes (Herzer, Grosse-Wilde et al. 2008). It also has been demonstrated that TRAIL plays an important role in TGF- $\beta$ -induced apoptosis in liver tumor cells (Herzer, Grosse-Wilde et al. 2008).

Therefore, co-culture experiments were performed to investigate whether myoepithelial cells could regulate TRAIL expression. The level of TRAIL was measured in Jurkat and primary T cell populations following co-culture with  $\beta 4$  or  $\beta 6$  myoepithelial cells for 48 hrs. This demonstrated primary T cells, but not Jurkat T cells, express higher levels of TRAIL when they were co-cultured with  $\beta 6$  myoepithelial cells than when co-cultured with  $\beta 4$  myoepithelial cells. The lack of response in the established cell line may be a reflection of its immortalisation, and the lack of 'plasticity' in a cell line, in comparison to primary cells. It has been shown that TRAIL is induced in activated T cells and CD69 is considered to be an early marker of T cell activation. In the immunohistochemical study on DCIS tissues, we demonstrated higher numbers of CD69-positive T cells in the peri-ductal environment of  $\alpha\beta 6$ -positive myoepithelial cells compared to  $\alpha\beta 6$ -negative ducts. Thus, it is possible that up-regulation of  $\alpha\beta 6$  can lead to T cell activation. Co-culture studies followed by detailed phenotypic analysis of T cells, for example using FACS analysis, could address this. Similar studies in our laboratory have shown that  $\alpha\beta 6$ -positive myoepithelial cells can modulate macrophage phenotype and activation (M Allen, personal communication), making this a plausible theory.

## **7.5 Effect of TRAIL on DCIS-associated myoepithelial cells**

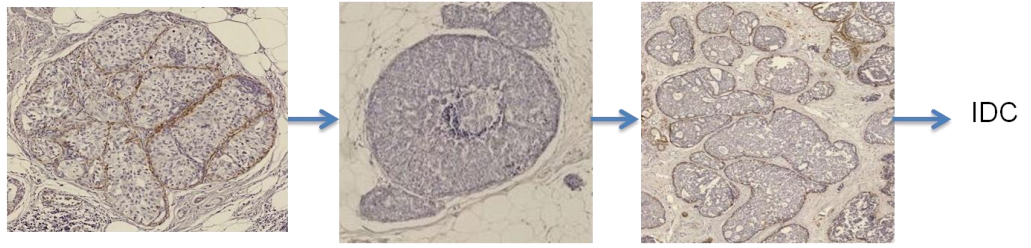
TRAIL mediates its actions through specific TRAIL receptors, DR4 and DR5. These receptors have been detected on breast cancer cells and high DR5 expression is strongly correlated with decreased survival in patients with breast cancer (McCarthy, Sznol et al. 2005). The level of both receptors was



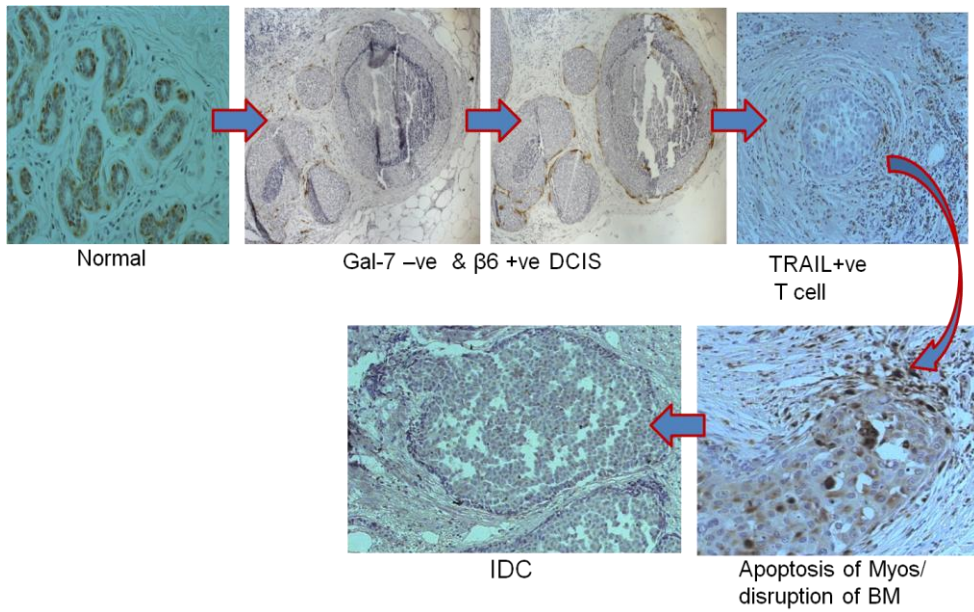
significantly higher in  $\beta 6$  myoepithelial cells compared to  $\beta 4$  myoepithelial cells. Unfortunately attempts to measure DR4 and DR5 at the protein level were unsuccessful as the antibodies could not be optimised.

To investigate the effect of TRAIL on myoepithelial cell apoptosis,  $\beta 6$  and  $\beta 4$  myoepithelial cells were treated with recombinant TRAIL for 2, 4 and 8 hrs, after which the cells were analysed for expression of cleaved PARP, as a marker of apoptosis. This demonstrated enhanced apoptosis in the  $\beta 6$ +ve myoepithelial cell line compared to the  $\beta 6$ -ve myoepithelial cells at each time point. This provides some indirect evidence that  $\beta 6$ +ve myoepithelial cells may be more susceptible to the effect of Treg cells, but this requires further investigation. In addition, exposure of both myoepithelial cell lines to Etoposide also demonstrated that  $\beta 6$ +ve myoepithelial cells were more susceptible to apoptosis compared to  $\beta 6$ -ve myoepithelial cells. Therefore, the effect is not specific to TRAIL.

A model for the involvement of altered myoepithelial cell phenotype and impact on inflammatory cell infiltrate and myoepithelial apoptosis is indicated below.



Gal-7	+	-	-
$\beta 6$	-	-	+
T cells	↓	↓	↑
Apoptosis	↓	↓	↑



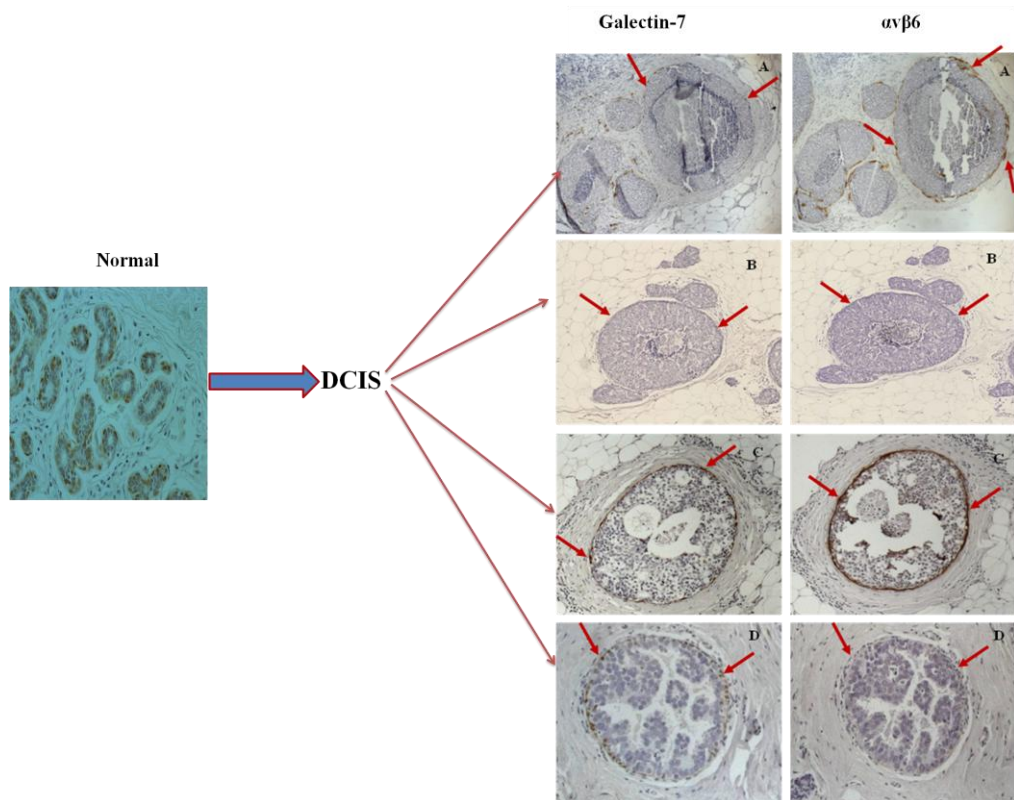
## **7.6 Clinical relevance of myoepithelial cell apoptosis**

In order to evaluate the clinical relevance of myoepithelial cell apoptosis, a series of DCIS samples was assessed for the presence of apoptosis, specifically relating to the myoepithelial compartment. Cases were selected that were  $\alpha\text{v}\beta\text{6}^{\text{+ve}}$  with high levels of infiltration with Treg cells, and were stained for caspase-3 antigen as a marker of apoptosis. This confirmed positive staining for caspase-3 in myoepithelial cells in some of the DCIS ducts. This provides some very preliminary support for the hypothesis that myoepithelial cells may be lost through apoptosis however further work is needed to provide definitive evidence.

## **7.7 Down-regulation of galectin-7 in myoepithelial cells and its relationship to $\alpha\text{v}\beta\text{6}$**

It has been shown that normal myoepithelial cells express galectin-7 and its expression is altered during breast cancer progression (Demers, Rose et al. 2010). Therefore, galectin-7 expression was examined in a series of DCIS tissue samples, in conjunction with  $\alpha\text{v}\beta\text{6}$  expression in order to investigate the relationship between these molecules. In keeping with previous reports, galectin-7 expression was found to be limited to the myoepithelial cells in normal breast tissue. In DCIS cases there was more variable expression of galectin-7. Some ducts entirely lacked expression, others retained myoepithelial cell expression, whilst in others the pattern of staining was

heterogeneous. When compared to  $\alpha\beta6$  status, there was an inverse relationship between the two markers, thus positivity for  $\alpha\beta6$  on myoepithelial cells was associated with loss of galectin-7 ( $p= 0.001$ ). Thus this result may be proposed that progression of DCIS to invasive disease is a multi-step process.



## 7.8 Clinical impact of galectin-7 expression in DCIS-associated myoepithelial cells

One of the major biological roles played by galectin-7 relates to its modulatory effects on apoptosis; while it seems to display pro-apoptotic activity in some tumour cell lines (Bernerd, Sarasin et al. 1999, Kuwabara, Kuwabara et al. 2002), other studies have suggested that galectin-7 may display anti-apoptotic effects (Gendronneau, Sidhu et al. 2008, Demers, Rose et al. 2010).

It has been reported that ectopic expression of Galectin-7 in HeLa cells and in the colon carcinoma cell line DLD-1 renders them more susceptible to apoptosis induced by actinomycin D and UVB (Kuwabara, Kuwabara et al. 2002). Similarly, an increase in galectin-7 expression has been demonstrated in apoptotic keratinocytes of human skin explants exposed to UVB (Bernerd, Sarasin et al. 1999). On the contrary, exposure of skin from wild type (wt) or galectin-7<sup>-/-</sup> adult mice to UVB revealed a twofold increase in apoptotic cells in galectin-7<sup>-/-</sup> compared with wt epidermis at 6 h (Gendronneau, Sidhu et al. 2008). In the breast, Demers and his colleagues (Demers, Rose et al. 2010) suggest that galectin-7 has the ability to render mammary cells more resistant to apoptosis. This study demonstrated that the mouse breast cancer cell line 4T1, when transfected with galectin-7, becomes more resistant to apoptosis when exposed to epigallocatechin galatte, a pharmacological agent known to induce apoptosis in 4T1 cells (Demers, Rose et al. 2010). Thus, it appears from the literature that galectin-7 certainly has a role in apoptosis, and whereas most evidence suggests it is pro-apoptotic some models suggest it may be anti-apoptotic, and this is context-dependent. Therefore, this study aimed to investigate whether there was any change in galectin-7 expression in DCIS-

associated myoepithelial cells, and whether this could influence their response to apoptosis-inducing stimuli.

To further investigate the relationship between  $\alpha\beta6$ , galectin-7 and susceptibility to apoptosis,  $\beta4$  and  $\beta6$  myoepithelial cells were examined for expression of galectin-7. This showed reduced expression of galectin-7 in the  $\beta6$  cells. To determine whether galectin-7 has the ability to protect myoepithelial cells from apoptosis, galectin-7 was knocked down in  $\beta4$  cells, which were then exposed to recombinant TRAIL. This demonstrated that the  $\beta4$  cells appeared to be more sensitive to TRAIL when galectin-7 levels were reduced compared to non-target control cells. This was measured by western blot for cleaved PARP, however, it recognised that further analysis is required.

## **7.9 Putative mechanisms to explain the impact of $\alpha\beta6$ on inflammatory cell phenotype**

### **7.9.1 Effect of $\alpha\beta6$ on phenotype of T cells**

We previously have demonstrated up-regulation of  $\alpha\beta6$  on myoepithelial cells in a subset of DCIS which is associated with invasive disease (Allen, Thomas et al. 2014). We also have observed in this study that there is a correlation between the type of inflammatory cell infiltrate in DCIS and the expression of  $\alpha\beta6$  on myoepithelial cells. Expression of  $\alpha\beta6$  on DCIS-associated myoepithelial cells is associated with a higher level of CD4<sup>+</sup>ve cells and a lower level of CD8<sup>+</sup> cells. Therefore, we investigated the influence of  $\alpha\beta6$ <sup>+</sup> myoepithelial cells on phenotype of inflammatory cells and also investigated influence of T cells on myoepithelial cell cytokines.

$\beta 6$  myoepithelial cells were used as a model of  $\alpha\beta 6^{+ve}$  myoepithelial cells and  $\beta 4$  cells were used as a model of  $\alpha\beta 6^{-ve}$  myoepithelial cells. Both types of myoepithelial cells were co-cultured with primary T cells and Jurkat T cells for 24, 48 and 72 hrs and the levels of CD4 and CD8 expression were measured in the T cells by flow cytometry. No difference in the levels of CD4 and CD8 were identified between cells co-cultured with  $\beta 4$  cells and those co-cultured with  $\beta 6$  cells at any time points. This does not reflect the observations from the tissue study but is probably a limitation in the study design, since in-vitro there is no new recruitment of T cell populations. The matrigel plugs assays containing  $\beta 4$  cells were associated with lower numbers of CD4+ve cells compared to matrigel plugs containing  $\beta 6$  cells, and this supports the idea that the environment of  $\beta 6^{+ve}$  myoepithelial cells leads to effects on recruitment of T cell populations.

### **7.9.2 Altered cytokine expression by myoepithelial cells**

Myoepithelial cells in DCIS differ from normal myoepithelial cells (Allinen, Beroukhim et al. 2004): SAGE (serial analysis of gene expression) was employed to identify differences between isolated normal and DCIS-associated cell populations and demonstrated that DCIS-associated myoepithelial cells exhibited the greatest change in gene expression of all cells in DCIS, including up-regulation of certain chemokines such as CXCL14 (Allinen, Beroukhim et al. 2004). In order to address whether myoepithelial cells influence the inflammatory infiltrate through altered cytokine release, the cytokine profile of  $\beta 6$  and  $\beta 4$  myoepithelial cells with or without co-culture with T cells was analysed.

This demonstrated that  $\beta 6$  myoepithelial cells expressed a higher level of IL-1 $\alpha$  compared to  $\beta 4$  cells.  $\beta 6$  cells also expressed higher levels of IL-5 compared to  $\beta 4$  cells, which has been shown to induce CD4 T cells (Hogan, Koskinen et al. 1998). In addition,  $\beta 6$  cells expressed more of IL-16, which has a role in the induction and recruitment of Treg cells (McFadden, Morgan et al. 2007).

Thus, up-regulation of IL-5 and IL-16 in  $\beta 6$  cells may be one of the mechanisms leading to the higher numbers of CD4<sup>+</sup> and FOXP3<sup>+</sup> T cells in  $\alpha\beta 6$  positive DCIS cases. The cytokine analysis also demonstrated that  $\beta 6$  cells expressed and released more IFN $\gamma$  compared to  $\beta 4$  cells, which previously has been shown to augment TRAIL-induced apoptosis (Park, Seol et al. 2004). These are promising results but ideally the cytokine arrays should be confirmed by ELISA and the functional relevance of these cytokines confirmed in co-culture assays with knockdown.

## 7.10 Strengths and Weaknesses of the Study

The strength of this study is that the hypothesis is based on observations made in human DCIS tissue, that is, that there is a change in myoepithelial phenotype in a subset of DCIS cases, and this correlates with an increased periductal inflammatory infiltrate. Also, access to primary cell populations, both myoepithelial and T cell, as well as cell lines allowed results to be assessed in physiologically relevant systems.

The study used different approaches to address the same question, in order to achieve robust results. Thus, the assessment of inflammatory cell populations in human tissues was cross-referenced to in-vivo Matrigel plug assays.



Furthermore, the functional impact of molecules was analysed using both knock-down and over-expression systems, also providing more robust data.

The main weakness of the study lies in sample numbers, and this should be addressed in future work.

Also, the Matrigel plug assays, although a potentially powerful approach to directly measure the impact of myoepithelial phenotype on inflammatory populations, were very difficult to interpret owing to high levels of background.

## **7.11 Recommendation**

One of the most challenging areas of the study was quantifying the number of positive inflammatory cells in the Matrigel plugs sections because of the background staining. Therefore, it will be recommended that considerable effort should be made to improve the Matrigel plug technique in order enhance staining.

# Chapter 8 Summary and Conclusion

## 8.0 Summary and Conclusion

---

### 8.1 Influence of DCIS-associated myoepithelial cell phenotype on inflammatory cell infiltrate

This study has shown that there is a correlation between the inflammatory infiltrate in DCIS and expression of  $\alpha\beta6$  integrin by myoepithelial cells. The important findings are summarised below.

- It has shown higher infiltration of regulatory T cells, as determined by CD4 and FOXP3, in  $\alpha\beta6$ +ve DCIS cases compared to  $\alpha\beta6$ -negative cases.
- It also has demonstrated that the  $\alpha\beta6$ +ve DCIS cases are associated with higher numbers of TAMs compared to  $\alpha\beta6$ -ve DCIS cases.
- Overall, analysis of DCIS tissue suggests that the DCIS microenvironment contains high infiltration of CD4+ve T cells. The number of FOXP3 + cells and arginase-1+ cells indicates they are a minor inflammatory cell population in DCIS, whilst MHCII cells numbers are very low in  $\alpha\beta6$ +ve but represents the second dominant cell population in  $\alpha\beta6$ -ve cases.
- In addition, the *in-vivo* study has also shown a direct link between myoepithelial phenotype and inflammatory infiltrate, as indicated by a positive correlation between the numbers of CD4 and FOXP3 cells and up-regulation of  $\alpha\beta6$ .

In conclusion, this work demonstrated that there is variation in the extent and nature of the inflammatory infiltrate in DCIS and this is influenced by myoepithelial cell phenotype.

## **8.2 Impact of up-regulation of $\beta 6$ on DCIS-associated myoepithelial cells on T cell TRAIL levels**

- This work has shown that up-regulation of  $\beta 6$  in DCIS-associated myoepithelial cells promotes enhanced TRAIL expression in primary T cells
- $\beta 6$  myoepithelial cells express higher levels of DR4 and DR5 (TRAIL receptors ) RNA compared to  $\beta 6$ -ve myoepithelial cells.

## **8.3 Role of T cells in progression of DCIS**

- Expression of  $\beta 6$  by myoepithelial cells appears to increase their sensitivity to TRAIL induced apoptosis.
- Knockdown of galectin-7 in a myoepithelial cell line increases their sensitivity to apoptosis mediated by TRAIL.
- Cleaved caspase-3, a marker of apoptosis, has been detected in myoepithelial cells of  $\alpha v\beta 6$  positive DCIS cases highly infiltrated with T cells.

## 8.4 Altered myoepithelial cell phenotype during DCIS

- This study has demonstrated that galectin-7, expressed by myoepithelial cells in normal breast, is down-regulated in a sub-set of DCIS.
- An inverse correlation is evident between galectin-7 and  $\alpha v\beta 6$  expression in myoepithelial cells as demonstrated by duct-duct analysis.

Thus it may be proposed that there is evolution of DCIS in a multi-step manner towards a phenotype likely to progress to invasive disease.

# Chapter 9 Future directions

## 9.0 Future directions

---

- Knockdown of galectin-7 and over-expression of  $\alpha\beta 6$  in primary myoepithelial cells has been successfully achieved. These primary myoepithelial cells will be used as another model to investigate our hypothesis and extend the work beyond myoepithelial cell lines.
- Specific caspase-3 staining has been detected in myoepithelial cells of  $\alpha\beta 6$  positive DCIS cases. To assess the relationship between galectin-7,  $\alpha\beta 6$  expression and apoptosis of myoepithelial cells, double staining for galectin-7 and caspase-3 or  $\alpha\beta 6$  and caspase-3 will be applied to a wider series of DCIS samples.
- Further functional assays to establish the role of altered myoepithelial cytokine profile would be undertaken, specifically knockdown of IL-5 and IL-16.
- Finally, the study will be extended to include earlier stages of disease, including hyperplasia and atypical hyperplasia, in order to establish at what stage changes in galectin-7 and  $\alpha\beta 6$  molecules occur and to investigate this multi-stage hypothesis of breast cancer.

Together, these experiments aim to determine some of the mechanisms involved in the disruption and loss of the myoepithelial cell population in DCIS that may promote progression to invasive disease.



## References

---

- Adriance, M. C., J. L. Inman, O. W. Petersen and M. J. Bissell (2005). "Myoepithelial cells: good fences make good neighbors." Breast Cancer Res **7**(5): 190-197.
- Agrez, M., A. Chen, R. I. Cone, R. Pytela and D. Sheppard (1994). "The alpha v beta 6 integrin promotes proliferation of colon carcinoma cells through a unique region of the beta 6 cytoplasmic domain." J Cell Biol **127**(2): 547-556.
- Akbar, A. N., M. Salmon and G. Janossy (1991). "The synergy between naive and memory T cells during activation." Immunol Today **12**(6): 184-188.
- Akbar, A. N., L. Terry, A. Timms, P. C. Beverley and G. Janossy (1988). "Loss of CD45R and gain of UCHL1 reactivity is a feature of primed T cells." J Immunol **140**(7): 2171-2178.
- Allen, M. D., G. J. Thomas, S. Clark, M. M. Dawoud, S. Vallath, S. J. Payne, J. J. Gomm, S. A. Dreger, S. Dickinson, D. R. Edwards, C. J. Pennington, I. Sestak, J. Cuzick, J. F. Marshall, I. R. Hart and J. L. Jones (2014). "Altered microenvironment promotes progression of preinvasive breast cancer: myoepithelial expression of alphavbeta6 integrin in DCIS identifies high-risk patients and predicts recurrence." Clin Cancer Res **20**(2): 344-357.
- Allinen, M., R. Beroukhi, L. Cai, C. Brennan, J. Lahti-Domenici, H. Huang, D. Porter, M. Hu, L. Chin, A. Richardson, S. Schnitt, W. R. Sellers and K. Polyak (2004). "Molecular characterization of the tumor microenvironment in breast cancer." Cancer Cell **6**(1): 17-32.
- Alpaugh, M. L., M. C. Lee, M. Nguyen, M. Deato, L. Dishakjian and S. H. Barsky (2000). "Myoepithelial-specific CD44 shedding contributes to the anti-invasive and antiangiogenic phenotype of myoepithelial cells." Exp Cell Res **261**(1): 150-158.
- Angele, S., C. Jones, J. S. Reis Filho, L. G. Fulford, I. Treilleux, S. R. Lakhani and J. Hall (2004). "Expression of ATM, p53, and the MRE11-Rad50-NBS1 complex in myoepithelial cells from benign and malignant proliferations of the breast." J Clin Pathol **57**(11): 1179-1184.
- Antoniou, A., P. D. Pharoah, S. Narod, H. A. Risch, J. E. Eyfjord, J. L. Hopper, N. Loman, H. Olsson, O. Johannsson, A. Borg, B. Pasini, P. Radice, S. Manoukian, D. M. Eccles, N. Tang, E. Olah, H. Anton-Culver, E. Warner, J. Lubinski, J. Gronwald, B. Gorski, H. Tulinius, S. Thorlacius, H. Eerola, H. Nevanlinna, K. Syrjakoski, O. P. Kallioniemi, D. Thompson, C. Evans, J. Peto, F. Lalloo, D. G. Evans and D. F. Easton (2003). "Average risks of breast and ovarian cancer associated with BRCA1 or BRCA2 mutations detected in case Series unselected for family history: a combined analysis of 22 studies." Am J Hum Genet **72**(5): 1117-1130

## References

- Ashida, A., N. Boku, K. Aoyagi, H. Sato, Y. Tsubosa, K. Minashi, M. Muto, A. Ohtsu, A. Ochiai, T. Yoshida, S. Yoshida and H. Sasaki (2006). "Expression profiling of esophageal squamous cell carcinoma patients treated with definitive chemoradiotherapy: clinical implications." Int J Oncol **28**(6): 1345-1352.
- Aspod, C., A. Pedroza-Gonzalez, M. Gallegos, S. Tindle, E. C. Burton, D. Su, F. Marches, J. Banchereau and A. K. Palucka (2007). "Breast cancer instructs dendritic cells to prime interleukin 13-secreting CD4+ T cells that facilitate tumor development." J Exp Med **204**(5): 1037-1047.
- Augier, S., T. Ciucci, C. Luci, G. F. Carle, C. Blin-Wakkach and A. Wakkach (2010). "Inflammatory blood monocytes contribute to tumor development and represent a privileged target to improve host immunosurveillance." J Immunol **185**(12): 7165-7173.
- Baan, R., K. Straif, Y. Grosse, B. Secretan, F. El Ghissassi, V. Bouvard, A. Altieri, V. Coglianò and W. H. O. I. A. f. R. o. C. M. W. Group (2007). "Carcinogenicity of alcoholic beverages." Lancet Oncol **8**(4): 292-293.
- Bacher, M., C. N. Metz, T. Calandra, K. Mayer, J. Chesney, M. Lohoff, D. Gemsa, T. Donnelly and R. Bucala (1996). "An essential regulatory role for macrophage migration inhibitory factor in T-cell activation." Proc Natl Acad Sci U S A **93**(15): 7849-7854.
- Badoual, C., S. Hans, J. Rodriguez, S. Peyrard, C. Klein, H. Agueznay Nel, V. Mosseri, O. Laccourreye, P. Bruneval, W. H. Fridman, D. F. Brasnu and E. Tartour (2006). "Prognostic value of tumor-infiltrating CD4+ T-cell subpopulations in head and neck cancers." Clin Cancer Res **12**(2): 465-472.
- Badve, S., R. P. A'Hern, A. M. Ward, R. R. Millis, S. E. Pinder, I. O. Ellis, B. A. Gusterson and J. P. Sloane (1998). "Prediction of local recurrence of ductal carcinoma in situ of the breast using five histological classifications: a comparative study with long follow-up." Hum Pathol **29**(9): 915-923.
- Baker, K., J. Lachapelle, I. Zlobec, T. A. Bismar, L. Terracciano and W. D. Foulkes (2011). "Prognostic significance of CD8+ T lymphocytes in breast cancer depends upon both oestrogen receptor status and histological grade." Histopathology **58**(7): 1107-1116.
- Balkwill, F., K. A. Charles and A. Mantovani (2005). "Smoldering and polarized inflammation in the initiation and promotion of malignant disease." Cancer Cell **7**(3): 211-217.
- Bando, M., Y. Miyake, M. Shiina, M. Wachi, K. Nagai and T. Kataoka (2002). "Actin cytoskeleton is required for early apoptosis signaling induced by anti-Fas antibody but not Fas ligand in murine B lymphoma A20 cells." Biochemical and Biophysical Research Communications **290**(1): 268-274.

## References

- Banks, W. M. (1882). "On Free Removal of Mammary Cancer, with Extirpation of the Axillary Glands as a Necessary Accompaniment." Br Med J **2**(1145): 1138-1141.
- Barondes, S. H., D. N. Cooper, M. A. Gitt and H. Leffler (1994). "Galectins. Structure and function of a large family of animal lectins." J Biol Chem **269**(33): 20807-20810.
- Barsky, S. H. (2003). "Myoepithelial mRNA expression profiling reveals a common tumor-suppressor phenotype." Exp Mol Pathol **74**(2): 113-122.
- Bates, G. J., S. B. Fox, C. Han, R. D. Leek, J. F. Garcia, A. L. Harris and A. H. Banham (2006). "Quantification of regulatory T cells enables the identification of high-risk breast cancer patients and those at risk of late relapse." J Clin Oncol **24**(34): 5373-5380.
- Bates, R. C., D. I. Bellovin, C. Brown, E. Maynard, B. Wu, H. Kawakatsu, D. Sheppard, P. Oettgen and A. M. Mercurio (2005). "Transcriptional activation of integrin beta6 during the epithelial-mesenchymal transition defines a novel prognostic indicator of aggressive colon carcinoma." J Clin Invest **115**(2): 339-347.
- Bennett, S. R., F. R. Carbone, F. Karamalis, R. A. Flavell, J. F. Miller and W. R. Heath (1998). "Help for cytotoxic-T-cell responses is mediated by CD40 signalling." Nature **393**(6684): 478-480.
- Benoit, M., B. Desnues and J. L. Mege (2008). "Macrophage polarization in bacterial infections." J Immunol **181**(6): 3733-3739.
- Beral, V. (2003). "Breast cancer and hormone-replacement therapy in the Million Women Study." Lancet **362**(9382): 419-427.
- Bernengo, M. G., P. Quaglino, N. Cappello, F. Lisa, S. Osella-Abate and M. T. Fierro (2000). "Macrophage-mediated immunostimulation modulates therapeutic efficacy of interleukin-2 based chemoimmunotherapy in advanced metastatic melanoma patients." Melanoma Res **10**(1): 55-65.
- Bernerd, F., A. Sarasin and T. Magnaldo (1999). "Galectin-7 overexpression is associated with the apoptotic process in UVB-induced sunburn keratinocytes." Proceedings of the National Academy of Sciences of the United States of America **96**(20): 11329-11334.
- Beverley, P. C. (1992). "Functional analysis of human T cell subsets defined by CD45 isoform expression." Semin Immunol **4**(1): 35-41.
- Bissell, M. J. and D. Radisky (2001). "Putting tumours in context." Nat Rev Cancer **1**(1): 46-54.

## References

- Bissell, M. J., D. C. Radisky, A. Rizki, V. M. Weaver and O. W. Petersen (2002). "The organizing principle: microenvironmental influences in the normal and malignant breast." Differentiation **70**(9-10): 537-546.
- Biswas, S. K. and A. Mantovani (2010). "Macrophage plasticity and interaction with lymphocyte subsets: cancer as a paradigm." Nat Immunol **11**(10): 889-896.
- Bodian, C. A., K. H. Perzin, R. Lattes and P. Hoffmann (1993). "Reproducibility and validity of pathologic classifications of benign breast disease and implications for clinical applications." Cancer **71**(12): 3908-3913.
- Bohling, S. D. and K. H. Allison (2008). "Immunosuppressive regulatory T cells are associated with aggressive breast cancer phenotypes: a potential therapeutic target." Mod Pathol **21**(12): 1527-1532.
- Bolat, F., F. Kayaselcuk, T. Z. Nursal, M. C. Yagmurdu, N. Bal and B. Demirhan (2006). "Microvessel density, VEGF expression, and tumor-associated macrophages in breast tumors: correlations with prognostic parameters." J Exp Clin Cancer Res **25**(3): 365-372.
- Boldin, M. P., T. M. Goncharov, Y. V. Goltsev and D. Wallach (1996). "Involvement of MACH, a novel MORT1/FADD-interacting protease, in Fas/APO-1- and TNF receptor-induced cell death." Cell **85**(6): 803-815.
- Bombonati, A. and D. C. Sgroi (2011). "The molecular pathology of breast cancer progression." J Pathol **223**(2): 307-317.
- Borner, C. (2003). "The Bcl-2 protein family: sensors and checkpoints for life-or-death decisions." Mol Immunol **39**(11): 615-647.
- Bouillet, P. and A. Strasser (2002). "BH3-only proteins - evolutionarily conserved proapoptotic Bcl-2 family members essential for initiating programmed cell death." J Cell Sci **115**(Pt 8): 1567-1574.
- Boyd, N. F., G. S. Dite, J. Stone, A. Gunasekara, D. R. English, M. R. McCredie, G. G. Giles, D. Tritchler, A. Chiarelli, M. J. Yaffe and J. L. Hopper (2002). "Heritability of mammographic density, a risk factor for breast cancer." N Engl J Med **347**(12): 886-894.
- Breasted JH (1930). The Edwin Smith Surgical Papyrus. Chicago, IL: The University of Chicago Press, Special Edition. 1984. The Classics of Surgery Library. Division of Gryphon Editions, Ltd. Birmingham (AB). Frontispiece.
- Breuss, J. M., J. Gallo, H. M. DeLisser, I. V. Klimanskaya, H. G. Folkesson, J. F. Pittet, S. L. Nishimura, K. Aldape, D. V. Landers, W. Carpenter and et al. (1995). "Expression of the beta 6 integrin subunit in development, neoplasia and tissue repair suggests a role in epithelial remodeling." J Cell Sci **108** ( Pt 6): 2241-2251.

## References

- Brocker, E. B., G. Zwadlo, B. Holzmann, E. Macher and C. Sorg (1988). "Inflammatory cell infiltrates in human melanoma at different stages of tumor progression." Int J Cancer **41**(4): 562-567.
- Bukowski, R. M., W. Sharfman, S. Murthy, P. Rayman, R. Tubbs, J. Alexander, G. T. Budd, J. S. Sergi, L. Bauer, V. Gibson and et al. (1991). "Clinical results and characterization of tumor-infiltrating lymphocytes with or without recombinant interleukin 2 in human metastatic renal cell carcinoma." Cancer Res **51**(16): 4199-4205.
- Burton, J. D., S. Ely, P. K. Reddy, R. Stein, D. V. Gold, T. M. Cardillo and D. M. Goldenberg (2004). "CD74 is expressed by multiple myeloma and is a promising target for therapy." Clin Cancer Res **10**(19): 6606-6611.
- Cabado, A. G., F. Leira, M. R. Vieytes, J. M. Vieites and L. M. Botana (2003). "Cytoskeletal disruption is the key factor that triggers apoptosis in okadaic acid-treated neuroblastoma cells." Archives of Toxicology **78**(2): 74-85.
- Calandra, T., J. Bernhagen, R. A. Mitchell and R. Bucala (1994). "The macrophage is an important and previously unrecognized source of macrophage migration inhibitory factor." J Exp Med **179**(6): 1895-1902.
- Calandra, T. and T. Roger (2003). "Macrophage migration inhibitory factor: a regulator of innate immunity." Nat Rev Immunol **3**(10): 791-800.
- Cao, Z., N. Said, H. K. Wu, I. Kuwabara, F. T. Liu and N. Panjwani (2003). "Galectin-7 as a potential mediator of corneal epithelial cell migration." Arch Ophthalmol **121**(1): 82-86.
- Cassol, E., L. Cassetta, M. Alfano and G. Poli (2010). "Macrophage polarization and HIV-1 infection." J Leukoc Biol **87**(4): 599-608.
- Cebrian, M., E. Yague, M. Rincon, M. Lopez-Botet, M. O. de Landazuri and F. Sanchez-Madrid (1988). "Triggering of T cell proliferation through AIM, an activation inducer molecule expressed on activated human lymphocytes." J Exp Med **168**(5): 1621-1637.
- Chan, M. F., M. Dowsett, E. Folkard, S. Bingham, N. Wareham, R. Luben, A. Welch and K. T. Khaw (2007). "Usual physical activity and endogenous sex hormones in postmenopausal women: the European prospective investigation into cancer-norfolk population study." Cancer Epidemiol Biomarkers Prev **16**(5): 900-905.
- Chang, C. I., J. C. Liao and L. Kuo (2001). "Macrophage arginase promotes tumor cell growth and suppresses nitric oxide-mediated tumor cytotoxicity." Cancer Res **61**(3): 1100-1106.
- Charles, A. J., Jr, Paul Travers, Mark Walport, and Mark J Shlomchik., Ed. (2001). Immunobiology. The Immune System in Health and Disease New York: , Garland Science;

## References

- Charras, G. T., C. K. Hu, M. Coughlin and T. J. Mitchison (2006). "Reassembly of contractile actin cortex in cell blebs." J Cell Biol **175**(3): 477-490.
- Chen, J., Y. Yao, C. Gong, F. Yu, S. Su, J. Chen, B. Liu, H. Deng, F. Wang, L. Lin, H. Yao, F. Su, K. S. Anderson, Q. Liu, M. E. Ewen, X. Yao and E. Song (2011). "CCL18 from tumor-associated macrophages promotes breast cancer metastasis via PITPNM3." Cancer Cell **19**(4): 541-555.
- Chen, L., S. N. Willis, A. Wei, B. J. Smith, J. I. Fletcher, M. G. Hinds, P. M. Colman, C. L. Day, J. M. Adams and D. C. Huang (2005). "Differential targeting of prosurvival Bcl-2 proteins by their BH3-only ligands allows complementary apoptotic function." Mol Cell **17**(3): 393-403.
- Chen, S. Y., A. G. Yang, J. D. Chen, T. Kute, C. R. King, J. Collier, Y. Cong, C. Yao and X. F. Huang (1997). "Potent antitumour activity of a new class of tumour-specific killer cells." Nature **385**(6611): 78-80.
- Chen, W. (2006). "Dendritic cells and (CD4+)CD25+ T regulatory cells: crosstalk between two professionals in immunity versus tolerance." Front Biosci **11**: 1360-1370.
- Cheng, R. J., W. G. Deng, C. B. Niu, Y. Y. Li and Y. Fu (2011). "Expression of macrophage migration inhibitory factor and CD74 in cervical squamous cell carcinoma." Int J Gynecol Cancer **21**(6): 1004-1012.
- Chin, K., C. O. de Solorzano, D. Knowles, A. Jones, W. Chou, E. G. Rodriguez, W. L. Kuo, B. M. Ljung, K. Chew, K. Myambo, M. Miranda, S. Krig, J. Garbe, M. Stampfer, P. Yaswen, J. W. Gray and S. J. Lockett (2004). "In situ analyses of genome instability in breast cancer." Nat Genet **36**(9): 984-988.
- Chinnaiyan, A. M., U. Prasad, S. Shankar, D. A. Hamstra, M. Shanaiah, T. L. Chenevert, B. D. Ross and A. Rehemtulla (2000). "Combined effect of tumor necrosis factor-related apoptosis-inducing ligand and ionizing radiation in breast cancer therapy." Proc Natl Acad Sci U S A **97**(4): 1754-1759.
- Clark, S. E., J. Warwick, R. Carpenter, R. L. Bowen, S. W. Duffy and J. L. Jones (2011). "Molecular subtyping of DCIS: heterogeneity of breast cancer reflected in pre-invasive disease." Br J Cancer **104**(1): 120-127.
- Clarke, R., N. Brunner, B. S. Katzenellenbogen, E. W. Thompson, M. J. Norman, C. Koppi, S. Paik, M. E. Lippman and R. B. Dickson (1989). "Progression of human breast cancer cells from hormone-dependent to hormone-independent growth both in vitro and in vivo." Proc Natl Acad Sci U S A **86**(10): 3649-3653.
- Clement, L. T. (1992). "Isoforms of the CD45 common leukocyte antigen family: markers for human T-cell differentiation." J Clin Immunol **12**(1): 1-10.

## References

- Coleman, M. L. and M. F. Olson (2002). "Rho GTPase signalling pathways in the morphological changes associated with apoptosis." Cell Death Differ **9**(5): 493-504.
- Collaborative Group on Hormonal Factors in Breast, C. (2002). "Breast cancer and breastfeeding: collaborative reanalysis of individual data from 47 epidemiological studies in 30 countries, including 50302 women with breast cancer and 96973 women without the disease." Lancet **360**(9328): 187-195.
- Collaborative Group on Hormonal Factors in Breast, C. (2012). "Menarche, menopause, and breast cancer risk: individual participant meta-analysis, including 118 964 women with breast cancer from 117 epidemiological studies." Lancet Oncol **13**(11): 1141-1151.
- Collins, L. C., R. M. Tamimi, H. J. Baer, J. L. Connolly, G. A. Colditz and S. J. Schnitt (2005). "Outcome of patients with ductal carcinoma in situ untreated after diagnostic biopsy: results from the Nurses' Health Study." Cancer **103**(9): 1778-1784.
- Colotta, F., P. Allavena, A. Sica, C. Garlanda and A. Mantovani (2009). "Cancer-related inflammation, the seventh hallmark of cancer: links to genetic instability." Carcinogenesis **30**(7): 1073-1081.
- Condeelis, J. and J. W. Pollard (2006). "Macrophages: obligate partners for tumor cell migration, invasion, and metastasis." Cell **124**(2): 263-266.
- Coombes, J. L., N. J. Robinson, K. J. Maloy, H. H. Uhlig and F. Powrie (2005). "Regulatory T cells and intestinal homeostasis." Immunol Rev **204**: 184-194.
- Coombes, J. L., K. R. Siddiqui, C. V. Arancibia-Carcamo, J. Hall, C. M. Sun, Y. Belkaid and F. Powrie (2007). "A functionally specialized population of mucosal CD103+ DCs induces Foxp3+ regulatory T cells via a TGF-beta and retinoic acid-dependent mechanism." J Exp Med **204**(8): 1757-1764.
- Cooper, J. A. (1991). "The role of actin polymerization in cell motility." Annu Rev Physiol **53**: 585-605.
- Coronella-Wood, J. A. and E. M. Hersh (2003). "Naturally occurring B-cell responses to breast cancer." Cancer Immunol Immunother **52**(12): 715-738.
- Coronella, J. A., P. Telleman, G. A. Kingsbury, T. D. Truong, S. Hays and R. P. Junghans (2001). "Evidence for an antigen-driven humoral immune response in medullary ductal breast cancer." Cancer Res **61**(21): 7889-7899.
- Correa, I., T. Plunkett, A. Vlad, A. Mungul, J. Candelora-Kettel, J. M. Burchell, J. Taylor-Papadimitriou and O. J. Finn (2003). "Form and pattern of MUC1 expression on T cells activated in vivo or in vitro suggests a function in T-cell migration." Immunology **108**(1): 32-41.

## References

- Correale, P., M. S. Rotundo, M. T. Del Vecchio, C. Remondo, C. Migali, C. Ginanneschi, K. Y. Tsang, A. Licchetta, S. Mannucci, L. Loiacono, P. Tassone, G. Francini and P. Tagliaferri (2010). "Regulatory (FoxP3+) T-cell tumor infiltration is a favorable prognostic factor in advanced colon cancer patients undergoing chemo or chemoimmunotherapy." *J Immunother* **33**(4): 435-441.
- Cory, S. and J. M. Adams (2002). "The BCL2 family: Regulators of the cellular life-or-death switch." *Nature Reviews Cancer* **2**(9): 647-656.
- Cosulich, M. E., A. Rubartelli, A. Risso, F. Cozzolino and A. Bargellesi (1987). "Functional characterization of an antigen involved in an early step of T-cell activation." *Proc Natl Acad Sci U S A* **84**(12): 4205-4209.
- Cotlar, A. M., J. J. Dubose and D. M. Rose (2003). "History of surgery for breast cancer: radical to the sublime." *Curr Surg* **60**(3): 329-337.
- Coussens, L. M. and Z. Werb (2002). "Inflammation and cancer." *Nature* **420**(6917): 860-867.
- Curiel, T. J., G. Coukos, L. Zou, X. Alvarez, P. Cheng, P. Mottram, M. Evdemon-Hogan, J. R. Conejo-Garcia, L. Zhang, M. Burow, Y. Zhu, S. Wei, I. Kryczek, B. Daniel, A. Gordon, L. Myers, A. Lackner, M. L. Disis, K. L. Knutson, L. Chen and W. Zou (2004). "Specific recruitment of regulatory T cells in ovarian carcinoma fosters immune privilege and predicts reduced survival." *Nat Med* **10**(9): 942-949.
- Curtis, C., S. P. Shah, S. F. Chin, G. Turashvili, O. M. Rueda, M. J. Dunning, D. Speed, A. G. Lynch, S. Samarajiwa, Y. Yuan, S. Graf, G. Ha, G. Haffari, A. Bashashati, R. Russell, S. McKinney, A. Langerod, A. Green, E. Provenzano, G. Wishart, S. Pinder, P. Watson, F. Markowitz, L. Murphy, I. Ellis, A. Purushotham, A. L. Borresen-Dale, J. D. Brenton, S. Tavare, C. Caldas and S. Aparicio (2012). "The genomic and transcriptomic architecture of 2,000 breast tumours reveals novel subgroups." *Nature* **486**(7403): 346-352.
- Dairkee, S. H., C. Blayney, H. S. Smith and A. J. Hackett (1985). "Monoclonal antibody that defines human myoepithelium." *Proc Natl Acad Sci U S A* **82**(21): 7409-7413.
- De Maria, R., M. G. Cifone, R. Trotta, M. R. Rippo, C. Festuccia, A. Santoni and R. Testi (1994). "Triggering of human monocyte activation through CD69, a member of the natural killer cell gene complex family of signal transducing receptors." *J Exp Med* **180**(5): 1999-2004.
- De Moulin, D. (1983). "A short history of breast cancer." *Boston: Martinus Nijhof* **6**(2): 99-107.
- de Visser, K. E., A. Eichten and L. M. Coussens (2006). "Paradoxical roles of the immune system during cancer development." *Nat Rev Cancer* **6**(1): 24-37.



## References

- Deapen, D., L. Liu, C. Perkins, L. Bernstein and R. K. Ross (2002). "Rapidly rising breast cancer incidence rates among Asian-American women." Int J Cancer **99**(5): 747-750.
- Degli-Esposti, M. A., W. C. Dougall, P. J. Smolak, J. Y. Waugh, C. A. Smith and R. G. Goodwin (1997). "The novel receptor TRAIL-R4 induces NF-kappaB and protects against TRAIL-mediated apoptosis, yet retains an incomplete death domain." Immunity **7**(6): 813-820.
- Degli-Esposti, M. A., P. J. Smolak, H. Walczak, J. Waugh, C. P. Huang, R. F. DuBose, R. G. Goodwin and C. A. Smith (1997). "Cloning and characterization of TRAIL-R3, a novel member of the emerging TRAIL receptor family." J Exp Med **186**(7): 1165-1170.
- Degterev, A. and J. Yuan (2008). "Expansion and evolution of cell death programmes." Nat Rev Mol Cell Biol **9**(5): 378-390.
- Demers, M., A. A. Rose, A. A. Grosset, K. Biron-Pain, L. Gaboury, P. M. Siegel and Y. St-Pierre (2010). "Overexpression of galectin-7, a myoepithelial cell marker, enhances spontaneous metastasis of breast cancer cells." Am J Pathol **176**(6): 3023-3031.
- DeNardo, D. G., J. B. Barreto, P. Andreu, L. Vasquez, D. Tawfik, N. Kolhatkar and L. M. Coussens (2009). "CD4(+) T cells regulate pulmonary metastasis of mammary carcinomas by enhancing protumor properties of macrophages." Cancer Cell **16**(2): 91-102.
- DeNardo, D. G., D. J. Brennan, E. Rexhepaj, B. Ruffell, S. L. Shiao, S. F. Madden, W. M. Gallagher, N. Wadhvani, S. D. Keil, S. A. Junaid, H. S. Rugo, E. S. Hwang, K. Jirstrom, B. L. West and L. M. Coussens (2011). "Leukocyte complexity predicts breast cancer survival and functionally regulates response to chemotherapy." Cancer Discov **1**(1): 54-67.
- DeNardo, D. G. and L. M. Coussens (2007). "Inflammation and breast cancer. Balancing immune response: crosstalk between adaptive and innate immune cells during breast cancer progression." Breast Cancer Res **9**(4): 212.
- Desouza, M., P. W. Gunning and J. R. Stehn (2012). "The actin cytoskeleton as a sensor and mediator of apoptosis." Bioarchitecture **2**(3): 75-87.
- Dewson, G. and R. M. Kluck (2009). "Mechanisms by which Bak and Bax permeabilise mitochondria during apoptosis." Journal of Cell Science **122**(16): 2801-2808.
- Dickson, S. R. and M. J. Warburton (1992). "Enhanced synthesis of gelatinase and stromelysin by myoepithelial cells during involution of the rat mammary gland." J Histochem Cytochem **40**(5): 697-703.
- Dixit, R. B., A. Chen, J. Chen and D. Sheppard (1996). "Identification of a sequence within the integrin beta6 subunit cytoplasmic domain that is

## References

- required to support the specific effect of alphavbeta6 on proliferation in three-dimensional culture." J Biol Chem **271**(42): 25976-25980.
- Donegan, W. (2002). Cancer of the breast, 5th ed. Philadelphia:, W.B. Saunders Co;.
  - Dong, C. (2008). "TH17 cells in development: an updated view of their molecular identity and genetic programming." Nat Rev Immunol **8**(5): 337-348.
  - Dunn, G. P., L. J. Old and R. D. Schreiber (2004). "The three Es of cancer immunoediting." Annu Rev Immunol **22**: 329-360.
  - Dupont, W. D., F. F. Parl, W. H. Hartmann, L. A. Brinton, A. C. Winfield, J. A. Worrell, P. A. Schuyler and W. D. Plummer (1993). "Breast cancer risk associated with proliferative breast disease and atypical hyperplasia." Cancer **71**(4): 1258-1265.
  - Ebert, L. M., B. S. Tan, J. Browning, S. Svobodova, S. E. Russell, N. Kirkpatrick, C. Gedye, D. Moss, S. P. Ng, D. MacGregor, I. D. Davis, J. Cebon and W. Chen (2008). "The regulatory T cell-associated transcription factor FoxP3 is expressed by tumor cells." Cancer Res **68**(8): 3001-3009.
  - El Kasmi, K. C., J. E. Qualls, J. T. Pesce, A. M. Smith, R. W. Thompson, M. Heno-Tamayo, R. J. Basaraba, T. Konig, U. Schleicher, M. S. Koo, G. Kaplan, K. A. Fitzgerald, E. I. Tuomanen, I. M. Orme, T. D. Kanneganti, C. Bogdan, T. A. Wynn and P. J. Murray (2008). "Toll-like receptor-induced arginase 1 in macrophages thwarts effective immunity against intracellular pathogens." Nature Immunology **9**(12): 1399-1406.
  - Eliassen, A. H., S. A. Missmer, S. S. Tworoger and S. E. Hankinson (2006). "Endogenous steroid hormone concentrations and risk of breast cancer: does the association vary by a woman's predicted breast cancer risk?" J Clin Oncol **24**(12): 1823-1830.
  - Elmore, S. (2007). "Apoptosis: a review of programmed cell death." Toxicol Pathol **35**(4): 495-516.
  - Emery, J. G., P. McDonnell, M. B. Burke, K. C. Deen, S. Lyn, C. Silverman, E. Dul, E. R. Appelbaum, C. Eichman, R. DiPrinzio, R. A. Dodds, I. E. James, M. Rosenberg, J. C. Lee and P. R. Young (1998). "Osteoprotegerin is a receptor for the cytotoxic ligand TRAIL." J Biol Chem **273**(23): 14363-14367.
  - Ernster, V. L., J. Barclay, K. Kerlikowske, H. Wilkie and R. Ballard-Barbash (2000). "Mortality among women with ductal carcinoma in situ of the breast in the population-based surveillance, epidemiology and end results program." Arch Intern Med **160**(7): 953-958.
  - Esplugues, E., D. Sancho, J. Vega-Ramos, C. Martinez, U. Syrbe, A. Hamann, P. Engel, F. Sanchez-Madrid and P. Lauzurica (2003). "Enhanced antitumor immunity in mice deficient in CD69." J Exp Med **197**(9): 1093-1106.

## References

- Esplugues, E., J. Vega-Ramos, D. Cartoixa, B. N. Vazquez, I. Salaet, P. Engel and P. Lauzurica (2005). "Induction of tumor NK-cell immunity by anti-CD69 antibody therapy." Blood **105**(11): 4399-4406.
- Falk, R. T., P. Maas, C. Schairer, N. Chatterjee, J. E. Mabie, C. Cunningham, S. S. Buys, C. Isaacs and R. G. Ziegler (2014). "Alcohol and risk of breast cancer in postmenopausal women: an analysis of etiological heterogeneity by multiple tumor characteristics." Am J Epidemiol **180**(7): 705-717.
- Ferguson, D. J. and T. J. Anderson (1981). "Morphological evaluation of cell turnover in relation to the menstrual cycle in the "resting" human breast." Br J Cancer **44**(2): 177-181.
- Ferlay, J., D. M. Parkin and E. Steliarova-Foucher (2010). "Estimates of cancer incidence and mortality in Europe in 2008." Eur J Cancer **46**(4): 765-781.
- Fong, T. A. and T. R. Mosmann (1990). "Alloreactive murine CD8+ T cell clones secrete the Th1 pattern of cytokines." J Immunol **144**(5): 1744-1752.
- Fontenot, J. D., M. A. Gavin and A. Y. Rudensky (2003). "Foxp3 programs the development and function of CD4+CD25+ regulatory T cells." Nat Immunol **4**(4): 330-336.
- Fontenot, J. D., J. P. Rasmussen, L. M. Williams, J. L. Dooley, A. G. Farr and A. Y. Rudensky (2005). "Regulatory T cell lineage specification by the forkhead transcription factor foxp3." Immunity **22**(3): 329-341.
- Franklin-Tong, V. E. and C. W. Gourlay (2008). "A role for actin in regulating apoptosis/programmed cell death: evidence spanning yeast, plants and animals." Biochemical Journal **413**: 389-404.
- Fridman, W. H., J. Galon, F. Pages, E. Tartour, C. Sautes-Fridman and G. Kroemer (2011). "Prognostic and predictive impact of intra- and peritumoral immune infiltrates." Cancer Res **71**(17): 5601-5605.
- Fujiwara, T., J. Fukushi, S. Yamamoto, Y. Matsumoto, N. Setsu, Y. Oda, H. Yamada, S. Okada, K. Watari, M. Ono, M. Kuwano, S. Kamura, K. Iida, Y. Okada, M. Koga and Y. Iwamoto (2011). "Macrophage infiltration predicts a poor prognosis for human ewing sarcoma." Am J Pathol **179**(3): 1157-1170.
- Fukunaga, A., M. Miyamoto, Y. Cho, S. Murakami, Y. Kawarada, T. Oshikiri, K. Kato, T. Kurokawa, M. Suzuoki, Y. Nakakubo, K. Hiraoka, T. Itoh, T. Morikawa, S. Okushiba, S. Kondo and H. Katoh (2004). "CD8+ tumor-infiltrating lymphocytes together with CD4+ tumor-infiltrating lymphocytes and dendritic cells improve the prognosis of patients with pancreatic adenocarcinoma." Pancreas **28**(1): e26-31.
- Galon, J., A. Costes, F. Sanchez-Cabo, A. Kirilovsky, B. Mlecnik, C. Lagorce-Pages, M. Tosolini, M. Camus, A. Berger, P. Wind, F. Zinzindohoue, P. Bruneval, P. H. Cugnenc, Z. Trajanoski, W. H. Fridman and F. Pages (2006).

## References

- "Type, density, and location of immune cells within human colorectal tumors predict clinical outcome." Science **313**(5795): 1960-1964.
- Galon, J., F. Pages, F. M. Marincola, M. Thurin, G. Trinchieri, B. A. Fox, T. F. Gajewski and P. A. Ascierto (2012). "The immune score as a new possible approach for the classification of cancer." J Transl Med **10**: 1.
  - Garcia-Closas, M., L. A. Brinton, J. Lissowska, N. Chatterjee, B. Peplonska, W. F. Anderson, N. Szeszenia-Dabrowska, A. Bardin-Mikolajczak, W. Zatonski, A. Blair, Z. Kalaylioglu, G. Rymkiewicz, D. Mazepa-Sikora, R. Kordek, S. Lukaszek and M. E. Sherman (2006). "Established breast cancer risk factors by clinically important tumour characteristics." Br J Cancer **95**(1): 123-129.
  - Geissmann, F., M. G. Manz, S. Jung, M. H. Sieweke, M. Merad and K. Ley (2010). "Development of monocytes, macrophages, and dendritic cells." Science **327**(5966): 656-661.
  - Gendronneau, G., S. S. Sidhu, D. Delacour, T. Dang, C. Calonne, D. Houzelstein, T. Magnaldo and F. Poirier (2008). "Galectin-7 in the Control of Epidermal Homeostasis after Injury." Molecular Biology of the Cell **19**(12): 5541-5549.
  - Gerloni, M. and M. Zanetti (2005). "CD4 T cells in tumor immunity." Springer Semin Immunopathol **27**(1): 37-48.
  - Glukhova, M., V. Koteliansky, X. Sastre and J. P. Thiery (1995). "Adhesion systems in normal breast and in invasive breast carcinoma." Am J Pathol **146**(3): 706-716.
  - Goede, V., L. Brogelli, M. Ziche and H. G. Augustin (1999). "Induction of inflammatory angiogenesis by monocyte chemoattractant protein-1." Int J Cancer **82**(5): 765-770.
  - Gomm, J. J., P. J. Browne, R. C. Coope, Q. Y. Liu, L. Buluwela and R. C. Coombes (1995). "Isolation of pure populations of epithelial and myoepithelial cells from the normal human mammary gland using immunomagnetic separation with Dynabeads." Anal Biochem **226**(1): 91-99.
  - Gomm, J. J., J. Smith, G. K. Ryall, R. Baillie, L. Turnbull and R. C. Coombes (1991). "Localization of basic fibroblast growth factor and transforming growth factor beta 1 in the human mammary gland." Cancer Res **51**(17): 4685-4692.
  - Gordon, L. A., K. T. Mulligan, H. Maxwell-Jones, M. Adams, R. A. Walker and J. L. Jones (2003). "Breast cell invasive potential relates to the myoepithelial phenotype." Int J Cancer **106**(1): 8-16.
  - Gordon, S. (2003). "Alternative activation of macrophages." Nat Rev Immunol **3**(1): 23-35.
  - Gordon, S. and P. R. Taylor (2005). "Monocyte and macrophage heterogeneity." Nat Rev Immunol **5**(12): 953-964.

## References

- Green, D. R., T. Ferguson, L. Zitvogel and G. Kroemer (2009). "Immunogenic and tolerogenic cell death." Nature Reviews Immunology **9**(5): 353-363.
- Greenwood, C., G. Metodieva, K. Al-Janabi, B. Lausen, L. Alldridge, L. Leng, R. Bucala, N. Fernandez and M. V. Metodiev (2012). "Stat1 and CD74 overexpression is co-dependent and linked to increased invasion and lymph node metastasis in triple-negative breast cancer." J Proteomics **75**(10): 3031-3040.
- Grewal, J. S., Y. V. Mukhin, M. N. Garnovskaya, J. R. Raymond and E. L. Greene (1999). "Serotonin 5-HT2A receptor induces TGF-beta1 expression in mesangial cells via ERK: proliferative and fibrotic signals." Am J Physiol **276**(6 Pt 2): F922-930.
- Gudjonsson, T., L. Ronnov-Jessen, R. Villadsen, F. Rank, M. J. Bissell and O. W. Petersen (2002). "Normal and tumor-derived myoepithelial cells differ in their ability to interact with luminal breast epithelial cells for polarity and basement membrane deposition." J Cell Sci **115**(Pt 1): 39-50.
- Guelstein, V. I., T. A. Tchypysheva, V. D. Ermilova, L. V. Litvinova, S. M. Troyanovsky and G. A. Bannikov (1988). "Monoclonal antibody mapping of keratins 8 and 17 and of vimentin in normal human mammary gland, benign tumors, dysplasias and breast cancer." Int J Cancer **42**(2): 147-153.
- Guidos, C. (2006). "Thymus and T-lymphocyte development: what is new in the 21st century?" Immunol Rev **209**: 5-9.
- Gunter, M. J., D. R. Hoover, H. Yu, S. Wassertheil-Smoller, T. E. Rohan, J. E. Manson, J. Li, G. Y. Ho, X. Xue, G. L. Anderson, R. C. Kaplan, T. G. Harris, B. V. Howard, J. Wylie-Rosett, R. D. Burk and H. D. Strickler (2009). "Insulin, insulin-like growth factor-I, and risk of breast cancer in postmenopausal women." J Natl Cancer Inst **101**(1): 48-60.
- Gusterson, B. A., P. Monaghan, R. Mahendran, J. Ellis and M. J. O'Hare (1986). "Identification of myoepithelial cells in human and rat breasts by anti-common acute lymphoblastic leukemia antigen antibody A12." J Natl Cancer Inst **77**(2): 343-349.
- Hacker, G. (2000). "The morphology of apoptosis." Cell Tissue Res **301**(1): 5-17.
- Hagemann, T., J. Wilson, H. Kulbe, N. F. Li, D. A. Leinster, K. Charles, F. Klemm, T. Pukrop, C. Binder and F. R. Balkwill (2005). "Macrophages induce invasiveness of epithelial cancer cells via NF-kappa B and JNK." J Immunol **175**(2): 1197-1205.
- Hahn, H. and S. H. Kaufmann (1981). "The role of cell-mediated immunity in bacterial infections." Rev Infect Dis **3**(6): 1221-1250.

## References

- Hamajima, N., K. Hirose, K. Tajima, T. Rohan, E. E. Calle, C. W. Heath, Jr., R. J. Coates, J. M. Liff, R. Talamini, N. Chantarakul, S. Koetsawang, D. Rachawat, A. Morabia, L. Schuman, W. Stewart, M. Szklo, C. Bain, F. Schofield, V. Siskind, P. Band, A. J. Coldman, R. P. Gallagher, T. G. Hislop, P. Yang, L. M. Kolonel, A. M. Nomura, J. Hu, K. C. Johnson, Y. Mao, S. De Sanjose, N. Lee, P. Marchbanks, H. W. Ory, H. B. Peterson, H. G. Wilson, P. A. Wingo, K. Ebeling, D. Kunde, P. Nishan, J. L. Hopper, G. Colditz, V. Gajalanski, N. Martin, T. Pardthaisong, S. Silpisornkosol, C. Theetranont, B. Boosiri, S. Chutivongse, P. Jimakorn, P. Virutamasen, C. Wongsrichanalai, M. Ewertz, H. O. Adami, L. Bergkvist, C. Magnusson, I. Persson, J. Chang-Claude, C. Paul, D. C. Skegg, G. F. Spears, P. Boyle, T. Evstifeeva, J. R. Daling, W. B. Hutchinson, K. Malone, E. A. Noonan, J. L. Stanford, D. B. Thomas, N. S. Weiss, E. White, N. Andrieu, A. Bremond, F. Clavel, B. Gairard, J. Lansac, L. Piana, R. Renaud, A. Izquierdo, P. Viladiu, H. R. Cuevas, P. Ontiveros, A. Palet, S. B. Salazar, N. Aristizabel, A. Cuadros, L. Tryggvadottir, H. Tulinius, A. Bachelot, M. G. Le, J. Peto, S. Franceschi, F. Lubin, B. Modan, E. Ron, Y. Wax, G. D. Friedman, R. A. Hiatt, F. Levi, T. Bishop, K. Kosmelj, M. Primic-Zakelj, B. Ravnihar, J. Stare, W. L. Beeson, G. Fraser, R. D. Bullbrook, J. Cuzick, S. W. Duffy, I. S. Fentiman, J. L. Hayward, D. Y. Wang, A. J. McMichael, K. McPherson, R. L. Hanson, M. C. Leske, M. C. Mahoney, P. C. Nasca, A. O. Varma, A. L. Weinstein, T. R. Moller, H. Olsson, J. Ranstam, R. A. Goldbohm, P. A. van den Brandt, R. A. Apelo, J. Baens, J. R. de la Cruz, B. Javier, L. B. Lacaya, C. A. Ngelangel, C. La Vecchia, E. Negri, E. Marubini, M. Ferraroni, M. Gerber, S. Richardson, C. Segala, D. Gatei, P. Kenya, A. Kungu, J. G. Mati, L. A. Brinton, R. Hoover, C. Schairer, R. Spirtas, H. P. Lee, M. A. Rookus, F. E. van Leeuwen, J. A. Schoenberg, M. McCredie, M. D. Gammon, E. A. Clarke, L. Jones, A. Neil, M. Vessey, D. Yeates, P. Appleby, E. Banks, V. Beral, D. Bull, B. Crossley, A. Goodill, J. Green, C. Hermon, T. Key, N. Langston, C. Lewis, G. Reeves, R. Collins, R. Doll, R. Peto, K. Mabuchi, D. Preston, P. Hannaford, C. Kay, L. Rosero-Bixby, Y. T. Gao, F. Jin, J. M. Yuan, H. Y. Wei, T. Yun, C. Zhiheng, G. Berry, J. Cooper Booth, T. Jelihovsky, R. MacLennan, R. Shearman, Q. S. Wang, C. J. Baines, A. B. Miller, C. Wall, E. Lund, H. Stalsberg, X. O. Shu, W. Zheng, K. Katsouyanni, A. Trichopoulou, D. Trichopoulos, A. Dabancens, L. Martinez, R. Molina, O. Salas, F. E. Alexander, K. Anderson, A. R. Folsom, B. S. Hulka, L. Bernstein, S. Enger, R. W. Haile, A. Paganini-Hill, M. C. Pike, R. K. Ross, G. Ursin, M. C. Yu, M. P. Longnecker, P. Newcomb, L. Bergkvist, A. Kalache, T. M. Farley, S. Holck, O. Meirik and C. Collaborative Group on Hormonal Factors in Breast (2002). "Alcohol, tobacco and breast cancer--collaborative reanalysis of individual data from 53 epidemiological studies, including 58,515 women with breast cancer and 95,067 women without the disease." *Br J Cancer* **87**(11): 1234-1245.
- Hamperl, H. (1970). "The myoepithelia (myoepithelial cells). Normal state; regressive changes; hyperplasia; tumors." *Curr Top Pathol* **53**: 161-220.
- Han, Y., Q. Guo, M. Zhang, Z. Chen and X. Cao (2009). "CD69+ CD4+ CD25- T cells, a new subset of regulatory T cells, suppress T cell proliferation through membrane-bound TGF-beta 1." *J Immunol* **182**(1): 111-120.
- Hanahan, D. and R. A. Weinberg (2000). "The hallmarks of cancer." *Cell* **100**(1): 57-70.

## References

- Hanahan, D. and R. A. Weinberg (2011). "Hallmarks of cancer: the next generation." Cell **144**(5): 646-674.
- Hao, N. B., M. H. Lu, Y. H. Fan, Y. L. Cao, Z. R. Zhang and S. M. Yang (2012). "Macrophages in tumor microenvironments and the progression of tumors." Clin Dev Immunol **2012**: 948098.
- Hartveit, F. (1998). "Breast cancer: poor short-term prognosis in cases with moderate lymphocyte infiltration at the tumour edge: a preliminary report." Oncol Rep **5**(2): 423-426.
- Harvey, J., D. B. Jones and D. H. Wright (1989). "Leucocyte common antigen expression on T cells in normal and inflamed human gut." Immunology **68**(1): 13-17.
- Haupt, S., M. Berger, Z. Goldberg and Y. Haupt (2003). "Apoptosis - the p53 network." J Cell Sci **116**(Pt 20): 4077-4085.
- He, X. X., K. Chen, J. Yang, X. Y. Li, H. Y. Gan, C. Y. Liu, T. R. Coleman and Y. Al-Abed (2009). "Macrophage migration inhibitory factor promotes colorectal cancer." Mol Med **15**(1-2): 1-10.
- Hengartner, M. O. (2000). "The biochemistry of apoptosis." Nature **407**(6805): 770-776.
- Hertlein, E., G. Triantafyllou, E. J. Sass, J. D. Hessler, X. Zhang, D. Jarjoura, D. M. Lucas, N. Muthusamy, D. M. Goldenberg, R. J. Lee and J. C. Byrd (2010). "Milatuzumab immunoliposomes induce cell death in CLL by promoting accumulation of CD74 on the surface of B cells." Blood **116**(14): 2554-2558.
- Herzer, K., A. Grosse-Wilde, P. H. Krammer, P. R. Galle and S. Kanzler (2008). "Transforming growth factor-beta-mediated tumor necrosis factor-related apoptosis-inducing ligand expression and apoptosis in hepatoma cells requires functional cooperation between Smad proteins and activator protein-1." Mol Cancer Res **6**(7): 1169-1177.
- Hill, M. A. and P. Gunning (1993). "Beta and gamma actin mRNAs are differentially located within myoblasts." J Cell Biol **122**(4): 825-832.
- Hinz, S., L. Pagerols-Raluy, H. H. Oberg, O. Ammerpohl, S. Grussel, B. Sipos, R. Grutzmann, C. Pilarsky, H. Ungefroren, H. D. Saeger, G. Kloppel, D. Kabelitz and H. Kalthoff (2007). "Foxp3 expression in pancreatic carcinoma cells as a novel mechanism of immune evasion in cancer." Cancer Res **67**(17): 8344-8350.
- Ho, V. W. and L. M. Sly (2009). "Derivation and characterization of murine alternatively activated (M2) macrophages." Methods Mol Biol **531**: 173-185.
- Hogan, S. P., A. Koskinen, K. I. Matthaiei, I. G. Young and P. S. Foster (1998). "Interleukin-5-producing CD4+ T cells play a pivotal role in aeroallergen-

## References

- induced eosinophilia, bronchial hyperreactivity, and lung damage in mice." Am J Respir Crit Care Med **157**(1): 210-218.
- Hoock, T. C., P. M. Newcomb and I. M. Herman (1991). "Beta actin and its mRNA are localized at the plasma membrane and the regions of moving cytoplasm during the cellular response to injury." J Cell Biol **112**(4): 653-664.
  - Hori, S., T. Nomura and S. Sakaguchi (2003). "Control of regulatory T cell development by the transcription factor Foxp3." Science **299**(5609): 1057-1061.
  - Hotta, K., M. Sho, K. Fujimoto, K. Shimada, I. Yamato, S. Anai, N. Konishi, Y. Hirao, K. Nonomura and Y. Nakajima (2011). "Prognostic significance of CD45RO+ memory T cells in renal cell carcinoma." Br J Cancer **105**(8): 1191-1196.
  - Huang, D. C. and A. Strasser (2000). "BH3-Only proteins-essential initiators of apoptotic cell death." Cell **103**(6): 839-842.
  - Huang, X., J. Wu, S. Spong and D. Sheppard (1998). "The integrin alphavbeta6 is critical for keratinocyte migration on both its known ligand, fibronectin, and on vitronectin." J Cell Sci **111 ( Pt 15)**: 2189-2195.
  - Huang, X. Z., J. F. Wu, D. Cass, D. J. Erle, D. Corry, S. G. Young, R. V. Farese, Jr. and D. Sheppard (1996). "Inactivation of the integrin beta 6 subunit gene reveals a role of epithelial integrins in regulating inflammation in the lung and skin." J Cell Biol **133**(4): 921-928.
  - Hudson, J. D., M. A. Shoaibi, R. Maestro, A. Carnero, G. J. Hannon and D. H. Beach (1999). "A proinflammatory cytokine inhibits p53 tumor suppressor activity." J Exp Med **190**(10): 1375-1382.
  - Huseby, R., A. and Thomas, L.,B (1954). "Histological and histochemical alteration in advanced breast cancer being treated with Estrogen Hormones " Cancer **7**: 54-74.
  - Hwang, E. S., S. DeVries, K. L. Chew, D. H. Moore, 2nd, K. Kerlikowske, A. Thor, B. M. Ljung and F. M. Waldman (2004). "Patterns of chromosomal alterations in breast ductal carcinoma in situ." Clin Cancer Res **10**(15): 5160-5167.
  - Ichihara, F., K. Kono, A. Takahashi, H. Kawaida, H. Sugai and H. Fujii (2003). "Increased populations of regulatory T cells in peripheral blood and tumor-infiltrating lymphocytes in patients with gastric and esophageal cancers." Clin Cancer Res **9**(12): 4404-4408.
  - Iliopoulos, D., H. A. Hirsch and K. Struhl (2009). "An Epigenetic Switch Involving NF-kappa B, Lin28, Let-7 MicroRNA, and IL6 Links Inflammation to Cell Transformation." Cell **139**(4): 693-706.
  - Inagaki, Y., K. Higashi, M. Kushida, Y. Y. Hong, S. Nakao, R. Higashiyama, T. Moro, J. Itoh, T. Mikami, T. Kimura, G. Shiota, I. Kuwabara and I. Okazaki



## References

- (2008). "Hepatocyte growth factor suppresses profibrogenic signal transduction via nuclear export of Smad3 with galectin-7." Gastroenterology **134**(4): 1180-1190.
- Ioachim, H. L., S. E. Pambuccian, M. Hekimgil, F. R. Giancotti and B. H. Dorsett (1996). "Lymphoid monoclonal antibodies reactive with lung tumors. Diagnostic applications." Am J Surg Pathol **20**(1): 64-71.
  - Irvine, T. and I. S. Fentiman (2007). "Biology and treatment of ductal carcinoma in situ." Expert Rev Anticancer Ther **7**(2): 135-145.
  - Ishigami, S., S. Natsugoe, K. Tokuda, A. Nakajo, H. Iwashige, K. Aridome, S. Hokita and T. Aikou (2001). "Invariant chain expression in gastric cancer." Cancer Lett **168**(1): 87-91.
  - Janes, S. M. and F. M. Watt (2004). "Switch from alpha5beta1 to alpha5beta2 integrin expression protects squamous cell carcinomas from anoikis." J Cell Biol **166**(3): 419-431.
  - Janeway, C. A., Jr. (1998). "Presidential Address to The American Association of Immunologists. The road less traveled by: the role of innate immunity in the adaptive immune response." J Immunol **161**(2): 539-544.
  - Jensen, E., DeSombre ER, Jungblut PW (1967). Estrogen receptors in hormone responsive tissues and tumors. In: Wissler RW, Dao TL, Wood S Jr., editors. Endogenous factors influencing host-tumor balance. Chicago: University of Chicago Press;.
  - Jensen, T. O., H. Schmidt, H. J. Moller, M. Hoyer, M. B. Maniecki, P. Sjoegren, I. J. Christensen and T. Steiniche (2009). "Macrophage markers in serum and tumor have prognostic impact in American Joint Committee on Cancer stage I/II melanoma." J Clin Oncol **27**(20): 3330-3337.
  - Jeremias, I., I. Herr, T. Boehler and K. M. Debatin (1998). "TRAIL/Apo-2-ligand-induced apoptosis in human T cells." Eur J Immunol **28**(1): 143-152.
  - Jones, C., A. Mackay, A. Grigoriadis, A. Cossu, J. S. Reis-Filho, L. Fulford, T. Dexter, S. Davies, K. Bulmer, E. Ford, S. Parry, M. Budroni, G. Palmieri, A. M. Neville, M. J. O'Hare and S. R. Lakhani (2004). "Expression profiling of purified normal human luminal and myoepithelial breast cells: identification of novel prognostic markers for breast cancer." Cancer Res **64**(9): 3037-3045.
  - Jones, J. L., J. A. Shaw, J. H. Pringle and R. A. Walker (2003). "Primary breast myoepithelial cells exert an invasion-suppressor effect on breast cancer cells via paracrine down-regulation of MMP expression in fibroblasts and tumour cells." J Pathol **201**(4): 562-572.
  - Kaaks, R., F. Berrino, T. Key, S. Rinaldi, L. Dossus, C. Biessy, G. Secreto, P. Amiano, S. Bingham, H. Boeing, H. B. Bueno de Mesquita, J. Chang-Claude, F. Clavel-Chapelon, A. Fournier, C. H. van Gils, C. A. Gonzalez, A. B. Gurrea, E. Critselis, K. T. Khaw, V. Krogh, P. H. Lahmann, G. Nagel, A. Olsen, N. C. Onland-Moret, K. Overvad, D. Palli, S. Panico, P. Peeters, J. R. Quiros, A.

## References

- Roddam, A. Thiebaut, A. Tjonneland, M. D. Chirlaque, A. Trichopoulou, D. Trichopoulos, R. Tumino, P. Vineis, T. Norat, P. Ferrari, N. Slimani and E. Riboli (2005). "Serum sex steroids in premenopausal women and breast cancer risk within the European Prospective Investigation into Cancer and Nutrition (EPIC)." J Natl Cancer Inst **97**(10): 755-765.
- Kawai, O., G. Ishii, K. Kubota, Y. Murata, Y. Naito, T. Mizuno, K. Aokage, N. Saijo, Y. Nishiwaki, A. Gemma, S. Kudoh and A. Ochiai (2008). "Predominant infiltration of macrophages and CD8(+) T Cells in cancer nests is a significant predictor of survival in stage IV nonsmall cell lung cancer." Cancer **113**(6): 1387-1395.
  - Kayalar, C., T. Ord, M. P. Testa, L. T. Zhong and D. E. Bredesen (1996). "Cleavage of actin by interleukin 1 beta-converting enzyme to reverse DNase I inhibition." Proceedings of the National Academy of Sciences of the United States of America **93**(5): 2234-2238.
  - Keane, M. M., S. A. Ettenberg, M. M. Nau, E. K. Russell and S. Lipkowitz (1999). "Chemotherapy augments TRAIL-induced apoptosis in breast cell lines." Cancer Res **59**(3): 734-741.
  - Keene, J. A. and J. Forman (1982). "Helper activity is required for the in vivo generation of cytotoxic T lymphocytes." J Exp Med **155**(3): 768-782.
  - Kelso, A. and A. L. Glasebrook (1984). "Secretion of interleukin 2, macrophage-activating factor, interferon, and colony-stimulating factor by alloreactive T lymphocyte clones." J Immunol **132**(6): 2924-2931.
  - Key, T., P. Appleby, I. Barnes, G. Reeves, H. Endogenous and G. Breast Cancer Collaborative (2002). "Endogenous sex hormones and breast cancer in postmenopausal women: reanalysis of nine prospective studies." J Natl Cancer Inst **94**(8): 606-616.
  - Key, T. J., P. N. Appleby, G. K. Reeves and A. W. Roddam (2010). "Insulin-like growth factor 1 (IGF1), IGF binding protein 3 (IGFBP3), and breast cancer risk: pooled individual data analysis of 17 prospective studies." Lancet Oncol **11**(6): 530-542.
  - Khaitlina, S. Y. (2001). "Functional specificity of actin isoforms." International Review of Cytology - a Survey of Cell Biology, Vol. 202 **202**: 35-98.
  - Kim, M., T. Grimmig, M. Grimm, M. Lazariotou, E. Meier, A. Rosenwald, I. Tsaour, R. Blaheta, U. Heemann, C. T. Germer, A. M. Waaga-Gasser and M. Gasser (2013). "Expression of Foxp3 in colorectal cancer but not in Treg cells correlates with disease progression in patients with colorectal cancer." PLoS One **8**(1): e53630.
  - Kim, Y. S., R. F. Schwabe, T. Qian, J. J. Lemasters and D. A. Brenner (2002). "TRAIL-mediated apoptosis requires NF-kappaB inhibition and the mitochondrial permeability transition in human hepatoma cells." Hepatology **36**(6): 1498-1508.

## References

- Ko, K., S. Yamazaki, K. Nakamura, T. Nishioka, K. Hirota, T. Yamaguchi, J. Shimizu, T. Nomura, T. Chiba and S. Sakaguchi (2005). "Treatment of advanced tumors with agonistic anti-GITR mAb and its effects on tumor-infiltrating Foxp3+CD25+CD4+ regulatory T cells." J Exp Med **202**(7): 885-891.
- Koebel, C. M., W. Vermi, J. B. Swann, N. Zerafa, S. J. Rodig, L. J. Old, M. J. Smyth and R. D. Schreiber (2007). "Adaptive immunity maintains occult cancer in an equilibrium state." Nature **450**(7171): 903-907.
- Koukoulis, G. K., A. A. Howedy, M. Korhonen, I. Virtanen and V. E. Gould (1993). "Distribution of tenascin, cellular fibronectins and integrins in the normal, hyperplastic and neoplastic breast." J Submicrosc Cytol Pathol **25**(2): 285-295.
- Kristensson, K., C. A. Borrebaeck and R. Carlsson (1992). "Human CD4+ T cells expressing CD45RA acquire the lymphokine gene expression of CD45RO+ T-helper cells after activation in vitro." Immunology **76**(1): 103-109.
- Krop, I. E., D. Sgroi, D. A. Porter, K. L. Lunetta, R. LeVangie, P. Seth, C. M. Kaelin, E. Rhei, M. Bosenberg, S. Schnitt, J. R. Marks, Z. Pagon, D. Belina, J. Razumovic and K. Polyak (2001). "HIN-1, a putative cytokine highly expressed in normal but not cancerous mammary epithelial cells." Proc Natl Acad Sci U S A **98**(17): 9796-9801.
- Kruger, J. M., C. Wemmert, L. Sternberger, C. Bonnas, G. Dietmann, P. Gancarski and F. Feuerhake (2013). "Combat or surveillance? Evaluation of the heterogeneous inflammatory breast cancer microenvironment." J Pathol **229**(4): 569-578.
- Kumar, S., H. Kishimoto, H. L. Chua, S. Badve, K. D. Miller, R. M. Bigsby and H. Nakshatri (2003). "Interleukin-1 alpha promotes tumor growth and cachexia in MCF-7 xenograft model of breast cancer." Am J Pathol **163**(6): 2531-2541.
- Kumar, V., Fausto, N., Abbas, A., Ed. (2005). Robbins & Cotran Pathologic Basis of Disease. 1525, William Schmitt.
- Kurtzman, S. H., K. H. Anderson, Y. Wang, L. J. Miller, M. Renna, M. Stankus, R. R. Lindquist, G. Barrows and D. L. Kreutzer (1999). "Cytokines in human breast cancer: IL-1alpha and IL-1beta expression." Oncol Rep **6**(1): 65-70.
- Kuwabara, I., Y. Kuwabara, R. Y. Yang, M. Schuler, D. R. Green, B. L. Zuraw, D. K. Hsu and F. T. Liu (2002). "Galectin-7 (PIG1) exhibits pro-apoptotic function through JNK activation and mitochondrial cytochrome c release." Journal of Biological Chemistry **277**(5): 3487-3497.
- Ladoire, S., L. Arnould, L. Apetoh, B. Coudert, F. Martin, B. Chauffert, P. Fumoleau and F. Ghiringhelli (2008). "Pathologic complete response to neoadjuvant chemotherapy of breast carcinoma is associated with the disappearance of tumor-infiltrating foxp3+ regulatory T cells." Clin Cancer Res **14**(8): 2413-2420.

## References

- Lai, Y. P., C. C. Lin, W. J. Liao, C. Y. Tang and S. C. Chen (2009). "CD4+ T cell-derived IL-2 signals during early priming advances primary CD8+ T cell responses." PLoS One **4**(11): e7766.
- Lakhani, S. R., R. Chaggar, S. Davies, C. Jones, N. Collins, C. Odel, M. R. Stratton and M. J. O'Hare (1999). "Genetic alterations in 'normal' luminal and myoepithelial cells of the breast." J Pathol **189**(4): 496-503.
- Lakhani, S. R. and M. J. O'Hare (2001). "The mammary myoepithelial cell--Cinderella or ugly sister?" Breast Cancer Res **3**(1): 1-4.
- Lala, P. K. (1998). "Significance of nitric oxide in carcinogenesis, tumor progression and cancer therapy." Cancer Metastasis Rev **17**(1): 1-6.
- Larsson, S. C., C. S. Mantzoros and A. Wolk (2007). "Diabetes mellitus and risk of breast cancer: a meta-analysis." Int J Cancer **121**(4): 856-862.
- Laster, S. M. and J. M. Mackenzie, Jr. (1996). "Bleb formation and F-actin distribution during mitosis and tumor necrosis factor-induced apoptosis." Microsc Res Tech **34**(3): 272-280.
- Lazard, D., X. Sastre, M. G. Frid, M. A. Glukhova, J. P. Thiery and V. E. Kotliansky (1993). "Expression of smooth muscle-specific proteins in myoepithelium and stromal myofibroblasts of normal and malignant human breast tissue." Proc Natl Acad Sci U S A **90**(3): 999-1003.
- Lazebnik, Y. A., S. H. Kaufmann, S. Desnoyers, G. G. Poirier and W. C. Earnshaw (1994). "Cleavage of Poly(Adp-Ribose) Polymerase by a Proteinase with Properties Like Ice." Nature **371**(6495): 346-347.
- Le Rhun, Y., J. B. Kirkland and G. M. Shah (1998). "Cellular responses to DNA damage in the absence of poly(ADP-ribose) polymerase." Biochemical and Biophysical Research Communications **245**(1): 1-10.
- Ledbetter, J. A., L. M. Rose, C. E. Spooner, P. G. Beatty, P. J. Martin and E. A. Clark (1985). "Antibodies to common leukocyte antigen p220 influence human T cell proliferation by modifying IL 2 receptor expression." J Immunol **135**(3): 1819-1825.
- Lee, A. H., L. C. Happerfield, L. G. Bobrow and R. R. Millis (1997). "Angiogenesis and inflammation in invasive carcinoma of the breast." J Clin Pathol **50**(8): 669-673.
- Lee, A. H., L. C. Happerfield, R. R. Millis and L. G. Bobrow (1996). "Inflammatory infiltrate in invasive lobular and ductal carcinoma of the breast." Br J Cancer **74**(5): 796-801.
- Lee, H. E., S. W. Chae, Y. J. Lee, M. A. Kim, H. S. Lee, B. L. Lee and W. H. Kim (2008). "Prognostic implications of type and density of tumour-infiltrating lymphocytes in gastric cancer." Br J Cancer **99**(10): 1704-1711.

## References

- Leek, R. D., N. C. Hunt, R. J. Landers, C. E. Lewis, J. A. Royds and A. L. Harris (2000). "Macrophage infiltration is associated with VEGF and EGFR expression in breast cancer." J Pathol **190**(4): 430-436.
- Leek, R. D., R. J. Landers, A. L. Harris and C. E. Lewis (1999). "Necrosis correlates with high vascular density and focal macrophage infiltration in invasive carcinoma of the breast." Br J Cancer **79**(5-6): 991-995.
- Leek, R. D., C. E. Lewis, R. Whitehouse, M. Greenall, J. Clarke and A. L. Harris (1996). "Association of macrophage infiltration with angiogenesis and prognosis in invasive breast carcinoma." Cancer Res **56**(20): 4625-4629.
- Leffers, N., M. J. Gooden, R. A. de Jong, B. N. Hoogeboom, K. A. ten Hoor, H. Hollema, H. M. Boezen, A. G. van der Zee, T. Daemen and H. W. Nijman (2009). "Prognostic significance of tumor-infiltrating T-lymphocytes in primary and metastatic lesions of advanced stage ovarian cancer." Cancer Immunol Immunother **58**(3): 449-459.
- Leffler, H., S. Carlsson, M. Hedlund, Y. Qian and F. Poirier (2004). "Introduction to galectins." Glycoconj J **19**(7-9): 433-440.
- Leng, L., C. N. Metz, Y. Fang, J. Xu, S. Donnelly, J. Baugh, T. Delohery, Y. Chen, R. A. Mitchell and R. Bucala (2003). "MIF signal transduction initiated by binding to CD74." J Exp Med **197**(11): 1467-1476.
- Li, J. Q., Q. X. Li, C. C. Xie, H. M. Zhou, Y. Q. Wang, N. Zhang, H. J. Shao, S. C. Chan, X. X. Peng, S. C. Lin and J. H. Han (2004). "beta-actin is required for mitochondria clustering and ROS generation in TNF-induced, caspase-independent cell death." Journal of Cell Science **117**(20): 4673-4680.
- Li, Q., Z. Guo, X. Xu, S. Xia and X. Cao (2008). "Pulmonary stromal cells induce the generation of regulatory DC attenuating T-cell-mediated lung inflammation." Eur J Immunol **38**(10): 2751-2761.
- Li, X., Y. Yang, Y. Hu, D. Dang, J. Regezi, B. L. Schmidt, A. Atakilit, B. Chen, D. Ellis and D. M. Ramos (2003). "Alphavbeta6-Fyn signaling promotes oral cancer progression." J Biol Chem **278**(43): 41646-41653.
- Lin, J., V. K. Brown and L. B. Justement (1992). "Regulation of basal tyrosine phosphorylation of the B cell antigen receptor complex by the protein tyrosine phosphatase, CD45." J Immunol **149**(10): 3182-3190.
- Liu, F. T. and G. A. Rabinovich (2005). "Galectins as modulators of tumour progression." Nat Rev Cancer **5**(1): 29-41.
- Liu, S., J. Lachapelle, S. Leung, D. Gao, W. D. Foulkes and T. O. Nielsen (2012). "CD8+ lymphocyte infiltration is an independent favorable prognostic indicator in basal-like breast cancer." Breast Cancer Res **14**(2): R48.

## References

- Livasy, C. A., C. M. Perou, G. Karaca, D. W. Cowan, D. Maia, S. Jackson, C. K. Tse, S. Nyante and R. C. Millikan (2007). "Identification of a basal-like subtype of breast ductal carcinoma in situ." Hum Pathol **38**(2): 197-204.
- Liyanage, U. K., T. T. Moore, H. G. Joo, Y. Tanaka, V. Herrmann, G. Doherty, J. A. Drebin, S. M. Strasberg, T. J. Eberlein, P. S. Goedegebuure and D. C. Linehan (2002). "Prevalence of regulatory T cells is increased in peripheral blood and tumor microenvironment of patients with pancreas or breast adenocarcinoma." J Immunol **169**(5): 2756-2761.
- Locksley, R. M., N. Killeen and M. J. Lenardo (2001). "The TNF and TNF receptor superfamilies: integrating mammalian biology." Cell **104**(4): 487-501.
- Lorsbach, R. B., W. J. Murphy, C. J. Lowenstein, S. H. Snyder and S. W. Russell (1993). "Expression of the nitric oxide synthase gene in mouse macrophages activated for tumor cell killing. Molecular basis for the synergy between interferon-gamma and lipopolysaccharide." J Biol Chem **268**(3): 1908-1913.
- Ma, X. J., R. Salunga, J. T. Tuggle, J. Gaudet, E. Enright, P. McQuary, T. Payette, M. Pistone, K. Stecker, B. M. Zhang, Y. X. Zhou, H. Varnholt, B. Smith, M. Gadd, E. Chatfield, J. Kessler, T. M. Baer, M. G. Erlander and D. C. Sgroi (2003). "Gene expression profiles of human breast cancer progression." Proc Natl Acad Sci U S A **100**(10): 5974-5979.
- Macchetti, A. H., H. R. Marana, J. S. Silva, J. M. de Andrade, A. Ribeiro-Silva and S. Bighetti (2006). "Tumor-infiltrating CD4+ T lymphocytes in early breast cancer reflect lymph node involvement." Clinics (Sao Paulo) **61**(3): 203-208.
- Mackay, C. R. (1991). "T-cell memory: the connection between function, phenotype and migration pathways." Immunol Today **12**(6): 189-192.
- MacMahon, B. (2006). "Epidemiology and the causes of breast cancer." Int J Cancer **118**(10): 2373-2378.
- Madsen, P., H. H. Rasmussen, T. Flint, P. Gromov, T. A. Kruse, B. Honore, H. Vorum and J. E. Celis (1995). "Cloning, expression, and chromosome mapping of human galectin-7." J Biol Chem **270**(11): 5823-5829.
- Magnaldo, T., F. Bernerd and M. Darmon (1995). "Galectin-7, a human 14-kDa S-lectin, specifically expressed in keratinocytes and sensitive to retinoic acid." Dev Biol **168**(2): 259-271.
- Mahmoud, S. M., A. H. Lee, E. C. Paish, R. D. Macmillan, I. O. Ellis and A. R. Green (2012). "Tumour-infiltrating macrophages and clinical outcome in breast cancer." J Clin Pathol **65**(2): 159-163.
- Mahmoud, S. M., E. C. Paish, D. G. Powe, R. D. Macmillan, M. J. Grainge, A. H. Lee, I. O. Ellis and A. R. Green (2011). "Tumor-infiltrating CD8+ lymphocytes predict clinical outcome in breast cancer." J Clin Oncol **29**(15): 1949-1955.

## References

- Mahmoud, S. M., E. C. Paish, D. G. Powe, R. D. Macmillan, A. H. Lee, I. O. Ellis and A. R. Green (2011). "An evaluation of the clinical significance of FOXP3+ infiltrating cells in human breast cancer." Breast Cancer Res Treat **127**(1): 99-108.
- Majno, G. and I. Joris (1995). "Apoptosis, oncosis, and necrosis. An overview of cell death." Am J Pathol **146**(1): 3-15.
- Makitie, T., P. Summanen, A. Tarkkanen and T. Kivela (2001). "Tumor-infiltrating macrophages (CD68+) cells) and prognosis in malignant uveal melanoma." Invest Ophthalmol Vis Sci **42**(7): 1414-1421.
- Man, Y. G. (2007). "Focal degeneration of aged or injured myoepithelial cells and the resultant auto-immunoreactions are trigger factors for breast tumor invasion." Med Hypotheses **69**(6): 1340-1357.
- Man, Y. G., L. Tai, R. Barner, R. Vang, J. S. Saenger, K. M. Shekitka, G. L. Brattbauer, D. T. Wheeler, C. Y. Liang, T. N. Vinh and B. L. Strauss (2003). "Cell clusters overlying focally disrupted mammary myoepithelial cell layers and adjacent cells within the same duct display different immunohistochemical and genetic features: implications for tumor progression and invasion." Breast Cancer Res **5**(6): R231-241.
- Mantovani, A., P. Allavena, A. Sica and F. Balkwill (2008). "Cancer-related inflammation." Nature **454**(7203): 436-444.
- Mantovani, A., A. Sica, P. Allavena, C. Garlanda and M. Locati (2009). "Tumor-associated macrophages and the related myeloid-derived suppressor cells as a paradigm of the diversity of macrophage activation." Hum Immunol **70**(5): 325-330.
- Mantovani, A., A. Sica and M. Locati (2005). "Macrophage polarization comes of age." Immunity **23**(4): 344-346.
- Mantovani, A., A. Sica and M. Locati (2007). "New vistas on macrophage differentiation and activation." Eur J Immunol **37**(1): 14-16.
- Mantovani, A., A. Sica, S. Sozzani, P. Allavena, A. Vecchi and M. Locati (2004). "The chemokine system in diverse forms of macrophage activation and polarization." Trends Immunol **25**(12): 677-686.
- Mantovani, A., S. Sozzani, M. Locati, P. Allavena and A. Sica (2002). "Macrophage polarization: tumor-associated macrophages as a paradigm for polarized M2 mononuclear phagocytes." Trends Immunol **23**(11): 549-555.
- Marathias, K. P., F. I. Preffer, C. Pinto and R. L. Kradin (1991). "Most human pulmonary infiltrating lymphocytes display the surface immune phenotype and functional responses of sensitized T cells." Am J Respir Cell Mol Biol **5**(5): 470-476.

## References

- Martorell, J., R. Vilella, L. Borche, I. Rojo and J. Vives (1987). "A second signal for T cell mitogenesis provided by monoclonal antibodies CD45 (T200)." Eur J Immunol **17**(10): 1447-1451.
- Mashima, T., M. Naito, N. Fujita, K. Noguchi and T. Tsuruo (1995). "Identification of actin as a substrate of ICE and an ICE-like protease and involvement of an ICE-like protease but not ICE in VP-16-induced U937 apoptosis." Biochemical and Biophysical Research Communications **217**(3): 1185-1192.
- Mashima, T., M. Naito, K. Noguchi, D. K. Miller, D. W. Nicholson and T. Tsuruo (1997). "Actin cleavage by CPP-32/apopain during the development of apoptosis." Oncogene **14**(9): 1007-1012.
- Mashima, T., M. Naito and T. Tsuruo (1999). "Caspase-mediated cleavage of cytoskeletal actin plays a positive role in the process of morphological apoptosis." Oncogene **18**(15): 2423-2430.
- Matkowski, R., I. Gisterek, A. Halon, A. Lacko, K. Szewczyk, U. Staszek, M. Pudelko, B. Szynglarewicz, J. Szelachowska, A. Zolnierek and J. Kornafel (2009). "The prognostic role of tumor-infiltrating CD4 and CD8 T lymphocytes in breast cancer." Anticancer Res **29**(7): 2445-2451.
- Mavaddat, N., A. C. Antoniou, D. F. Easton and M. Garcia-Closas (2010). "Genetic susceptibility to breast cancer." Mol Oncol **4**(3): 174-191.
- McCarthy, M. M., M. Sznol, K. A. DiVito, R. L. Camp, D. L. Rimm and H. M. Kluger (2005). "Evaluating the expression and prognostic value of TRAIL-R1 and TRAIL-R2 in breast cancer." Clinical Cancer Research **11**(14): 5188-5194.
- McClelland, M., L. Zhao, S. Carskadon and D. Arenberg (2009). "Expression of CD74, the receptor for macrophage migration inhibitory factor, in non-small cell lung cancer." Am J Pathol **174**(2): 638-646.
- McCormack, V. A. and I. dos Santos Silva (2006). "Breast density and parenchymal patterns as markers of breast cancer risk: a meta-analysis." Cancer Epidemiol Biomarkers Prev **15**(6): 1159-1169.
- McFadden, C., R. Morgan, S. Rahangdale, D. Green, H. Yamasaki, D. Center and W. Cruikshank (2007). "Preferential migration of T regulatory cells induced by IL-16." J Immunol **179**(10): 6439-6445.
- Menard, S., G. Tomasic, P. Casalini, A. Balsari, S. Pilotti, N. Cascinelli, B. Salvadori, M. I. Colnaghi and F. Rilke (1997). "Lymphoid infiltration as a prognostic variable for early-onset breast carcinomas." Clin Cancer Res **3**(5): 817-819.
- Meyer-Siegler, K. and P. B. Hudson (1996). "Enhanced expression of macrophage migration inhibitory factor in prostatic adenocarcinoma metastases." Urology **48**(3): 448-452.



## References

- Miller, J. F. (1961). "Immunological function of the thymus." Lancet **2**(7205): 748-749.
- Mills, C. D., J. Shearer, R. Evans and M. D. Caldwell (1992). "Macrophage arginine metabolism and the inhibition or stimulation of cancer." J Immunol **149**(8): 2709-2714.
- Mitchell, R. A., H. Liao, J. Chesney, G. Fingerle-Rowson, J. Baugh, J. David and R. Bucala (2002). "Macrophage migration inhibitory factor (MIF) sustains macrophage proinflammatory function by inhibiting p53: regulatory role in the innate immune response." Proc Natl Acad Sci U S A **99**(1): 345-350.
- Mitchison, N. A. (1971). "The carrier effect in the secondary response to hapten-protein conjugates. V. Use of antilymphocyte serum to deplete animals of helper cells." Eur J Immunol **1**(2): 68-75.
- Mittler, R. S., R. S. Greenfield, B. Z. Schacter, N. F. Richard and M. K. Hoffmann (1987). "Antibodies to the common leukocyte antigen (T200) inhibit an early phase in the activation of resting human B cells." J Immunol **138**(10): 3159-3166.
- Mohammed, Z. M., J. J. Going, J. Edwards, B. Elsberger, J. C. Doughty and D. C. McMillan (2012). "The relationship between components of tumour inflammatory cell infiltrate and clinicopathological factors and survival in patients with primary operable invasive ductal breast cancer." Br J Cancer **107**(5): 864-873.
- Mohammed, Z. M., J. J. Going, J. Edwards and D. C. McMillan (2012). "The role of the tumour inflammatory cell infiltrate in predicting recurrence and survival in patients with primary operable breast cancer." Cancer Treat Rev **38**(8): 943-955.
- Moll, R. (1993). "[Cytokeratins as markers of differentiation. Expression profiles in epithelia and epithelial tumors]." Veroff Pathol **142**: 1-197.
- Monaghan, P., C. Clarke, N. P. Perusinghe, D. W. Moss, X. Y. Chen and W. H. Evans (1996). "Gap junction distribution and connexin expression in human breast." Exp Cell Res **223**(1): 29-38.
- Monninkhof, E. M., S. G. Elias, F. A. Vlems, I. van der Tweel, A. J. Schuit, D. W. Voskuil, F. E. van Leeuwen and Tfpac (2007). "Physical activity and breast cancer: a systematic review." Epidemiology **18**(1): 137-157.
- Morgan, M. R., G. J. Thomas, A. Russell, I. R. Hart and J. F. Marshall (2004). "The integrin cytoplasmic-tail motif EKQKVDLSTDC is sufficient to promote tumor cell invasion mediated by matrix metalloproteinase (MMP)-2 or MMP-9." J Biol Chem **279**(25): 26533-26539.

## References

- Mork, C., B. van Deurs and O. W. Petersen (1990). "Regulation of vimentin expression in cultured human mammary epithelial cells." Differentiation **43**(2): 146-156.
- Morton, B. A., W. G. Ramey, H. Paderon and R. E. Miller (1986). "Monoclonal antibody-defined phenotypes of regional lymph node and peripheral blood lymphocyte subpopulations in early breast cancer." Cancer Res **46**(4 Pt 2): 2121-2126.
- Munger, J. S., X. Huang, H. Kawakatsu, M. J. Griffiths, S. L. Dalton, J. Wu, J. F. Pittet, N. Kaminski, C. Garat, M. A. Matthay, D. B. Rifkin and D. Sheppard (1999). "The integrin alpha v beta 6 binds and activates latent TGF beta 1: a mechanism for regulating pulmonary inflammation and fibrosis." Cell **96**(3): 319-328.
- Murray, P. J. and T. A. Wynn (2011). "Protective and pathogenic functions of macrophage subsets." Nat Rev Immunol **11**(11): 723-737.
- Muzio, M., A. M. Chinnaiyan, F. C. Kischkel, K. O'Rourke, A. Shevchenko, J. Ni, C. Scaffidi, J. D. Bretz, M. Zhang, R. Gentz, M. Mann, P. H. Krammer, M. E. Peter and V. M. Dixit (1996). "FLICE, a novel FADD-homologous ICE/CED-3-like protease, is recruited to the CD95 (Fas/APO-1) death--inducing signaling complex." Cell **85**(6): 817-827.
- Nagata, S., Y. F. Jin, K. Yoshizato, M. Tomoeda, M. Song, N. Iizuka, M. Kitamura, H. Takahashi, H. Eguchi, H. Ohigashi, O. Ishikawa and Y. Tomita (2009). "CD74 is a novel prognostic factor for patients with pancreatic cancer receiving multimodal therapy." Ann Surg Oncol **16**(9): 2531-2538.
- Nagle, R. B., W. Bocker, J. R. Davis, H. W. Heid, M. Kaufmann, D. O. Lucas and E. D. Jarasch (1986). "Characterization of breast carcinomas by two monoclonal antibodies distinguishing myoepithelial from luminal epithelial cells." J Histochem Cytochem **34**(7): 869-881.
- Nair, S., D. Boczkowski, M. Fassnacht, D. Pisetsky and E. Gilboa (2007). "Vaccination against the forkhead family transcription factor Foxp3 enhances tumor immunity." Cancer Res **67**(1): 371-380.
- Nakano, O., M. Sato, Y. Naito, K. Suzuki, S. Orikasa, M. Aizawa, Y. Suzuki, I. Shintaku, H. Nagura and H. Ohtani (2001). "Proliferative activity of intratumoral CD8(+) T-lymphocytes as a prognostic factor in human renal cell carcinoma: clinicopathologic demonstration of antitumor immunity." Cancer Res **61**(13): 5132-5136.
- Nakazono-Kusaba, A., F. Takahashi-Yanaga, S. Morimoto, M. Furue and T. Sasaguri (2002). "Staurosporine-induced cleavage of alpha-smooth muscle actin during myofibroblast apoptosis." Journal of Investigative Dermatology **119**(5): 1008-1013.

## References

- Nardin, A. and J. P. Abastado (2008). "Macrophages and cancer." Front Biosci **13**: 3494-3505.
- Natali, P. G., M. R. Nicotra, C. Botti, M. Mottolese, A. Bigotti and O. Segatto (1992). "Changes in expression of alpha 6/beta 4 integrin heterodimer in primary and metastatic breast cancer." Br J Cancer **66**(2): 318-322.
- Naukkarinen, A. and K. J. Syrjanen (1990). "Quantitative immunohistochemical analysis of mononuclear infiltrates in breast carcinomas--correlation with tumour differentiation." J Pathol **160**(3): 217-222.
- Negrini, S., V. G. Gorgoulis and T. D. Halazonetis (2010). "Genomic instability--an evolving hallmark of cancer." Nat Rev Mol Cell Biol **11**(3): 220-228.
- Newmeyer, D. D. and S. Ferguson-Miller (2003). "Mitochondria: releasing power for life and unleashing the machineries of death." Cell **112**(4): 481-490.
- Nguyen, M., M. C. Lee, J. L. Wang, J. S. Tomlinson, Z. M. Shao, M. L. Alpaugh and S. H. Barsky (2000). "The human myoepithelial cell displays a multifaceted anti-angiogenic phenotype." Oncogene **19**(31): 3449-3459.
- Nguyen, Q. H., R. L. Moy, M. D. Roth, R. Yamamoto, S. Tomono and S. M. Dubinett (1993). "Expression of CD45 isoforms in fresh and IL-2-cultured tumor-infiltrating lymphocytes from basal cell carcinoma." Cell Immunol **146**(2): 421-430.
- Niranjana, B., L. Buluwela, J. Yant, N. Perusinghe, A. Atherton, D. Phippard, T. Dale, B. Gusterson and T. Kamalati (1995). "HGF/SF: a potent cytokine for mammary growth, morphogenesis and development." Development **121**(9): 2897-2908.
- Nosho, K., Y. Baba, N. Tanaka, K. Shima, M. Hayashi, J. A. Meyerhardt, E. Giovannucci, G. Dranoff, C. S. Fuchs and S. Ogino (2010). "Tumour-infiltrating T-cell subsets, molecular changes in colorectal cancer, and prognosis: cohort study and literature review." J Pathol **222**(4): 350-366.
- O'Connell, P., V. Pekkel, S. A. Fuqua, C. K. Osborne, G. M. Clark and D. C. Allred (1998). "Analysis of loss of heterozygosity in 399 premalignant breast lesions at 15 genetic loci." J Natl Cancer Inst **90**(9): 697-703.
- O'Garra, A. and K. Murphy (1994). "Role of cytokines in determining T-lymphocyte function." Curr Opin Immunol **6**(3): 458-466.
- O'Hare, M. J., J. Bond, C. Clarke, Y. Takeuchi, A. J. Atherton, C. Berry, J. Moody, A. R. Silver, D. C. Davies, A. E. Alsop, A. M. Neville and P. S. Jat (2001). "Conditional immortalization of freshly isolated human mammary fibroblasts and endothelial cells." Proc Natl Acad Sci U S A **98**(2): 646-651.

## References

- Odegaard, J. I. and A. Chawla (2008). "Mechanisms of macrophage activation in obesity-induced insulin resistance." Nat Clin Pract Endocrinol Metab **4**(11): 619-626.
- Ogawa, H., J. Nishihira, Y. Sato, M. Kondo, N. Takahashi, T. Oshima and S. Todo (2000). "An antibody for macrophage migration inhibitory factor suppresses tumour growth and inhibits tumour-associated angiogenesis." Cytokine **12**(4): 309-314.
- Oliver, F. J., G. de la Rubia, V. Rolli, M. C. Ruiz-Ruiz, G. de Murcia and J. Menissier-de Murcia (1998). "Importance of poly(ADP-ribose) polymerase and its cleavage in apoptosis - Lesson from an uncleavable mutant." Journal of Biological Chemistry **273**(50): 33533-33539.
- Olson, J. A., C. McDonald-Hyman, S. C. Jameson and S. E. Hamilton (2013). "Effector-like CD8(+) T Cells in the Memory Population Mediate Potent Protective Immunity." Immunity **38**(6): 1250-1260.
- Oza, A. M. and N. F. Boyd (1993). "Mammographic parenchymal patterns: a marker of breast cancer risk." Epidemiol Rev **15**(1): 196-208.
- Pages, F., A. Berger, M. Camus, F. Sanchez-Cabo, A. Costes, R. Molidor, B. Mlecnik, A. Kirilovsky, M. Nilsson, D. Damotte, T. Meatchi, P. Bruneval, P. H. Cugnenc, Z. Trajanoski, W. H. Fridman and J. Galon (2005). "Effector memory T cells, early metastasis, and survival in colorectal cancer." N Engl J Med **353**(25): 2654-2666.
- Pages, F., A. Kirilovsky, B. Mlecnik, M. Asslaber, M. Tosolini, G. Bindea, C. Lagorce, P. Wind, F. Marliot, P. Bruneval, K. Zatloukal, Z. Trajanoski, A. Berger, W. H. Fridman and J. Galon (2009). "In situ cytotoxic and memory T cells predict outcome in patients with early-stage colorectal cancer." J Clin Oncol **27**(35): 5944-5951.
- Paliard, X., R. de Waal Malefijt, H. Yssel, D. Blanchard, I. Chretien, J. Abrams, J. de Vries and H. Spits (1988). "Simultaneous production of IL-2, IL-4, and IFN-gamma by activated human CD4+ and CD8+ T cell clones." J Immunol **141**(3): 849-855.
- Pan, G., J. Ni, Y. F. Wei, G. Yu, R. Gentz and V. M. Dixit (1997). "An antagonist decoy receptor and a death domain-containing receptor for TRAIL." Science **277**(5327): 815-818.
- Pan, G., K. O'Rourke, A. M. Chinnaiyan, R. Gentz, R. Ebner, J. Ni and V. M. Dixit (1997). "The receptor for the cytotoxic ligand TRAIL." Science **276**(5309): 111-113.
- Pan, H., Z. He, L. Ling, Q. Ding, L. Chen, X. Zha, W. Zhou, X. Liu and S. Wang (2014). "Reproductive factors and breast cancer risk among BRCA1 or BRCA2 mutation carriers: results from ten studies." Cancer Epidemiol **38**(1): 1-8.

## References

- Parker, D. C. (1993). "T cell-dependent B cell activation." Annu Rev Immunol **11**: 331-360.
- Parkin, D. M. (2011). "15. Cancers attributable to reproductive factors in the UK in 2010." Br J Cancer **105 Suppl 2**: S73-76.
- Parton, M., M. Dowsett and I. Smith (2001). "Studies of apoptosis in breast cancer." British Medical Journal **322**(7301): 1528-1532.
- Pasare, C. and R. Medzhitov (2004). "Toll-dependent control mechanisms of CD4 T cell activation." Immunity **21**(5): 733-741.
- Patey, D. H. and W. H. Dyson (1948). "The prognosis of carcinoma of the breast in relation to the type of operation performed." Br J Cancer **2**(1): 7-13.
- Pedroza-Gonzalez, A., K. Xu, T. C. Wu, C. Aspod, S. Tindle, F. Marches, M. Gallegos, E. C. Burton, D. Savino, T. Hori, Y. Tanaka, S. Zurawski, G. Zurawski, L. Bover, Y. J. Liu, J. Banchereau and A. K. Palucka (2011). "Thymic stromal lymphopoietin fosters human breast tumor growth by promoting type 2 inflammation." J Exp Med **208**(3): 479-490.
- Perou, C. M., T. Sorlie, M. B. Eisen, M. van de Rijn, S. S. Jeffrey, C. A. Rees, J. R. Pollack, D. T. Ross, H. Johnsen, L. A. Akslen, O. Fluge, A. Pergamenschikov, C. Williams, S. X. Zhu, P. E. Lonning, A. L. Borresen-Dale, P. O. Brown and D. Botstein (2000). "Molecular portraits of human breast tumours." Nature **406**(6797): 747-752.
- Peto, J. (2001). "Cancer epidemiology in the last century and the next decade." Nature **411**(6835): 390-395.
- Pharoah, P. D., N. E. Day, S. Duffy, D. F. Easton and B. A. Ponder (1997). "Family history and the risk of breast cancer: a systematic review and meta-analysis." Int J Cancer **71**(5): 800-809.
- Plebanski, M., M. Saunders, S. S. Burtles, S. Crowe and D. C. Hooper (1992). "Primary and secondary human in vitro T-cell responses to soluble antigens are mediated by subsets bearing different CD45 isoforms." Immunology **75**(1): 86-91.
- Pollard, T. D. and J. A. Cooper (1986). "Actin and Actin-Binding Proteins - a Critical-Evaluation of Mechanisms and Functions." Annual Review of Biochemistry **55**: 987-1035.
- Polyak, K. and R. Kalluri (2010). "The role of the microenvironment in mammary gland development and cancer." Cold Spring Harb Perspect Biol **2**(11): a003244.
- Polyak, K., Y. Xia, J. L. Zweier, K. W. Kinzler and B. Vogelstein (1997). "A model for p53-induced apoptosis." Nature **389**(6648): 300-305.

## References

- Porter, D., J. Lahti-Domenici, A. Keshaviah, Y. K. Bae, P. Argani, J. Marks, A. Richardson, A. Cooper, R. Strausberg, G. J. Riggins, S. Schnitt, E. Gabrielson, R. Gelman and K. Polyak (2003). "Molecular markers in ductal carcinoma in situ of the breast." Mol Cancer Res **1**(5): 362-375.
- Quiding-Jarbrink, M., S. Raghavan and M. Sundquist (2010). "Enhanced M1 macrophage polarization in human helicobacter pylori-associated atrophic gastritis and in vaccinated mice." PLoS One **5**(11): e15018.
- Ramirez, R., J. Carracedo, M. Castedo, N. Zamzami and G. Kroemer (1996). "CD69-induced monocyte apoptosis involves multiple nonredundant signaling pathways." Cell Immunol **172**(2): 192-199.
- Rasbridge, S. A., C. E. Gillett, S. A. Sampson, F. S. Walsh and R. R. Millis (1993). "Epithelial (E-) and placental (P-) cadherin cell adhesion molecule expression in breast carcinoma." J Pathol **169**(2): 245-250.
- Rastogi, R. P., Richa and R. P. Sinha (2009). "Apoptosis: Molecular Mechanisms and Pathogenicity." Excli Journal **8**: 155-181.
- Reed, J. C. (1994). "Bcl-2 and the regulation of programmed cell death." J Cell Biol **124**(1-2): 1-6.
- Reis-Filho, J. S. and S. R. Lakhani (2003). "The diagnosis and management of pre-invasive breast disease: genetic alterations in pre-invasive lesions." Breast Cancer Res **5**(6): 313-319.
- Ren, X., F. Ye, Z. Jiang, Y. Chu, S. Xiong and Y. Wang (2007). "Involvement of cellular death in TRAIL/DR5-dependent suppression induced by CD4(+)CD25(+) regulatory T cells." Cell Death Differ **14**(12): 2076-2084.
- Ren, Y., H. T. Tsui, R. T. Poon, I. O. Ng, Z. Li, Y. Chen, G. Jiang, C. Lau, W. C. Yu, M. Bacher and S. T. Fan (2003). "Macrophage migration inhibitory factor: roles in regulating tumor cell migration and expression of angiogenic factors in hepatocellular carcinoma." Int J Cancer **107**(1): 22-29.
- Ren, Y. G., K. W. Wagner, D. A. Knee, P. Aza-Blanc, M. Nasoff and Q. L. Deveraux (2004). "Differential regulation of the TRAIL death receptors DR4 and DR5 by the signal recognition particle." Molecular Biology of the Cell **15**(11): 5064-5074.
- Ridge, J. P., F. Di Rosa and P. Matzinger (1998). "A conditioned dendritic cell can be a temporal bridge between a CD4+ T-helper and a T-killer cell." Nature **393**(6684): 474-478.
- Romagnani, S. (1997). "The Th1/Th2 paradigm." Immunol Today **18**(6): 263-266.

## References

- Ronnov-Jessen, L., B. Van Deurs, M. Nielsen and O. W. Petersen (1992). "Identification, paracrine generation, and possible function of human breast carcinoma myofibroblasts in culture." In Vitro Cell Dev Biol **28A**(4): 273-283.
- Rosenberg, L., D. A. Boggs, L. A. Wise, L. L. Adams-Campbell and J. R. Palmer (2010). "Oral contraceptive use and estrogen/progesterone receptor-negative breast cancer among African American women." Cancer Epidemiol Biomarkers Prev **19**(8): 2073-2079.
- Ross, M., and Pawlina, W (2006). Histology: A Text and Atlas, Lippincott Williams & Wilkins.
- Rudland, P. S., C. M. Hughes, S. A. Ferns and M. J. Warburton (1989). "Characterization of human mammary cell types in primary culture: immunofluorescent and immunocytochemical indicators of cellular heterogeneity." In Vitro Cell Dev Biol **25**(1): 23-36.
- Runswick, S. K., M. J. O'Hare, L. Jones, C. H. Streuli and D. R. Garrod (2001). "Desmosomal adhesion regulates epithelial morphogenesis and cell positioning." Nat Cell Biol **3**(9): 823-830.
- Rutella, S., C. Rumi, M. B. Lucia, T. Barberi, P. L. Puggioni, M. Lai, A. Romano, R. Cauda and G. Leone (1999). "Induction of CD69 antigen on normal CD4+ and CD8+ lymphocyte subsets and its relationship with the phenotype of responding T-cells." Cytometry **38**(3): 95-101.
- Saelens, X., N. Festjens, E. Parthoens, I. Vanoverberghe, M. Kalai, F. van Kuppeveld and P. Vandenabeele (2005). "Protein synthesis persists during necrotic cell death." Journal of Cell Biology **168**(4): 545-551.
- Sager, R. (1997). "Expression genetics in cancer: shifting the focus from DNA to RNA." Proc Natl Acad Sci U S A **94**(3): 952-955.
- Sakaguchi, S., M. Ono, R. Setoguchi, H. Yagi, S. Hori, Z. Fehervari, J. Shimizu, T. Takahashi and T. Nomura (2006). "Foxp3+ CD25+ CD4+ natural regulatory T cells in dominant self-tolerance and autoimmune disease." Immunol Rev **212**: 8-27.
- Salagianni, M., E. Lekka, A. Moustaki, E. G. Iliopoulou, C. N. Baxevanis, M. Papamichail and S. A. Perez (2011). "NK cell adoptive transfer combined with Ontak-mediated regulatory T cell elimination induces effective adaptive antitumor immune responses." J Immunol **186**(6): 3327-3335.
- Salazar, H., H. Tobon and J. B. Josimovich (1975). "Developmental, gestational and postgestational modifications of the human breast." Clin Obstet Gynecol **18**(2): 113-137.
- Salehi, E., M. Vodjgani, A. Massoud, A. Keyhani, A. Rajab, B. Shafaghi, Z. Gheflati and T. Aboufazeli (2007). "Increased expression of TRAIL and its

## References

- receptors on peripheral T-cells in type 1 diabetic patients." Iran J Immunol **4**(4): 197-205.
- Salmon, M., G. D. Kitz and P. A. Bacon (1989). "Production of lymphokine mRNA by CD45R+ and CD45R- helper T cells from human peripheral blood and by human CD4+ T cell clones." J Immunol **143**(3): 907-912.
  - Sancho, D., M. Gomez and F. Sanchez-Madrid (2005). "CD69 is an immunoregulatory molecule induced following activation." Trends Immunol **26**(3): 136-140.
  - Sancho, D., M. Gomez, F. Viedma, E. Esplugues, M. Gordon-Alonso, M. A. Garcia-Lopez, H. de la Fuente, A. C. Martinez, P. Lauzurica and F. Sanchez-Madrid (2003). "CD69 downregulates autoimmune reactivity through active transforming growth factor-beta production in collagen-induced arthritis." J Clin Invest **112**(6): 872-882.
  - Sancho, D., A. G. Santis, J. L. Alonso-Lebrero, F. Viedma, R. Tejedor and F. Sanchez-Madrid (2000). "Functional analysis of ligand-binding and signal transduction domains of CD69 and CD23 C-type lectin leukocyte receptors." J Immunol **165**(7): 3868-3875.
  - Sanders, M. E., M. W. Makgoba, S. O. Sharrow, D. Stephany, T. A. Springer, H. A. Young and S. Shaw (1988). "Human memory T lymphocytes express increased levels of three cell adhesion molecules (LFA-3, CD2, and LFA-1) and three other molecules (UCHL1, CDw29, and Pgp-1) and have enhanced IFN-gamma production." J Immunol **140**(5): 1401-1407.
  - Sanders, M. E., P. A. Schuyler, W. D. Dupont and D. L. Page (2005). "The natural history of low-grade ductal carcinoma in situ of the breast in women treated by biopsy only revealed over 30 years of long-term follow-up." Cancer **103**(12): 2481-2484.
  - Santis, A. G., M. R. Campanero, J. L. Alonso, A. Tugores, M. A. Alonso, E. Yague, J. P. Pivel and F. Sanchez-Madrid (1992). "Tumor necrosis factor-alpha production induced in T lymphocytes through the AIM/CD69 activation pathway." Eur J Immunol **22**(5): 1253-1259.
  - Santisteban, M., J. M. Reiman, M. K. Asiedu, M. D. Behrens, A. Nassar, K. R. Kalli, P. Haluska, J. N. Ingle, L. C. Hartmann, M. H. Manjili, D. C. Radisky, S. Ferrone and K. L. Knutson (2009). "Immune-induced epithelial to mesenchymal transition in vivo generates breast cancer stem cells." Cancer Res **69**(7): 2887-2895.
  - Sasieni, P. D., J. Shelton, N. Ormiston-Smith, C. S. Thomson and P. B. Silcocks (2011). "What is the lifetime risk of developing cancer?: the effect of adjusting for multiple primaries." Br J Cancer **105**(3): 460-465.
  - Saslow, D., C. Boetes, W. Burke, S. Harms, M. O. Leach, C. D. Lehman, E. Morris, E. Pisano, M. Schnall, S. Sener, R. A. Smith, E. Warner, M. Yaffe, K. S. Andrews, C. A. Russell and G. American Cancer Society Breast Cancer



## References

- Advisory (2007). "American Cancer Society guidelines for breast screening with MRI as an adjunct to mammography." CA Cancer J Clin **57**(2): 75-89.
- Sato, E., S. H. Olson, J. Ahn, B. Bundy, H. Nishikawa, F. Qian, A. A. Jungbluth, D. Frosina, S. Gnjatic, C. Ambrosone, J. Kepner, T. Odunsi, G. Ritter, S. Lele, Y. T. Chen, H. Ohtani, L. J. Old and K. Odunsi (2005). "Intraepithelial CD8+ tumor-infiltrating lymphocytes and a high CD8+/regulatory T cell ratio are associated with favorable prognosis in ovarian cancer." Proc Natl Acad Sci U S A **102**(51): 18538-18543.
  - Sato, K., A. Niessner, S. L. Kopecky, R. L. Frye, J. J. Goronzy and C. M. Weyand (2006). "TRAIL-expressing T cells induce apoptosis of vascular smooth muscle cells in the atherosclerotic plaque." J Exp Med **203**(1): 239-250.
  - Sato, K., T. Nuki, K. Gomita, C. M. Weyand and N. Hagiwara (2010). "Statins reduce endothelial cell apoptosis via inhibition of TRAIL expression on activated CD4 T cells in acute coronary syndrome." Atherosclerosis **213**(1): 33-39.
  - Schevzov, G., C. Lloyd and P. Gunning (1992). "High level expression of transfected beta- and gamma-actin genes differentially impacts on myoblast cytoarchitecture." J Cell Biol **117**(4): 775-785.
  - Schmid, K. W., I. O. Ellis, J. M. Gee, B. M. Darke, W. E. Lees, J. Kay, A. Cryer, J. M. Stark, A. Hittmair, D. Ofner and et al. (1993). "Presence and possible significance of immunocytochemically demonstrable metallothionein over-expression in primary invasive ductal carcinoma of the breast." Virchows Arch A Pathol Anat Histopathol **422**(2): 153-159.
  - Schnitt, S. J. (2003). "The diagnosis and management of pre-invasive breast disease: flat epithelial atypia--classification, pathologic features and clinical significance." Breast Cancer Res **5**(5): 263-268.
  - Schoenberger, S. P., R. E. Toes, E. I. van der Voort, R. Offringa and C. J. Melief (1998). "T-cell help for cytotoxic T lymphocytes is mediated by CD40-CD40L interactions." Nature **393**(6684): 480-483.
  - Scholl, S. M., C. Pallud, F. Beuvon, K. Hacene, E. R. Stanley, L. Rohrschneider, R. Tang, P. Pouillart and R. Lidereau (1994). "Anti-colony-stimulating factor-1 antibody staining in primary breast adenocarcinomas correlates with marked inflammatory cell infiltrates and prognosis." J Natl Cancer Inst **86**(2): 120-126.
  - Schroder, K., P. J. Hertzog, T. Ravasi and D. A. Hume (2004). "Interferon-gamma: an overview of signals, mechanisms and functions." J Leukoc Biol **75**(2): 163-189.
  - Schwarz, B. A. and A. Bhandoola (2006). "Trafficking from the bone marrow to the thymus: a prerequisite for thymopoiesis." Immunol Rev **209**: 47-57.
  - Sestak, I., R. Kealy, M. Nikoloff, M. Fontecha, J. F. Forbes, A. Howell and J. Cuzick (2012). "Relationships between CYP2D6 phenotype, breast cancer and

## References

- hot flushes in women at high risk of breast cancer receiving prophylactic tamoxifen: results from the IBIS-I trial." Br J Cancer **107**(2): 230-233.
- Shao, Z. M., M. Nguyen, M. L. Alpaugh, J. T. O'Connell and S. H. Barsky (1998). "The human myoepithelial cell exerts antiproliferative effects on breast carcinoma cells characterized by p21WAF1/CIP1 induction, G2/M arrest, and apoptosis." Exp Cell Res **241**(2): 394-403.
  - Sheikh, M. S., M. Garcia, P. Pujol, J. A. Fontana and H. Rochefort (1994). "Why are estrogen-receptor-negative breast cancers more aggressive than the estrogen-receptor-positive breast cancers?" Invasion Metastasis **14**(1-6): 329-336.
  - Smith, C. M., N. S. Wilson, J. Waithman, J. A. Villadangos, F. R. Carbone, W. R. Heath and G. T. Belz (2004). "Cognate CD4(+) T cell licensing of dendritic cells in CD8(+) T cell immunity." Nat Immunol **5**(11): 1143-1148.
  - Smyth, M. J., G. P. Dunn and R. D. Schreiber (2006). "Cancer immunosurveillance and immunoediting: the roles of immunity in suppressing tumor development and shaping tumor immunogenicity." Adv Immunol **90**: 1-50.
  - Solinas, G., G. Germano, A. Mantovani and P. Allavena (2009). "Tumor-associated macrophages (TAM) as major players of the cancer-related inflammation." J Leukoc Biol **86**(5): 1065-1073.
  - Starling, G. C., S. E. Davidson, J. L. McKenzie and D. N. Hart (1987). "Inhibition of natural killer-cell mediated cytotoxicity with monoclonal antibodies to restricted and non-restricted epitopes of the leucocyte common antigen." Immunology **61**(3): 351-356.
  - Steidl, C., T. Lee, S. P. Shah, P. Farinha, G. Han, T. Nayar, A. Delaney, S. J. Jones, J. Iqbal, D. D. Weisenburger, M. A. Bast, A. Rosenwald, H. K. Muller-Hermelink, L. M. Rimsza, E. Campo, J. Delabie, R. M. Braziel, J. R. Cook, R. R. Tubbs, E. S. Jaffe, G. Lenz, J. M. Connors, L. M. Staudt, W. C. Chan and R. D. Gascoyne (2010). "Tumor-associated macrophages and survival in classic Hodgkin's lymphoma." N Engl J Med **362**(10): 875-885.
  - Stein, R., Z. Qu, T. M. Cardillo, S. Chen, A. Rosario, I. D. Horak, H. J. Hansen and D. M. Goldenberg (2004). "Antiproliferative activity of a humanized anti-CD74 monoclonal antibody, hLL1, on B-cell malignancies." Blood **104**(12): 3705-3711.
  - Sternlicht, M. D., S. Safarians, S. P. Rivera and S. H. Barsky (1996). "Characterizations of the extracellular matrix and proteinase inhibitor content of human myoepithelial tumors." Lab Invest **74**(4): 781-796.
  - Sterry, W., S. Bruhn, N. Kunne, B. Lichtenberg, K. Weber-Matthiesen, J. Brasch and V. Mielke (1990). "Dominance of memory over naive T cells in contact dermatitis is due to differential tissue immigration." Br J Dermatol **123**(1): 59-64.

## References

- Stout, R. D. and K. Bottomly (1989). "Antigen-specific activation of effector macrophages by IFN-gamma producing (TH1) T cell clones. Failure of IL-4-producing (TH2) T cell clones to activate effector function in macrophages." J Immunol **142**(3): 760-765.
- Stratton, M. R., N. Collins, S. R. Lakhani and J. P. Sloane (1995). "Loss of heterozygosity in ductal carcinoma in situ of the breast." J Pathol **175**(2): 195-201.
- Suri-Payer, E., A. Z. Amar, A. M. Thornton and E. M. Shevach (1998). "CD4+CD25+ T cells inhibit both the induction and effector function of autoreactive T cells and represent a unique lineage of immunoregulatory cells." J Immunol **160**(3): 1212-1218.
- Suria, H., L. A. Chau, E. Negrou, D. J. Kelvin and J. Madrenas (1999). "Cytoskeletal disruption induces T cell apoptosis by a caspase-3 mediated mechanism." Life Sciences **65**(25): 2697-2707.
- Svensson, H., V. Olofsson, S. Lundin, C. Yakkala, S. Bjorck, L. Borjesson, B. Gustavsson and M. Quiding-Jarbrink (2012). "Accumulation of CCR4(+)/CTLA-4/FOXP3(+)/CD25(hi) regulatory T cells in colon adenocarcinomas correlate to reduced activation of conventional T cells." PLoS One **7**(2): e30695.
- Swain, S. L., L. M. Bradley, M. Croft, S. Tonkonogy, G. Atkins, A. D. Weinberg, D. D. Duncan, S. M. Hedrick, R. W. Dutton and G. Huston (1991). "Helper T-cell subsets: phenotype, function and the role of lymphokines in regulating their development." Immunol Rev **123**: 115-144.
- Tai, X., M. Cowan, L. Feigenbaum and A. Singer (2005). "CD28 costimulation of developing thymocytes induces Foxp3 expression and regulatory T cell differentiation independently of interleukin 2." Nat Immunol **6**(2): 152-162.
- Takahashi, N., J. Nishihira, Y. Sato, M. Kondo, H. Ogawa, T. Ohshima, Y. Une and S. Todo (1998). "Involvement of macrophage migration inhibitory factor (MIF) in the mechanism of tumor cell growth." Mol Med **4**(11): 707-714.
- Tamimi, R. M., H. J. Baer, J. Marotti, M. Galan, L. Galaburda, Y. Fu, A. C. Deitz, J. L. Connolly, S. J. Schnitt, G. A. Colditz and L. C. Collins (2008). "Comparison of molecular phenotypes of ductal carcinoma in situ and invasive breast cancer." Breast Cancer Res **10**(4): R67.
- Tamimi, R. M., C. Byrne, G. A. Colditz and S. E. Hankinson (2007). "Endogenous hormone levels, mammographic density, and subsequent risk of breast cancer in postmenopausal women." J Natl Cancer Inst **99**(15): 1178-1187.
- Testi, R., J. H. Phillips and L. L. Lanier (1989). "T cell activation via Leu-23 (CD69)." J Immunol **143**(4): 1123-1128.

## References

- Thomas, G. J., M. L. Nystrom and J. F. Marshall (2006). "Alphavbeta6 integrin in wound healing and cancer of the oral cavity." J Oral Pathol Med **35**(1): 1-10.
- Thomas, M. L. (1989). "The leukocyte common antigen family." Annu Rev Immunol **7**: 339-369.
- Tian, B., Y. Zhang, N. Li, X. Liu and J. Dong (2012). "CD74: a potential novel target for triple-negative breast cancer." Tumour Biol **33**(6): 2273-2277.
- Toussaint, J., V. Durbecq, S. Altintas, V. Doriath, G. Rouas, M. Paesmans, P. Bedard, B. Haibe-Kains, W. A. Tjalma, D. Larsimont, M. Piccart and C. Sotiriou (2010). "Low CD10 mRNA expression identifies high-risk ductal carcinoma in situ (DCIS)." PLoS One **5**(8).
- Trump, B. F., I. K. Berezsky, S. H. Chang and P. C. Phelps (1997). "The pathways of cell death: oncosis, apoptosis, and necrosis." Toxicol Pathol **25**(1): 82-88.
- Trzonkowski, P., E. Szmit, J. Mysliwska and A. Mysliwski (2006). "CD4+CD25+ T regulatory cells inhibit cytotoxic activity of CTL and NK cells in humans-impact of immunosenescence." Clin Immunol **119**(3): 307-316.
- Tsutsui, S., K. Yasuda, K. Suzuki, K. Tahara, H. Higashi and S. Era (2005). "Macrophage infiltration and its prognostic implications in breast cancer: the relationship with VEGF expression and microvessel density." Oncol Rep **14**(2): 425-431.
- Tworoger, S. S., A. H. Eliassen, P. Sluss and S. E. Hankinson (2007). "A prospective study of plasma prolactin concentrations and risk of premenopausal and postmenopausal breast cancer." J Clin Oncol **25**(12): 1482-1488.
- Urdiales-Viedma, M., F. Nogales-Fernandez, S. Martos-Padilla and E. Sanchez-Cantalejo (1986). "Correlation of histologic grade and lymph node status with some histopathologic discriminants in breast cancer." Tumori **72**(1): 43-51.
- van der Kooij, M. A., E. M. von der Mark, J. K. Kruijt, A. van Velzen, T. J. van Berkel and O. H. Morand (1997). "Human monocyte-derived macrophages express an approximately 120-kD Ox-LDL binding protein with strong identity to CD68." Arterioscler Thromb Vasc Biol **17**(11): 3107-3116.
- van Dongen, J. A., R. Holland, J. L. Peterse, I. S. Fentiman, M. D. Lagios, R. R. Millis and A. Recht (1992). "Ductal carcinoma in-situ of the breast; second EORTC consensus meeting." Eur J Cancer **28**(2-3): 626-629.
- Varney, M. L., S. L. Johansson and R. K. Singh (2005). "Tumour-associated macrophage infiltration, neovascularization and aggressiveness in malignant melanoma: role of monocyte chemotactic protein-1 and vascular endothelial growth factor-A." Melanoma Res **15**(5): 417-425.

## References

- Verjans, E., E. Noetzel, N. Bektas, A. K. Schutz, H. Lue, B. Lennartz, A. Hartmann, E. Dahl and J. Bernhagen (2009). "Dual role of macrophage migration inhibitory factor (MIF) in human breast cancer." BMC Cancer **9**: 230.
- Volodko N, R. A., Rudas M (1998). "Tumour-associated macrophages in breast cancer and their prognostic correlations. ." The Breast **7**: 99-105.
- Walczak, H., M. A. Degli-Esposti, R. S. Johnson, P. J. Smolak, J. Y. Waugh, N. Boiani, M. S. Timour, M. J. Gerhart, K. A. Schooley, C. A. Smith, R. G. Goodwin and C. T. Rauch (1997). "TRAIL-R2: a novel apoptosis-mediating receptor for TRAIL." EMBO J **16**(17): 5386-5397.
- Walczak, H., R. E. Miller, K. Ariail, B. Gliniak, T. S. Griffith, M. Kubin, W. Chin, J. Jones, A. Woodward, T. Le, C. Smith, P. Smolak, R. G. Goodwin, C. T. Rauch, J. C. Schuh and D. H. Lynch (1999). "Tumoricidal activity of tumor necrosis factor-related apoptosis-inducing ligand in vivo." Nat Med **5**(2): 157-163.
- Wald, O., U. Izhar, G. Amir, S. Avniel, Y. Bar-Shavit, H. Wald, I. D. Weiss, E. Galun and A. Peled (2006). "CD4+CXCR4highCD69+ T cells accumulate in lung adenocarcinoma." J Immunol **177**(10): 6983-6990.
- Wallace, D. L. and P. C. Beverley (1990). "Phenotypic changes associated with activation of CD45RA+ and CD45RO+ T cells." Immunology **69**(3): 460-467.
- Walsh, G. M., M. L. Williamson, F. A. Symon, G. B. Willars and A. J. Wardlaw (1996). "Ligation of CD69 induces apoptosis and cell death in human eosinophils cultured with granulocyte-macrophage colony-stimulating factor." Blood **87**(7): 2815-2821.
- Wang, H. Y. and R. F. Wang (2007). "Regulatory T cells and cancer." Curr Opin Immunol **19**(2): 217-223.
- Warburton, M. J., D. Mitchell, E. J. Ormerod and P. Rudland (1982). "Distribution of myoepithelial cells and basement membrane proteins in the resting, pregnant, lactating, and involuting rat mammary gland." J Histochem Cytochem **30**(7): 667-676.
- Weinacker, A., A. Chen, M. Agrez, R. I. Cone, S. Nishimura, E. Wayner, R. Pytela and D. Sheppard (1994). "Role of the integrin alpha v beta 6 in cell attachment to fibronectin. Heterologous expression of intact and secreted forms of the receptor." J Biol Chem **269**(9): 6940-6948.
- Wendling, U., H. Walczak, J. Dorr, C. Jaboci, M. Weller, P. H. Krammer and F. Zipp (2000). "Expression of TRAIL receptors in human autoreactive and foreign antigen-specific T cells." Cell Death Differ **7**(7): 637-644.
- Wernicke, M. (1975). "Quantitative morphologic assessment of immunoreactivity in regional lymph nodes of patients with carcinoma of the breast." Surg Gynecol Obstet **140**(6): 919-924.

## References

- White, E. S., K. R. Flaherty, S. Carskadon, A. Brant, M. D. Iannettoni, J. Yee, M. B. Orringer and D. A. Arenberg (2003). "Macrophage migration inhibitory factor and CXC chemokine expression in non-small cell lung cancer: role in angiogenesis and prognosis." Clin Cancer Res **9**(2): 853-860.
- White, S. R., P. Williams, K. R. Wojcik, S. Sun, P. S. Hiemstra, K. F. Rabe and D. R. Dorscheid (2001). "Initiation of apoptosis by actin cytoskeletal derangement in human airway epithelial cells." American Journal of Respiratory Cell and Molecular Biology **24**(3): 282-294.
- Wiechmann, L. and H. M. Kuerer (2008). "The molecular journey from ductal carcinoma in situ to invasive breast cancer." Cancer **112**(10): 2130-2142.
- Wilgenbus, K. K., C. J. Kirkpatrick, R. Knuechel, K. Willecke and O. Traub (1992). "Expression of Cx26, Cx32 and Cx43 gap junction proteins in normal and neoplastic human tissues." Int J Cancer **51**(4): 522-529.
- Willis, S. N. and J. M. Adams (2005). "Life in the balance: how BH3-only proteins induce apoptosis." Current Opinion in Cell Biology **17**(6): 617-625.
- Wong, P. Y., E. D. Staren, N. Tereshkova and D. P. Braun (1998). "Functional analysis of tumor-infiltrating leukocytes in breast cancer patients." J Surg Res **76**(1): 95-103.
- Woo, E. Y., C. S. Chu, T. J. Goletz, K. Schlienger, H. Yeh, G. Coukos, S. C. Rubin, L. R. Kaiser and C. H. June (2001). "Regulatory CD4(+)CD25(+) T cells in tumors from patients with early-stage non-small cell lung cancer and late-stage ovarian cancer." Cancer Res **61**(12): 4766-4772.
- Xie, K. and I. J. Fidler (1998). "Therapy of cancer metastasis by activation of the inducible nitric oxide synthase." Cancer Metastasis Rev **17**(1): 55-75.
- Xu, X., B. Wang, C. Ye, C. Yao, Y. Lin, X. Huang, Y. Zhang and S. Wang (2008). "Overexpression of macrophage migration inhibitory factor induces angiogenesis in human breast cancer." Cancer Lett **261**(2): 147-157.
- Yacyshyn, M. B., S. Poppema, A. Berg, G. D. MacLean, M. A. Reddish, A. Meikle and B. M. Longenecker (1995). "CD69+ and HLA-DR+ activation antigens on peripheral blood lymphocyte populations in metastatic breast and ovarian cancer patients: correlations with survival following active specific immunotherapy." Int J Cancer **61**(4): 470-474.
- Yakirevich, E., O. B. Izhak, G. Rennert, Z. G. Kovacs and M. B. Resnick (1999). "Cytotoxic phenotype of tumor infiltrating lymphocytes in medullary carcinoma of the breast." Mod Pathol **12**(11): 1050-1056.
- Yamazaki, Y., M. Tsuruga, D. Zhou, Y. Fujita, X. Y. Shang, Y. Dang, K. Kawasaki and S. Oka (2000). "Cytoskeletal disruption accelerates caspase-3 activation and alters the intracellular membrane reorganization in DNA damage-induced apoptosis." Experimental Cell Research **259**(1): 64-78.

## References

- Yan, N. and Y. Shi (2005). "Mechanisms of apoptosis through structural biology." Annu Rev Cell Dev Biol **21**: 35-56.
- Yang, S. B., Y. Du, B. Y. Wu, S. P. Xu, J. B. Wen, M. Zhu, C. H. Cai and P. C. Yang (2012). "Integrin alphavbeta6 promotes tumor tolerance in colorectal cancer." Cancer Immunol Immunother **61**(3): 335-342.
- Yarar, D., C. M. Waterman-Storer and S. L. Schmid (2005). "A dynamic actin cytoskeleton functions at multiple stages of clathrin-mediated endocytosis." Mol Biol Cell **16**(2): 964-975.
- Yokosaki, Y., H. Monis, J. Chen and D. Sheppard (1996). "Differential effects of the integrins alpha9beta1, alphavbeta3, and alphavbeta6 on cell proliferative responses to tenascin. Roles of the beta subunit extracellular and cytoplasmic domains." J Biol Chem **271**(39): 24144-24150.
- Young, A. N., M. B. Amin, C. S. Moreno, S. D. Lim, C. Cohen, J. A. Petros, F. F. Marshall and A. S. Neish (2001). "Expression profiling of renal epithelial neoplasms: a method for tumor classification and discovery of diagnostic molecular markers." Am J Pathol **158**(5): 1639-1651.
- Yousefi, M., R. Mattu, C. Gao and Y. G. Man (2005). "Mammary ducts with and without focal myoepithelial cell layer disruptions show a different frequency of white blood cell infiltration and growth pattern: implications for tumor progression and invasion." Appl Immunohistochem Mol Morphol **13**(1): 30-37.
- Yuan, J. and H. R. Horvitz (2004). "A first insight into the molecular mechanisms of apoptosis." Cell **116**(2 Suppl): S53-56, 51 p following S59.
- Zeiss, C. J. (2003). "The apoptosis-necrosis continuum: insights from genetically altered mice." Vet Pathol **40**(5): 481-495.
- Zhang, L., J. R. Conejo-Garcia, D. Katsaros, P. A. Gimotty, M. Massobrio, G. Regnani, A. Makrigiannakis, H. Gray, K. Schlienger, M. N. Liebman, S. C. Rubin and G. Coukos (2003). "Intratumoral T cells, recurrence, and survival in epithelial ovarian cancer." N Engl J Med **348**(3): 203-213.
- Zhang, X. D., G. D. Schiller, P. G. Gill and B. J. Coventry (1998). "Lymphoid cell infiltration during breast cancer growth: a syngeneic rat model." Immunol Cell Biol **76**(6): 550-555.
- Zhao, Q., D. M. Kuang, Y. Wu, X. Xiao, X. F. Li, T. J. Li and L. Zheng (2012). "Activated CD69+ T cells foster immune privilege by regulating IDO expression in tumor-associated macrophages." J Immunol **188**(3): 1117-1124.
- Zheng, Y. X., M. Yang, T. T. Rong, X. L. Yuan, Y. H. Ma, Z. H. Wang, L. S. Shen and L. Cui (2012). "CD74 and macrophage migration inhibitory factor as therapeutic targets in gastric cancer." World J Gastroenterol **18**(18): 2253-2261.

## References

- Ziegler, R. G., R. N. Hoover, M. C. Pike, A. Hildesheim, A. M. Nomura, D. W. West, A. H. Wu-Williams, L. N. Kolonel, P. L. Horn-Ross, J. F. Rosenthal and M. B. Hyer (1993). "Migration patterns and breast cancer risk in Asian-American women." J Natl Cancer Inst **85**(22): 1819-1827.
- Ziegler, S. F., F. Ramsdell and M. R. Alderson (1994). "The activation antigen CD69." Stem Cells **12**(5): 456-465.
- Zingoni, A., G. Palmieri, S. Morrone, M. Carretero, M. Lopez-Botel, M. Piccoli, L. Frati and A. Santoni (2000). "CD69-triggered ERK activation and functions are negatively regulated by CD94 / NKG2-A inhibitory receptor." Eur J Immunol **30**(2): 644-651.
- Zou, Z., A. Anisowicz, M. J. Hendrix, A. Thor, M. Neveu, S. Sheng, K. Rafidi, E. Seftor and R. Sager (1994). "Maspin, a serpin with tumor-suppressing activity in human mammary epithelial cells." Science **263**(5146): 526-529.



# Appendices

## Appendix 1

### 1.1 Mycoplasma PCR

#### 1) Culture Supernatant

- I. Collect supernatant and centrifuge.
- II. Discard excess and leave behind 500µl.
- III. Flick tube resuspend debris.

#### 2) PCR

(GPO1) FWd 1 ACT CTT ACG GGA GGC AGC AGT A

(GPO2) Fwd 2 CTT AAA GGA ATT GAC GGG AAC CCG

(GPO3) Rev TGC ACC ATC TGT CAT TCT GTT AAC CTC

1<sup>st</sup> Round – Band at 720bp

Culture supernatant	1µl
GPO1 Forward Primer 1 (10 uM)	1µl
MGSO Reverse Primer (10 uM)	1µl
Formamide	0.5µl
Megamix	16.5µl

Cycling condition

95° C X 30s	
95° C X 30s	} 35 cycles
55° C X 30s	
72° C X 1 min	
72° C X 1 min	

2 <sup>nd</sup> Round- Band at 145bp	
1 <sup>st</sup> Round PCR product	1µl
GPO1 Forward Primer 1 (10 uM)	1µl
MGSO Reverse Primer (10 uM)	1µl
Formamide	0.5µl
Megamix	16.5µl

## 1.2 1X RIPA Buffer

20 mM Tris-HCl (pH 7.5)

150 mM NaCl,

1 mM Na<sub>2</sub>EDTA

1 mM EGTA

1% NP-40

1% sodium deoxycholate

2.5 mM sodium pyrophosphate

1 mM β-glycerophosphate

1 mM Na<sub>3</sub>VO<sub>4</sub>

1 µg/ml leupeptin.

### 1.3 SDS–polyacrylamide gel

	<b>8%</b>	<b>12%</b>
22.2% Acrylamide/0.6% Bis	10.81 mls	7.21 mls
1M Tris/HCl pH=8.8	7.5 mls	7.5 mls
Distilled water	1.38 mls	4.99 mls
10% SDS	200µl	200µl
10% Ammonium Persulfate	100µl	100µl
TEMED	10µl	10µl

### 1.4 Stacking gel

22.2% Acrylamide/Bisacrylamide	2.2ml
Distilled Water	6.6ml
1M Tris/HCl pH=6.8	1.25ml
10% SDS	100µl
10% Ammonium Persulfate	50µl
TEMED	50µl

### 1.5 SDS-PAGE: Running buffer

<b>Contents</b>	<b>weight</b>	<b>final</b>
<b>concentration</b>		
TRIS base	15.15 g	25Mm
Glycine	72g	192Mm
SDS	5g	0.1%
(w/v)		
Distilled water	5liters	

### 1.6 SDS- PAGE: Transfer buffer

<b>Contents</b>	<b>volume</b>	<b>final</b>
<b>concentration</b>		
Triglycin	25 ml	8%
Methanol	50ml	25%
Distilled water	250ml	

### 1.7 RNA extraction

1. Cell pellet was collected by centrifugation and resuspended in 600  $\mu$ l of ZR RNA Buffer.
2. Then, the cell pellet was vortexed for few seconds and transferred to Zymo-Spin III C column in a collection tube and centrifuged for at 12.000 rpm for 1 minute.

3. The flow-through was discarded and 400  $\mu$ l RNA pre-wash Buffer was added to the column and centrifuged at 12.000 rpm for 1 minute.
4. The flow-through was discarded and 700  $\mu$ l of RNA wash Buffer was added and centrifuged at 12.000 rpm for 30 seconds. Then, the flow-through was discarded and this step was repeated with 400  $\mu$ l of RNA wash Buffer.
5. Then, the column was placed in a new collection tube and centrifuged at 12.000 rpm for 2 minutes to ensure complete removal of the wash Buffer.
6. The column placed into an RNase-free tube, 35  $\mu$ l of DNase/ RNase-free water was added directly to the column and incubated at room temperature for 1 minute then centrifuged at high speed for 30 seconds. Eluted RNA was used immediately or stored at  $< 70^{\circ}$  C

## Appendix 2

### Source of reagents

Product	Source
A	
Acetic acid	Sigma, UK
Acrylamide	Invitrogen, UK
Acrylamide gel	Invitrogen, UK
Ammonium acetate	Sigma, UK
APC	National Diagnostics, UK
Avidin biotin complex (ABC)	Dakocyomation, UK
B	
$\beta$ -actin	Sigma, UK
BioRad DC protein assay kit (Reagent A, Reagent B and Reagent C)	BioRad, UK
C	
C57/BLK6 mice	Harlan
Calcium chloride	Sigma, UK
CD40L ELISA	R & D, UK
Centrifuge tube	BD, UK
Chemiluminescence film	Amersham, UK
Coverslips	CR-UK
Cryotubes	BD,UK
D	
DAP	Sigma, UK
Distilled water ( dH <sub>2</sub> O)	CR-UK

DMEM	Sigma, UK
DMSO	Laboratory supplies, UK
DNase (RNase free water)	Promega,UK
DPX (Mountant)	VWR International
E	
ECL plus Western Blotting Detection System	Amersham Bioscience, UK
EDTA	Sigma, UK
EGF	Sigma, UK
Eosin	Sigma, UK
Ethanol	Fischer Scientific, UK
Etoposide chemotherapy	Sigma, UK
F	
FBS (heat inactivated)	Marathon laboratories,UK
Flow cytometry tube	BD, UK
Formalin saline	CR-UK
G	
L-glutamine	CR-UK
H	
H&E	Sigma, UK
Haemocytometer	Fischer Scientific, UK
Ham's F12	Sigma, UK
Hydrogen peroxidase	Fischer Scientific,UK
Hydrocortisone	Sigma, UK
I	



IgG isotype control antibody	Sigma, UK
Insulin	Sigma, UK
M	
Matrigel	BD, UK
Methanol	Fischer Scientific, UK
Milk powder	Marvel
N	
Nitrocellulose filter	Pall Life Science, UK
Nunc EASY Flask T75 (75cm <sup>2</sup> ) plastic culture flasks	Sigma
P	
PAP pen	Zymed,UK
PBS	CR-UK
PCR-grade water	Sigma, UK
Pepsin	Invitrogen, UK
PI (propidium iodide)	Calbiochem, UK
Plates for culture	BD, UK
Ponceau S solution	Sigma, UK
Power Syber green PCR Master Mix	Applied Biosystem
Protease inhibitor cocktail	Calbiochem, UK
R	
Rabbit anti-mouse IgG Dyanbeads	Invitrogen, UK
Resolving buffer	National Diagnostics, UK
Recombinant TRAIL	Peprtech,UK
RIPA buffer	Millipore, USA

RPMI medium	Sigma, UK
S	
SDS	Qiage,UK
Sodium chloride	Sigma, UK
T	
TRAIL ELISA	R& D, UK
TBS (TRIS-buffered saline )	CR-UK
TEMED	National Diagnostics, UK
Trypan Blue	Sigma, UK
Trypsin/EDTA	CR-UK
Tween	Sigma, UK
W	
Whatmann paper / sponges	Invitrogen, UK
X	
X –ray film	GE healthcare,UK
Xylene	Fischer Scientific, UK

## Appendix3

### Presentations

- 1- Khairiya Ahmed, Michael Allen, John Marshall, J Louise Jones  
Changes in the microenvironment of DCIS: the relationship between altered myoepithelial cell phenotype and inflammatory infiltrate, William Harvey day 2010.
- 2- Khairiya Ahmed, Michael Allen, Jenny Gomm, John Marshall, J Louise Jones  
Myoepithelial control of the inflammatory microenvironment promotes transition of DCIS to invasive disease, William Harvey day 2012.
- 3- Khairiya Ahmed, Michael Allen, Jenny Gomm, John Marshall, J Louise Jones  
T regulatory cells in the DCIS microenvironment induce myoepithelial apoptosis: a role in transition of DCIS to invasive disease? Keystone Symposia conference (The Role of Inflammation during Carcinogenesis conference), Dublin, Ireland 2012.
- 4- Khairiya Ahmed, Michael Allen, Jenny Gomm, John Marshall, J Louise Jones  
Myoepithelial control of the inflammatory microenvironment promotes transition of DCIS to invasive disease, ESMO, IMPAKT Breast Cancer conference Brussels, Belgium 2012.
- 5- Khairiya Ahmed, Michael Allen, Jenny Gomm, John Marshall, J Louise Jones  
Changes in the microenvironment of DCIS: the relationship between altered myoepithelial cell phenotype and inflammatory infiltrate, William Harvey day 2013.

